

REPUBLIQUE ALGERIENNE DEMOCRATIQUE ET POPULAIRE
MINISTERE DE L'ENSEIGNEMENT SUPERIEUR ET DE LA RECHERCHE SCIENTIFIQUE
UNIVERSITE MOULOU D MAMMERI DE TIZI-OUZOU
FACULTE DES SCIENCES BIOLOGIQUES ET DES SCIENCES AGRONOMIQUES



THÈSE

Présentée

Par **Sarah LAMMI**

En vue de l'obtention du titre de

DOCTEUR EN SCIENCES BIOLOGIQUES

Option : Microbiologie Appliquée et Biotechnologie Microbienne

Thème

**DEVELOPPEMENT D'UN EMBALLAGE ACTIF ET
BIODEGRADABLE A BASE DE GRIGNONS D'OLIVES EN VUE
D'UNE APPLICATION DANS LA CONSERVATION DES ALIMENTS**

Soutenue publiquement le 13/09/2018, devant le jury composé de :

Mr MATI Abderrahmane	Professeur à l'U.M.M.T.O.	Président
Mr DJENANE Djamel	Professeur à l'U.M.M.T.O.	Directeur de thèse
Mme ANGELLIER-COUSSY Hélène	Maître de Conférences à l'Université de Montpellier (France)	Co-Directrice de thèse
Mme CHEMANI Halima	Professeur à l'U.M.B.(Boumerdes)	Examinatrice
Mr HAZZIT Mohamed	Professeur à l'E.N.S.A.(El-Harrach)	Examineur
Mme FERNANE Farida	Professeur à l'U.M.M.T.O.	Examinatrice

Remerciements

La présente thèse est effectuée au Laboratoire de Qualité et Sécurité des Aliments (LQSA) de l'université Mouloud MAMMARI de Tizi-Ouzou (UMMTO) et l'Unité Mixte de Recherche Ingénierie des Agropolymères et Technologies Emergentes (UMR IATE) de Montpellier (France).

En premier lieu, je remercie mon Directeur de thèse Djamel DJENANE, Professeur à l'UMMTO pour m'avoir proposé ce sujet de thèse et ouvert son laboratoire ; qu'il trouve ici le témoignage de mon respect.

Je tiens à exprimer toute ma reconnaissance au Professeur Nathalie GONTARD, Directrice de laboratoire à l'UMR IATE, de m'avoir accueillie au sein de son équipe de recherche.

Mes vifs remerciements s'adressent à Madame Hélène ANGELLIER-COUSSY, Maître de conférences à l'Université de Montpellier, d'avoir accepté de codiriger ce travail de thèse malgré ses multiples tâches. Ses suggestions précieuses, sa rigueur scientifique et ses conseils éclairés m'ont permis de mener à bien ce projet de recherche multidisciplinaire. Qu'elle trouve ici l'expression de mon respect et mes remerciements les plus sincères pour tout le temps qu'elle m'a consacré depuis nos réunions au laboratoire, jusqu'à la rédaction d'articles et les corrections du manuscrit de thèse et pour toutes les connaissances scientifiques qu'elle m'a transmises notamment dans le domaine des matériaux composites.

Je voudrais également adresser mes remerciements aux membres du jury d'avoir accepté d'examiner ce travail.

Je remercie Claire MAYER-LAIGLE et Abdellatif BARAKAT pour leurs précieuses aide et orientations dans les travaux menés sur le fractionnement des grignons.

Je remercie également Nicolas LE MOIGNE de m'avoir accueilli dans son laboratoire à l'Ecole des Mines d'Alès et pour sa contribution dans la partie matériaux. Merci aussi à Benjamin GALLARD pour son aide technique dans la mise en œuvre des composites.

Je suis très reconnaissante à Emmanuelle GASTALDI, pour m'avoir initiée sur les principes de la biodégradation, pour sa gentillesse et ses qualités humaines.

Mes sincères remerciements s'adressent à Fabrice GAUBIAC, pour le temps qu'il m'a consacré (même pendant ses séances de TP), afin que je puisse réaliser les tests des propriétés antibactériennes. Je le remercie pour les échanges enrichissants qu'on a eus autour de la microbiologie des aliments.

C'est aussi un grand plaisir d'exprimer mes remerciements à Cécile SOTTO de m'avoir formée aux différents appareils de broyage et de fractionnement, pour sa patience et sa gentillesse.

Je souhaite aussi remercier tous les thésards et stagiaires que j'ai côtoyés durant mon séjour à Montpellier : Valentin, Céline, Amélie, Charlie, Sara, Grégoire, Anaïs, Ali, Aida, Modeste, Chutima et Daniel, pour leur encouragement et leur amitié.

Je tiens particulièrement à remercier mon amie Hamida AKLI de l'UMMTO, pour ses encouragements et sa gentillesse.

Je dois de la reconnaissance à mes très chers Parents, mon frère et mes sœurs, pour leurs encouragements et soutien permanent pendant mes longues années d'études.

Enfin, je suis très reconnaissante au Ministère Algérien de l'Enseignement Supérieur et de la Recherche Scientifique de m'avoir octroyé une bourse de 11 mois, qui m'a été indispensable pour finaliser mes travaux de recherches en France dans des meilleures conditions.

“Expliquer toute la nature est une tâche trop ardue pour un seul homme ou une seule époque. Il est plus sage de faire peu en étant sûr de soi et laisser le reste à ceux qui viendront après, que présumer de tout sans être sûr de rien”

Isaac Newton

“ Face à la roche, le ruisseau l’emporte toujours, non pas par la force mais par la persévérance ”

Henry Jackson Brown

ASTM: “*American Society for Testing and Materials*”

BHA: Butyl hydroxy anisole

BHT: Butyl hydroxy toluène

CIP: Collection de l'Institut Pasteur

DSC: “*Differential Scanning Calorimetry*”

E: module d'Young

F0: Grignon d'olives brut broyé

GPa: Géga Pascal

GRAS: “*Generally Recognized As Safe*”

Hz: Hertz

MEB: Microscope Electronique à Balayage

MPa: Mega Pascal

OP: Grignon d'olives brut “*Olive pomace*”

OTR: “*Oxygen Transmission Rate*”

PF: Fraction riche en pulpe

PHA: Polyhydroxyalkanoate

PHB: Polyhydroxybutyrate

PHBV: Poly (3-hydroxybutyrate-co-3-hydroxyvalérate)

PHV: Polyhydroxyvalérate

PP: Polypropylène

SF: Fraction riche en noyau

T_c: Température de cristallisation

T_f: Température de fusion

T_g: Température de transition vitreuse

TGA: “*Thermogravimetric analysis*”

WVP: “*Water vapor permeability*”

WVTR: “*Water vapor transmission rate*”

X_c: Taux de cristallinité

ε: Déformation à la rupture

σ: Contrainte à la rupture

Figure 1 : Les différents effets physiques et chimiques qui permettent à un matériau de devenir actif.	9
Figure 2 : Schéma général d'un composite.	18
Figure 3 : Classification des bioplastiques selon leur origine, leur voie de synthèse et leur fin de vie.	20
Figure 4 : Image de cellules bactériennes contenant des granules de PHA, prise par microscopie électronique à transmission.	22
Figure 5 : Structure chimique générale du PHBV.	22
Figure 6 : Représentation de la structure lignocellulosique montrant la cellulose, l'hémicellulose et la lignine.	25
Figure 7: <i>“Evolution of the number of peer-reviewed journal articles published (bars) and cited (●) with the keyword “olive pomace”. Data obtained from Web of Science (5th of April 2018)”.</i>	31
Figure 8: <i>“Main producers of olive and olive oil in the world”.</i>	32
Figure 9: <i>“Longitudinal section of the olive fruit”.</i>	34
Figure 10: <i>“Simplified processes for olive oil production. Bold names correspond to the different by-products, the boxes in dotted points correspond to the facultative steps.”</i>	36
Figure 11: <i>“ATG and DTG curves of stone-rich and pulp-rich fractions under air atmosphere”.</i>	45
Figure 12: <i>“Fractionation process of crude olive pomace investigated to obtain stone (S) and pulp (P) rich fractions”.</i>	82
Figure 13: <i>“TGA and DTG curves of stone and pulp rich-fractions produced either by wet fractionation or dry fractionation with sieving”.</i>	95
Figure 14: <i>“Dry fractionation process of crude olive pomace”.</i>	109
Figure 15: <i>“Biochemical composition of olive pomace-based fractions”.</i>	116
Figure 16: <i>“Particle size distribution of olive pomace fractions”.</i>	118
Figure 17: <i>“SEM images of F0, SF and PF fillers”.</i>	119
Figure 18: <i>“TGA and DTG curves of F0, SF and PF fractions under air and nitrogen”.</i>	120
Figure 19: <i>“SEM images of cryo-fractured surfaces of PP-based composites”.</i>	125
Figure 20: <i>“TGA and DTG curves of (a) PP and (b) PHBV-based biocomposites under air”.</i>	128
Figure 21: <i>“Experimental values of the stress at break of PHBV and PBHV-based composites and resulting fitted curves with Pukanszky’s model”.</i>	131
Figure 22: <i>“Kinetic of biodegradation of OP-based fillers in sol”.</i>	143

Figure 23: “ <i>SEM pictures of olive pomace-based fillers</i> ”.	145
Figure 24: “ <i>Antibacterial results of OP-based fillers and OP-based composites</i> ”.	146
Figure 25: “ <i>Kinetic of biodegradation of OP/PHBV-based composites in sol</i> ”.	148
Figure 26: “ <i>SEM pictures of OP/PHBV-based biocomposites surfaces</i> ”.	149

Tableau 1 : Principales applications des technologies d'emballage actif.	14
Tableau 2 : Exemples d'emballage actif actuellement connus.	
Tableau 3 : Quelques systèmes d'emballage actif commercialisés, type de présentation et fonction.	15
Tableau 4: <i>“Composition of the different parts and by-products of the olive”.</i>	16
Tableau 5: <i>“Terminology used to describe the wastes generated in olive oil mills, in different languages”.</i>	35
Tableau 6: <i>“The main valorization routes of the various olive oil by-products”.</i>	37
Tableau 7: <i>“Lignocellulose composition of olive pomace reported in the literature”.</i>	38
Tableau 8: <i>“Main bioactive compounds with potential food technological functions of olive pomace”.</i>	44
Tableau 9: <i>“Scientific papers focusing on the valorization of olive pomace tissues as fillers in biocomposite materials”.</i>	54
Tableau 10: <i>“Mechanical properties of olive pomace-based biocomposites, normalized towards the properties of the neat matrix”.</i>	57
Tableau 11: <i>“Color parameters of OP-based fractions”.</i>	59
Tableau 12: <i>“Biochemical composition of different olive pomace fractions produced by wet and dry process”.</i>	87 88
Tableau 13: <i>“Temperatures corresponding to the different degradation rates of the olive pomace fractions”.</i>	97
Tableau 14: <i>“Contact angle measurements and solid surface free energy of different fractions”.</i>	99
Tableau 15: <i>“Polar and dispersive component of some polymer matrices and the predicted work of adhesion between these polymer matrices and the olive pomace-based fractions produced by wet process and dry process with friction”.</i>	101
Tableau 16: <i>“True density, color parameters, morphological parameters and thermal degradation temperatures recorded under air flow of olive pomace-based fillers”.</i>	117
Tableau 17: <i>“Contact angle, polar and dispersive components of the solid surface free energy and predicted work of adhesion between polymer matrices and OP-based fillers”.</i>	122
Tableau 18: <i>“Colorimetric attributes of biocomposites filled with 15 wt% of OP-based fillers”.</i>	124

Tableau 19: *“Thermal properties of biocomposites filled with 15 wt% of OP-based fillers”.* 127

Tableau 20: *“Mechanical properties, water vapor permeability and oxygen permeability of olive pomace-based biocomposites”.* 129

Tableau 21: *“Biochemical composition (% dry basis) of olive pomace fractions”.* 144

Valorisation des travaux scientifiques

Les résultats obtenus durant cette thèse ont fait l'objet de :

Publications internationales

- [1] **Lammi S.**, Barakat A., Mayer-Laigle C., Djenane D., Gontard N., Angellier-Coussy H. 2018. Dry fractionation of olive pomace as a sustainable process to produce fillers for biocomposites. *Powder Technology* 326, 44-53. DOI.org/10.1016/j.powtec.2017.11.060
- [2] **Lammi S.**, Le Moigne N., Djenane D., Gontard N., Angellier-Coussy H. 2018. Dry fractionation of olive pomace for the development of food packaging biocomposites. *Industrial Crops and Products* 120, 250-261. DOI.org/10.1016/j.indcrop.2018.04.052
- [3] **Lammi S.**, Gastaldi E., Gaubiac F., Djenane D., Gontard N., Angellier-Coussy H. Biodegradability of olive pomace-based biocomposites: Impact of filler composition. Article en préparation pour soumission.
- [4] **Lammi S.**, Djenane D., Gontard N., Angellier-Coussy H. Potential routes of valorizing olive pomace residues: A review. Revue en préparation pour soumission.

Communications scientifiques

- [1] **Lammi S.**, Djenane D. Valorization of olive pomace and durum wheat flour in the manufacture of biodegradable food packaging. The first International Conference in Integrated Management of Environment, 25-28 September 2014, Hammamet -TUNISIA.
- [2] **Lammi S.**, Akli H., Djenane D. Approche écologique pour l'utilisation du grignon d'olive. 2^{ème} Congrès International de la Société Algérienne de Nutrition sur l'Alimentation Méditerranéenne et Santé, 13-15 Octobre 2015, Alger - ALGERIE.
- [3] **Lammi S.**, Gontard N., Angellier-Coussy H. Biocomposites from PHBV and olive pomace-based fillers: Impact of filler composition. 9th European Symposium of BioPolymers, 5 - 7 July 2017, INSA Toulouse - FRANCE.
- [4] **Lammi S.**, Gastaldi E., Djenane D., Gontard N., Angellier-Coussy H. Valorisation du grignon d'olives dans l'élaboration de matériaux biodégradables. La 1^{ère} Ecole d'Hiver sur l'Analyse du Cycle de Vie et l'Eco-conception 18-19 Février 2018, Boumerdes - ALGERIE.
- [5] **Lammi S.**, Gastaldi E., Djenane D., Gontard N., Angellier-Coussy H. Etude de la biodégradation de matériaux biocomposites à base de différentes charges de grignon d'olives. 4^{ème} Conférence Internationale sur l'Energie, les Matériaux, l'Energétique appliquée et la Pollution, 29-30 avril 2018, Constantine - ALGERIE.

Table des matières

Liste des abréviations et symboles

Liste des figures

Liste des tableaux

INTRODUCTION GENERALE

I. SYNTHÈSE BIBLIOGRAPHIQUE

I.1. L'emballage actif **1**

I. 1.1. Introduction	1
I. 1. 2. L'emballage alimentaire : fonctions et enjeux	1
I. 1. 3. L'emballage actif	3
I. 1. 3.1. Principe	3
I. 1. 3.2. Histoire et développement	3
I. 1. 4. Les différentes technologies de l'emballage actif	4
I. 1.4.1. Les émetteurs	5
I. 1.4.2. Les absorbeurs	7
I. 1.4.3. Autres systèmes	8
I. 1.5. Applications de l'emballage actif	9

I.2. Les biocomposites **13**

I. 2.1. Introduction	13
I. 2.2. Les matériaux composites	13
I. 2.3. Les biocomposites	14
I. 2.3.1. Définitions	14
I. 2.3.2. Choix de la matrice polymère	16
I. 2.3.2.1. Classification des biopolymères	16
I. 2.3.2.2. Les polyhydroxylalkanoates (PHAs)	18
I. 2.3.3. Choix de la charge	20
I. 2.3.3.1. La biomasse lignocellulosique	20
I. 2.3.4. Biocomposites à base de PHBV et de particules lignocellulosiques	23

I.3. Potential routes of valorizing olive pomace residues: Review **24**

I.3.1. Introduction	25
I.3.2. Key features of the olives, olive oil and olive by-products	28
I.3.2.1. Main producers and consumers of olive oil	28
I.3.2.2. Olive composition	29
I.3.3. Olive by-products	31
I.3.3.1. Olive pomace	33
I.3.3.1.1. Types of olive pomace	33
I.3.3.1.2. Composition of olive pomace	34
I.3.3.3. Use of olive pomace as filler in biocomposite materials	36
I. 3.4. Conclusion	39

II. MATERIEL ET METHODES

<i>II.1. Production des charges de renfort</i>	42
II.1.1. Matériel	42
II.1.2. Fractionnement du grignon d'olives	42
II.1.2.1. Fractionnement par voie humide	42
II.1.2.2. Fractionnement par voie sèche	43
II.1.3. Caractérisation des fractions de grignon d'olives	44
II.1.3.1. La taille des particules	44
II.1.3.2. Couleur	44
II.1.3.3. Composition biochimique	45
II.1.3.4. Analyse thermogravimétrique	46
II.1.3.5. Mesures d'angle de contact	46
<i>II. 2. Développement et caractérisation des biocomposites pour l'emballage alimentaire</i>	47
II.2.1. Matériel	47
II.2.2. Préparation des charges à base de grignon d'olives	48
II.2.3. Préparation de films biocomposites à base de grignons d'olive	48
II.2.3.1. Compoundage	48
II.2.3.2. Mise en forme des films	49
II.2.3.3. Epaisseur des film et conditionnement	49
II.2.4. Caractérisation des charges et des biocomposites à base de grignon d'olives	49
II.2.4.1. Taille et morphologie des particules	49
II.2.4.2. Densité de particules	50
II.2.4.3. Composition biochimique	50
II.2.4.4. Energie libre de surface et travail d'adhésion	50
II.2.4.5. Couleur	51
II.2.4.6. Analyse thermogravimétrique (ATG)	51
II.2.4.7. Calorimétrie différentielle à balayage (DSC)	51
II.2.4.8. Tests de traction	52
II.2.4.9. Perméabilité à la vapeur d'eau (WVP)	52
II.2.4.10. Perméabilité à l'oxygène	53
II.2.4.11. Microscopie électronique à balayage (MEB)	53
II.2.4.12. Activité antibactérienne	53
II.2.4.13. Tests de biodégradation	54
III. RESULTATS ET DISCUSSION	
<i>III.1. Dry fractionation of olive pomace as a sustainable process to produce fillers for biocomposites (Article n°1)</i>	56
III.1.1. Introduction	57
III.1.2. Materials and methods	60
III.1.2.1. Materials	60
III.1.2.2. Fractionation of olive pomace	61
III.1.2.2.1. Wet fractionation	61
III.1.2.2.2. Dry fractionation	61
III.1.2.3. Characterization of olive pomace fractions	64
III.1.2.3.1. Particle size	64

III.1.2.3.2. Color	64
III.1.2.3.3. Biochemical composition	64
III.1.2.3.4. Thermogravimetric analysis	65
III.1.2.3.5. Contact angle measurements	65
III.1.3. Results and discussion	65
III.1.3.1. Wet fractionation	66
III.1.3.2. Dry fractionation	70
III.1.3.3. Potentiality of using OP-based fractions as raw resources for the production of fillers	73
III.1.4. Conclusion	82
<i>III.2. Dry fractionation of olive pomace for the development of food packaging biocomposites (Article n°2)</i>	84
III.2.1. Introduction	86
III.2.2. Materials and methods	88
III.2.2.1. Raw materials	88
III.2.2.2. Preparation of olive pomace-based fillers	90
III.2.2.3. Preparation of olive pomace-based composite films	90
III.2.2.3.1. Compounding	90
III.2.2.3.2. Film shaping	90
III.2.2.3.3. Film thickness and conditioning	91
III.2.2.4. Characterization of olive pomace-based fillers and biocomposites	91
III.2.2.4.1. Particle size and morphology	91
III.2.2.4.2. Particle density	91
III.2.2.4.3. Biochemical composition	92
III.2.2.4.4. Surface free energy and work of adhesion	92
III.2.2.4.5. Color	92
III.2.2.4.6. Thermogravimetric analysis (TGA)	93
III.2.2.4.7. Differential scanning calorimetry (DSC)	93
III.2.2.4.8. Tensile tests	93
III.2.2.4.9. Scanning electron microscopy (SEM)	94
III.2.2.4.10. Water vapour permeability (WVP)	94
III.2.2.4.11. Oxygen permeability	95
III.2.3. Results and discussion	95
III.2.3.1. Effect of dry fractionation on the characteristics of olive pomace-based fillers	95
III.2.3.1.1. Effect of dry fractionation on biochemical composition, color and particle density	98
III.2.3.1.2. Effect of dry fractionation on particle size and morphology	99
III.2.3.1.3. Effect of dry fractionation on the thermal stability of olive pomace-based fillers	101
III.2.3.1.4. Effect of dry fractionation on the surface energy of olive-pomace based fillers	103
III.2.3.2. Structure of olive pomace-based biocomposites	103
III.2.3.2.1. Visual appearance of films	104
III.2.3.2.2. Observation of the microstructure	104
III.2.3.2.3. Melting and crystallization behavior	106
III.2.3.3. Functional properties of olive-pomace based biocomposites films	106
III.2.3.3.1. Thermal stability	108
III.2.3.3.2. Mechanical properties	111
III.2.3.3.3. Water vapour and oxygen permeability	

III.2.4. Conclusion	113
III.3. Biodegradability of olive pomace–based biocomposites: Impact of filler composition (Article n°3)	115
III.3.1. Introduction	116
III.3.2. Materials and methods	118
III.3.2.1. Materials	118
III.3.2.2. Preparation and characterization of olive pomace-based fillers	119
III.3.2.3. Preparation and characterization of OP/PHBV-based biocomposites	120
III.3.2.4. Biodegradation tests	121
III.3.3. Results and discussion	122
III.3.3.1. Biodegradability of OP-based fillers	122
III.3.3.2. Biodegradability of OP-based biocomposites	127
III.3.4. Conclusion	130
IV. DISCUSSION GENERALE	131
CONCLUSION	140
Références bibliographiques	
Annexes	
Abstract	
Résumé	

Introduction générale

La plupart des polymères synthétiques disponibles de nos jours sont produits à partir de dérivés pétrochimiques et ne sont pas biodégradables. Ces polymères persistants s'accumulent dans notre environnement et génèrent des sources importantes de pollution. Leur substitution par des plastiques biosourcés et biodégradables en conditions naturelles ont ainsi suscité un grand intérêt (Avérous et Pollet, 2012).

L'emballage alimentaire est le secteur qui consomme le plus de plastiques, avec environ 40% de la demande mondiale. Le polypropylène (PP) est à la tête des polymères utilisés dans ce domaine, avec plus de 19 % d'utilisations (Plastics Europe, 2016). Les exigences en matière de fonctionnalité et d'impact environnemental suscitent actuellement une attention importante de la part de tous les acteurs de la chaîne d'emballage alimentaire, avec pour objectif de réduire les pertes et gaspillages alimentaires, tout en réduisant les effets nocifs des résidus plastiques pétrochimiques sur l'environnement. A cet effet, les problématiques environnementales sont de nos jours intégrées dès la phase de conception des matériaux d'emballage.

En plus de son rôle de stockage et de protection mécanique, la fonction principale de l'emballage alimentaire est d'assurer la qualité et la sécurité du produit emballé tout au long de sa conservation, en contrôlant les transferts de nombreux types de molécules (Chea *et al.*, 2015). Les propriétés de transfert de l'emballage doivent être adaptées aux besoins du produit à emballer et à l'application finale prévue (Siracusa *et al.*, 2008 ; Peelman *et al.*, 2013). La vapeur d'eau et l'oxygène sont deux des principaux perméats étudiés dans les applications d'emballage, car ils peuvent provenir de l'environnement interne ou externe à l'emballage, ce qui entraîne un changement continu de la qualité du produit et de sa durée de conservation. Par exemple, dans le cas des fruits et légumes frais qui ont un métabolisme continu, il est nécessaire d'avoir des matériaux « respirants » adaptés à leur activité respiratoire (Turan *et al.*, 2017).

Dans ce contexte, l'objectif de cette thèse est d'explorer le potentiel de renfort des grignons d'olives pour le développement de matériaux biocomposites fonctionnels et biodégradables, en vue d'une application dans le domaine de l'emballage alimentaire. Pour cela, notre but était - sur le plan pratique - de valoriser le grignon d'olive dans son ensemble, tel qu'il est abandonné dans la nature et selon une démarche écologique. L'enjeu scientifique de ce travail, était de comprendre l'influence des caractéristiques de la charge sur les propriétés fonctionnelles, ainsi que la biodégradabilité des matériaux biocomposites développés.

Afin de répondre à la problématique de ce projet de thèse, le présent manuscrit est partagé en trois parties :

La « première partie » est consacrée à une synthèse bibliographique, dans laquelle nous présentons un aperçu sur les emballages actifs, les biocomposites et une revue de littérature scientifique rédigée en anglais dédiée aux grignon d'olives, avec un accent sur ses principales voies de valorisation disponibles de nos jours, notamment son application dans les matériaux biocomposites.

La « deuxième partie » présentera les différentes matières premières utilisées et les diverses techniques de caractérisation et méthodes expérimentales mises en place, pour mener à bien ce projet de recherche.

Ensuite, les résultats des travaux réalisés et leurs discussions sont présentés sous formes d'articles scientifiques dans la « troisième partie » de la thèse. Le premier article, traite une étude réalisée sur la possibilité de séparer la pulpe du noyau à partir du grignon d'olives brut par voie sèche, pour la production de charges de renfort. Le deuxième article s'intéresse à la mise en œuvre ainsi que la caractérisation des propriétés fonctionnelles des matériaux biocomposites à base de charges de grignon. Le troisième article présente le travail mené pour comprendre l'influence de l'incorporation de charges issues de grignon d'olive sur le mécanisme de biodégradation des matériaux biocomposites développés.

Pour finir, une discussion générale ainsi que des conclusions et perspectives sont présentées.

I. Synthèse bibliographique

I.1. L'emballage actif

I.1. L'EMBALLAGE ACTIF

I.1.1. Introduction

Tous les aliments sont soumis à une transformation progressive de leurs propriétés microbiologiques, chimiques, physiques et organoleptiques. La durée de conservation des aliments intéresse l'ensemble des acteurs de la chaîne alimentaire, du producteur jusqu'au consommateur. Elle est contrôlée par de nombreux facteurs et l'emballage est l'un des facteurs les plus importants (Parisi, 2002).

Sans développement de l'emballage, les systèmes de récolte, du traitement et de la distribution des produits alimentaires n'auraient pas été développés à leur niveau actuel, les consommateurs n'auraient pas eu un accès facile à la vaste gamme d'aliments offerts aujourd'hui, les déchets et les pertes dus à la détérioration des aliments, auraient été plus élevés (Cirillo *et al.*, 2015). Des systèmes d'emballage ont été mis en œuvre pour atteindre ces objectifs et des efforts considérables ont été faits pour développer des matériaux plus efficaces d'un point de vue mécanique et fonctionnel (Volpe *et al.*, 2015).

I.1.2. L'emballage alimentaire : fonctions et enjeux

Avant de communiquer, tracer, transporter, commercialiser, l'emballage a pour fonction primaire de protéger et de stabiliser l'aliment (Zhang et Mittal, 2010). Qu'il soit en plastique, papier-carton, verre, bois, métal ou composite, l'emballage est mis en œuvre le plus souvent, à la fin de la chaîne de production de l'aliment et fait partie intégrante des technologies de conservation de l'aliment (Gontard, 2015).

La première fonction de l'emballage alimentaire est en effet de protéger, transporter et stocker ces denrées périssables que sont nos aliments. Cette nécessité est apparue durant la deuxième partie du vingtième siècle où l'emballage a été célébré par une intensification et une diversification considérables de ses formes et de ses utilisations. Deux prix Nobels ont été co-attribués en 1963 dans le domaine de la chimie des plastiques pour la découverte de catalyseurs permettant la polymérisation des polyéthylène et polypropylène qui sont aujourd'hui couramment utilisés comme emballage alimentaire. En réduisant les pertes des denrées alimentaires au cours des étapes de distribution, stockage et commercialisation, ces matériaux contribuaient ainsi déjà à d'importants enjeux de sécurité alimentaire (Gontard *et al.*, 2017).

Les systèmes d'emballage et les techniques de conditionnement peuvent être considérés comme des outils technologiques mis en œuvre pour assurer la conservation des denrées alimentaires

(Multon, 1998). Pour ces applications, les emballages sont avant tout des systèmes de protection passive des denrées alimentaires (exemple : une barrière physique entre le produit et le milieu environnant). La fonction de protection des emballages prend en compte la protection mécanique (contre les chocs), la protection contre les transferts de matière (essentiellement les gaz et les liquides), la protection contre les transferts d'énergie (lumière et chaleur) et la protection contre les micro-organismes. Les emballages participent ainsi pleinement au maintien de la qualité hygiénique et microbiologique des aliments tout au long des chaînes de distribution (Cuq et Redl, 2000).

La conservation des aliments pourrait être définie en termes de réduction des réactions de dégradation, à savoir des réactions physico-chimiques et microbiennes pour les produits non vivants et aussi des réactions physiologiques pour les produits vivants. La qualité et la salubrité des aliments dépendent de la qualité initiale des matières premières et du taux de réactions de dégradation qui surviennent pendant le traitement des aliments, du stockage, de la distribution et des étapes de préparation à domicile (Steele, 2004). L'emballage définit matériellement autour de l'aliment une atmosphère favorable à la préservation des qualités gustatives, nutritionnelles et de la sécurité sanitaire des aliments. Il permet de maîtriser les transferts de vapeur d'eau, d'oxygène et/ou de gaz carbonique qui conditionnent les vitesses de nombreuses réactions d'oxydation des constituants de l'aliment (vitamines, acides gras essentiels, composés d'arôme etc.), le développement microbien ou encore les réactions physiologiques de maturation des produits vivants (Guillard et Gontard, 2017).

Centre d'importants enjeux économiques, environnementaux et de santé publique, l'emballage alimentaire impose aujourd'hui aux acteurs économiques de faire évoluer les matériaux et les technologies vers des solutions plus respectueuses à la fois de l'environnement et du consommateur (Gontard *et al.*, 2017).

Le principal enjeu de la recherche et développement se situe aujourd'hui sur l'amélioration de l'impact environnemental du système « aliment emballé » dans son ensemble, non seulement en minimisant l'impact négatif du matériau d'emballage sur l'environnement mais aussi en améliorant son rôle positif sur la réduction des pertes et gaspillages alimentaires qui impactent très fortement notre environnement (Angellier *et al.*, 2013).

En outre, la demande des consommateurs pour des aliments frais, légèrement transformés, faciles à préparer et prêts à consommer tout en conservant leur aspect attrayant pendant plusieurs jours, ainsi que les exigences de plus en plus strictes concernant la santé du

consommateur, posent des défis majeurs pour la qualité et la sécurité des aliments (Vermeiren *et al.*, 1999 ; Yam *et al.*, 2005). Par conséquent, un emballage simple avec une couche barrière passive est souvent insuffisant (Hauser and Wunderlich, 2011).

I.1. 3. L'emballage actif

I.1. 3.1. Principe

L'emballage actif est actuellement l'une des technologies les plus dynamiques pouvant être utilisées pour prolonger la durée de conservation des aliments emballés (Bentayeb *et al.*, 2007). Plusieurs définitions sont rapportées dans la littérature scientifique :

« Un emballage actif offre plus qu'une simple protection. Il interagit avec le produit et dans certains cas répond à des changements du milieu environnant ou du produit lui-même » (Wagner, 1989).

« Ces nouveaux emballages dits "actifs" ou "fonctionnels" remplissent un autre rôle que celui de barrière inerte, car ils peuvent à titre d'exemple éliminer des agents indésirables de l'atmosphère environnant le produit ou relarguer progressivement des composés prolongeant la durée de conservation du produit » (Gontard, 2000).

« L'expression "emballage fonctionnel" désigne les solutions d'emballage qui interagissent de façon constante et active avec l'atmosphère interne d'un emballage, en libérant des substances utiles ou en absorbant des substances indésirables pour améliorer la qualité de l'aliment emballé. Les systèmes d'emballage actif sont développés dans le but d'allonger la durée de conservation de l'aliment » (Yam *et al.*, 2005).

« L'emballage actif interagit positivement avec l'aliment emballé et son environnement, pour améliorer/préserver sa qualité plus longtemps que l'emballage conventionnel » (Kerry *et al.*, 2006).

« L'emballage actif fait référence à l'incorporation de certains additifs dans des films d'emballage ou dans des récipients d'emballage dans le but de maintenir et prolonger la durée de conservation du produit » (Day, 2008).

I.1. 3.2. Histoire et développement

Le concept d'emballage actif s'inscrit dans des traditions ancestrales de certaines régions du globe. Dans toutes les régions tropicales, les feuilles végétales sont abondamment utilisées pour

l'emballage des produits alimentaires. Au-delà d'un simple effet barrière, des composés aromatiques, des colorants, des enzymes (comme la papaine) ou encore des agents ralentissant la croissance microbiennes (comme certaines huiles essentielles) migrent au cours de la conservation, de la feuille végétale vers le produit emballé. L'emballage interagit avec l'aliment en modifiant favorablement sa couleur, sa texture et en limitant le développement de certains micro-organismes indésirables.

Les absorbeurs d'oxygène sont les premiers systèmes d'emballages actifs à avoir vu le jour au tout début des années 1970 au Japon. Ils sont apparus aux États-Unis au début des années 80 avec notamment une utilisation importante par le marché militaire. Un peu plus tard, la société « Mark & Spencer » a grandement contribué au lancement de l'utilisation des absorbeurs d'oxygène en Europe, en proposant dans ses rayons à Londres, un produit innovant : du poisson frais fumé sous emballage contenant un absorbeur d'oxygène. L'intérêt pour les emballages actifs s'est considérablement accru ces dernières années et a donné naissance à de nombreux brevets sur le sujet (Gontard, 2000).

I.1. 4. Les différentes technologies de l'emballage actif

La mise en œuvre d'un emballage actif est différente selon que le produit emballé est vivant ou inerte. Dans le cas d'aliments dits « inertes » (ou « morts »), les conditions optimales de conservation pourront être établies dès la fermeture de l'emballage et ne seront perturbées que par les transferts s'opérant au travers de l'emballage s'il n'est pas assez « barrière ».

Les produits dits « vivants » (ou « respirants »), par définition, ont des activités métaboliques qui engendrent en continu la production et la consommation de composés gazeux. C'est le cas des fruits et légumes frais ou faiblement transformés, des crustacés et autres produits de la mer vivants, ou bien encore des produits contenant une flore microbienne en activité (certains fromages, saucissons, pâtes fraîches de type boulangères, légumes fermentés, etc.) nécessaire à l'affinage ou à la maturation du produit en cours de stockage. Le maintien de conditions optimales de conservation sera donc plus complexe et nécessitera une action permanente de l'emballage au cours du stockage pour satisfaire les besoins respiratoires de ces produits. La mise en œuvre de systèmes actifs peut dans ces cas, être d'un grand secours aux problèmes de conservation de ces produits qui ne s'accommodent pas d'un simple mélange gazeux et d'un film barrière (Gontard, 2000).

Les emballages actifs agissent de façon contrôlée sur l'aliment. Leur objectif principal est de préserver la qualité du produit en créant ou en maintenant des conditions optimales pour sa

conservation. Tous les mécanismes de détérioration des aliments sont visés par l'action de ces emballages : oxydation des matières grasses, brunissement, dégradation des vitamines, des pigments, des composés aromatiques, développement des micro-organismes, activité respiratoire des végétaux frais, etc. (Gontard, 2000). Les technologies d'emballage actif sont multiples et variées (Figure 1), elles peuvent être divisées en trois catégories : les émetteurs (les systèmes de libération ou bien, les relargueurs), les absorbeurs et autres systèmes (Ahvenainen, 2003).

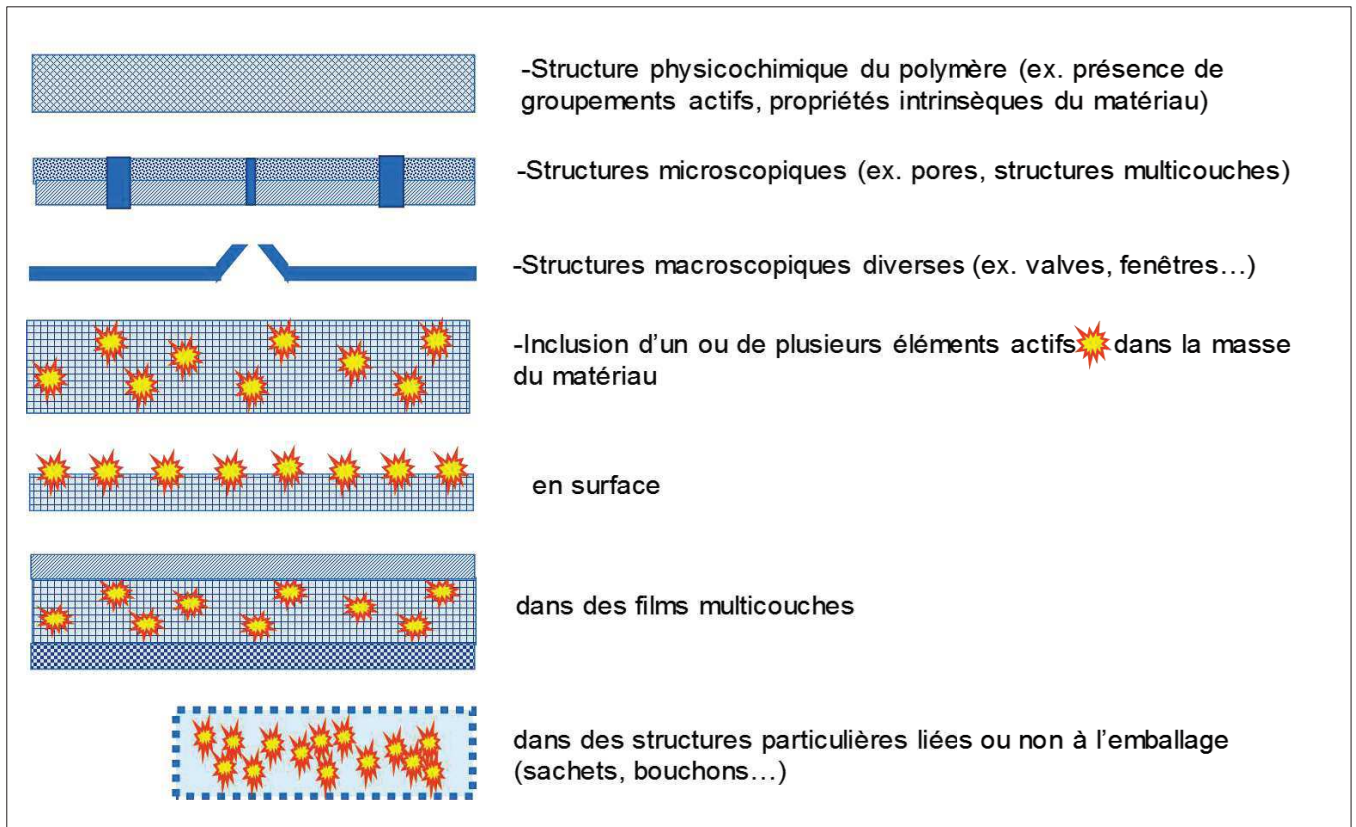


Figure 1 : Les différents effets physiques et chimiques qui permettent à un matériau de devenir actif (Gontard, 2000).

I.1. 4.1. Les émetteurs

L'industrie alimentaire concentre ses efforts pour offrir aux consommateurs des produits plus sûrs, plus nutritifs et de meilleure qualité. La contamination microbienne des produits alimentaires provoque des conséquences graves sur la santé du consommateur et des pertes économiques considérables (Ture *et al.*, 2012). Ainsi, l'addition d'agents bactéricides ou inhibiteurs de croissance dans la formulation des aliments par des méthodes de pulvérisation ou d'immersion a été utilisée pour surmonter ce problème. Cependant, l'application directe des agents antimicrobiens a certaines limites, car ils peuvent être neutralisés, évaporés ou diffusés

rapidement et de façon inadéquate dans la masse de la matrice alimentaire, réduisant ainsi leur concentration sur la surface (Quattara *et al.*, 2000). Dans ce contexte, une tendance actuelle consiste à incorporer des additifs antimicrobiens dans les emballages alimentaires en vue d'améliorer leur fonctionnalité (Cagri *et al.*, 2001). Les agents actifs ajoutés à la matrice du film (Figure 1) sont lentement libérés vers la surface des aliments pendant le temps d'exposition, où ils restent à une concentration élevée pendant une longue période (Chollet *et al.*, 2008). Lorsque l'activité antimicrobienne est conférée au matériau d'emballage, la croissance microbienne est limitée ou empêchée en réduisant le taux de croissance ou en diminuant le nombre de micro-organismes vivants, augmentant ainsi la sécurité du consommateur (Galotto *et al.*, 2012 ; Mastromateo *et al.*, 2012).

Différentes substances antimicrobiennes ont été testées en laboratoire pour leurs applications potentielles dans les emballages alimentaires antimicrobiens. Ces substances comprennent les acides organiques (acide benzoïque, sorbates), les enzymes (lysozyme, glucose oxydase), les bactériocines (nisine, pédiocine), les fongicides (bénomyl, imazalil), les polymères (principalement le chitosane), les extraits naturels de plantes (notamment les huiles essentielles) et les antibiotiques. Chaque substance antimicrobienne présente un mécanisme d'action unique, spécifique à une gamme particulière d'aliments et de micro-organismes (Lopez *et al.*, 2015). Le relargage contrôlé d'agent antimicrobiens tels que l'éthanol, le gaz carbonique ou le dioxyde de soufre est lui aussi aujourd'hui largement utilisé par les industriels de l'agroalimentaire (Gontard, 2000).

Un autre problème sérieux auquel l'industrie alimentaire doit faire face, consiste à protéger les aliments contre les réactions d'oxydation, qui entraînent une perte de leur qualité nutritionnelle et des modifications de leur composition chimique. En raison de la présence d'insaturations dans leur structure, les composants alimentaires les plus sensibles à l'oxydation sont les graisses et les huiles (Benzie, 1996). L'oxydation des lipides dans le système alimentaire entraîne non seulement la réduction de la durée de conservation, mais affecte également le goût, la perte de valeur nutritive, la sécurité des aliments et le développement de nombreuses maladies chroniques (Eriksson, 1987).

Moore et ses collaborateurs (2000), rapportent que l'incorporation de substances antioxydantes (comme le BHT, le BHA, l'alpha-tocophérol et l'extrait de romarin) dans l'emballage peut être plus efficace que l'utilisation directe d'additifs sur la surface de la viande. Des systèmes d'emballage actif ont été développés en utilisant des extraits naturels comme le romarin, l'origan et le thé vert avec des propriétés antimicrobiennes et antioxydantes pour augmenter la stabilité

de différents produits de viande et ainsi prolonger leur durée de conservation (Calatayud *et al.*, 2013 ; Camo *et al.*, 2011 ; Nerín *et al.*, 2006 ; Siripatrawan et Noipha, 2012).

Lorsque les agents conservateurs sont incorporés dans la formulation du matériau d'emballage, dans le but d'être libérés ultérieurement dans l'atmosphère interne qui entoure l'aliment, ils doivent répondre aux règles de sécurité strictes de la *Food and Drug Administration* (FDA). Ils sont contrôlés en tant qu'ingrédients alimentaires et doivent être de qualité GRAS (Galotto *et al.*, 2015).

I.1. 4.2. Les absorbeurs

Les systèmes absorbeurs éliminent les composants indésirables tels que l'oxygène, le dioxyde de carbone, l'éthylène et l'humidité (Cirillo *et al.*, 2015).

La présence d'oxygène dans l'espace de tête, que celui-ci soit déjà présent au moment de la fermeture de l'emballage ou qu'il provienne de la diffusion au travers du matériau, constitue un facteur déterminant de la vitesse d'oxydation des liaisons éthyléniques, notamment des acides gras insaturés, présents dans l'aliment. Ces détériorations se traduisent non seulement par une diminution de la valeur nutritive de l'aliment mais aussi par l'apparition de caractéristiques organoleptiques inacceptables (Gontard, 2000).

Les absorbeurs d'oxygène sont capables de fixer, grâce à des réactions chimiques ou biochimiques, de façon irréversible l'oxygène présent dans l'espace de tête d'un emballage clos, favorisant ainsi la désorption de l'oxygène dissout dans l'aliment. La vitesse d'adsorption de l'oxygène doit être suffisamment élevée pour inhiber le plus rapidement possible les réactions de détérioration. La sélection d'un absorbeur sera donc basée sur la capacité (volume d'oxygène à absorber), la vitesse d'absorption souhaitée, la durée de conservation, mais aussi la température de stockage (certains absorbeurs fonctionnent aux températures de réfrigération et même de congélation), de l'activité de l'eau du produit (certains ne fonctionnent qu'en présence d'humidité, d'autres dans des atmosphères sèches) et les propriétés de perméabilités de l'emballage utilisé. L'utilisation d'absorbeurs d'oxygène, permet de préserver la couleur des viandes ou encore de réduire considérablement la vitesse d'oxydation des matières grasses des charcuteries, plats cuisinés, pâtisseries, etc. (Andersen et Rasmussen, 1992). Il existe sur le marché des absorbeurs d'oxygène présentant simultanément d'autres fonctions telles que l'absorption (pour le café torréfié) ou le relargage (pour les produits fragiles) de gaz carbonique ou encore de vapeur d'éthanol. Des sachets absorbeurs de CO₂ sont aussi disponibles sur le marché.

L'utilisation d'absorbants d'oxygène présente les avantages de pouvoir réduire et de maintenir au cours du stockage, la présence d'oxygène à des teneurs extrêmes faibles, inférieures à 0.01%, valeurs impossibles à atteindre par balayage de gaz dans l'espace de tête. Ils représentent aussi une alternative à l'emballage sous vide de produits trop fragiles (de type pâtisserie) pour supporter l'écrasement occasionné par le vide.

De nombreux absorbants d'humidité ou d'eau liquide sont aussi proposés sur le marché sous forme de sachets, de films, de feuilles ou de barquettes. Les barquettes sont constituées d'une première couche en polystyrène expansé présentant des perforations en forme d'entonnoir pour permettre l'écoulement des exsudats (de viandes prédécoupées par exemple), d'un buvard intégré absorbant, puis d'une deuxième coque rigide qui possède des cannelures pour guider l'exsudat. L'absorption d'eau peut être couplée au relargage de gaz carbonique. Au fond de la barquette, l'eau est drainée vers un sachet contenant du bicarbonate de sodium et de l'acide ascorbique pour piéger l'oxygène et dégager du gaz carbonique.

Des sachets absorbants d'odeurs sont proposés pour éliminer certains composés aromatiques indésirables (Gontard, 2000).

I.1. 4.3. Autres systèmes

D'autres systèmes d'emballages actifs peuvent avoir des mécanismes divers permettant de prolonger la durée de vie de l'aliment emballé.

Les films offrant une perméabilité sélective vis-à-vis des gaz de l'atmosphère, sont actuellement très recherchés pour le conditionnement sous atmosphère modifiée de végétaux frais ou faiblement transformés. Le conditionnement sous atmosphère modifiée est un procédé qui consiste soit à injecter un mélange gazeux dans un emballage étanche, soit à prévoir la création d'une atmosphère particulière à l'intérieur de l'emballage, résultant des simples transferts de gaz au travers de l'emballage et des consommations et/ou productions de gaz par le produit emballé (Gontard, 2000).

En jouant sur leur activité respiratoire et sur les perméabilités aux gaz de l'emballage, on peut obtenir au bout d'un certain temps nécessaire à la mise en équilibre, des proportions « teneur en oxygène/teneur en gaz carbonique » optimales pour leur conservation. En sélectionnant en quelque sorte les gaz qui vont traverser l'emballage, une nouvelle génération de films offrant une sélectivité bien supérieure à celles des emballages conventionnels, permettant de générer à l'intérieur de l'emballage, des atmosphères gazeuses tout à fait originales et adaptées à la

conservation de nombreux végétaux. Ces emballages sélectifs répondent à des besoins importants dans le domaine de la conservation des fruits et des légumes.

D'autres systèmes d'emballage actifs s'adaptent aux conditions extérieures : par exemple leurs perméabilités à l'oxygène et au gaz carbonique, augmente avec la température pour répondre à une augmentation naturelle de la respiration d'un produit végétal.

Dans d'autres cas l'activité est basée sur un contact direct entre l'emballage et le produit alimentaire. Par exemple, une des couches proches de l'aliment, des matériaux antimicrobiens, contient un agent actif à la surface qui n'agit que par contact direct avec l'aliment. Certains matériaux d'emballage peuvent posséder des propriétés fonctionnelles particulières. Ces propriétés, pourront être le résultat de la présence ou d'un greffage de groupements actifs sur la chaîne polymérique soit dans la masse ou en surface du matériaux (Figure 1). Ces groupements chimiques confèrent au matériau des propriétés, par exemple antibactérienne, durables (Gontard, 2000).

I.1. 5. Applications de l'emballage actif

La grande diversité des dispositifs d'emballage actif a des applications spécifiques aux produits alimentaires individuels, grâce auxquels la durée de conservation peut être considérablement prolongée, à condition que les mécanismes de détérioration de l'aliment soient compris et contrôlés (Restuccia *et al.*, 2015). À cet égard, des données récentes sont disponibles sur l'application de l'emballage actif dans l'industrie alimentaire (tableau 1) ou sur les technologies d'emballage actif (tableaux 2 et 3).

Tableau 1 : Principales applications des technologies d'emballage actif
(Restuccia *et al.*, 2010)

Type de technologie	Aliments
Absorbeurs d'oxygène	Café moulu, thé, noix grillées, chocolat, lait écrémé, boissons en poudre, pain, pizza, pâte à pizza, pâtes fraîches réfrigérée, gâteaux, biscuits, bière, charcuterie, viandes, poisson, fromage
Absorbeurs de dioxyde de carbone	Café moulu
Émetteurs de dioxyde de carbone	Viande, poisson
Absorbeurs d'humidité	Produits secs et déshydratés, viande, volaille, poisson
Absorbeurs d'éthylène	Kiwi, banane, avocat, kaki
Émetteurs d'éthanol	Pain, gâteaux, poisson
Films libérant des antimicrobiens	Abricots secs
Films libérant des antioxydants	Céréales
Films perméables au gaz / respirants	Salades prêtes à consommer, fruits et légumes frais.

Tableau 2 : Exemples de certains systèmes d'emballage actif actuellement connus
(Ozdemir et Floros, 2004)

Type de technologie	Substances utilisées et mode d'action
Absorbeurs d'oxygène	-Systèmes enzymatiques : glucose oxydase-glucose. -Systèmes chimiques: oxyde de fer en poudre, catéchine, carbonate ferreux, fer-soufre, sulfate de cuivre, oxydation de colorant photosensible, oxydation de l'acide ascorbique.
Absorbeurs/Émetteurs de dioxyde de carbone	Poudre de fer-hydroxyde de calcium, carbonate de métal ferreux
Absorbeurs d'humidité	Gel de silice, propylène glycol, alcool polyvinylique, diatomite
Absorbeurs d'éthylène	Charbon actif, gel de silice-permanganate de potassium, bentonite, poudre de dioxyde de silicium, zéolite, ozone
Émetteurs d'éthanol	Éthanol encapsulé
Films libérant des antimicrobiens	Sorbates, benzoates, propionates, éthanol, ozone, peroxyde, dioxyde de soufre, antibiotiques, zéolite d'argent, sels d'ammonium quaternaire
Films libérant des antioxydants	BHA, BHT, acide ascorbique, tocophérol
Films perméables au gaz / respirants	Films traités en surface, perforés ou microporeux

Tableau 3 : Quelques systèmes d'emballage actif commercialisés, type de présentation et fonction (Day, 2003)

Fabricant	Pays	Nom commercial	À base de	Forme d'emballage
Mitsubishi Gas Chemical Co. Ltd	Japon	Ageless	Fer	Sachets et étiquettes
Toppan Printing Co. Ltd	Japon	Freshilizer	Fer	Sachets
Toagosei Chem. Industry Co. Ltd	Japon	Vitalon	Fer	Sachets
Nippon Soda Co. Ltd	Japon	Seagul	Fer	Sachets
Toyo Seikan Kaisha Ltd	Japon	Oxyguard	Fer	Barquettes en plastique
Multisorb Technologies Inc.	Etats-Unis	FreshMax FreshPax Fresh Pack	Fer Fer Fer	Etiquettes Etiquettes Etiquettes
Chevron Chemicals	Etats-Unis	N/A	Acrylate de benzyle	Film plastique
W. R. Grace Co. Ltd	Etats-Unis	PureSeal	Ascorbate / sels métalliques	Bouchons de bouteilles
Food Science Australia/Visy Industries	Australie	ZERO2	Colorant photosensible / composé organique	Film plastique
CMB Technologies	France	Oxbar	Catalyseur au cobalt	Bouteilles en plastique
Standa Industries	France	ATCO Oxycap	Fer Fer	Sachets Bouchons de bouteilles
EMCO Packaging Systems	Royaume-Uni	ATCO	Fer	Etiquettes
Johnson Matthey Plc	Royaume-Uni	N/A	Platine	Etiquettes
Bioka Ltd	Finlande	Bioka	Enzyme	Sachets

1.2. Les biocomposites

I.2. LES BIOCOMPOSITES

I.2.1. Introduction

La production de plastiques en 2017 a atteint 340 millions de tonnes. Actuellement plus de 90 % des plastiques tous secteurs confondus sont issus de ressources fossiles, 6 % de la production pétrolière mondiale est dédiée à cette production. Si la progression du plastique continue sur sa lancée, en 2050, le secteur représentera 20 % de la consommation mondiale de ressources fossiles. Le plus souvent après une durée d'usage très courte, inhérente à leur utilisation en tant qu'emballage alimentaire, 40% de ces plastiques sont aujourd'hui enfouis, soit 9 millions de tonnes de déchets de plastiques par an, qui s'accumulent dans les sols. 32 % des déchets plastiques fuient nos systèmes de collecte et de traitement et finissent dans les sols et les océans (connu sous le nom de 6^{ème} continent). Ces déchets se dégradent en micro- puis en nanoparticules qui peuvent pénétrer aisément dans les organismes vivants de la chaîne alimentaire dont l'homme, maillon final, avec des effets délétères à long terme qui sont encore mal connus (Ellen MacArthur Foundation, 2016 ; Geyer *et al.*, 2017).

Les préoccupations environnementales planétaires, telles que le réchauffement climatique, l'épuisement ainsi que la hausse des prix des ressources fossiles, la sensibilisation croissante à la gestion des déchets, ont intensifié la pression sur les industries dépendantes du pétrole (Thakur, 2014). Ces préoccupations ont conduit à d'intenses investigations dans l'utilisation des biopolymères dans le développement de composites écologiques (Bledzki *et al.*, 2010).

I.2.2. Les matériaux composites

Le terme "composite" vient du mot latin *compositus*, issu de la racine du mot *componere*, ce qui signifie « rassembler » (Singha et Thakur, 2012). Plusieurs chercheurs ont défini les matériaux composites de différentes manières.

En général, les composites sont définis comme des matériaux d'ingénierie fabriqués à partir de deux ou plusieurs constituants non miscibles, présentant des différences significatives de propriétés physiques ou chimiques (Thakur *et al.*, 2011). Un composite est constitué d'au moins deux matériaux, dont l'un agit essentiellement comme agent de liaison (la matrice), tandis que l'autre agit comme un renfort (Thakur, 2014).

Les matériaux composites résultent habituellement de l'association d'au moins deux matériaux non miscibles dont les propriétés se combinent. Le *renfort*, qui constitue l'armature du composite, assure la tenue mécanique (résistance à la traction et rigidité), améliore la tenue

à la chaleur et peut parfois réduire le coût du matériau final. La *matrice* joue le rôle de liant, répartit les efforts (résistance à la flexion ou à la compression) et assure la cohésion du matériau. Les propriétés mécaniques des composites matrice/renfort ne dépendent pas seulement des propriétés intrinsèques de chaque constituant élémentaire, mais également de la géométrie du renfort et de la nature des liaisons entre la charge et la matrice qui contrôlent le mécanisme de transfert de contrainte à l'interface. Ainsi, un problème inhérent à ces matériaux hétérogènes est la réalisation d'une bonne *interface* matrice/renfort (Angellier, 2005). La figure 2 montre le schéma général d'un composite.

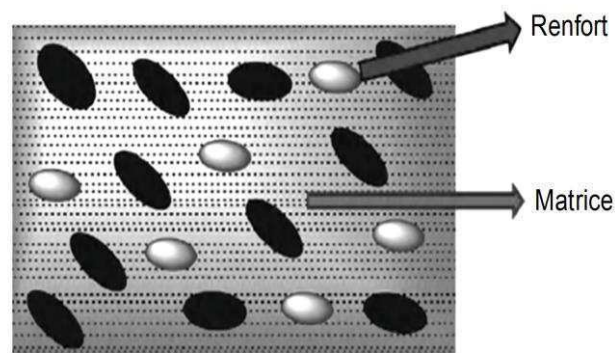


Figure 2 : Schéma général d'un composite (Thakur, 2014)

Le gros avantage des composites par rapport aux matériaux conventionnels est de pouvoir combiner deux constituants pour optimiser les propriétés finales du matériau. Ils sont donc utilisés dans de nombreuses technologies telles que les élastomères chargés, les conducteurs thermiques, les isolants électriques ou en tant que matériaux haute performance pour l'automobile et l'aéronautique.

I.2.3. Les biocomposites

I.2.3.1. Définitions

Les biocomposites sont une classe spécifique de composites, dont au moins l'un des constituants (la matrice ou le renforcement) est obtenu à partir de ressources naturelles (Netravali et Chabba, 2003). Les termes composites verts, biocomposites et éocomposites se réfèrent tous à la même classe de matériaux (Oksman et Sain, 2008).

Les composites renforcés de fibres naturelles ont été utilisés par l'Homme depuis le début de la civilisation humaine, comme matériau pour fabriquer des abris, des vêtements et des outils. Dans l'Égypte ancienne, il y a 3000 ans, les gens utilisaient la paille comme élément de

renforcement pour les matériaux de mur à base de boue, dans la construction de leurs maisons (Thakur *et al.*, 2011). Les nombreux avantages des fibres végétales (faible coût, faible densité comparativement aux fibres de verre, renouvelable et biodégradable, non abrasif) les placent parmi les renforts de haute performance présentant des avantages économiques et environnementaux (Voichita, 2011).

Une large gamme de polymères est disponible pour la fabrication de biocomposites, y compris le polyéthylène, le polypropylène, le polystyrène, les polyesters, les résines époxy, l'amidon thermoplastique, l'acide polylactique, et les polyhydroxylalkanoates (Garlotta, 2001 ; Ouajai et Shanks, 2009).

Les biocomposites peuvent être divisés en deux groupes principaux selon l'origine des constituants :

- Composites partiellement renouvelables, dans lesquels soit la matrice ou la charge de renfort est obtenue à partir de ressources renouvelables ;
- Composites totalement renouvelables (connus sous le nom de « *full* » biocomposites), dans lesquels la matrice et la charge proviennent de ressources renouvelables. Nous nous concentrerons sur cette classe de biocomposites dans la suite de ce chapitre. A noter que de récents travaux de recherche s'intéressent aux matériaux biocomposites entièrement issus de ressources renouvelables et totalement biodégradables en conditions naturelles (Berthet *et al.*, 2015a ; Berthet *et al.*, 2015b ; Hassaini *et al.*, 2017).

Les biocomposites peuvent être des matériaux économiquement viables et respectueux de l'environnement pour de multiples applications (Thakur, 2014).

Dans l'industrie du bâtiment et de la construction, les applications incluent des panneaux de séparation, cadres de fenêtres et de portes, tuiles et bâtiments. On les trouve également dans les applications aérospatiales, militaires et marines ; dans l'industrie de transport, de l'automobile et des autocars de chemin de fer ; dans les dispositifs de stockage, tels que les boîtes aux lettres, des silos de stockage de céréales ou des conteneurs de biogaz ; et dans les meubles, les douches, les unités de bain, les composants de portes, les fenêtres, les surfaces de pont et de nombreux autres produits (Gomes, 2004, Shibata *et al.*, 2013).

Pour qu'un matériau soit utilisé efficacement dans les applications d'emballage, les matières premières de base devraient être renouvelables et les produits finaux devraient être

compostables pour réduire l'utilisation de carburants fossiles et limiter les coûts et l'impact environnemental du traitement des déchets (Rowell, 2012). Les procédés de production à l'échelle industrielle utilisés pour préparer différents types de matériaux d'emballage utilisant des biopolymères devraient être efficaces, économiquement compétitifs, et respectueux de l'environnement (Dufresne *et al.*, 1999).

Ces composites offrent de nombreux avantages, leurs caractéristiques doivent être soigneusement évaluées lors du choix d'un matériau pour une application donnée.

I.2.3.2. Choix de la matrice polymère

I.2.3.2.1. Classification des biopolymères

Les biopolymères ne constituent pas une seule classe de matériaux mais toute une famille de produits ayant un impact environnemental plus faible que les matières plastiques conventionnelles (Guilbert *et al.*, 2011). Le terme « bio » est attribué lorsqu'une des trois caractéristiques suivantes est remplie : **l'origine** biosourcée (par opposition à l'origine fossile), **la production** du polymère par biosynthèse (par opposition aux voies de polymérisation conventionnelles à partir de monomères pétro-sourcés ou issus de la biomasse) ou leur **fin de vie** compostable ou biodégradable (par opposition à l'incinération ou l'enfouissement) (Figure 3).

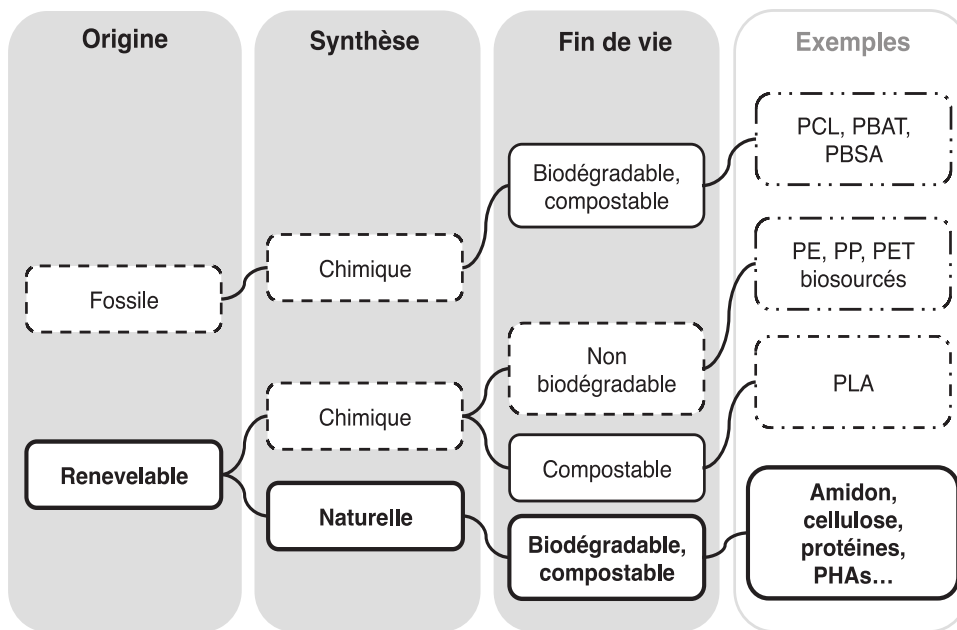


Figure 3 : Classification des bioplastiques selon leur origine, leur voie de synthèse et leur fin de vie (Guilbert *et al.*, 2011).

Une première catégorie regroupe donc les biopolymères **biodégradables/compostables** obtenus par **polymérisation conventionnelle** de monomères issus du craquage du **pétrole**. On trouve notamment les copolyesters biodégradables tels que le poly (butylène co-apidate téréphtalate) (PBAT) ou le poly (butylène succinate co-adipate) (PBSA) qui sont synthétisés par réaction de polycondensation de glycols et d'acides carboxyliques aliphatiques ou aromatiques.

Une deuxième catégorie regroupe les biopolymères biosourcés mais **non biodégradables/compostables** produits par **synthèse chimique** à partir de monomères issus d'**agro-ressources**. Cette catégorie connaît un plein essor pour palier à l'épuisement des ressources fossiles. On trouve ainsi le bio-PE, le bio-PP et le bio-PET.

Une troisième catégorie regroupe les biopolymères biosourcés et **biodégradables/compostables**, mais synthétisés par **polymérisation conventionnelle** de monomères issus de la déconstruction de **la biomasse**. Le principal avantage de cette catégorie de polymères est la possibilité de produire des polymères avec des propriétés contrôlées, mais le bénéfice environnemental reste très controversé. Parmi ces biopolymères, on trouve le poly (acide lactique) (PLA) produit par polycondensation de l'acide lactique. L'acide lactique est lui-même obtenu par homo-fermentation à partir de sources carbonées renouvelables comme le glucose ou le maltose, par des bactéries de type *Lactobacillus sp.* Le principal verrou du PLA est le fait qu'il ne s'agit pas d'un polymère biodégradable en milieu naturel, mais d'un polymère qui est seulement compostable en conditions industrielles (du fait de la Tg supérieure à la température ambiante).

Enfin, une quatrième catégorie regroupe les biopolymères répondant à l'ensemble des critères « bio », produits par **biosynthèse** dans **les cellules végétales** ou par **fermentation bactérienne** (poly(hydroxyalcanoates)). Ces biopolymères sont extraits, éventuellement purifiés et modifiés. Les propriétés fonctionnelles de ces biopolymères (par exemple les propriétés barrière) se distinguent souvent de celles des polymères conventionnels, permettant ainsi d'envisager de nouvelles applications telles que les emballages actifs et intelligents (Guilbert *et al.*, 2011).

I.2. 3.2.2. Les polyhydroxylalkanoates (PHAs)

Les PHAs sont des polyesters synthétisés par de nombreuses bactéries à Gram positif et à Gram négatifs, provenant d'au moins 75 genres différents. Les bactéries accumulent ces polymères sous forme de granules intracellulaires (Figure 4) à des taux aussi élevés que 90% de leur poids sec, dans des conditions de stress nutritionnel et agissent comme une réserve de carbone et d'énergie (Madison et Huisman, 1999).

Plus de 100 monomères de PHA

différents ont été identifiés (Reddy *et al.*, 2003). Le poly (3-hydroxy butyrate) (PHB) et le poly (3-hydroxybutyrate-co-3-hydroxyvalérate) (PHBV) sont les principaux représentants des PHAs. Le PHBV est le plus étudié (Figure 5), c'est un copolymère constitué d'unités d'hydroxybutyrate (HB) et d'hydroxyvalérate (HV) disposées au hasard (Misra *et al.*, 2011).

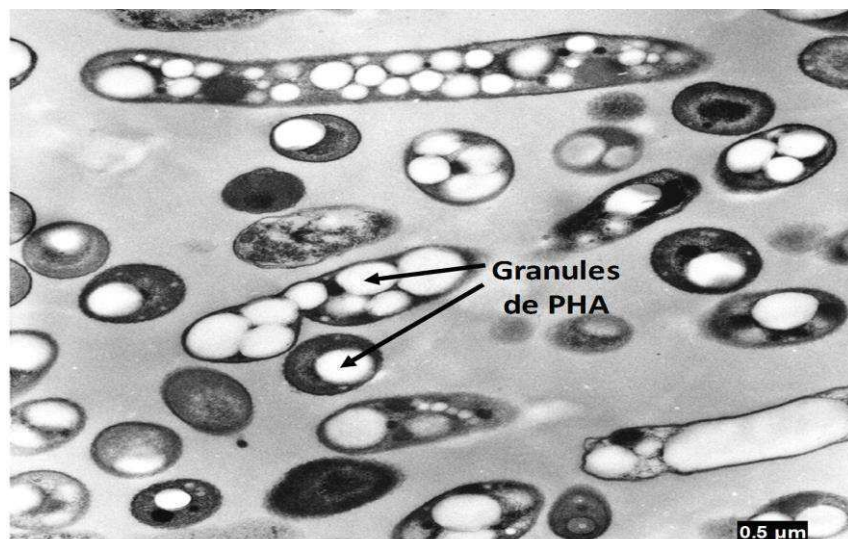


Figure 4 : Image de cellules bactériennes contenant des granules de PHA, prise par microscopie électronique à transmission (Tian *et al.*, 2005)

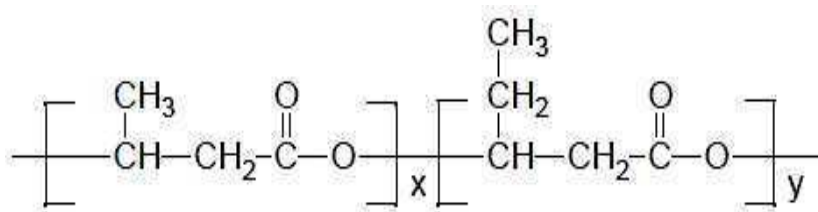


Figure 5 : Structure chimique générale du PHBV (Misra *et al.*, 2011).

➤ **Propriétés et applications pratiques des PHAs**

Les PHAs sont des polymères thermoplastiques non toxiques, qui peuvent être produits à partir de ressources renouvelables. Ils ont un haut degré de polymérisation, sont hautement cristallins et insolubles dans l'eau. Ces caractéristiques les rendent très compétitifs avec le polypropylène dérivé de la pétrochimie (Reddy *et al.*, 2003).

La propriété qui distingue les PHAs des plastiques à base de pétrole est leur biodégradabilité. Ces polymères se dégradent lorsqu'ils sont exposés au sol, au compost ou aux sédiments marins. La biodégradation dépend d'un certain nombre de facteurs tels que l'activité microbienne de l'environnement, la surface exposée, l'humidité, la température, le pH et la masse moléculaire (Boopathy, 2000). La composition du PHA et son degré de cristallinité jouent également un rôle important (Lee, 1996). Les micro-organismes sécrètent des enzymes qui décomposent le polymère en ses unités moléculaires appelées hydroxyacides, qui sont utilisées comme source de carbone pour la croissance.

La biodégradation des PHAs dans des conditions aérobies entraîne la formation de dioxyde de carbone et d'eau ; alors que dans les conditions anaérobies, les produits de dégradation sont le dioxyde de carbone et le méthane. Les PHAs sont compostables sur une large gamme de températures, même à un maximum d'environ 60°C avec des taux d'humidité de 55%. En outre, il a été rapporté que les PHAs se dégradent dans les milieux aquatiques (lac de Lugano, Suisse) en 254 jours même à des températures ne dépassant pas 6°C (Johnstone, 1990).

Les applications potentielles des PHAs sont nombreuses et couvrent différents domaines : emballage, médecine, agriculture, nanocomposites, mélanges de polymères (Philip *et al.*, 2007).

Les PHA ont été utilisés depuis longtemps pour fabriquer des produits de la vie courante, notamment des matériaux d'emballages. Ainsi, dès 1990, une bouteille de shampoing a été fabriquée en Allemagne avec un copolymère de PHB et de PHV. Divers articles jetables comme des rasoirs, des sacs d'approvisionnement ont également été réalisés avec des PHAs (Chen, 2009).

La médecine constitue un autre champ d'application important des PHAs. Ainsi, le PHB et le PHBV par exemple, sont fréquemment employés, dans la fabrication de plaques osseuses, de sutures chirurgicales, de prothèses vasculaires ou d'autres matériaux d'ostéosynthèse. Certains PHAs peuvent aussi être utilisés pour la libération contrôlée de médicaments

(Akaraonye *et al.*, 2010). On peut également citer le domaine de l'agriculture, avec la production de films de paillage biodégradables (Philip *et al.*, 2007).

De nombreuses études ont été menées sur la production des PHAs et leurs applications. La plupart d'entre elles sont basées sur la recherche de sources de carbone bon marché, pour réduire le coût de production des PHAs et sur l'augmentation de la productivité par l'ingénierie génétique (Chanprateep, 2010).

Les biocomposites à base de PHAs ont été récemment développés dans le but de réduire le prix du polymère. Cependant, beaucoup plus d'efforts sont nécessaires dans ce domaine pour augmenter la production de bioplastiques et remplacer avec succès les plastiques non dégradables.

I.2.3.3. Choix de la charge

Dans les biocomposites, la charge sert de renfort et fournit la force et la rigidité à la structure composite résultante (Rowell, 2012). L'utilisation des agro-ressources en emballage alimentaire est actuellement un enjeu très important, car il est nécessaire de substituer les emballages actuels, pétro-sourcés, par des matériaux à la fois biosourcés (sans compétition avec les ressources alimentaires) et biodégradables en conditions naturelles. La biomasse naturelle lignocellulosique est considérée comme l'un des composants les plus importants des composites verts.

I.2.3.3.1. La biomasse lignocellulosique

La biomasse lignocellulosique est une matière organique inépuisable, renouvelable et omniprésente sur Terre. Elle se trouve en grande quantité en tant que résidus agricoles, forestiers et déchets générés par différentes industries, y compris les déchets municipaux solides. La biomasse lignocellulosique, source de carbone non fossile sur terre, est une alternative prometteuse au pétrole brut qui peut être utilisé pour la production de biocarburants, biomolécules, produits chimiques et matériaux. Elle est principalement constituée de cellulose, d'hémicellulose et de lignine (Figure 6) (Isikgor et Becer, 2015 ; Singh *et al.*, 2016).

La cellulose : principal constituant de la biomasse lignocellulosique. C'est un homopolymère fibreux, insoluble et de haut poids moléculaire composé d'unités de glucose anhydre liées par

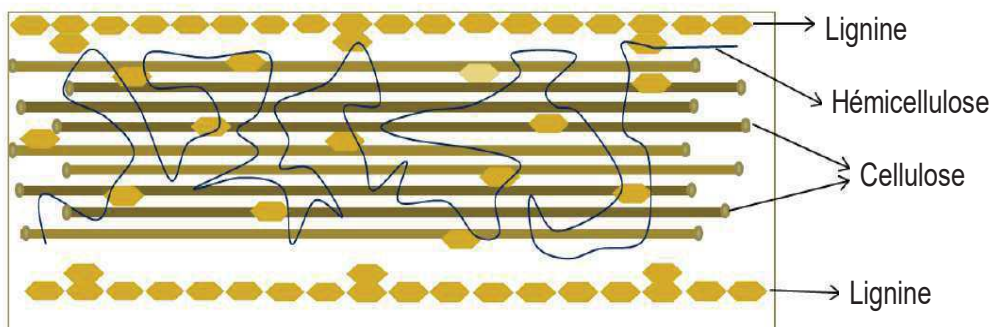


Figure 6 : Représentation de la structure lignocellulosique montrant la cellulose, l'hémicellulose et la lignine (Singh *et al.*, 2016)

les liaisons glycosidiques (β -1,4) et constitue le principal composant structurel des plantes. Les polymères celluloses à longue chaîne sont liés entre eux par de nombreuses liaisons croisées, telles que les interactions d'hydrogène et de Van Der Waal pour empaqueter la cellulose en microfibrilles (Isikgor et Becer, 2015).

L'arrangement hautement ordonné des chaînes de cellulose entraîne le développement de la région cristalline alors que dans la région amorphe, il s'agit d'une disposition des chaînes moins ordonnée (Gardner et Blackwell, 1974 ; Li *et al.*, 2009). Le degré de polymérisation de la chaîne cellulosique est très variable allant de 250 à 10000 et influence les propriétés physiologiques, mécaniques et biologiques de la cellulose. La longueur de la chaîne cellulosique ou le degré de polymérisation dépend de la source du matériau et des méthodes de traitement (Sukumaran *et al.*, 2005, Santos *et al.*, 2016).

L'hémicellulose : c'est le deuxième composant le plus abondant de la biomasse lignocellulosique. C'est un polymère hétérogène de pentoses (principalement le xylose et l'arabinose), d'hexoses (principalement le mannose, moins de glucose et de galactose) et d'acides sucrés. Généralement, il est composé de cinq sucres différents, le L-arabinose, le D-galactose, le D-glucose, le D-mannose et le D-xylose ainsi que d'autres composants tels que les acides acétique et glucuronique (Singh *et al.*, 2016). La distribution des différents sucres dans l'hémicellulose varie selon le bois et les conditions de culture (Sorieul *et al.*, 2016). En général, dans les parties de bois mou, l'hémicellulose est principalement composée de mannose alors qu'elle est remplacée par le xylose dans les bois durs (Persson *et al.*, 2006). Habituellement, les hémicelluloses constituent 15 à 35% de la biomasse lignocellulosique et le degré de polymérisation varie de 100 à 200 (Kuhad *et al.*, 1997).

La lignine : c'est le troisième polymère hétérogène principal de la biomasse lignocellulosique. C'est une molécule complexe formée de trois alcools phénylpropioniques dont l'alcool coniférylique, sinapylique et *p*-coumarylique. La lignine est incorporée dans la matrice polymère de la cellulose et l'hémicellulose, et fournit la rigidité et le soutien structural à la paroi cellulaire. Elle confère une imperméabilité à l'eau au vaisseau du xylème et forme une barrière contre les attaques biologiques et chimiques. C'est la composante la plus récalcitrante de la biomasse lignocellulosique (Hamelinck *et al.*, 2005). Semblable à la diversité des hydrates de carbone dans l'hémicellulose, la distribution de l'alcool aromatique varie également en fonction du bois. Le bois tendre est constitué de plus de 90% d'alcool coniférylique, alors que les bois durs sont composés de divers degrés d'alcools coniféryliques et sinapyliques (Harmsen *et al.*, 2010).

Les propriétés des charges naturelles varient considérablement, en fonction de la méthode de traitement utilisée pour les obtenir (Hon, 1996). Plusieurs études sur les composites renforcés de fibres naturelles ont révélé que leurs propriétés mécaniques sont fortement influencées par des paramètres tels que la fraction des fibres (volume/poids), l'orientation des fibres, le rapport des fibres, la longueur des fibres, l'adhésion fibre-matrice à l'interface (Hepworth *et al.*, 2000). Ces fibres contribuent souvent à la performance structurale de la plante et lorsqu'elles sont utilisées dans des matériaux composites, elles peuvent fournir un renforcement significatif (Joshi *et al.*, 2004 ; Karus et Kaup, 2002).

Bien que le renforcement de fibres naturelles a été utilisé dans diverses applications au cours des deux dernières décennies, des recherches approfondies sont encore nécessaires pour bien comprendre et explorer le potentiel des fibres naturelles (Voichita, 2006). L'utilisation efficace des fibres naturelles dérivées de ressources renouvelables offrent des avantages environnementaux en ce qui concerne la disponibilité ultime et l'utilisation de la matière première (Singha et Thakur, 2012). Par conséquent, de nombreux secteurs industriels considèrent les fibres naturelles comme substituts pour le renforcement synthétique.

I.2.3.4. Biocomposites à base de PHBV et de particules lignocellulosiques

Ces dernières années de nombreuses recherches ont été menées sur le développement de matériaux composites entièrement biosourcés et biodégradables (Berthet *et al.*, 2016). Dans ce contexte, en vue de moduler les propriétés du PHBV en fonction des applications envisagées et réduire son coût tout en maintenant sa biodégradabilité complète, une stratégie pertinente consiste à le mélanger avec des fibres lignocellulosiques à faible coût telles que les fibres de bois (Reinsch et Kelley, 1997), les fibres d'épicéa (Dufresne *et al.*, 2003), les fibres de lin (Wong *et al.*, 2004), les fibres de jute et d'abaca (Bledzki et Jaszkiwicz, 2010), ou des fibres de paille de blé (Avella *et al.*, 2000; Ahankari *et al.*, 2011). Récemment, certaines études ont été consacrées à l'utilisation de fibres lignocellulosiques issues des grignons d'olives comme agents de renforcement dans le PHBV, ouvrant ainsi des débouchés prometteurs pour la valorisation de ce sous-produit oléicole (Berthet *et al.*, 2015 ; Hassaini *et al.*, 2017). Ce concept sera développé dans le chapitre suivant de cette thèse.

Cependant, le principal problème des biocomposites est l'incompatibilité entre les fibres naturelles « hydrophiles » et les matrices thermoplastiques « hydrophobes », ce qui entraîne une dégradation de leurs propriétés fonctionnelles. En conséquence, diverses stratégies ont été adoptées pour améliorer l'adhésion interfaciale entre charge de renfort et matrice, y compris le traitement des fibres lignocellulosiques avec de l'hydroxyde de sodium ou l'incorporation d'un agent de couplage comme le silane (Djidjelli *et al.*, 2007 ; Harikumar *et al.*, 1999).

***1.3. Potential routes of
valorizing olive pomace
residues: Review***

Chapitre adapté de la revue :

Potential routes of valorizing olive pomace residues: A review

Revue en préparation pour soumission

Sarah Lammi^{a,b}, Djamel Djenane^b, Nathalie Gontard^a, Hélène Angellier-Coussy^{a,*}

^aJRU IATE 1208 – CIRAD/INRA/Montpellier SupAgro/University of Montpellier, 2 place Pierre Viala, F-34060 Montpellier, France.

^bLaboratory of Food Quality and Food Safety, Department of Agronomic Sciences, University of Mouloud MAMMERI, BP 17, 15000 Tizi-Ouzou, Algeria.

*Corresponding author : helene.coussy@umontpellier.fr / +33(0)4 99 61 24 32

Résumé

L'extraction de l'huile d'olive génère d'énormes quantités de déchets, y compris le grignon d'olives, qui correspond au résidu lignocellulosique solide et représente environ 40 kg par 100 kg d'olives et 20 L d'huile produite. Son élimination soulève des problèmes environnementaux dans les principaux pays producteurs d'olives, notamment l'inhibition des populations microbiennes du sol et la réduction de la germination des graines. Ainsi, l'éco-conversion de ce résidu agricole en produits à valeur ajoutée doit être encouragée. Des études ont récemment été menées pour évaluer sa composition, ses caractéristiques physico-chimiques, biologiques et toxicologiques. Cette revue a pour but de discuter des différents sous-produits issus du procédés d'extraction d'huile d'olive et de mettre en évidence leurs principaux usages, en mettant l'accent sur le grignon d'olives. Les voies de valorisation du grignon d'olives, déjà disponibles à l'échelle industrielle ou encore en phase de recherche et développement, font l'objet d'un examen critique. Le document comprend la production d'huile de grignon d'olives, l'utilisation des grignons dans l'alimentation animale, la production de bioénergie, les biocarburants et les biofertilisants, l'extraction de biomolécules et de composés bioactifs, ainsi que sa conversion en constituants de matériaux.

Mots clés : grignon d'olives, sous-produits de l'huile d'olive, composition, valorisation.

Abstract

Extraction of olive oil generates huge amounts of residual wasted biomasses, including olive pomace, which corresponds to the solid lignocellulosic residue and represents an amount of around 40 kg per 100 kg of olives and 20 L of oil produced. Its disposal in raises environmental issues in the main olive-producing countries, including the inhibition of soil microbial populations and the reduction in seed germination. So, the eco-conversion into added-value products of this agricultural residue is to be encouraged. Studies have recently been carried out on assessing their composition, physical-chemical, biological and toxicological characteristics. This paper aims at discussing the different olive oil by-products and highlighting their main usages, with a special focus given on olive pomace. The valorization routes of olive pomace, which are already available on an industrial scale or still at the research and development stage, are critically reviewed. The paper includes the production of olive pomace oil, its use in animal feeding, the production of bioenergy, biofuels and biofertilizers, the extraction of biomolecules and bioactive compounds, and also its conversion into material constituents.

Keywords: Olive pomace, olive oil by-products, composition, valorization.

I.3.1. Introduction

In all Mediterranean civilizations, the olive plays a very important role in the life of the populations and olive tree has a very strong cultural and religious symbolism. Notably, the official seal and emblem of the World Health Organization features the rod of Asclepius over a world map surrounded by olive tree branches, chosen as a symbol of peace and health (Barbaro *et al.*, 2014). The discovery of the benefits of its oil, which is now an integral part of what is commonly called the "Mediterranean diet", gave rise to a lightning return to grace and deserved of culture of the olive tree (Villa, 2003). The rising popularity of olive oil is predominantly attributed to its oleic acid and phenolic compounds contents (Fki *et al.*, 2005), which act as natural antioxidants to prevent human diseases (Owen *et al.*, 2000). In addition, phenolic compounds are also known to display anti-inflammatory, anti-proliferative and anti-atherogenic properties (Loizzo *et al.*, 2011; Perez-Jimenez *et al.*, 2005; Tuck and Hayball, 2002).

With currently more than ten million hectares of olive culture, the production of olives and virgin olive oil in the world was reported to be 15.40 and 3.05 million tons respectively, for

the year 2014 (FAOSTAT, 2016). Olive cultivation is particularly spread in the entire Mediterranean region where it plays an important role in protecting the economy, local heritage and the environment. The production of olive oil provides income and employment to millions of people in natural environments where the possibility of establishing alternative activities could be difficult. The largest olive-growing countries are located in areas around the Mediterranean, with 98% of the total cultivated area and 99% of the total production of olive fruits (Naghmouchi *et al.*, 2015; Niaounakis and Halvadakis, 2006).

In addition to residues generated in the field such as olive tree pruning, the olive oil extraction industry generates large amounts of others by-products, including olive tree leaves and a solid residue called olive pomace or olive cake as well as an effluent known as olive mill wastewater, the two latter being preponderant. These by-products are currently still considered as olive mill wastes. Each olive tree produces 15 to 50 kg of olives per year, depending on the nature of the olives and environmental conditions, with the generation of on average 25 kg of leaves and twigs annually (Lazzeri, 2009; Nefzaoui, 1987). One hectare of olive tree generates on average about 2500 kg of olives (Rodrigues *et al.*, 2015), which are converted into 500 L of oil. Generally, 100 kg of olives produce around 20 L of oil, 40 kg of solid pomace and 100 L of wastewater (Nefzaoui, 1987). It is estimated that the production of olive pomace reaches 2,881,500 tons per year worldwide (Ravindran and Jaiswal, 2016). One key point is that olive pomace and olive mill wastewater are known to be harmful to the environment, as several studies have demonstrated their negative effects on soil microbial populations, aquatic ecosystems and air through phenol and sulfur dioxide emissions (Dermeche *et al.*, 2013).

During the last years the interest in the recovery, recycling and upgrading of food industry by-products has increased drastically (Laufenberg *et al.*, 2003) in the framework of overall efforts to achieve progresses toward circular bio-economy. These by-products are promising sources of compounds that can be recovered and used as valuable substances by developing new processes (Fernández-Bolaños *et al.*, 2006). The optimal solution for disposing waste should be their valorization to transform several ecological problems into a range of economic opportunities.

An increasing number of papers have been published since the years 2000 on olive pomace, starting from 1992 (Figure 7). However, existing reviews on the subject are mainly focused either on olive oil by-products as a whole or on a particular area of application, such as food

(Antónia Nunes *et al.*, 2016), pharmaceuticals (Araújo *et al.*, 2015), cosmetic (Rodrigues *et al.*, 2015), energy (Rajaeifar *et al.*, 2016) and the environment (Muktadirul *et al.*, 2013). The only published review on olive pomace (Kalderis and Diamadopoulou, 2010) deserves to be updated as for example it does not include one of the most promising recovery routes, *i.e.* the use of olive pomace as raw materials for the production of building material constituent or filler in biocomposites.

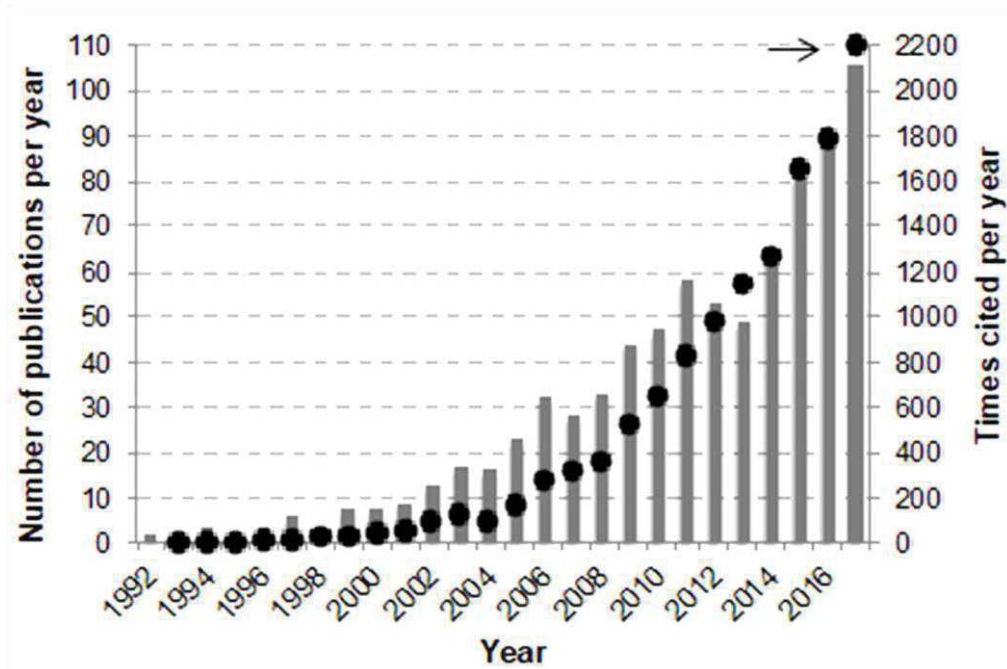


Figure 7 : Evolution of the number of peer-reviewed journal articles published (bars) and cited (●) with the keyword “olive pomace”

Data obtained from Web of Science (5th of April 2018)

The aim of this paper is to propose an updated and critical review focusing on olive pomace and its current and potential ways of eco-conversion. The first part of the review will present the key features of the olives and olive oil in such a way as to get an overview of the availability and potentiality of the resource, including the main producers and consumers, the different olive varieties, the olive average composition and the different olive oil extraction processes. The second part will present the key characteristics, including the biochemical composition, of the different olive by-products, *i.e.* the olive tree biomass from pruning, the olive leaves, the olive stones, the olive-mill wastewater and the olive pomace, with more attention paid to olive pomace. Finally, the third part will focus on the valorization routes of

olive pomace, whether they are already available at industrial scale or still at the research and development stage.

I.3.2. Key features of the olives, olive oil and olive by-products

I.3.2.1. Main producers and consumers of olive oil

The olive and oil production covers areas between the 25th and 45th degree of latitude North and South (Latin America), preferably close to the sea (Villa, 2003). The Mediterranean basin is still the productive and commercial heart of the olive due to its favorable climate for the cultivation of this tree, characterized by a mild and humid winter and a warm dry summer. Mediterranean countries produce about 98% of the olive oil and more than 75% of table olives worldwide (Benhayoun and Lazzeri, 2007).

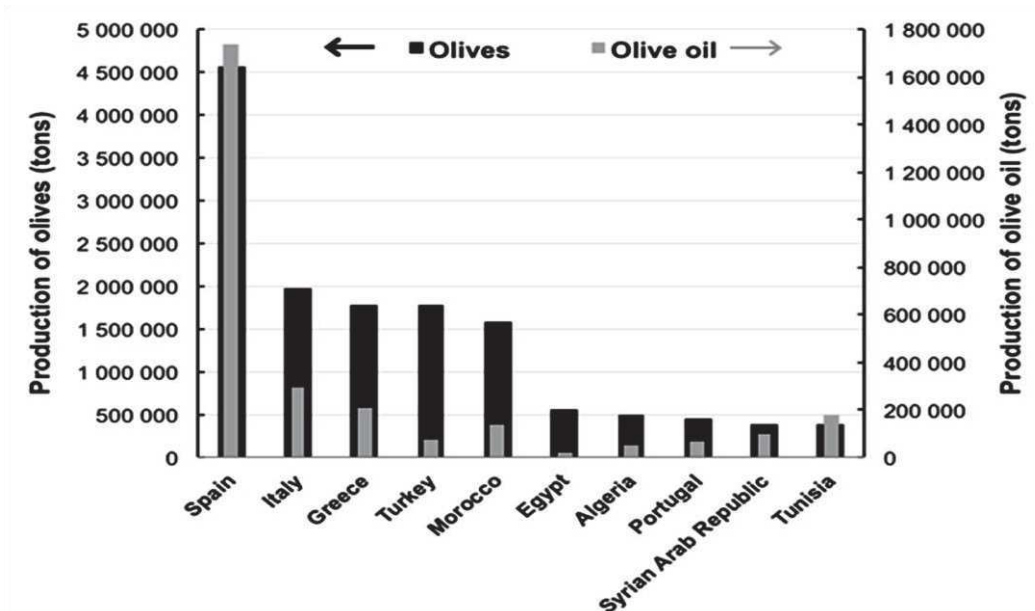


Figure 8: Main producers of olive and olive oil in the world. Data from (FAOSTAT, 2016)

Olive oil is for the main part produced by Spain with approximately 50 % of the world production, 2.3 million hectares and 2.7-3 million tons of olive oil. Italy comes next with about 20% of the world production, followed by Greece with 10%, Tunisia with 8%, Syria with 6% and the rest of the countries contributing with about 6% of world production (Figure 8). The coming years should see the arrival of some major countries with a Mediterranean climate, on the international olive oil scene, including Argentina and Chile. The United States, with a consumption of over 220 000 tons per year since the 90s, are now the second largest market after the European Union. There is also an increase in olive oil consumption in

Australia, Japan, Canada and Brazil, with consumption between 25000 to 35000 tons per year in each of these countries. Since the 2000s the Indian market in olive oil also seems promising.

I.3.2.2. Olive composition

Olive fruit is essentially made up of 3 parts, *i.e.* epicarp (or skin), mesocarp (or pulp) and endocarp (or stone) (Figure 9). The epicarp is covered with waxes, during the growth phase its color turns from light green to purple and brown or black. The mesocarp, with a soft and pulpy flesh, accounts for 70–90% (of the total fruit mass). Finally, the hard endocarp containing the seed or kernel may differ from 13 to 30% of fruit weight. The olive fruit's average composition includes water (50 wt%), oil (22 wt% wet basis (w.b.)), lignin (19 wt% w.b.), cellulose (6 wt% w.b.), extractives including phenolic compounds (1-3 wt% w.b.), protein (1-2 wt% w.b.) and inorganic substances corresponding to ashes (1-2 wt% w.b.). Other important compounds present in olive fruit are pectins, organic acids, and pigments (Boskou, 1996). The richest part in oil is the mesocarp (52 wt% w.b. fats, 12 wt% w.b. crude cellulose and 10wt% w.b. proteins), while the endocarp is the richest in cellulose (74 wt% w.b. crude cellulose, 1 wt% w.b. proteins and 1 wt% w.b. fats) (Table 4). The olive phenols impart antimicrobial properties to the different parts of the plant and are also responsible for the extent of browning in the fruit. These phenolic components also contribute towards the sensory and aromatic characteristics of the olive as well as imparting pharmaceutical and physiological benefits (Bianchi, 2003; Ghanbari *et al.*, 2012).

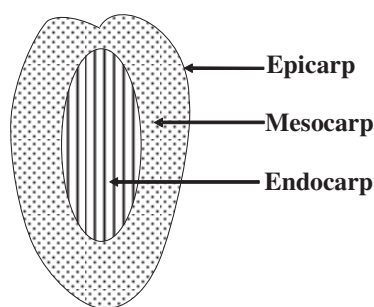


Figure 9: Longitudinal section of the olive fruit

I. Synthèse bibliographique

Table 4: Composition (wt% w.b.) of the different parts and by-products of the olive
(n.d.: not determined, *: depending on the olive oil extraction process)

	Water	Fats	Cellulose	Hemicellulose	Lignin	Extractives not nitrogenous	Proteins	Ashes	References	
Parts of the olive										
Olive	50	22	6		19	1-3	1-2	1-2	Boskou, 1996	
Epicarp	n.d.	3.4	2.4			82.8	9.8	1.6	Maymone <i>et al.</i> , 1961	
Mesocarp	n.d.	51-52	12.0			24.2	9-10	2.3	Bianchi, 2003 Ghanbari <i>et al.</i> , 2012	
By-products of olive oil production										
Biomass from pruning	8.1	n.d.	26-37	20-25	17-28	14-31	n.d.	6.7	Romero <i>et al.</i> , 2007 Al bkoor Alrawashdeh <i>et al.</i> , 2017	
Leaves	51	3.2	5.7	3.8	39.6	36.5	7.2	2.4	Aydinoglu and Sargin, 2013 García-Maraver <i>et al.</i> , 2013	
Olive stones	n.d.	n.d.	25-54	18-35	25-35	n.d.	n.d.	5	Matos <i>et al.</i> , 2010 Rodríguez <i>et al.</i> , 2008 Naghmoushi <i>et al.</i> , 2014 Abou-Zeid <i>et al.</i> , 2015	
Olive waste water	83-94	4-16							0.4-2.5	Davies <i>et al.</i> , 2004 Inglezakis <i>et al.</i> , 2012
Olive pomace	35-70*	2-5	5-25	6-35	20-48	n.d.	1.5	2.5	REACM, 2008 El Mouhtadi <i>et al.</i> , 2014 Rigane <i>et al.</i> , 2012	

I.3.3. Olive by-products

The production of olive oil generates many residues or by-products, which significantly affects the environmental sustainability of this agricultural activity. It includes agro-residues generated by olive cultivation, *i.e.* biomass from pruning and leaves, residues from table olives, *i.e.* olive stones, and by-products from the oil extraction process it-self, *i.e.* an aqueous sludge and a solid residue. Generally, from 100 kg of olives, about 20% of oil is recovered while 30% of solid residue and 50% of aqueous liquor are generated. Due to their high phenolic content (e.g. concentration in hydroxytyrosol 10-100 fold higher than olive oil) (Lesage-Meessen *et al.*, 2001), these two latter by-products are not easily degradable by natural processes, and their disposal creates a major environmental issue in the main olive-producing countries (Gharbi *et al.*, 2014; Rigane *et al.*, 2012). Table 5 summarizes the main terms used in literature to call these by-products in the Mediterranean countries. The main valuation routes of the different olive by-products are synthesized in Table 6 and summarized in the following paragraphs.

Table 5: Terminology used to describe the wastes generated in olive oil mills, in different languages (En: English, Fr: French, Gr: Greek, It: Italian, Sp: Spanish, Tk: Turkish)
(CAR/PP, 2000)

	3-phases process	2-phases process
Solid waste	Orujo (Sp)	Alperujo or Orujo de 2 fases (Sp)
	Sansa (It)	Sansa umida (It)
	Grignon (Fr)	Grignon(Fr)
	Pirina (Gr/Tk)	Pirina (Gr/Tk)
	Pomace or Husk or Cake (En)	Pomace or Husk or Cake (En)
Liquid waste	Alpechín or Jamila (Sp)	
	Aque di vegetazione (It)	
	Margine (Fr)	Not concerned
	Katsigaros (Gr)	
	Olive-mill wastewater or olive vegetation water (En)	

I. Synthèse bibliographique

Table 6: The main valorization routes of the various olive oil by-products (*: % of the pruning biomass weight; n.d: not determined; -: not used; +: still at the lab scale, less than 10 publications; ++: still at the lab scale, more than 10 publications; +++: already at the industrial scale)

By-products	Yield (%)	Bioenergy		Biofertilizers		Biomolecules			Biomaterials				
		Combustion	Production of biofuels	Composting	Culture medium	Pharmaceutical/ Food ingredient	Animal Feed	Cosmetics (Exfoliating agent)	Reinforcing filler	Building materials	Paper industry	Furniture manufacturing	Adsorbent Material
Biomass from pruning	10-30	+++	-	-	-	-	-	-	-	-	++	+	-
Leaves	25*	+++	-	+	-	+++	+++	-	-	-	-	-	-
Olive stones	n.d	+++	+	-	-	+	+	+++	++	+	+	-	++
Olive wastewater	30	-	-	-	++	+++	-	-	-	-	-	-	-
Olive pomace	20	+++	++	++	+	++	+++	-	+	++	-	-	+

I.3.3.1. Olive pomace

Olive pomace (OP) is a lignocellulosic by-product containing olive skin, pulp and stone, with a significant moisture and residual oil content, depending on the cultivation region and extraction process (Akay *et al.*, 2015) (Table 4). Among the negative effects resulting from the spread of OP in the field, we can cite (i) the inhibition of microorganisms' activities, (ii) the reduction in seed germination, and (iii) the alteration of the soil characteristics in terms of the porosity and the humus concentration (Cardelli and Benitez, 1998). OP is considered as a source of pollution, either because it is contaminated with fungi or because it releases toxic substances into the environment. Fungal toxins or polyphenolic compounds that are resistant to bacterial degradation can then leach and pollute water sources nearby, threatening human health and the environment. Phenolic compounds are pollutants when the by-products, which contain them are left in their raw state in the environment. This is why several recent works are interested in their extraction and valorization for different targeted applications. Accordingly, research into finding new possible uses for olive pomace is of great relevance not only to the economy, but also to the environment (Gharbi *et al.*, 2014). This will be further developed.

I.3.3.1.1. Types of olive pomace

Different types of pomace can be obtained according to the final destination (Nefzaoui, 1987):

- **Raw (or crude) pomace.** It is the solid residue of the whole olive oil extraction. 100 kg of olives give (after triturating with the classical system) on average 35-45 kg of crude pomace (with a water content ranging from 40 to 70 wt%). Its high content of water and oil make it very vulnerable for rapid deterioration by fungal contamination and/or oxidation when left in the open air.

- **Partially pitted (or strained) pomace.** It results from the partial separation of the fragments of pit (also called stone) from the pulp, by sieving or ventilation. This residue is called "fat" if the oil is not extracted by solvent or "degreased or exhausted" if the oil is extracted by solvent. The main difference between the 3-phase pomace and pomace from the 2-phase process lies in the method used to remove the stone. In the 3-phase process, the pneumatic removal of the stone is done just after drying. The stone is separated, in the majority of cases, using separating machines where the air which flows against the pomace current pulls off the lighter pulp particles, leaving behind the heavier and larger stone pieces. Cyclones are used to

separate the pulp from the air flow, which enables the air to be cleaned before being emitted into the atmosphere. The pressed pomace and pomace from the three-phase process must be directly subjected to a drying process immediately after leaving the mills in order to prevent the rapid deterioration of the oil, particularly free acidity. In the 2-phase process, Stone removal occurs prior to drying and is carried out using mills with filters with approximately 3mm spaces, which allow solids smaller than this size to pass through, expelling the larger stone directly to the drying phase.

- **Exhausted pomace.** It is the residue obtained after deoiling of the crude pomace by solvent, generally hexane. After exhaustion, 25-26 kg of pomace are obtained (for an initial weight of 100 kg of olives), with a humidity of 15 wt%, and consisting of 13 to 14 kg of stone and 12 to 13 kg of pulp.

I.3.3.1.2. Composition of olive pomace

The average composition of olive pomace is 35-70 wt% of water depending on the olive oil production process, 5-25 wt% w.b. of cellulose, 6-35 wt% w.b. of hemicellulose, 20-48 wt% w.b. of lignin, 2-5 wt% w.b. of oil (retained in the pulp) and 2.5 % of ashes (Tables 4 and 7). Other organic components are sugars (3 wt%), proteins (1.5 wt%), total volatile fatty acids (C2–C7) (1 %), polyphenols (0.2%) and pigments (0.5 %) (Rigane *et al.*, 2012).

It is important to note that the composition of OP may differ depending on the variety of the olives, the stage of maturity, the process of oil extraction, the extent of exhaustion by solvents and also the methodology used to analyze the composition. As an example, the two-phase separation mode (Figure 9) produces a pomace with a higher moisture content (55-70%) than the one obtained in the three-phase operation (40-45%) (Borja *et al.*, 2006).

Different studies showed that olive pomace is a very good source of phenolic compounds. Phenolic compounds are variably detected and concentrated in olive pomace according to the treatment applied. According to Goldsmith *et al.*, (2014), about 30% of the total phenolic compounds and 21% of the oleuropein are recovered in olive pomace resulting from the traditional press oil extraction method. Related to that, they showed that the pomace exhibited 32% of the antioxidant activity originally measured in the whole olive. Lower phenolic contents were found (8%) in the case of freeze-dried samples (Jerman Klen and Mozetic Vodopivec, 2012). The total phenolic content of the olive fruit can reach 98% in OP (Rodis, 2002; Rubio-Senent *et al.*, 2015).

The storage of the crude olive pomace is relatively tricky due to its high water and oil contents, contributing therefore to mold development and rancidity in contact of air (Ghanbari *et al.*, 2012). It is estimated that crude residue obtained by centrifugation deteriorates after 4-5 days while the residue obtained by pressure deteriorates after about 15 days. Dehydration of crude pomace during the extraction could be a way to increase the conservation duration up to one year (Sansoucy, 1991). However, the dehydration is a costly process in terms of energy required to remove water from the olive cake (Ghanbari *et al.*, 2012).

Table 7: Lignocellulose composition (wt% w.b.) of olive pomace reported in the literature
(n.d: not determined)

Geographical origin	Process	Hemicellulose	Cellulose	Lignin	Others	Reference
Spain	two-phase	11.3	5.2	19.7	63.8	De la Lama <i>et al.</i> , 2017
Spain	n.d	21.5	24.3	38	16.2	Garcia-Ibanes <i>et al.</i> , 2006
Turkey	n.d	23.6	24	48.4	4	Demirbas, 2004
Turkey	n.d	6.6	14.5	8.5	70.4	Ayrilmis and Buyuksari, 2010
Portugal	two-phase	22.3	12.5	43.2	22	Leite <i>et al.</i> , 2016
Tunisia	n.d	35	25	35	5	Gharbi <i>et al.</i> , 2014
Tunisia	two-phase	34	25	34.5	6.5	Naghmouchi <i>et al.</i> , 2015
Tunisia	Press	32-45		30	25-38	Nefzaoui, 1987
Spain	n.d	44		45	11	Jauhiainen <i>et al.</i> , 2005
Algeria	n.d	40.2		27	32.8	Rabouhi <i>et al.</i> , 2010

III.3.3.3. Use of olive pomace as filler in biocomposite materials

During the last few decades, extensive researches have been conducted on the development of biodegradable materials from renewable agricultural resources, including full-biocomposites, *i.e.* composite materials based on constituents all biosourced and biodegradable (Berthet *et al.*, 2016). The cheapest and most environmentally virtuous lignocellulosic fibers would be those obtained from food industry, agricultural or forestry solid by-products since their up-cycling in biocomposites would give value to a zero-value waste while helping waste reduction in the food industry. Recently, some studies were devoted to the use of lignocellulosic fibers stemming from olive pomace as reinforcing agents in polymer matrices, thus opening promising outlets with added value to this waste (Amar *et al.*, 2011; Berthet *et al.*, 2015; De Moraes Crizel *et al.*, 2018; Dufresne *et al.*, 2003; Gharbi *et al.*, 2014; Hassaini *et al.*, 2017; Lammi *et al.*, 2018 a, b ; Siracusa *et al.*, 2001). Either the crude olive pomace or the stone-rich fraction is generally used for that purpose, with filler contents up to 50 wt% and a focus on mechanical performance and water absorbance of biocomposites (Tables 9 et 10). Up to now, only two studies have been devoted to the valorization of olive pulp (Banat and Fares, 2015; Lammi *et al.*, 2018a). It has been shown that the incorporation of the OP-based fillers leads to a decrease in mechanical and barrier properties of composites material as compared to the polymer matrix. The decrease in mechanical performance was ascribed to a poor affinity between the hydrophilic natural fibers and the hydrophobic thermoplastic matrices (Berthet *et al.*, 2015; Gharbi *et al.*, 2014; Hassaini *et al.*, 2017). As a result, some authors suggested different physicochemical treatments of the filler surface to improve the interfacial adhesion between the OP fibers and the thermoplastic matrices (Gharbi *et al.*, 2014; Banat *et al.*, 2015; Naghmouchi *et al.*, 2015; Tserki *et al.*, 2015; Tserki *et al.*, 2016; Hammoui *et al.*, 2015; Khemakhem *et al.*, 2016; Boussehel *et al.*, 2016b; Hassaini *et al.*, 2017). Changes in the mechanical properties as well as the water absorption behavior were shown to be greatly affected by the treatment (Table 8). For example, in the work of Gharbi *et al.* (2014), the evolution of mechanical properties and water absorbance was investigated as a function of the filler content. These properties were greatly affected by the silane treatment of the OP stone-based filler, with a higher enhancement in the stiffening effect and a more pronounced reduction in water absorption as compared to untreated fillers. In a recent work, dry fractionation (combination of grinding and sorting processes) has been demonstrated as an efficient process to produce contrasted and pure stone-rich and pulp-rich fractions from crude olive pomace that could be further exploited as fillers in composite materials (Lammi *et al.*,

2018a). It was shown that the properties of PP and PHBV-based biocomposites could be modulated according to the nature of the OP-based filler (Table 8). As an example, a better preservation of mechanical characteristics was achieved in the case of pulp-rich filler due to better filler/matrix interactions and hence higher interfacial adhesion.

Targeted fields of applications are building, automotive industry, park benches and indoor furniture, gardening products and food packaging (Berthet *et al.*, 2015; De Moraes Crizel *et al.*, 2018; Djidjelli *et al.*, 2007; Siracusa *et al.*, 2001). As regards food packaging applications, the advantage of olive pomace is its anti-oxydant property, which was highlighted in the case of chitosan-based biocomposites (De Moraes Crizel *et al.*, 2018).

Table 8: Scientific papers focusing on the valorization of olive pomace tissues as fillers in biocomposite materials

PP: Polypropylene; PHBV: Poly(3hydroxybutyrate-co-valerate); PVC: Polyvinyl chloride; PLA: Polylactic acid; PBSA: Poly(butylène succinate co-adipate)

Type of filler	Polymer matrix	Evaluated properties	References
Olive pomace	PP	Mechanical properties	Siracusa <i>et al.</i> , 2001; Ayrimis and Buyuksari, 2010; Lammi <i>et al.</i> , 2018b
		Water vapour permeability	Ayrimis and Buyuksari, 2010; Lammi <i>et al.</i> , 2018b
		Thermal properties	Lammi <i>et al.</i> , 2018b
		Oxygen permeability	Lammi <i>et al.</i> , 2018b
	PVC	Mechanical properties	Djidjelli <i>et al.</i> , 2007
		Thermal properties	Djidjelli <i>et al.</i> , 2007
		Dielectric properties	Djidjelli <i>et al.</i> , 2007
	PBSA	Mechanical properties	Tserki <i>et al.</i> , 2006
		Water absorption	Tserki <i>et al.</i> , 2006
	PHBV	Mechanical properties	Berthet <i>et al.</i> , 2015; Hassaini <i>et al.</i> , 2017 ; Lammi <i>et al.</i> , 2018b
		Water vapour permeability	Berthet <i>et al.</i> , 2015; Hassaini <i>et al.</i> , 2017 ; Lammi <i>et al.</i> , 2018b
		Thermal properties	Berthet <i>et al.</i> , 2015; Hassaini <i>et al.</i> , 2017 ; Lammi <i>et al.</i> , 2018b
		Water absorbance	Hassaini <i>et al.</i> , 2017
		Oxygen permeability	Lammi <i>et al.</i> , 2018
	Olive stone	PP	Mechanical properties
Thermal properties			Lammi <i>et al.</i> , 2018b

		Water vapour permeability	Lammi <i>et al.</i> , 2018b	
		Oxygen permeability	Lammi <i>et al.</i> , 2018b	
		Water absorbance	Naghmouchi <i>et al.</i> , 2015	
	PVC	Mechanical properties	Djidjelli <i>et al.</i> , 2007 ; Naghmouchi <i>et al.</i> , 2014	
		Thermal properties	Djidjelli <i>et al.</i> , 2007 ; Naghmouchi <i>et al.</i> , 2014	
		Dielectric properties	Djidjelli <i>et al.</i> , 2007	
	PS	Mechanical properties	Boussehel <i>et al.</i> , 2015 ; Boussehel <i>et al.</i> , 2016	
		Water absorbance	Boussehel <i>et al.</i> , 2015 ; Boussehel <i>et al.</i> , 2016	
	Epoxy matrix	Mechanical properties	Papanicolaou <i>et al.</i> , 2011	
	Stearic acid and Graphite	Thermal properties	Djefel <i>et al.</i> , 2015	
	Unsaturated polyester	Mechanical properties	Gharbi <i>et al.</i> , 2014	
		Water absorbance	Gharbi <i>et al.</i> , 2014	
	PLA	Thermal properties	Perinovic <i>et al.</i> , 2010 ; Koutsomitopoulou <i>et al.</i> , 2014	
		Mechanical properties	Koutsomitopoulou <i>et al.</i> , 2014	
	Wheat gluten	Mechanical properties	Hammoui <i>et al.</i> , 2015	
		Thermal properties	Hammoui <i>et al.</i> , 2015	
		Water absorption	Hammoui <i>et al.</i> , 2015	
	PHBV	Mechanical properties	Hassaini <i>et al.</i> , 2017; Lammi <i>et al.</i> , 2018b	
		Thermal properties	Hassaini <i>et al.</i> , 2017; Lammi <i>et al.</i> , 2018b	
		Water vapour permeability	Lammi <i>et al.</i> , 2018b	
		Oxygen permeability	Lammi <i>et al.</i> , 2018b	
Olive pulp	PP	Mechanical properties	Lammi <i>et al.</i> , 2018b	
		Thermal properties	Lammi <i>et al.</i> , 2018b	
		Water vapour permeability	Lammi <i>et al.</i> , 2018b	
		Oxygen permeability	Lammi <i>et al.</i> , 2018b	
		Mechanical properties	Banat <i>et al.</i> , 2015	
			Water absorbance	Banat <i>et al.</i> , 2015
	PHBV	Mechanical properties	Lammi <i>et al.</i> , 2018b	
		Thermal properties	Lammi <i>et al.</i> , 2018b	
		Water vapour permeability	Lammi <i>et al.</i> , 2018b	
		Oxygen permeability	Lammi <i>et al.</i> , 2018b	

Table 8: Mechanical properties of olive pomace-based biocomposites, normalized towards the properties of the neat matrix.

(OP: olive pomace; d_{50} : apparent particle median diameter; n.d.: not determined)

Matrix	Filler type (d_{50})	Filler content (wt%)	Relative Young's modulus	Relative stress at break	Relative elongation at break	References
Polypropylene	Crude OP (n.d.)	30	1.68	-	-	Siracusa <i>et al.</i> , 2001
		40	1.30	-	-	
		50	1.13	-	-	
Unsaturated polyester	Stone of OP (50 -200 μm)	10	1.36	-	-	Gharbi <i>et al.</i> , 2014
		30	1.90	-	-	
		40	2.07	-	-	
Poly(3hydroxy butyrate-co-valerate)	Crude OP (59 μm)	5	1.07	0.81	0.73	Lammi <i>et al.</i> , 2018b
		15	0.88	0.52	0.52	
		30	0.81	0.34	0.43	
	Stone of OP (56 μm)	5	1	0.77	0.60	
		15	0.92	0.54	0.52	
		30	0.81	0.22	0.26	
	Pulp of OP (84 μm)	5	0.88	0.78	0.91	
		15	0.81	0.52	0.65	
		30	0.88	0.63	0.65	
Polypropylene	Crude OP (59 μm)	15	1	0.65	0.43	Lammi <i>et al.</i> , 2018b
	Stone of OP (56 μm)	15	1.07	0.60	0.38	
	Pulp of OP (84 μm)	15	0.92	0.66	0.61	
Poly(3hydroxy butyrate-co-valerate)	Treated OP (46 μm)	20	0.92	0.63	0.66	Berthet <i>et al.</i> , 2015

III.3.4. Conclusion

Over the last few years, there is an awareness of the scientific community about the environmental problems that threaten our planet, mainly related to the over-exploitation of farmland, consumption of large quantities of water and our dependence on fossil resources, especially for the production of energy and materials, which have become the most polluting sectors. At the same time, enormous quantity of food waste is becoming a global concern. Thus, multiple efforts have been directed to address this persistent problem. Using food waste as potential feedstock in bioprocesses is now possible. Adapting biorefinery strategy with integrated approach can lead to the development of circular bioeconomy.

The olive pomace has been largely studied for different purposes. Indeed, the increase of interest in the olive oil industry and the huge quantities generated require the development of adequate and alternative management solutions. As mentioned in this review, the main valorization routes of OP available to date, highlights four major opportunities, namely: bioenergy / biofuels, biofertilizers, biomolecules and biomaterials. However, some applications do not answer to the current requirements of sustainable development, and need to be reviewed or improved. Indeed, despite its great energy production, the combustion of OP is non-clean process due to its pollutants emissions, while olive pomace oil is unfit for human consumption because of its composition. Also, some OP recovery strategies allow only a partial valorization of this lignocellulosic residue, such as the extraction of biomolecules and the use of OP as reinforcing filler in composite materials. For this last application, mainly the olive stone has been used as filler in biocomposites. Moreover, the conventional available pre-treatments of OP use a large amount of water and chemicals, in order to separate the pulp from the stone. In addition to the consumption of a large quantity of water, such wet processes generate toxic effluents with negative environmental impact and certainly the loss of some interesting substances that consequently, limits the possible valorization fields of OP. Thus, it would be more relevant in the future to exploit this by-product in the whole by eco-friendly technologies, like the dry fractionation process, to effectively remedy these problems. Nevertheless, the emergence of new non Mediterranean producers and consumers on the one hand, the explosion of demand for olive oil on the other hand, engender an intense production of OP. Furthermore, the constant shortage of energy and food raw materials, incite to develop new feasible and viable ways of OP valorization.

To conclude, olive by-products represent greater tonnage than olive oil and their composition lends them to a multitude of uses. They will play a vital role in sustainable development of the olive sector. Therefore, it is important to consider them as raw materials in the same way as the oil and evaluate the economic conditions, for developing reproducible solutions on a large scale. It is also necessary that emerging valorization routes avoid the creation of more issues than solving the existing ones. Finally, biorefinery schemes should include cascading bioprocesses and be developed in a regional and seasonal reasoning. Thus, we will be able to solve environmental problems, and increase the competitiveness of the olive oil sector.

Acknowledgements

We are grateful to the PNE Program (2016-2017) of the Algerian Ministry of Higher Education and Scientific Research for its financial support in the 11-months doctoral fellowship of S. Lammi at the JRU IATE. Direct costs were covered by the MALICE project (call “Chercheur d’avenir 2015”), which is co-financed by the European Regional Development Fund (FEDER) and the Languedoc-Roussillon region.

II. Matériel et méthodes

II.1. PRODUCTION DES CHARGES DE RENFORT

La première partie de l'étude visait à explorer la potentialité d'utiliser le fractionnement par voie sèche, pour produire des poudres riches en pulpe et en noyau avec la plus grande pureté et un rendement élevé à partir du grignon d'olive brut, qui seront utilisées pour la production de charges.

Différents modes de broyage sont testés et combinés en sélectionnant les équipements appropriés. Les poudres broyées sont ensuite séparées en fractions intéressantes par une succession d'étapes de tri. Les propriétés intrinsèques des fractions résultantes sont caractérisées. Un procédé de séparation par voie humide est appliqué pour comparaison.

II.1. Matériel

Le grignon d'olives (OP) est obtenu à partir de l'extraction d'huile de la variété *Chemlal* en utilisant un système de presse traditionnel. Il a été gracieusement fourni par les producteurs locaux d'olives de la région d'Azazga (Tizi-Ouzou, Algérie), en février 2016. Ce résidu est composé de noyaux partiellement concassés, de pulpe et de peau. L'OP a été séché à l'air libre puis, stocké à 4°C à l'abri de la lumière jusqu'à son utilisation.

L'acide sulfurique, l'arabinose, le xylose et le glucose (SIGMA-ALDRICH), le formamide, le di-iodométhane (Acros Organics, Geel, Belgique), l'éthylène glycol (Aldrich Chemical Co. Inc., Milwaukee, USA) et le glycérol (Merck, Darmstadt, Allemagne) sont utilisés pour la caractérisation des fractions d'OP.

II.2. Fractionnement du grignon d'olives

Le fractionnement du grignon d'olives brut est effectué dans le but de produire des fractions riches en pulpe et en noyau suivant différentes voies. Toutes les fractions obtenues proviennent du même lot initial de grignon d'olives.

II.2.1. Fractionnement par voie humide

200 g d'OP brut sont mélangés avec 1 L d'eau distillée et laissés pendant 24 heures à température ambiante. Cette suspension est ensuite placée sous agitation à 400 tr / min et 30°C pendant 24 heures. Le mélange est d'abord tamisé à travers un tamis de 1 mm afin de séparer la fraction riche en noyau humide de la fraction riche en pulpe humide. La fraction liquide résiduelle est centrifugée à 10.000 tr / min pendant 10 min afin de séparer la fraction riche en pulpe de

l'effluent liquide. Les deux fractions obtenues sont séchées dans une étuve à 50°C pendant 24 heures et désignées par wS (fraction riche en noyau) et wP (fraction riche en pulpe).

II.2.2. Fractionnement par voie sèche

L'OP brut est d'abord broyé à l'aide d'un broyeur à couteaux (SM 300, Retch, Allemagne) avec une grille de 4 mm, puis a subi un deuxième broyage à travers une grille de 2 mm pour obtenir la fraction F0. Ensuite, deux types de tri sont testés afin de séparer la pulpe du noyau, à savoir le tri en fonction de la granulométrie par tamisage (voie A1), tri électrostatique selon la voie A2. Compte tenu du caractère friable du tissu pulpaire, une autre voie de séparation par friction (voie B) est étudiée, en utilisant des conditions douces de broyage à billes sans broyage préalable de la biomasse de départ :

- Tri par tamisage (voie A1) : 200 g d'échantillon F0 sont passés dans un tamis mécanique ROTEX à travers une ouverture de mailles de 0,8 mm pendant 10 minutes. Deux fractions sont obtenues. La première contient les particules de diamètre supérieur ou égal à 0,8 mm et correspondait à la fraction riche en noyaux (dS1) tandis que la fraction constituée de particules de taille inférieure à 0,8 mm représentait la fraction riche en pulpe (dP1).

- Tri électrostatique (TFS) (voie A2) : 200 g de F0 sont encore broyés à l'aide d'un broyeur à impact (Hosokawa-alpine, type UPZ, Augsburg, Allemagne) avec une grille de 0,3 mm. Les particules ultrafines résultantes présentaient un diamètre médian (d_{50}) mesuré par granulométrie laser, d'environ 100 μm (voir paragraphe 1.4.1). Un TFS à l'échelle pilote (système TEP, Tribo Flow Separations, Lexington, États-Unis) est utilisé pour le fractionnement électrostatique (EsF), en utilisant de fines particules comme matériau de départ. Cette technologie repose sur la séparation des particules en fonction de leurs propriétés de surface (composition chimique et charge), dans lesquelles les particules lignocellulosiques sont entraînées dans une ligne d'électrons où elles sont chargées par triboélectricité. Les particules chargées sont ensuite déplacées vers une chambre de séparation contenant un champ électrique élevé (10 kV), généré par deux électrodes haute tension. Les particules chargées positivement sont attirées par l'électrode négative et les particules chargées négativement sont attirées par l'électrode positive (Chuetor *et al.*, 2015; Barakat *et al.*, 2014). Les fractions chargées positivement (F+) sont généralement plus riches en protéines et hydrates de carbone hydrosolubles par rapport à la matière initiale F0. En revanche, les fractions chargées négativement (F-) sont plus riches en lignine et en

hydrates de carbone structurels (et donc en cellulose) que F+ (Basset *et al.*, 2016). Les poudres obtenues avec ce procédé sont désignées respectivement par (dS2) et (dP2) pour la fraction riche en noyau et la fraction riche en pulpe.

- Tri par friction et tamisage (voie B) : 200 g de grignons d'olive bruts sont soumis à des vibrations à l'aide d'un broyeur à billes (MM 400, Retch, Allemagne), sous une fréquence de 15 Hz pendant 2 min en présence de trois billes d'acier de 15 mm de diamètre. La poudre obtenue est ensuite tamisée dans un tamis mécanique ROTEX avec une ouverture de maille de 1 mm pendant 10 minutes, afin de séparer la pulpe noyau. Les particules grossières d'un diamètre supérieur ou égal à 1 mm sont retenues sur le tamis et correspondent à la fraction riche en noyau (dS3), les particules fines sont récupérées au fond du tamis et représentent la fraction riche en pulpe (dP3).

II.3. Caractérisation des fractions de grignon d'olives

Toutes les fractions, à l'exception de celles obtenues par fractionnement électrostatique (EsF), sont broyées avec un broyeur à billes (MM400) à une fréquence de 25 Hz pendant 2 min afin d'obtenir des échantillons homogènes avant d'être analysés. Cela n'était pas nécessaire dans le cas des fractions dS2 et dP2 car elles étaient déjà suffisamment fines pour subir d'autres analyses.

II.3.1. La taille des particules

Afin de piloter certains processus de fractionnement, c'est-à-dire le tri électrostatique dans la présente étude, il était nécessaire de contrôler la distribution granulométrique. La granulométrie des particules est mesurée en utilisant un analyseur de taille de particule à diffraction laser Mastersizer 2000 (Malvern Instruments Ltd., Royaume-Uni). A cet effet, les poudres sont mises en suspension dans de l'éthanol à 95% (v / v) directement dans la cellule expérimentale. Le diamètre médian des particules (d_{50}) est déterminé afin de caractériser les fractions.

II.3.2. Couleur

Les attributs de couleur de chaque fraction sont mesurés avec un colorimètre (Minolta), en utilisant le système de couleur L*, a*, b*. La valeur L* caractérise la luminance tandis que les valeurs a* et b* sont des indicateurs de la couleur de l'échantillon (a* du vert au rouge et b* du bleu au jaune). Les mesures ont été faites en double. La différence de couleur totale (ΔE) entre la fraction et la biomasse de départ est calculée selon l'équation suivante (CIE, 2004) :

$$\Delta E = [(L^* - L_{F0}^*)^2 + (a^* - a_{F0}^*)^2 + (b^* - b_{F0}^*)^2]^{0.5}$$

Avec L^* , a^* et b^* les composantes de couleur de la poudre obtenue. L_{F0}^* , a_{F0}^* et b_{F0}^* sont les composantes de la couleur de la biomasse de départ.

II.3.3. Composition biochimique

Les teneurs en cellulose et en hémicellulose des différentes fractions de grignon d'olives sont mesurées après une double hydrolyse acide concentrée. 10 mg d'échantillons séchés ont été traités avec H_2SO_4 à 72% pendant 1 h à 30°C, puis hydrolysés avec de l'acide sulfurique à 4% pendant 1 h à 120°C. Les monosaccharides libérés sont analysés par un système HPLC d'eau combiné, en utilisant une colonne BioRad HPX-87H à 40°C et 0,3 ml.min⁻¹ selon le protocole décrit par Barakat *et al.* (2014). La teneur en lignine est déterminée par la méthode de Klason (Nicholson *et al.*, 2014). Toutes les analyses sont effectuées en triple pour chaque fraction. La concentration en cellulose est déterminée par le taux de glucose tandis que le xylose et l'arabinose ont été utilisés pour calculer la concentration en hémicellulose dans le complexe lignocellulosique de chaque fraction, comme suit :

$$\text{Cellulose (g/100g}_{\text{Echantillon}}) = [(\text{Glucose (g/L)} * V_{\text{tot}}) / M_{\text{ini}}] * 100 / 1,11$$

$$\text{Hemicellulose (g/100g}_{\text{Echantillon}}) = [(\text{Xylose (g/L)} + \text{Arabinose (g/L)}) * V_{\text{tot}}] / M_{\text{ini}} * 100 / 1,13$$

$$\text{Lignine (g/100g}_{\text{Echantillon}}) = [(P_{\text{CE}} - P_{\text{C}}) * 100] / M_{\text{ini}} - \text{Cendres (g/100g}_{\text{Echantillon}})$$

Avec :

V_{tot} : volume total du milieu d'hydrolyse

M_{ini} : masse initial de l'échantillon

P_{CE} : poids du creuset + échantillon à 105°C

P_{C} : poids du creuset vide

1,11 : facteur de conversion entre glucose et cellulose

1,13 : facteur de conversion entre (xylose, arabinose) et hemicellulose

Les teneurs en humidité et en cendres sont déterminées par analyse thermogravimétrique sous air (voir paragraphe 1.4.4) en considérant le résidu de masse à 130°C et 900°C, respectivement.

Les teneurs en protéines des différentes fractions ont été déterminées avec (N x 6,25) selon

Jones (1941), après estimation de la teneur en azote dans chaque échantillon par analyse élémentaire.

II.3.4. Analyse thermogravimétrique

Une analyse thermogravimétrique (ATG) est réalisée afin d'étudier la stabilité thermique des différentes fractions. Des échantillons (environ 10 mg) sont chauffés à partir de la température ambiante jusqu'à 900°C, à une vitesse de chauffage de 10°C.min⁻¹ sous flux d'air et d'azote (50 mL.min⁻¹). La température de dégradation (T_{peak}) est mesurée à partir de la valeur maximale de la courbe dérivée de perte de poids.

II.3.5. Mesures d'angle de contact

Des mesures d'angles de contact sont effectuées sur des pastilles obtenues par compression des poudres de grignon dans un moule (diamètre de 13 mm) à l'aide d'une presse hydraulique (Perkin-Elmer) et sous une pression de 10 tonnes. Les pastilles résultantes sont préalablement séchées pendant 30 minutes sous vide et en présence de gel de silice. Les mesures de l'angle de contact sont effectuées à l'aide d'un instrument Digidrop (GBX, France). Le volume de la goutte est fixé à 3 µl dans tous les cas à l'aide d'une micro-seringue. La mesure de l'angle de contact est effectuée au moment de la stabilisation de la chute au-dessus de la surface de la pastille. Cinq liquides de référence sont utilisés afin d'estimer l'énergie libre de surface des pastilles de poudres : eau distillée, formamide, diiodométhane, éthylèneglycol et glycerol.

II.2. DEVELOPPEMENT ET CARACTERISATION DES BIOCOMPOSITES POUR L'EMBALLAGE ALIMENTAIRE

La deuxième partie de ce travail était consacrée dans un premier temps, à la mise en œuvre des matériaux biocomposites ensuite, à la caractérisation de leurs propriétés fonctionnelles et de biodégradabilité. A cet effet, nous avons exploré l'utilisation potentielle des deux principales parties du grignons d'olive, à savoir le « noyau » et la « pulpe », comme charges dans les biocomposites et les comparer à celle du « grignon brut ». Les poudres de grignon ont été d'abord produites par fractionnement à sec puis, incorporées dans deux matrices thermoplastiques : un polymère synthétique conventionnel, le "Polypropylène" et un polymère naturel biodégradable, le "Polyhydroxy-butyrates-co-valérate".

Différentes formulations de biocomposites à teneur croissante en charges, ont été préparées par un procédé thermomécanique disponible à échelle industrielle. Leurs propriétés optiques (couleur), microstructurales, thermiques, mécaniques (essais de traction), barrières (perméabilité à la vapeur d'eau et à l'oxygène), antibactérienne et de biodégradabilité ont été caractérisées. Une attention particulière a été accordée à la compréhension de l'impact de la composition des charges de grignon et notamment de leur affinité physico-chimique avec les matrices thermoplastiques, sur les propriétés fonctionnelles et la biodégradabilité des biocomposites, en vue d'évaluer leur éventuelle application dans le secteur de l'emballage alimentaire.

II.2.1. Matériel

Un lot de grignon d'olive brut de la variété *Chemlal* est gracieusement fourni en décembre 2016 par des producteurs d'olives locaux de la région d'Azeffoun (Tizi-Ouzou, Algérie). Il a été stocké dans une chambre froide à $4^{\circ}\text{C} \pm 1$ jusqu'à son utilisation. Ce résidu présentait un taux d'humidité initiale de 53% (P/P). Avant le fractionnement à sec, le grignon d'olives frais est séché dans une étuve à 60°C pendant 24 heures, jusqu'à atteindre une teneur en eau de 9% en poids (matière humide).

Le polyhydroxy-(butyrates-co-valérate) (PHBV) contenant 5% de valérate a été achetée auprès de la société NaturePlast (France) sous la forme de granules (grade PHI 002). Ces granules sont séchés pendant une nuit à 60°C avant utilisation. Le polypropylène (PP) sous la forme de granules (grade PPH 9020) a été acheté auprès de Total Petrochemicals (Belgique).

II.2.2. Préparation des charges à base de grignon d'olives

Le travail réalisé dans la première partie, nous a permis de sélectionner le schéma de fractionnement par voie sèche, le plus adapté à la biomasse de départ et de l'appliquer pour la séparation de la pulpe et le noyau à partir du nouveau lot d'OP brut.

L'OP sec est tout d'abord soumis à des forces de frottement dans un broyeur à boulets (Marne n°55, FAURE, France) fonctionnant à température ambiante, à 86 tr/min et pendant 30 min. Une jarre de 2 L est utilisée, avec 1/3 en volume de boulets en céramique (diamètre de 15, 20 et 25 mm) et 1/3 en volume d'OP brut. La poudre résultante est ensuite passée dans un tamis électrique (RITEC, modèle 400, France) à travers une maille de 1,25 mm. Deux fractions sont obtenues : la fraction fine est récupérée dans le fond du tamis et correspond à la fraction riche en pulpe (PF), tandis que la fraction grossière est retenue sur le tamis (Lammi *et al.*, 2018a). Cette fraction grossière est encore broyée à l'aide d'un broyeur à couteaux (SM 300, Retch, Allemagne) avec une grille de 1 mm et une vitesse de 1500 tr/min. Le produit broyé est ensuite tamisé à travers une ouverture de maille de 0,4 mm, afin de séparer la fraction riche en noyau (SF) de la fraction intermédiaire.

Enfin, pour obtenir des poudres de granulométrie similaire, les fractions SF et PF ainsi que l'OP brut correspondant à la biomasse de départ (F0) sont d'abord réduites dans un broyeur à couteaux à l'aide d'une grille de 0,25 mm à 1500 tr/min, puis encore réduites à l'aide d'un broyeur à impact de 0,3 mm (Hosokawa-alpine, type 100UPZ, Augsburg, Allemagne) fonctionnant à 18 000 tr/min.

II.2.3. Préparation de films biocomposites à base de grignons d'olive

II.2.3.1. Compoundage

Pour minimiser la dégradation hydrolytique, tous les constituants (granules de PHBV, poudres F0, SF et PF) sont séchés dans une étuve sous vide à 60°C pendant une nuit avant d'être mélangés. Les constituants sont mélangés à différents rapports polymère/charge (100/0, 95/5, 85/15, 70/30 P/P) en utilisant un mélangeur interne HAAKE Rheomix. Les granules de polymères et les charges à base d'OP sont d'abord mélangés manuellement. Le mélange résultant est ensuite introduit dans le mélangeur, fonctionnant à une vitesse de rotor de 60 tr/min pendant 5 minutes à des températures de 170°C et 180°C pour les matrices PHBV et PP, respectivement. Les composites obtenus sont refroidis à la température ambiante puis, broyés

dans un broyeur à couteaux (SM 300, Retch, Allemagne) à une vitesse de 2200 tr/min sur une grille de 4 mm pour obtenir des granulés de composites, qui sont ensuite stockés dans des sacs en plastique scellés contenant du gel de silice.

La codification de la formulation était selon l'exemple suivant : matrice-fraction de grignon (teneur en charge pondérale). Par exemple, la formulation PHBV-F0 (5%) correspond à un biocomposite à base de PHBV rempli de 5% en poids de la fraction F0.

II.2.3.2. Mise en forme des films

Les composites sont séchés à 60°C pendant au moins 8 heures avant la préparation des films. Des films biocomposites (carrés de 10,5 cm de large, épaisseur moyenne d'environ 250 µm) sont préparés par pressage à chaud des granules entre deux plaques revêtues de papier Téflon, à 170°C et 180°C pour les biocomposites PHBV et PP respectivement, à l'aide d'une presse hydraulique chauffante (PLM 10 T, Techmo, Nazelles, France). Les échantillons sont laissés pendant 3 minutes pour fondre puis, une pression de 150 bars est appliquée pendant 2 minutes comme décrit par Martino *et al.* (2015). Enfin, les films sont refroidis à température ambiante avant d'être retirés du moule. Le même processus est appliqué aux matrices PP et PHBV vierges.

II.2.3.3. Epaisseur des film et conditionnement

L'épaisseur du film est mesurée en utilisant une jauge de précision d'épaisseur (modèle Hanatek FT3, UK) sur au moins dix endroits différents pour chaque échantillon de film. Les valeurs moyennes d'épaisseur sont prises en compte dans le calcul des propriétés mécaniques, et de la perméabilité à la vapeur d'eau et à l'oxygène. Toutes les analyses sont effectuées sur des échantillons de films stockés dans des dessiccateurs en présence de gel de silice (humidité relative de 3%).

II.2.4. Caractérisation des charges et des biocomposites à base de grignon d'olives

II.2.4.1. Taille et morphologie des particules

Les distributions granulométriques des particules de charges, sont déterminées en utilisant un granulomètre laser comme il a été décrit plus haut.

L'analyse morphologique quantitative des particules est réalisée par analyse d'image en utilisant le logiciel Image J. Pour chaque échantillon, des images mosaïques sont assemblées en reconstruisant des images 10 x 4 par le logiciel d'imagerie NIS-Elements (Nikon, Japon) fonctionnant avec le système Multizoom AZ100, comme décrit par Montano *et al.* (2013). Les distributions pondérées en nombre et en surface des diamètres maximaux de Feret, c'est-à-dire la longueur maximale à l'intérieur de la projection de particules, sont déterminées sur la base de l'analyse d'environ 300 particules. L'analyse de l'image est réalisée sur un nombre croissant de particules, jusqu'à stabilisation de la moyenne de l'indicateur considéré, c'est-à-dire avec une variation inférieure à 5%, obtenue avec 80 particules dans la présente étude. Le rapport d'aspect des particules est calculé comme le diamètre maximal de Feret (dimension maximale à l'intérieur de la projection de particules) divisé par le diamètre minimum de Feret (rectangle équivalent côté court).

II.2.4.2. Densité de particules

La densité absolue des poudres de grignon est mesurée avec un pycnomètre à hélium (ULTRAPYCNOMETER 1000, instruments Quantachrome) en utilisant environ 2 g d'échantillon.

II.2.4.3. Composition biochimique

La teneur en humidité des poudres à base de grignon est déterminée en séchant deux grammes d'échantillon dans une étuve à 110°C jusqu'à un poids constant. La teneur en cendres est obtenue en brûlant environ un gramme d'échantillon dans un four à moufle à 600°C pendant cinq heures dans des creusets en porcelaine. Les teneurs en cellulose, hémicellulose, lignine et protéine sont quantifiées selon le protocole décrit précédemment.

II.2.4.4. Energie libre de surface et travail d'adhésion

Le même protocole décrit dans la première partie de l'étude a été appliqué pour la mesure d'angle de contact, aussi bien pour les charges (sur des pastilles de poudres) que les matrices polymères (des disques de films). Les valeurs d'énergie de surface (composantes polaire γ^p et dispersive γ^d) sont calculées en utilisant la formule d'Owens-Wendt (Owens et Wendt, 1969). Le travail d'adhésion (W_A) entre deux constituants solides, à savoir une matrice polymère (m) et une charge (f) peut être prédit en utilisant l'équation suivante :

$$W_A = 2 \left[\sqrt{\gamma_m^d \gamma_f^d} + \sqrt{\gamma_m^p \gamma_f^p} \right]$$

II.2.4.5. Couleur

Les attributs de couleur de toutes les fractions et biocomposites à base d'OP sont mesurés avec un colorimètre (Minolta), en utilisant le système de couleur L*, a*, b* comme il a été décrit précédemment. Les références sont respectivement F0 pour les fractions SF et PF, et les matrices de polymères purs pour les biocomposites. Toutes les mesures ont été effectuées en triplicata.

II.2.4.6. Analyse thermogravimétrique

La stabilité thermique des fractions et des biocomposites à base de grignon est évaluée par ATG selon la démarche décrite plus haut. Trois températures de dégradation thermique sont enregistrées : T_{pic} est mesurée à partir de la valeur maximale de la dérivée de perte de poids, T_{5%} et T_{20%}, correspondent aux températures auxquelles les pertes en poids sont respectivement de 5% et 20% par rapport au poids initial.

II.2.4.7. Calorimétrie différentielle à balayage (DSC)

La calorimétrie différentielle à balayage est utilisée pour mesurer les températures de cristallisation (T_c) et de fusion (T_m) des matériaux, ainsi que leur degré de cristallinité (X_c). Les mesures sont effectuées avec un calorimètre thermo-modulé (DSC modulé Q200, TA Instruments, New Castle, USA). Environ 10 mg de film sont placés dans des creusets hermétiques en aluminium (creuset hermétique Zero Aluminium, TA Instruments New Castle, USA). Chaque échantillon est d'abord chauffé à 200°C puis refroidi à -40°C à 10°C.min⁻¹ et chauffé à nouveau jusqu'à 200°C à une vitesse de chauffage de 10°C.min⁻¹. Le premier balayage est utilisé pour effacer l'histoire thermomécanique des échantillons.

La température de cristallisation est mesurée à partir du pic exothermique de la rampe de refroidissement. Les températures de fusion sont déduites des pics endothermiques de la première (T_{m1}) et deuxième (T_{m2}) rampe de chauffage. Les enthalpies de fusion sont déterminées par le logiciel DSC, à partir de la zone sous le pic observé à la fois sur la première (ΔH_{m1}) et la deuxième (ΔH_{m2}) rampe de chauffage. Le degré de cristallinité de chaque échantillon est calculé avec l'équation :

$$X_c = \left(\frac{\Delta H_m}{W \times \Delta H_m^*} \right) \times 100$$

où ΔH_m est l'enthalpie de fusion apparente de l'échantillon, W est le poids de la fraction de polymère dans l'échantillon et ΔH_m^* l'enthalpie de fusion théorique d'un polymère 100% cristallin. Des valeurs de 146 J.g^{-1} et 148 J.g^{-1} sont respectivement utilisées pour ΔH_m^* de PHBV et PP, comme rapporté par Barham *et al.* (1984) et Monasse et Haudin (1985).

II.2.4.8. Tests de traction

Les propriétés mécaniques des différents films sont évaluées à température ambiante par des tests de traction réalisés avec un analyseur de texture (Zwick BZ2.5/TN1S, France) sur des éprouvettes en forme d'os prédécoupées à l'aide d'un cutter (largeur de 4 mm et longueur de 45 mm) et en utilisant une vitesse transversale de 10 mm.min^{-1} . La contrainte nominale à la rupture (σ), l'allongement nominal à la rupture (ε) et le module de Young (E) sont déterminés à partir des courbes contrainte-déformation. Dix répétitions sont réalisées pour chaque formulation.

II.2.4.9. Perméabilité à la vapeur d'eau (WVP)

La perméabilité à la vapeur d'eau des films ($\text{mol.m}^{-1}.\text{s}^{-1}.\text{Pa}^{-1}$) est déterminée à 20°C en utilisant une méthode gravimétrique selon le protocole décrit par Angellier-Coussy *et al.* (2011) entre 0% (cellules de perméation placées dans un dessiccateur contenant du gel de silice) et 100% d'humidité relative (cellules contenant de l'eau). Les cellules sont pesées en utilisant une balance à quatre chiffres (BALCO -Type LX 220A, Suisse) toutes les 24 heures pendant une semaine. Cinq échantillons de chaque film sont testés et la perméabilité à la vapeur d'eau est calculée à partir de l'équation suivante :

$$WVP = \frac{w \cdot x}{A \cdot \Delta p}$$

où w est la pente de la perte de poids en fonction du temps (mol.s^{-1}), x est l'épaisseur du film à l'équilibre mesurée à l'extrémité (m), A est la surface du film exposée (m^2) et Δp est la différence de pression de vapeur d'eau à travers le film (à 20°C , $\Delta p = 2338 \text{ Pa}$).

II.2.4.10. Perméabilité à l'oxygène

La vitesse de transmission d'oxygène ($\text{m}^3 \cdot \text{m}^{-2} \cdot \text{d}^{-1}$) des films est mesurée à 20°C et 0% HR (humidité relative) sur des disques de films de 16 cm^2 , en utilisant une cellule de perméation à l'oxygène (OTR-Pst6, PresSens-GmbH, Allemagne) selon la procédure ASTM F1927-07 (2007) modifiée. Le taux de transmission d'oxygène à travers le matériau peut être détecté avec le capteur d'oxygène dans la chambre supérieure. Il a été déterminé pour tous les films en double et calculé selon la formule suivante :

$$\text{OTR} = \frac{\text{VO}_2}{A \cdot t}$$

Avec VO_2 est le volume d'oxygène dans la chambre supérieure (cm^3), A est la surface de la zone de l'échantillon (m^2), t est le temps (jour).

La perméabilité (PO_2) ($\text{cm}^3 \cdot \text{m}^{-2} \cdot \text{d}^{-1} \cdot \text{Pa}^{-1}$) des films a été calculée selon l'équation:

$$\text{PO}_2 = \frac{\text{OTR}}{P}$$

Où, P est la pression partielle d'oxygène dans la chambre supérieure.

Le coefficient de perméabilité à l'oxygène $P'O_2$ ($\text{mol} \cdot \text{m}^{-1} \cdot \text{s}^{-1} \cdot \text{Pa}^{-1}$) a été déterminé comme suit:

$$P'O_2 = \text{PO}_2 \times l$$

Où l (m) est l'épaisseur moyenne de l'échantillon de film, qui a été déterminée en cinq points répartis sur toute la zone d'essai.

II.2.4.11. Microscopie électronique à balayage (MEB)

Les observations au MEB ont été effectuées en utilisant un microscope électronique à balayage (SEM S-4500, Hitachi, Japon) avec une tension d'accélération de 2 kV et un détecteur pour les électrons secondaires. Pour l'observation des surfaces cryo-fracturées, les films sont préalablement congelés sous azote liquide, puis fracturés, montés et revêtus d'or / palladium sur des supports appropriés par pulvérisation ionique.

II.2.4.12. Activité antibactérienne

Les tests antibactériens sont effectués par la technique de contact direct sur gélose Mueller-Hinton, contre deux souches bactériennes cibles *Staphylococcus aureus* CIP 53156 et *Escherichia coli* 55B5 CIP 52170. Ces analyses sont réalisées afin d'évaluer à la fois, l'effet

antibactérien des charges et des films biocomposites. Les tests sont effectués sur des pré-cultures jeunes des deux bactéries dans le bouillon Mueller-Hinton. La concentration des suspensions bactériennes a été normalisée à 0,5 McFarland. Les charges à base d'OP (sous forme de poudres) sont déposées dans des puits de 10 mm de diamètre, obtenus avec un emporte-pièce sur le milieu gélosé. Dans le cas des matériaux, des disques de 10 mm de diamètre prédécoupés à partir des films biocomposites, sont déposés sur la surface de l'agar préalablement ensemencée avec les bactéries cibles. Les boîtes de Pétri sont incubées à 30°C pendant 24 heures. L'expression d'un effet antibactérien est définie par l'apparition d'une zone d'inhibition claire autour des puits/disques.

II.2.4.13. Tests de biodégradation

Des tests respirométriques ont été réalisés dans des conditions aérobies pour évaluer la biodégradabilité des charges à base d'OP, de la matrice PHBV et des composites OP/PHBV à 15% de charge. La méthode est adaptée de la norme américaine ASTM D5988-96, qui est une méthode d'essai standard pour la détermination de la biodégradation aérobie des matériaux plastiques dans le sol. Le CO₂ libéré étant proportionnel au pourcentage de substrat biodégradé, l'évolution du CO₂ mesure la dégradation ultime (c'est-à-dire la minéralisation) dans laquelle une substance est décomposée en ses produits finaux. Au préalable, les échantillons de film sont congelés dans de l'azote liquide puis broyés avec un broyeur domestique (Moulinex type DPA1, France) pour obtenir des particules de l'ordre de 1-2 mm.

Le sol utilisé dans cette étude provient du parc de l'Université de Montpellier (France) en avril 2017, après élimination de la couche de végétation superficielle. Les gros cailloux et les objets étrangers sont retirés manuellement pour obtenir un échantillon homogène. Le sol est séché à l'air libre pendant une semaine puis tamisé à travers un tamis de 2 mm. La teneur totale en matière sèche est déterminée en séchant le sol à 105°C jusqu'à un poids constant, elle est d'environ 97%.

La teneur en carbone des charges de grignon, de la matrice PHBV, des biocomposites et de la cellulose microcristalline est déterminée par analyse élémentaire.

Les essais de biodégradation sont effectués dans des récipients cylindriques en verre hermétiques (capacité de 1000 mL), contenant trois petits flacons en polypropylène ouverts (capacité de 60 mL). Le premier flacon contenait 25 g de sol sec mélangé avec des échantillons dont le poids correspondait à 50 mg de carbone. La teneur en eau des échantillons de sol est ajustée pour atteindre 80% de la capacité de rétention d'eau du sol (CRES). Le second flacon

contenait 10 ml de solution de NaOH (0,1 M) pour piéger le CO₂ produit par les microorganismes. Le troisième flacon contenait de l'eau distillée, afin de maintenir l'humidité relative à 100% à l'intérieur du récipient. Les récipients en verre sont fermés hermétiquement et incubés dans l'obscurité à 28 ± 1°C (Chevillard *et al.*, 2012).

Chaque semaine, les récipients en verre sont ouverts pour assurer le titrage en retour de l'excès de NaOH, qui n'a pas réagi avec le CO₂. Avant de titrer le NaOH résiduel avec une solution de HCl (0,1 M) en présence de thymophtaléine 0,10% (préparé dans l'éthanol 95,5), 5 ml de solution de chlorure de baryum (20% dans l'eau) sont ajoutés pour précipiter les ions carbonate. Les flacons contenant le sol sont pesés et une quantité appropriée d'eau est ajoutée afin de maintenir la teneur en eau constante, initialement fixée à 80% de CRES. Pendant cette procédure, les récipients en verre sont laissés ouverts pendant 2 minutes pour être aérés. A chaque dosage, un nouveau flacon contenant 10 ml de NaOH 0,1 M est introduit dans chaque récipient en verre avant d'être fermé et placé à l'obscurité à 28°C jusqu'à la prochaine mesure.

Les analyses de biodégradation comprenaient un échantillon témoin et un blanc. L'échantillon témoin était de la cellulose microcristalline, un matériau de référence positif bien connu par ses propriétés de biodégradation. L'échantillon blanc correspondait au sol seul, sans ajout d'une source externe de carbone. Toutes les expériences sont effectuées en triple.

Les résultats sont calculés après soustraction du CO₂ produit par le blanc. Le taux théorique maximal de CO₂ (CO₂ max (mg)) produit par l'oxydation totale du matériau est calculé à l'aide de l'équation suivante :

$$CO_{2 \max} = C \times \frac{44.01}{12.01}$$

Où (C) est la quantité de carbone de l'échantillon introduit dans le sol pour l'essai (mg).

Le pourcentage de biodégradation (B) est calculé par l'équation ci-dessous :

$$B = \frac{CO_2 \text{ matériau} - CO_2 \text{ blanc}}{CO_2 \max}$$

III. Résultats et discussion

***III.1. Dry fractionation of olive pomace
as a sustainable process to produce
fillers for biocomposites***

(Article n°1)

III.1. Dry fractionation of olive pomace as a sustainable process to produce fillers for biocomposites

Article publié dans le journal « Powder Technology »

Sarah Lammi^{1,2}, Abdellatif Barakat¹, Claire Mayer-Laigle¹, Djamel Djenane², Nathalie Gontard¹, Hélène Angellier-Coussy^{1*}

¹JRU IATE 1208 – CIRAD/INRA/Montpellier SupAgro/University of Montpellier, 2 place Pierre Viala, F-34060 Montpellier, France.

²Laboratory of Food Quality and Food Safety, Department of Agronomic Sciences, University of Mouloud MAMMARI, BP 17, 15000 Tizi-Ouzou, Algeria.

*Corresponding author : helene.coussy@umontpellier.fr - +33(0)4 99 61 24 32

Received 17 July 2017, Accepted 26 November 2017, Published 15 February 2018

DOI : 10.1016/j.powtec.2017.11.060

Résumé

Le grignon d'olive (OP) est le résidu agro-industriel de l'extraction de l'huile d'olive composé de pulpe résiduelle et de noyau. Ce travail vise à explorer la possibilité d'utiliser le fractionnement à sec (combinaison de procédés de broyage et de tri) pour produire des fractions riches en pulpe et en noyau avec la plus grande pureté et le meilleur rendement. Les caractéristiques physico-chimiques (composition, stabilité thermique, couleur, énergie libre de surface) des poudres obtenues ont été discutées en relation avec les procédés appliqués. Il a été démontré que le fractionnement à sec pouvait être utilisé avec succès pour transformer l'OP en fractions utiles en utilisant des procédés évitant la consommation d'eau et la génération d'effluents ou de coproduits. Les résultats ont révélé que la séparation de la pulpe du noyau en utilisant des sollicitations de friction dans un broyeur à boulets fonctionnant dans des conditions douces (2 min à 15 Hz) était aussi efficace que le fractionnement humide en termes de caractéristiques de poudres, atteignant un rendement total de 99,4% contre seulement 82,1% dans le cas du fractionnement humide et sans utiliser l'eau, alors qu'un rapport eau : biomasse de 5 : 1 était nécessaire pour le fractionnement humide. Les poudres produites présentaient une composition biochimique (soit riche en lignine ou en cellulose) et une énergie libre de surface contrastées, et étaient thermiquement stables jusqu'à au moins 210°C. Il a été conclu qu'il

pourrait être intéressant de les utiliser comme ressources brutes pour la production de charges qui seront incorporées dans des matrices de polymères pour produire une gamme de biocomposites.

Mots clés : grignon d'olive, fractionnement à sec, broyage, tri, caractérisation.

Abstract

Olive pomace (OP) is the agro-industrial residue of olive oil extraction composed of residual pulp and stone. This work aims at exploring the possibility of using dry fractionation (combination of grinding and sorting processes) to produce pulp-rich and stone-rich fractions with the highest purity and yield. The physical-chemical characteristics (composition, thermal stability, color, surface free energy) of the obtained powders were discussed in relation to the applied processes. It was shown that dry fractionation could be successfully used to convert OP into valuable fractions using processes avoiding the consumption of water and the generation of effluents or co-products. Results revealed that the separation of the pulp from the stone using friction solicitations in a ball mill operating in mild conditions (2 min at a frequency of 15 Hz) was as efficient as wet fractionation in terms of powder characteristics, achieving a total yield of 99.4% against only 82.1% in the case of wet fractionation and without using water while a water: biomass ratio of 5:1 was required for wet fractionation. Produced powders exhibited contrasted biochemical composition (either rich in lignin or cellulose) and surface free energy, and were thermally stable up to at least 210°C. It was concluded that they could be interestingly used as raw resources for the production of fillers that will be further incorporated in polymer matrices to produce a range of biocomposites.

Keywords: olive pomace, dry fractionation, grinding, sorting, characterization.

III.1.1. Introduction

In recent years, an increasing public concern has been noticed over the harmful effects of fossil-based plastic materials on the environment. The development of alternative materials that are both biodegradable and produced from natural resources is thus gaining considerable attention owing to environmental, economical, societal and technical advantages as compared to conventional synthetic polymers (Crocker, 2008). Lignocellulosic fillers based biocomposites constitute a promising answer since they allow to joint current requirements regarding the need to reduce our dependence to fossil resources, environmental pollution, while offering a way of sustainable eco-conversion of lignocellulosic solid wastes and by-products. A large range of

lignocellulosic residues obtained from agro-food industries have already been explored and effectively used as fillers in biocomposites due to their interesting properties, biodegradability, high availability and low price (Kengkhetkit and Amornsakchai, 2014; Nascimento *et al.*, 2010). Among this available lignocellulosic biomass, one valuable lignocellulosic biomass is olive pomace (Djidjelli *et al.*, 2007; Papanicolaou *et al.*, 2011). Recently, some studies were devoted to the use of olive pomace (OP), as reinforcing agents in polymer matrix (Gharbi *et al.*, 2014; Naghmouchi *et al.*, 2015). These authors consider the biocomposites based on olive pomace interesting and likely to become promising alternative to conventional plastic materials; their application can be envisaged in different fields: to produce containers and foods packaging, the automotive industry, in building, and indoor furniture as well as in gardening products, park benches., etc.

Over 95% of the world's olive trees are found in the Mediterranean basin, due to environmental factors that make the soil and the climate ideal for their cultivation, flowering and production of their fruit (Rubio-Senent *et al.*, 2012; Cavalheiro *et al.*, 2015). Olives are harvested in the autumn and winter and are mainly processed for olive oil production. Among the emerging producing countries, Algeria is considered as a new extra-virgin olive oil exporter. The area of the olive-growing orchard is annually increasing, reaching more than 38% of the total agricultural surface in the 2015/2016 harvest, with a production of 470 thousand tons of olive oil (ONFAA, 2016). *Chemlal* is the most common olive cultivar grown in this country, with 40% of the orchards. This olive variety is distributed mainly in north-central Algeria, particularly in Kabylia, its traditional area. Recently, this variety has become associated with high olive oil production, due to its large distribution and its high olive oil yield, *i.e.* 18 L/100 kg of olives (Haddadi and Yakoub-Bougdal, 2010; Bengana *et al.*, 2013; Abdessemed *et al.*, 2015). One hectare of olive tree originates on average about 2500 kg of olives (Rodrigues *et al.*, 2015). Generally, 100 kg of olives produce 20 liters of oil, 35 kg of olive pomace and 100 liters of wastewater (Nefzaoui, 1987). So, about 875 kg of OP are generated by hectare. It is estimated that the production of OP reaches 2,881,500 tons/year worldwide (Ravindran and Jaiswal, 2016).

OP is not easily degradable under natural conditions and its disposal causes serious environmental problems, particularly in the Mediterranean countries, where abundant quantities are produced during a short period of the year. It is responsible of inhibition of microorganisms' activities, reduction in the seed germination, and alteration of soil porosity and humus concentration. This is mainly due to its high phenolic content (some 98% of the total phenolic

compounds of the olive fruit), volatile fatty acids, low pH and relatively high salinity (Cardelli and Benitez, 1998). Thus, in order to reduce its harmful environmental impact, several works have been recently dedicated to its valorization in various fields, such as animal feed (Nefzaoui, 1983), composting (Plaza *et al.*, 2008), energy and biofuels (Benavente and Fullana, 2015; Rajaeifar *et al.*, 2016), cosmetics (Rodrigues *et al.*, 2015), food industry (Antónia Nunes *et al.*, 2016), and pharmaceutical areas (Barbaro *et al.*, 2014). Only few studies are describing the use of olive pomace (quasi exclusively olive stone) as raw materials for the production of reinforcing fillers (Papanicolaou *et al.*, 2011; Naghmouchi *et al.*, 2015; Gharbi *et al.*, 2014)

The olive fruit can structurally be separated into three compartments, *i.e.* (1) the skin, called epicarp, which contains chlorophylls, carotenoids and anthocyanins that account for the color, (2) the pulp or flesh, called mesocarp, which is the reserve supply of all the constituents (oil, ashes, proteins, cellulose and lignin), and (3) the stone, called woody endocarp, which contains the seed and is mainly composed of crude cellulose (Bianchi, 2003). OP is a mixture of residual skin, pulp and fragments of the crushed stone (Rigane *et al.*, 2012). The distribution of the various constituents and the physical-chemical characteristics of the OP are complex and fluctuate according to the fruit variety, cultivation practices, geographical origin, stage of maturity, storage time and process of oil extraction (Nefzaoui, 1983; Vlyssides *et al.*, 1998). The structural heterogeneity and complexity of OP constitute one of the obstacles to subsequent eco-conversion. Existing pre-treatments used to separate the pulp from the olive stone are based on chemical multistep processes consuming large amounts of water, chemicals and generating significant effluents that are necessary to treat. They include cleaning and washing with hot water (Djidjelli *et al.*, 2007; Papanicolaou *et al.*, 2011; Koutsomitopoulou *et al.*, 2014; Hammoui *et al.*, 2015; Hassaini *et al.*, 2017), with hot water and solvent (acetone-hexane) to remove pulp (Djefel *et al.*, 2015), or hot treatment by solvent (acetone and/or hexane) followed by separation with ventilation of the stone from the pulp (Gharbi *et al.*, 2014; Naghmouchi *et al.*, 2015). To raise this bottleneck and allow a better exploitation of OP, we believe that it would be more relevant to apply a non-polluting fractionation process in order to produce contrasted powders whose properties will be adapted to composite applications. In this context, dry fractionation appears as a promising alternative for the production of pulp-rich and stone-rich fractions without any consumption of water nor chemicals and therefore generate very few wastes (Barakat *et al.*, 2014; Licari *et al.*, 2016). Dry fractionation processes combining grinding and sorting technologies (air classification, electrostatic separation or sieving) have attracted a great deal of attention due to their use in various fields including electronic waste

valorization, food industry, pharmaceuticals, ceramics and materials science (Hemery *et al.*, 2011; Chuetor *et al.*, 2015). Dry fractionation has been widely applied to several lignocellulosic biomasses with promising results, namely wheat straw (Barakat *et al.*, 2014; Berthet *et al.*, 2017), rice straw (Chuetor *et al.*, 2015), bagasse (Licari *et al.*, 2016) and rapeseed press cake (Basset *et al.*, 2016). To our knowledge, these processes have never been applied to the treatment of crude olive pomace.

Furthermore, several studies demonstrated that the development of biocomposites at industrial scale requires a better control of the filler/matrix interface. The intrinsic characteristics of filler, mainly composition and surface properties are considered as key criteria for their use in composite materials. Indeed, it is well known that the barrier proprieties and the mechanical performances of a composite material strongly depend on the quality of the adhesion between the two components (Baley *et al.*, 2006; Berthet *et al.*, 2015c; Hassaini *et al.*, 2017).

In this context, the present study aimed at exploring the potentiality of using dry fractionation to produce pulp-rich and stone-rich fractions with the highest purity and yield from crude OP, that would be further used as raw resources for the production of fillers. Different milling modes (compression, shearing and impact, friction) were considered and combined by selecting appropriate equipment (knife milling, impact milling, ball milling). The ground powders were then separated in interesting fractions by sorting steps (sieving or electrostatic fractionation). Intrinsic properties (color, biochemical composition, surface free energy and thermal stability) of the resulting fractions were characterized and discussed in relation to the applied dry fractionation route. A wet separation process was tested for comparison. Finally, in view to draw an optimized biorefinery scheme for the conversion of OP, different added-value routes of valorization were proposed for each resulting powders, besides to their potential application as fillers in biocomposites.

III.1.2. Materials and methods

III.1.2.1. Materials

Olive pomace was obtained from the oil extraction of the *Chemlal* variety using a traditional press system. It was kindly supplied by local olive producers in the region of Azazga (Tizi-Ouzou) in north-central Algeria, in February 2016. This residue was composed of partially crushed stones, pulp and skin. Olive pomace was dried in ambient air for three days and then,

stored at 4°C and shielded from the light until its use. Only one batch of olive pomace was considered in the present study.

Sulfuric acid, arabinose, xylose and glucose (SIGMA-ALDRICH), formamide, diiodomethane (Acros Organics, Geel, Belgium), ethylene glycol (Aldrich chemical Co. Inc., Milwaukee, USA) and glycerol (Merck, Darmstadt, Germany) were used for characterization of olive pomace fractions.

III.1.2.2. Fractionation of olive pomace

Fractionation of crude olive pomace was carried out to produce pulp-rich and stone-rich fractions following different routes (Figure 12). All the obtained fractions came from the same initial olive pomace batch.

III.1.2.2.1. Wet fractionation

200 g of crude OP were mixed with 1 L of distilled water and left during 24 hours at room temperature. Then, this suspension was placed under agitation at 400 rpm and 30°C for 24 hours. The mixture was first sieved through a 1 mm sieve in order to separate the humid stone-rich fraction from the humid pulp-rich fraction. The residual liquid fraction was centrifuged at 10.000 rpm during 10 min in order to separate the pulp-rich fraction from the liquid effluent. The two obtained fractions were dried in an oven at 50°C during 24 hours and were designated as wS (stone-rich fraction) and wP (pulp-rich fraction) (Figure 12).

III.1.2.2.2. Dry fractionation

The crude OP was first ground using a knife milling (SM 300, Retch, Germany) with a grid size of 4 mm, and then passed through a second grinding with a grid size of 2 mm to obtain the fraction F0. Then, two types of sorting were tested in order to separate the pulp from the stone, *i.e.* sorting according to the particle size by sieving (route A1), sorting according to the particle surface charge by electrostatic separation (route A2). Given the crumbly character of the pulp tissue that can be easily mechanically detached from the stone, another sorting route has been investigated, *i.e.* friction (route B) using mild conditions of ball milling without preliminary grinding of crude OP (Figure 12).

III. Résultats et discussion

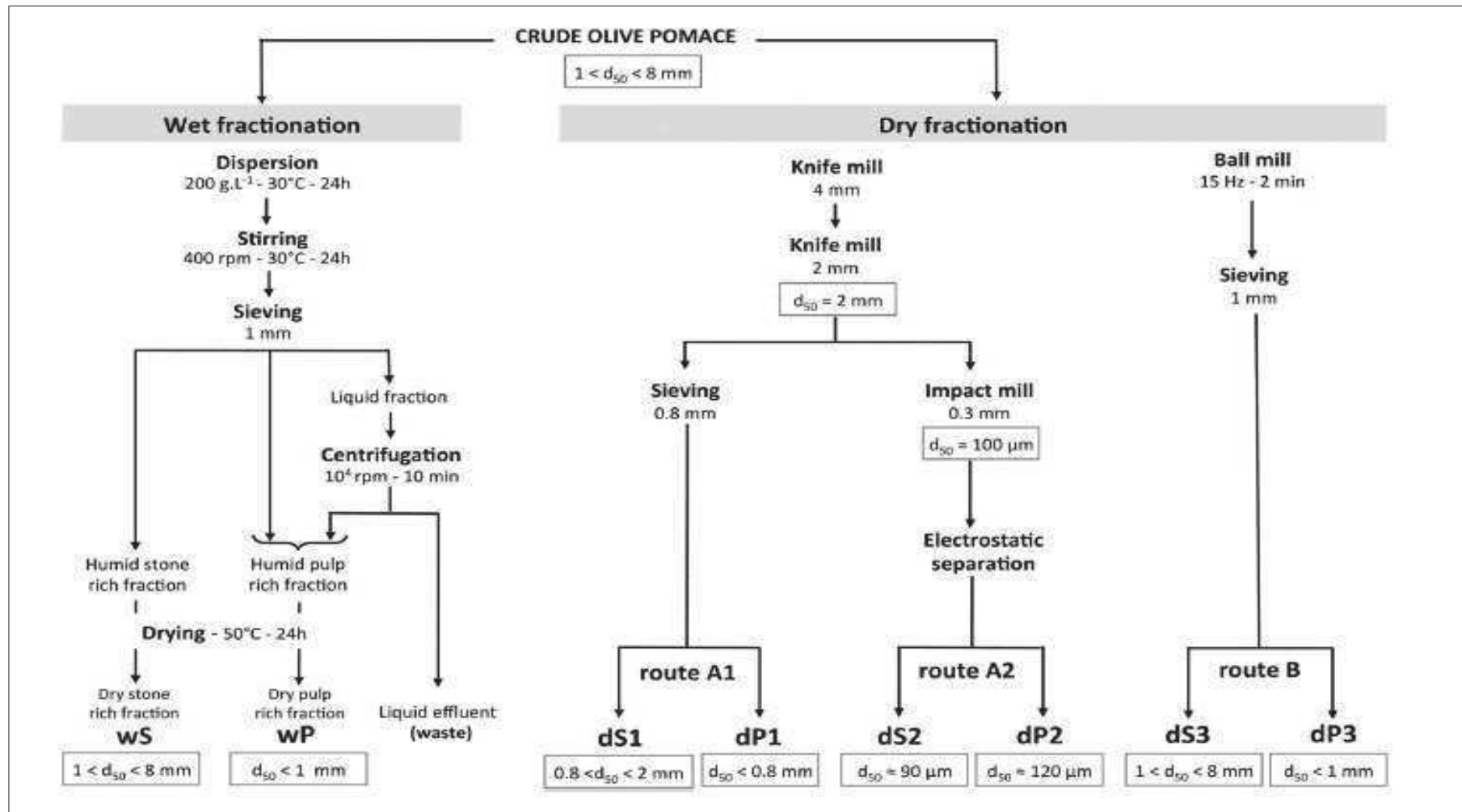


Figure 12: Fractionation process of crude olive pomace investigated to obtain stone (S) and pulp (P) rich fractions.

Sorting by sieving (route A1). 200 g of F0 sample were passed into a ROTEX mechanical sieve through a 0.8 mm mesh for 10 minutes. Two fractions were obtained. The first one contained the particles with a diameter greater than or equal to 0.8 mm and corresponded to the stone-rich fraction (dS1) while the fraction constituted of particles with a size smaller than 0.8 mm represented the pulp-rich fraction (dP1).

Electrostatic sorting (route A2). 200 g of F0 were further ground using impact milling (Hosokawa-alpine, type UPZ, Augsburg, Germany) with a grid size of 0.3 mm. Resulting ultrafine particles displayed a median diameter, measured by laser granulometry (d_{50}), of about 100 μm (see paragraph 2.3.1). A pilot-scale TFS (TEP System, Tribo Flow Separations, Lexington, USA) was used for the electrostatic fractionation (EsF), using fine particles as starting material. This technology is based on the separation of particles according to their surface properties (chemical composition and charges), in which lignocellulosic particles are trained in a charging line where they are charged by tribo-electricity. The charged particles are subsequently moved to a separator chamber containing a high electrical field (10 kV), generated by two high voltage electrodes. The positively charged particles are attracted by the negative electrode (F+) and the negatively charged particles are attracted by the positive electrode (F-) (Chuetor *et al.*, 2015; Barakat *et al.*, 2014). Positively charged fractions are generally richer in proteins and water-soluble carbohydrates in comparison to the initial F0 material. By contrast, negatively charged fractions are rather richer in lignin and structural carbohydrates (and thus cellulose) in comparison to F+ (Basset *et al.*, 2016). The powders obtained with this process are designated by (dS2) and (dP2) for the stone-rich fraction and the pulp-rich fraction, respectively (Figure 12).

Sorting by friction and sieving (route B). 200 g of crude olive pomace were submitted to vibrations using a ball mill (MM 400, Retch, Germany), under a frequency of 15 Hz for 2 min in the presence of three steel balls with a diameter of 15 mm. The obtained powder was then sieved into a ROTEX mechanical sieve 1 mm mesh for 10 minutes, in order to separate the pulp from the stone (Figure 12). Coarse particles with a diameter greater than or equal to 1 mm were retained on the sieve and corresponded to the stone-rich fraction (dS3), the fine particles were recovered from the bottom of the sieve and represented the pulp-rich fraction (dP3).

III.1.2.3. Characterization of olive pomace fractions

All fractions, except those obtained by electrostatic fractionation (EsF), were ground with a ball mill (MM400) at a frequency of 25 Hz for 2 min in order to get homogenous samples before being analyzed. This was not necessary in the case of dS2 and dP2 fractions because they were already fine enough for further analyses.

III.1.2.3.1. Particle size

In order to pilot some fractionation processes, *i.e.* electrostatic sorting in the present study, it was necessary to control the particle size distribution. The particle size distribution was measured by laser diffraction using a laser diffraction particle size analyzer Mastersizer 2000 (Malvern Instruments Ltd., United Kingdom). For that purpose, powders were suspended in ethanol 95% (v/v) directly in the experimental cell. The particle median diameter (d_{50}) was determined in order to characterize the fractions.

III.1.2.3.2. Color

The color attributes of each fraction were measured with a colorimeter (Minolta), using the L^* , a^* , b^* color system. The L^* value characterizes the luminance while a^* and b^* values are indicators of sample color (a^* from green to red and b^* from blue to yellow). The measurements were made in duplicate. The total color difference (ΔE) between the fraction and the starting biomass was calculated following Equation 1 (CIE, 2004).

$$\Delta E = [(L^* - L_{F0}^*)^2 + (a^* - a_{F0}^*)^2 + (b^* - b_{F0}^*)^2]^{0.5} \quad \text{Equation (1)}$$

with L^* , a^* and b^* the color components of the obtained powder. L_{F0}^* , a_{F0}^* and b_{F0}^* are the color components of the starting biomass.

III.1.2.3.3. Biochemical composition

The composition of olive pomace fractions was measured after concentrated acid hydrolysis according to Barakat *et al.* (2014). The lignin content in samples was determined by the Klason method. HPLC analysis enabled to quantify monosaccharides (glucose, xylose, and arabinose). The sugars analysis was done with a combined HPLC water system, using a BioRad HPX-87H column at 40°C and 0.3 mL.min⁻¹. All analyzes were carried out in triplicate for each OP fraction. The concentration of cellulose was determined by the glucose level whereas xylose and

arabinose were used to calculate the hemicellulose concentration in the lignocellulosic complex of each fraction. Humidity and ashes contents were determined by thermogravimetric analysis (TGA) under air (see paragraph 2.3.4) by considering the weight residue at 130°C and 900°C, respectively. Protein contents of the different fractions were determined with (N x 6.25) according to Jones (1941), after estimation of the nitrogen content in each sample by elementary analysis.

III.1.2.3.4. Thermogravimetric analysis

Thermogravimetric analysis (TGA) was carried out in order to study the thermal stability of the different fractions. Samples (about 10 mg) were heated from room temperature up to 900°C, at a heating rate of 10°C.min⁻¹ under air and nitrogen flow (50 mL.min⁻¹). The degradation temperature (T_{peak}) was measured from the maximum value of weight loss derivative.

III.1.2.3.5. Contact angle measurements

Contact angle measurements were carried out on tablets obtained by compression of powders in a mold (diameter of 13 mm) using a hydraulic press (Perkin-Elmer) and a pressure of 10 tons. Resulting tablets were dried during 30 min under vacuum and in presence of silica gel before measurement. Contact angle measurements were performed using a Digidrop (GBX, France) instrument. The volume of the drop was 3 µl in all cases using a micro-syringe. The measurement of the contact angle was carried out at the moment of the stabilization of drop above the surface of the pellet. Five reference liquids were used in order to estimate the surface free energy of compressed powders (polar and dispersive components), *i.e.* distilled water, formamide, diiodomethane, ethylene glycol and glycerol. Surface energy values were calculated by using the Owens-Wendt formula (Owens and Wendt, 1969). The work of adhesion between two solid constituents, *i.e.* a polymer matrix (m) and a filler (f) can be predicted using the following harmonic-mean equation:

$$W_{mf} = 2x \left(\sqrt{\gamma_m^d \gamma_f^d} + \sqrt{\gamma_m^p \gamma_f^p} \right) \quad \text{Equation (2)}$$

III.1.3. Results and discussion

The two fractions (pulp-rich and stone-rich fractions) obtained by wet fraction processed were considered as the targeted references in order to evaluate the efficiency of the different dry fractionation alternative routes proposed in the present study. The first parameter indicating the

efficiency of the separation was the color, the pulp being very dark (almost black) and the stone yellow/brown. The other characteristics were the biochemical composition, the thermal stability and polarity of powders. In addition to the evaluation of the dry fractionation efficiency, results have also been useful to propose potential routes of valorization for all olive pomace fractions.

III.1.3.1. Wet fractionation

Color is an intrinsic characteristic of the olive fruit. Literature reports that the pigment concentration greatly differs according to the variety, ripeness state, moment of picking and chloroplast pigment distribution through the tissues of the fruit (Gandul-Rojas *et al.*, 2000; Roca and Minguez-Mosquera, 2001). In contrast to the stone, whose growth stops after about two months, the pulp continues to grow through ripening. Olive contains greater amounts of chloroplasts in skin and pulp that are able to carry out photosynthesis, explaining that these two tissues retain chlorophylls and carotenoids pigments more than the stone.

A change in the color of the obtained fractions was thus considered as a first indicator of fractionation efficiency. Washing the crude olive pomace with water allowed to obtain two contrasted fractions, *i.e.* a dark brown (almost black) fraction corresponding to the pulp-rich fraction and a yellow/brown fraction corresponding to the stone-rich fraction (*Annex*). These visual observations were confirmed by the measurement of the color parameters (L^* , a^* , and b^*). According to the Commission Internationale de l'Eclairage (2004), L^* representing the luminance, ranges from 0 (black) to 100 (white) while the two chromatic components, a^* (from green to red) and b^* (from blue to yellow), range from -120 to +120. The starting biomass (F0), corresponding to a mixture of pulp and stone, exhibited L^* , a^* and b^* values of respectively 43.6, 9.4 and 15.7 (Table 11). The stone-rich fraction (wS) was significantly clearer than F0, with a higher value of L^* (65.8), and more yellow, with a slightly lower value of a^* (5.3) and higher value of b^* (18.6). On the opposite, the pulp-rich fraction (wP) was considerably darker, with a lower L^* value (34.9), and browner with a higher value of a^* (9.2) and lower value of b^* (11.6) (Table 11). It can be concluded, as expected, that washing in water is an efficient treatment to produce contrasted fractions, what justifies its application by several authors to remove the pulp from the stone (Koutsomitopoulou *et al.*, 2014; Hammoui *et al.*, 2015; Hassaini *et al.*, 2017).

Table 11: Color parameters of OP-based fractions

	F0	Wet fractionation		Dry fractionation					
		Ws	wP	dS1	dP1	dS2	dP2	dS3	dP3
L^*	43.6±0.2	65.8±0.9	34.9±0.6	55.4±0.7	37.8±0.0	56.7±1.5	44.9±1.1	51.0±0.5	29.1±0.8
a^*	9.4±0.0	5.3±0.1	9.2±0.0	8.0±0.0	9.7±0.0	5.5±0.0	7.3±0.0	8.6±0.0	9.5±0.1
b^*	15.7±0.1	18.6±0.1	11.6±0.1	17.8±0.1	13.2±0.0	14.6±0.0	12.2±0.3	19.4±0.2	13.0±0.3
ΔE	-	22.7±0.9	9.6±0.6	12.1±0.7	6.3±0.1	13.7±1.5	4.3±0.1	8.3±0.6	14.8±0.9

The biochemical composition was a second quantitative parameter to evaluate the separation efficiency of the two main tissues of olive pomace (Table 12). The starting biomass (F0) used in this study recorded a concentration of 14.8% in cellulose, 14.7% in hemicellulose and 37.8% of lignin. These values are in agreement with those found by Haddadin *et al.* (2009), which are about 18.3% for cellulose, 15.7% for hemicellulose and 38.5% for lignin. However, they differ from those registered by Gharbi *et al.* (2014), who found values of 25% in cellulose, 35% in hemicellulose and 35% in lignin. Concerning proteins and ashes, contents of 4.5% and 3.5% were respectively recorded for F0. These results are not far from those reported by Haddadin *et al.* (2009), which ranged from 5.5 to 6% for proteins and between 7.7 and 15% for ashes. As we have already reported, slight discrepancies between values are due the fact that the composition of olive pomace is variable, mainly depending on the fruit variety, growing region, and process of oil extraction (Nefzaoui,1983).

Concerning the powders produced by wet fractionation, results showed that the stone-rich fraction was characterized by higher cellulose and hemicellulose contents with a total value of 33% d.b. against 18% d.b. for the pulp-rich fraction. The two fractions could also be distinguished by their lignin concentration, with a significant lower lignin content in the stone-rich fraction (37 % d.b.) than in the pulp-rich fraction (43 % d.b.) (Table 12). These results are concordant with values reported in literature. Several authors agree that the stone contains higher contents in cellulose as compared to the pulp, with values ranging from 15 to over 70% (Maymone *et al.*, 1961; García-Maraver *et al.*, 2013; Rabouhi *et al.*, 2010); for Motos *et al.* (2010) and Rodríguez *et al.* (2008), the main components in stone are cellulose (28.1–40.4%), hemicelluloses (18.5–32.2%) and lignin (25.3–27.2%). On the other hand, lignin together with polyphenols is known to be more abundant in the pulp (Rubio-Senent *et al.*, 2012).

III. Résultats et discussion

Table 12: Biochemical composition (dry basis) of different olive pomace fractions produced by wet and dry process

	F0	Wet fractionation		Dry fractionation					
		wS	wP	dS1	dP1	dS2	dP2	dS3	dP3
Yield (%)	100	65.5	16.6	59.9	17.9	71.2	24.8	70.6	28.8
Humidity (%)	6.2±1.5	4.1±0.0	4.3±0.0	4.6±0.0	4.7±0.0	4.9±2.0	3.9±0.0	3.5±0.0	4.2±0.1
Ashes (%)	3.5±1.3	1.9±0.1	7.2±0.4	4.7±0.4	6.6±0.0	3.9±1.8	6.1±0.1	5.5±0.0	7.6±0.1
Cellulose (%)	14.8±1.3	14.2±1.0	11.5±0.4	15.1±1.3	13.0±1.0	15.7±1.1	10.2±1.6	15.7±0.8	9.2±0.0
Hemicellulose(%)	14.7±1.3	18.1±0.5	6.9±0.3	16.2±1.2	11.2±2.4	15.4±0.7	11.5±1.7	17.1±0.5	6.9±0.1
Lignin (%)	37.8±2.1	37.1±2.6	43.5±3.5	34.1±2.9	38.9 ±3.2	35.7±1.4	41.5±5.1	39.2±3.5	44.3±4.4
Glucose (%)	16.4±1.5	15.8±1.1	12.7±0.4	16.8±1.5	14.5±1.1	17.4±1.3	11.4±1.8	17.4±0.9	10.2±0.1
Xylose (%)	16.6±1.4	20.5±0.5	7.9±0.3	18.3±1.4	11.5±1.0	17.4±0.8	13.0±2.0	19.4±0.6	7.8±0.1
Proteins (%)	4.5	0.4	12.4	1.6	7.8	3.0	5.6	1.1	10.9
C (%)	47.91	47.10	49.82	47.20	48.64	48.12	48.95	46.98	50.14
H (%)	6.11	5.91	6.33	6.03	6.22	6.42	6.48	6.33	6.77
N (%)	0.72	0.07	1.98	0.25	1.25	0.48	0.90	0.18	1.75

Important differences were also noticed concerning the protein content, with a higher content in the pulp-rich fraction (12 % d.b.) and only traces in the stone-rich fraction (0.43%) (Table 12), in accordance with already published values (Maymone *et al.* 1961, Theriez and Boule 1970, Heredia *et al.* 1987, Bianchi 2003).

Finally, results showed that the stone-rich fraction was also characterized by a significant lower ashes content (around 2 % d.b.) as compared to the pulp-rich fraction (around 7% d.b.) (Table 12). This tendency was previously demonstrated by Maymone *et al.* (1961) who reported an ashes content of 0.8% for the stone against 4% for the pulp, whereas Ghanbari *et al.* (2012) reported values ranging from 0.01 to 0.68% for the stone. However, it is worth noting that the ashes content recorded for our stone-rich fraction was slightly higher than values reported for the stone. This can be ascribed to an incomplete separation of the stone from the pulp following our wet fractionation, or also to a bad washing of the olives at the mill and, consequently, to the persistence of soil in the olive pomace resulting from the presence of fruits collected at ground during the harvest. On the other hand, there is no work in the literature focusing on olive pulp indicating characteristic values concerning its biochemical composition; most publications transmit mainly composition of the crude olive pomace and only some of them, reporting data about the stone composition.

Different characteristics for the pulp-rich and stone-rich fractions obtained after washing the crude OP in water confirmed the efficiency of this treatment for the separation of OP in fractions richer in different tissues. Indeed, soaking the olive pomace into distilled water for 24 hours allows weakening the pulp tissue owing to water absorption, thus making easier the peeling of the pulp from the stone upon the second step of stirring. Furthermore, after sieving the stone sample is abundantly washed with water to remove any trace of residual pulp, allowing obtaining a purer fraction.

However, despite the efficient separation, this process presents some disadvantages. First, it is necessary to note the consumption of a large quantity of water (5 volumes of water per 1 volume of biomass), which is accompanied by the generation of a liquid effluent (Figure 12), whose composition seems to be similar to that of olive wastewater. This effluent, presenting an additional environmental problem, must be treated or co-valorized. Secondly it is likely that a prolonged contact of olive pomace with water (48 hours in this study) would promote the loss of some interesting hydrophilic substances (including carbohydrates, organic acid, phenols, polyphenols) in the aqueous phase (Rubio-Senent *et al.*, 2012), which can reduce the

valorization fields of the obtained fractions. Additionally, the loss of matter upon the wet fractionation process is not negligible, with a yield of about 82 %. Finally, obtained lignocellulosic fractions will require a drying step before further treatments such as grinding and then, incorporation as fillers in a polymer matrix. This is the reason why dry fractionation has recently emerged as a sustainable alternative to conventional wet treatments for the valorization of the lignocellulosic biomass stemming from agro-food industries.

III.1.3.2. Dry fractionation

The selected dry fractionation routes have been applied to the raw biomass in order to separate the pulp from the stone with the highest yield and lowest consumption of energy while preserving the integrity of the fractions. First, crude OP was beforehand subjected to two successive grindings in a knife mill in order to reduce the size of the particles from the cm down to the mm. This obtained powders followed then two different dry fractionation routes: (1) sorting by sieving and (2) electrostatic separation. Considering the crumbly nature of crude OP another fractionation route has been investigated, i.e. (3) friction mode, using mild conditions of ball milling without preliminary grinding. In this latter process the coarse particles correspond to the stone-rich fraction, which resist to the low friction forces due to its richness in cellulose. In contrast, the fine particles of the pulp-rich fraction are more brittle and consequently crumbly under the influence of applied frictions, owing to its low cellulose content. Indeed, according to Ciolacu *et al.*, (2008), the crystallinity of the cellulose is at the origin of its resistance. The resulting fractions were compared to both the starting biomass (F0) and the reference fractions obtained by wet fractionation, in terms of color and biochemical composition in order to assess the efficiency of the applied dry fractionation routes.

Colorimetric parameters (L^* , a^* , and b^*) varied according to the fraction and applied treatment. As previously observed for the wet fractionation, stone-rich fractions (dS1, dS2 and dS3) were globally clearer than F0, with higher L^* and b^* values and lower a^* values. For stone-rich fractions, L^* ranged from 51 to 56.7, values of b^* between 14.6 and 19.4, and a^* of 5 and 8.6. On the opposite, pulp-rich fractions (dP1, dP2 and dP3) were darker (lower L^* and b^* values and higher a^*) than F0, with L^* values ranging from 29.1 to 44.9, b^* around 12-13, and a^* around 7-10 (Table 11). Considering the results of ΔE , it can be noted that the most contrasted pulp and stone-rich fractions in term of color were obtained by wet fractionation with values of 9.6 and 22.7 respectively. For the dry fractionation, the pulp powder produced by friction (dP3) shows the greatest

difference in the color compared to F0 with ΔE of 14.8; on the other hand, the stone-rich fraction (dS3) shows the lowest difference with starting biomass compared to dS1 and dS2 fractions, with a value of 8.3 (Table 11). For the fractions obtained by sieving and electrostatic sorting, the obtained results don't allow to estimate the efficiency of separation at this stage of analysis.

The biochemical composition was also determined for different fractions. The analysis of the biochemical composition confirmed thus recorded for the wet process and also in accord with the literature (García-Maraver *et al.*, 2013; Rabouhi *et al.*, 2010) for OP composition. Indeed, the stone-rich fractions exhibited globally a higher cellulose-hemicellulose concentration, with about 16% of cellulose and of 17% hemicellulose in the fractions of stone, and 9-13 % of cellulose and 7-11 % of hemicellulose in the fractions of pulp whereas; the pulp- rich fractions were richer in lignin (38-44 %), proteins (5-10 %) and ashes (until 7 %) with regard to the stone-rich fractions which exhibit concentrations of 34-39 %; 1-3 %; 3-5 % for lignin, proteins and ashes respectively. The most contrasted pulp-stone couple and which differs from the other fractions, is obtained by friction; with lignin, protein and ashes contents of 44.3; 10.9 and 7.6 % respectively for dP3, and cellulose-hemicellulose concentrations exceeding 32 % for the dS3 fraction.

These results confirm that the fractionation process significantly affects the characteristics of the produced powders. The differences in the biochemical composition are related to the origin of the plant tissues and their localization in the cell wall of the olive fruit. Thus, the intensity of the color depends on the ratio between the stone and the pulp tissues in each fraction and consequently on its composition, which are the product of the solicitation and forces of applied processes.

The best results were obtained by sorting using friction solicitations in a ball milling owing to the crumbly nature of crude olive pomace. Indeed, applying a low vibration force during a short time (15 Hz / 2 min) was sufficient to remove the superficial layers of the pulp tissue that adhered to the stone, without grinding and thus avoiding mixing it with the pulp. A subsequent sieving step was necessary to separate the two constituents. Though, these operating conditions was very efficient to isolate a almost pure pulp-fraction but were not sufficient to completely purify the stone. Indeed, the applied frequencies didn't allow to remove the final layer of pulp which is strongly adhered to the stone. This explains the ΔE and the composition values

obtained for the fraction (dS3), which shows the highest rate of lignin (39%) and ashes (more than 5%) (Table 12), compared to other stone-rich fractions obtained by dry and wet process.

The compositions values obtained for fractions dS3 and dP3 closed to those obtained for wS and wP suggested that friction process allow the separation of the pulp from the stone with a greatest efficiency. However, the higher value of ΔE measured, show that the applied frequencies didn't allow removing the thin final layer of pulp, which is strongly adhered to the stone.

It was shown that dP1, dS1, dP2 and dS2 fractions displayed intermediate results in terms of color and composition (Tables 11 and 12). The reason of poor separation in the case of sieving and electrostatic sorting may be related to the two successive grinding operations applied to the crude OP before fractionation. Indeed, the knife milling steps destroyed the initial organization of the tissues in the raw biomass, reduces the size of particles and consequently, promotes mixing between the two compartments of the fruit *i.e.* pulp and stone. This effect is even more accentuated with the electrostatic process due to an additional grinding step (impact milling) before sorting (Figure 12). d_{50} (volume median diameter) values were respectively 100, 88 and 124 μm for F0, dS2 and dP2. The difference in size between dP2 and dS2 could be related to differences in composition, particles richer in cellulose being for prone to grinding. In the case of electrostatic sorting, this effect could be hindered by making successive passages of the biomass in the electrostatic system, as suggested in the works of Chuetor *et al.* (2015) for rice straw and by Basset *et al.* (2016) for rapeseed oil cakes.

On the other hand, yields of production were also strongly affected by the selected processes. The highest yield was recorded for the friction fractionation with only 0.6% of losses, followed by electrostatic sorting and sieving with losses of 4% and 22.2% respectively, against 17.9% for the wet fractionation (Table 12). These results were directly related to the applied treatment and depend on the number of grinding and separation steps. Indeed, friction was the shortest route (Figure 12). For the two other dry fractionation routes, losses were due to the biomass that remained adhered to the equipment in the multiple stages of the process. In addition, the results showed that the stone-rich fraction represents the most important part of the olive pomace used in this study.

The recorded yields of stone and pulp-rich fractions vary according to the applied process; rates of 16 to 28% are recorded for the pulp-rich fractions, and between 59-71% for the stone-rich fraction. As reported by Theriez and Boule (1970), this is one of the characteristics of olive varieties intended for the production of oil.

Based on the obtained results of our fractions and the literature data, we can admit that on the whole, both wet and dry fractionation processes applied in this study allow to separate the pulp and stone tissues but, at different degrees of purity. Fractionation routes were classified in terms of separation efficiency in the decreasing following order: in the first one the wet and dry fractionation by friction with a similar efficiency, followed by sieving sorting and electrostatic separation, which are less efficient than the first processes. Therefore, in the perspective to reduce the environmental impact of OP, it is clear that for an ecological and long-term solution that may be applied at industrial scale, dry fractionation by friction is more relevant option.

III.1.3.3. Potentiality of using OP-based fractions as raw resources for the production of fillers

In response to the growing environmental awareness, concepts of sustainable development and eco-friendly materials have become a necessity in order to preserve the environmental resources while improving economic activities (López *et al.*, 2012). In this context, the conversion of OP into reinforcing fillers for the production of biocomposites would allow transforming an abundant waste into an added-value product. The thermal stability of the constituents is of great importance for biocomposites manufacturing, since it affects their processability and their physical and mechanical behaviors (Koutsomitopoulou *et al.*, 2014). For this reason, the thermal stability of produced olive pomace-based powders was evaluated under both oxidative and inert conditions by thermal degradation analysis (TGA) in the temperature range from 20°C to 900°C. The degradation temperatures in oxidative conditions of each fraction are summarized in Table 13. Figure 13 shows the thermograms of weight loss and derivative weight loss of olive pomace powders obtained by wet process (wS; wP) and thus produced by dry process with sieving (dS1; dP1) compared to crude OP (F0).

During the thermal degradation in inert conditions, olive pomace base samples exhibited a two main steps decomposition (Figure 13a). The first step between 40 and 130 °C, corresponded to the evaporation of water entrapped into the molecular structure of each fraction particles. The moisture content of F0 is more than 6%, the produced samples are somewhat drier and exhibited moisture levels between 3 and 4% (Table 12). These results can be attributed to the drying of

the powders, as a result of the heating of the apparatus which they are in contact during the different steps of the process (grinding, friction and sieving); furthermore, the fractions produced by wet process were dried at 50°C for 24h (Figure 12).

The second step starts round 150°C and extends to 500°C, it can be deconvoluted in several peaks: in the first, the degradation of hemicellulose between 150 and 300°C followed by degradation of cellulose up to 400°C with a maximum around 343°C displayed by the stone-rich fraction (wS) due to its high cellulose content. As for lignin, its degradation takes place over a wide temperature range and extends to 500°C. The solid residue remaining after the thermal degradation of the main constituents of the biomass is estimated to be 19% for F0 and the fraction wS, and more than 22% for the wP fraction. Our results are in perfect correlation with those obtained by Benavente and Fullana (2015), who also studied the thermal stability under nitrogen, of the olive pomace produced by the two-phase extraction system. These authors noted a thermal degradation of the hemicellulose between 220-315°C, and cellulose thermal degradation ranges from 315 to 400 °C. These same authors also recorded 20% of solid residue at the end of degradation. On the other hand, other authors also report that lignin is thermally more stable and its degradation slowly happens under a wide temperature range from 100 to 900°C (Ozveren and Ozdogan, 2013).

During the thermal degradation in oxidative conditions, the DTG curves show three consecutive degradation steps of olive pomace based samples. As in inert conditions, the first step corresponded to water loss. Then, between 130 and around 200 °C, the olive pomace samples were relatively thermally stable (Figure 13b-c and Table 13), even if the degradation of lignin may have begun. Indeed, as has already been reported, lignin is known to start at relatively low temperatures, proceeding over a wide range of temperatures. The 130-200°C range can be thus considered as the optimal interval of temperatures for the process of olive pomace, as mentioned by Koutsomitopoulou *et al.* (2014). When the temperature increased beyond 200°C, *i.e.* once hemicellulose and then cellulose degradation has started, the degradation was very fast and gave rise to a characteristic sharp peak on the DTG curve. Hemicellulose is known to be the least thermally stable of lignocellulose components due to the presence of acetyl groups (Yang *et al.*, 2007). This is in agreement with already published results demonstrating that the decomposition of hemicellulose and cellulose occurred on average between 220 and 380°C (Monteiro *et al.*, 2012). The stone-rich powders prepared by washing (wS) or obtained by friction (dS3) exhibited the same degradation temperature (276°C, measured at the maximum rate of degradation), which corresponds to a 20% of mass loss. An increase of more than 10°C is noted

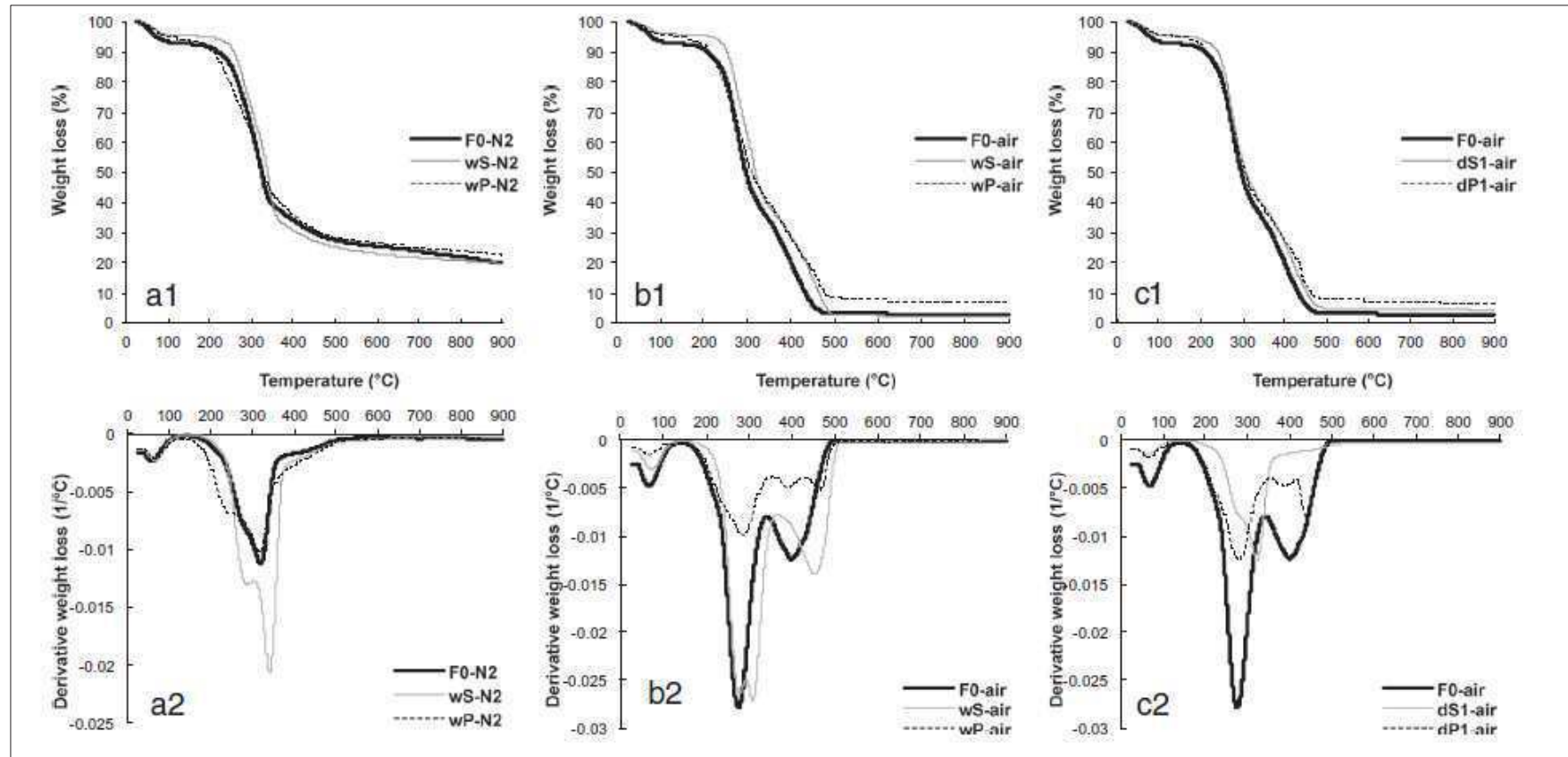


Figure 13: TGA (a1, b1 and c1) and DTG (a2, b2 and c2) curves of stone and pulp rich-fractions produced either by wet fractionation (a1 and a2 under nitrogen; b2 and b2 under air) and dry fractionation with sieving (c1 and c2 under air).

as compared to the crude pomace (262°C) (Table 13). This is due to their higher content in cellulose, about 32% for the stone-rich fractions against 29% for F0 (Table 12). Indeed, an increase in the thermal degradation temperature is known to be correlated to an increase in cellulose composition. Yang *et al.* (2007), report that cellulose is characterized by high thermal stability, seen is consisted of a long polymer of glucose without branches, its structure is in a good order and very strong. Koutsomitopoulou *et al.* (2014) reported that surpassed 300 °C, hemicellulose is essentially converted into gasses and acetic acid. When the hemicellulose is already decomposed, the contribution on the increase in weight loss rate is attributed to the cellulose decomposition.).

For the stone-rich fraction produced by wet process, the peaks associated respectively to the degradation of hemicellulose and cellulose are distinguished, unlike the stone fraction obtained by sieving (Figure 13 b2 and c2). This result indicates that the stone produced by washing is cleaner. In the case of sieving, the absence of these two peaks may be masked by the presence of the pulp, as it can be attributed to a loss of part of the stone in the pulp fraction after sieving. OP fractions exhibited peaks of maximum degradation at different values of temperature. From table 3, the highest peaks are recorded for the fractions of the pulp obtained by wet fractionation (wP) and friction (dP3) with very close values at 286 and 288°C respectively, which also display the highest lignin content 44% (Table 12). These results are close to the values recorded by Nabinejad *et al.* (2015), which report a degradation of lignin from 230 to 500 °C. These results may also reveal a similar purity rate of these two fractions.

The third step of degradation, recorded at temperatures above 400°C (Figure 13b-c), corresponds to the oxidation of the partially decomposed hemicellulose, cellulose and lignin (Yang *et al.*, 2007).

Referring to the results shown in Table 13, it can too be noted that overall degradation temperatures of the stone-rich fractions (228-309°C) are higher than those recorded for the pulp-rich fractions (208-288°C) with variations depend of the content in lignocellulose of each of them (Table 12). An exception is noted for the fractions obtained by electrostatic sorting (dS2 and dP2); the latter exhibit almost identical thermal degradation values (T5%, T20% and Tmax), certainly explained by their similar composition.

On the other hand, by comparing the values of the thermal degradation of the sample produced by dry process with those produced by wet process, we note that wS; wP; dS3; and dP3 fractions display almost similar thermal degradation profile. These results confirm, the influence of the

powder composition on its thermal stability, which depends on the nature and content tissues of each sample and therefore, depend on the applied fractionation treatment. The recorded values may be another indicator parameter of the fractions purity and thus, the efficiency of the separation. They demonstrate clearly that the least contrasted pulp-stone powders are produced by electrostatic sorting (similar thermal degradation temperatures) and the most contrasted correspond to the fractions obtained by washing in water followed by those produced by friction (different temperatures of degradation) (Table 13). So, this result allows confirming the possibility of substituting wet fractionation by dry fractionation with friction milling mode.

Table 13: Temperatures (°C) corresponding to the different degradation rates (% of the dry matter) of the olive pomace fractions (tests recorded under air atmosphere at a heating rate of 10 °C.min⁻¹) T_{5%}, T_{20%}, T_{max} correspond to the temperatures of 5%, 20% and maximum mass loss rates of dry matter

	T _{5%}	T _{20%}	T _{max}
F0	222±2	262±1	274±0
wS	250±0	276±1	309±1
wP	208±1	254±1	286±2
dS1	238±0	265±1	271±1
dP1	211±0	257±0	277±0
dS2	228±5	270±1	279±0
dP2	226±2	270±1	281±1
dS3	247±1	277±1	278±1
dP3	217±1	259±2	288±3

Another result which is interesting to indicate in this study is that a weight loss of 5% at temperatures higher than 200°C is recorded both for the crude OP and all obtained fractions (Table 3), which corresponds to temperatures higher than the melting point (T_m) of many thermoplastic conventional polymers such as polyethylene (PE) (T_m=130-170°C) (Li *et al.*, 2009; Babul Reddy *et al.*, 2016), polypropylene (PP) (T_m=165°C) (Ayrilmis and Buyuksari, 2010; Naghmouchi *et al.*, 2015) and polyvinyl chloride (PVC) (T_m=160-170°C) (Djidjelli *et al.*, 2007), or biosourced polymers such as poly(3-hydroxybutyrate-co-3 hydroxyvalerate)

(PHBV) ($T_m=165^\circ\text{C}$) (Hassaini *et al.*, 2017), polylactic acid (PLA) ($T_m=160-190^\circ\text{C}$) (Koutsomitopoulou *et al.*, 2014); it makes OP based fractions sufficiently thermally stable to be used as reinforcing fillers in several thermoplastic polymers for the production of biocomposites.

As has been already reported in this paper, the properties of the composites materials depend strongly on the intensity of the affinity between the fiber and matrix. In general, the interphase in polymer matrix composites can be formed by four basic mechanisms that can vary in magnitude and occur simultaneously: molecular segregation, chemical bonding, van der Waals bonding and mechanical interlocking (Kim and Mai, 1998). However, the main problem of natural fiber/polymer composites is the incompatibility between the hydrophilic nature of vegetal fibers that contrasts with the hydrophobic nature of most thermoplastic matrices, leading to poor Van der Waals interactions. According to Berthet *et al.* (2015c), the lignocellulosic biomass displays various physical and chemical structures, leading to a wide range of possible interactions with the polymer matrix. The strength of interactions between the filler and the polymer, which can be called “affinity”, mainly depends on the surface energy of the constituents since the interaction mechanisms of polymer with fillers is an adsorption process (Berthet *et al.*, 2017). Surface free energy is increasingly often used as a measure of adhesive properties (Rudawska and Jacniacka, 2009).

This is why the estimation of the solid surface free energy of the constituents from contact angle measurements can be useful to predict a work of adhesion and thus tailor new polymer-based composites (Rebouillat *et al.*, 1999). For that purpose, five reference liquids with different surface energies were used. First, the contact angle formed between a drop of each liquid on the surface of pellets of compressed particles was measured. Then, the surface free energy (γ) (polar (γ^p) and dispersive (γ^d) components) were estimated from the Owens-Wendt model (Owens and Wendt, 1969) for all samples (Table 4). The surface energy values recorded for all obtained fractions ranged from 29 to 36 $\text{mN}\cdot\text{m}^{-1}$. This range of valued is in agreement with those of Berthet *et al.* (2015c) who reported that the surface energy of lignocellulosic fibers varies from 30 to 50 $\text{mN}\cdot\text{m}^{-1}$ depending on botanical origin. It can be observed that the pulp/stone couples produced by the electrostatic and sieving sortings showed similar γ values, *i.e.* 35 $\text{mN}\cdot\text{m}^{-1}$ for dS1 and dP1 and 32 $\text{mN}\cdot\text{m}^{-1}$ for dS2 and dP2 (Table 4). On the contrary, the pulp/stone couples produced by either wet fractionation or dry friction recorded slightly but

III. Résultats et discussion

Table 14: Contact angle measurements and solid surface free energy of different fractions

(γ : solid surface free energy, γ^d : dispersive component of the solid surface free energy, γ^p polar component of the solid surface free energy, *nd*: not determined)

	Contact angle θ (°)					Surface energy (mJ.m ⁻²)		
	Water	Ethylene glycol	Diiodomethane	Formamide	Glycerol	Γ	γ^p	γ^d
F0	91.1±3.6	71.9±3.6	48.1±1.8	58.7±2.3	90.78±0.6	33	0.8	32.2
wS	75.2±2.0	53.7±4.9	nd	nd	nd	30.6	14.1	16.4
wP	96.4±2.4	68.8±5.3	52.8±4.4	61.9±0.3	94.8±1.5	32.4	0.3	32
dS1	83.4±2.9	69.4±2.3	40.7±4.5	47.6±0.5	92.3±1.1	35.5	1.5	33.9
dP1	95.4±4.0	68.1±2.1	44.1±1.6	62.5±2.5	91.8±3.6	35.5	0.2	35.3
dS2	86.3±3.3	66.2±5.5	45.2±3.4	62.8±1.6	95.1±6.1	32.2	1.4	30.8
dP2	87.2±3.7	67.2±1.3	41.6±3.9	66.8±3.0	94.3±1.6	32.5	1.1	31.4
dS3	82.4±3.3	63.9±1.8	42.3±1.7	48.7±1.2	99.2±1.6	34.5	1.7	32.8
dP3	93.7±3.8	71.3±1.2	56.7±0.6	59.2±1.8	97.6±2.9	29.9	0.8	29.2

significantly different γ values, *i.e.* 30.6 mN.m⁻¹ and 32.4 mN.m⁻¹ for wS and wP against 34.5 and 29.9 for dS3 and dP3 respectively (Table 4). It can also be underlined that these two last fractionation processes produced the most contrasted powders in terms of polarity, as revealed by polar component values and contact angles recorded with water. The highest the γ^p value and/or the lowest the contact angle with water, which implies the highest the polarity. For example, γ^p were 14.1 and 0.3 mN.m⁻¹ for wS and wP, and 1.7 and 0.8 mN.m⁻¹ for dS3 and dP3 respectively, while contact angle with water were 75.2 and 96.4° for wS and wP, and 82.4 and 93.7° for dS3 and dP3 (Table 14). These results clearly demonstrated the polar character of stone-rich fractions and a polar character of pulp-rich fractions, which is dependent on their chemical compositions and hence, on the applied fractionation process. The polar character of the stone is due to its high content in cellulose and hemicellulose as compared to the pulp which contains higher levels of lignin (Table 12) and also to its heterogeneous and porous structure allowing the penetration of water (Hassaini *et al.*, 2017). The more a polar character of pulp-rich fractions is attributed to the low amount of cellulose and hemicelluloses and also to the presence of a high level of lignin, whose main function is to bring rigidity and impermeability to water for the plant (Martone *et al.*, 2009).

It is worth noting that the stone-rich fraction obtained by washing is the most polar of all the fractions, with the highest γ^p value (14.1 mN.m⁻¹) as compared to all the other stone-rich fractions which present values between (1.4 and 1.7) (Table 14). This certainly justifies the applied treatments by different authors on the olive stone powder obtained mainly by the liquid route, in order to modify its surface properties and thus improve its affinity with a polar polymer matrix (Djidjelli *et al.*, 2007; Gharbi *et al.*, 2014; Hammoui *et al.*, 2015; Hassaini *et al.*, 2017).

Predicted values of adhesion work indicated that the affinity between the filler and the polymer matrix depends on the nature of each constituent (Table 15). Adhesion work was predicted to be greater with PP and PLA polymers for all OP-based fractions (around 56-78 mJ.m⁻²), these two polymers exhibiting the highest polarity (γ^p of 2 and 11 mJ.m⁻² respectively). On the opposite, adhesion work was predicted to be less important in the case of PE and PHBV polymers (between 46 and 65 mJ.m⁻²) that corresponded to the less polar polymers under consideration (γ^p of 0 and 0.5 mJ.m⁻² respectively). It is worth noting that OP-based fractions expressed different affinities towards a given polymer. For all polymers, the highest values of work of adhesion were predicted for dS3, leading to conclude that stone-rich fractions obtained by dry fractionation should be preferred to improve the interfacial adhesion with these kinds of polymer. It is interesting to note that a wet fractionation process is clearly in detriment of a high

work of adhesion, especially in highly apolar polymer matrices such as PE and PHBV. In the case of apolar matrices such as PE and PHBV, the difference of behavior between pulp-rich and stone-rich fractions was clearly reduced. Finally, not a so marked difference was observed between F0 and dS3. Based on these results, it is supposed that a range of biocomposites could be developed without adding coupling agents nor modifying the surface of fillers by appropriately choosing the filler/matrix couple. However, to date, no work does report the use of pulp-rich fractions nor F0 as raw resources for the production of reinforcing fillers in biocomposites. It would therefore be interesting in the future to also exploit these two latter fractions in this field of application.

Table 15: Polar component (γ^p) and dispersive component (γ^d) of some polymer matrices and the predicted work of adhesion (W) between these polymer matrices and the olive pomace-based fractions produced by wet process and dry process with friction.

	Surface energy of some polymer matrices (mJ.m^{-2})		Work of adhesion (W) (mJ.m^{-2})				
	γ^p	γ^d	F0	wS	wP	dS3	dP3
PE	0 ^(a)	33 ^(a)	65.2	46.5	65.0	65.8	62.1
PP	2 ^(a)	32 ^(a)	66.7	56.4	65.5	68.5	63.7
PLA	11 ^(a)	37 ^(a)	75.0	74.2	72.5	78.3	71.7
PHBV	0.5 ^(a)	27 ^(a)	60.2	47.4	59.6	61.4	57.4

^(a): data from Berthet *et al.*, 2015c

The production of a range of pulp-rich and stone-rich fractions by dry fractionation can be useful in other fields of applications than biocomposites. Concerning the pulp-rich fractions, given their high content of chlorophyll pigment demonstrated by colorimetric analyzes, they can present a natural source for the extraction of dyes which could be used as an additive in either agro-food industry or textile industry. This last application already exists for olive mill wastewater but not yet for OP (Meksi *et al.*, 2012). Regarding the potential application in food industry, the additional advantage of chlorophylls is their antioxidant properties that give the ability to reduce the oxidative damages associated to many human diseases (Fernandez-Orozco *et al.*, 2011).

Concerning the stone-rich fractions, one valuable use could be their incorporation in cosmetic formulations as an exfoliating agent (Cosmoliva, 2014). Additionally, given the high amounts

of cellulose and hemicellulose present in stone-rich fractions (Table 12), they may act as functional ingredients in cosmetic formulations, by improving physical and structural properties of hydration, oil holding capacity, emulsion and oxidative stability, viscosity, texture, sensory characteristics, and shelf-life of products (Rodrigues *et al.*, 2015). These fractions could also find applications in animal feeding. Indeed, numerous experiments have reported a "poor digestive use" of olive pomace when incorporated into animal feed rations due to its high content in lignin that may reduce the activity of the rumen flora (Theriez and Boule, 1970). Thus, the incorporation of pulp-poor fractions in animal feeding instead of crude OP could be interesting. Finally, the use of stone-rich fractions instead of crude OP could be proposed in the case of bioconversion processes for the production of biofuels or for composting. Indeed, the importance of lignin elimination by pre-treatments of the lignocellulosic biomass has been frequently suggested in these fields of applications due to its low decomposition rate (Fernandez-Orozco *et al.*, 2011).

III.1.4. Conclusion

Olive pomace is a lignocellulosic biomass displaying a complex composition, characterized by a heterogeneous distribution of its constituents through the different tissues of the fruit. With the prospect of a complete exploitation of this olive oil by-product, a treatment allowing the separation of the pulp from the stone while maintaining the integrity of components contained in the biomass constitutes the first step of its recycling and takes a major importance for potential valorizations. In the present work, different dry fractionation routes have been successfully investigated to produce contrasted and pure stone-rich and pulp-rich fractions from crude olive pomace. Results revealed that the separation of the pulp from the stone using friction solicitations in a ball mill operating in mild conditions (only 2 min at a frequency of 15 Hz) on a sample previously ground using a cut mill was the most efficient dry fractionation route. Obtained powders displayed similar biochemical composition, surface free energy, color and thermal stability as those obtained by wet fractionation. It was also demonstrated that dry fractionation allowed achieving a higher total yield than wet fractionation (99.4% against only 82.1% in the case of the wet fractionation followed in the present study). Finally, dry fractionation did not require the use of water while a water: biomass ratio of 5:1 was required in the case of wet fractionation.

Results demonstrated that it would be advantageous to exploit the stone-rich fraction, but also the crude OP and the pulp-rich fraction as raw resources for the production of fillers to develop

a wide range of biocomposites for targeted applications. It is worth noting that further grinding steps would be necessary to obtain fillers with controlled sizes. To conclude, this work opens a new and promising route for converting this agro-food residue into added value products either as fillers or other applications, through a clean technology for a better eco-friendly valorization.

Acknowledgments

We are grateful to the PNE Program (2016 - 2017, grant number 396 assigned on June 9th, 2016) of the Algerian Ministry of Higher Education and Scientific Research for its financial support in the 11-months doctoral fellowship of S. Lammi at the JRU IATE. Direct costs were covered by the MALICE project (call “Chercheur d'avenir 2015”), which is cofinanced by the European Regional Development Fund (FEDER) and the Languedoc-Roussillon region (grant number 2015-005910 assigned on November 20th, 2015). We acknowledge Cecile Sotto for her technical support in the realization of grinding experiments at the plant processing platform of JRU IATE.

***III.2. Dry fractionation of olive pomace
for the development of food packaging
biocomposites***

(Article n°2)

III.2. Dry fractionation of olive pomace for the development of food packaging biocomposites

Article publié dans le journal « Industrial Crops and Products »

Sarah Lammi^{1,2}, Nicolas Le Moigne³, Djamel Djenane², Nathalie Gontard¹, Hélène Angellier-Coussy^{1*}

¹JRU IATE 1208 – CIRAD/INRA/Montpellier SupAgro/University of Montpellier, 2 place Pierre Viala, F-34060 Montpellier, France.

²Laboratory of Food Quality and Food Safety, Department of Agronomic Sciences, University of Mouloud MAMMERI, BP 17, 15000 Tizi-Ouzou, Algeria.

³C2MA, IMT Mines Alès, Université Montpellier, 6 avenue de Clavières, 30319 Alès cedex France.

*Corresponding author: helene.coussy@umontpellier.fr

Received 6 December 2017, Accepted 18 Avril 2018, Available online 7 March 2018,

Will be published 15 September 2018

DOI: 10.1016/j.indcrop.2018.04.052

Résumé

Trois fractions lignocellulosiques présentant des propriétés contrastées sont produites par fractionnement sec de grignon d'olives (OP) : une fraction de noyau (SF) riche en cellulose et ayant une polarité élevée, une fraction de pulpe (PF) plus riche en lignine et moins polaire et le grignon brut (F0) présentant des propriétés intermédiaires. Ces fractions sont utilisées comme charges dans deux matrices thermoplastiques, le polypropylène (PP) et le polyhydroxybutyrate-co-valérate (PHBV). Les essais de traction ont montré une diminution à la fois de la contrainte et de l'allongement à la rupture pour tous les biocomposites, tandis que le module d'Young n'est pas significativement affecté. À faible teneur en charge, aucun effet de composition de charge n'est observé alors qu'à forte teneur en charge (30% en poids), la diminution de la contrainte à la rupture était moins prononcée pour le PHBV-PF avec des réductions respectives de 36%, 65% et 78% pour les composites PHBV-PF (30%), PHBV-F0 (30%) et PHBV-SF (30%), comparativement au PHBV pur. L'allongement à la rupture a également fortement diminué en fonction de la teneur en charge. La réduction la plus élevée est enregistrée dans le cas de la charge SF, avec une valeur de 74% pour les composites PHBV-SF. Les propriétés mécaniques sont mieux conservées dans le cas de la charge PF grâce à une meilleure adhérence interfaciale avec les matrices, comme le révèlent les calculs du travail d'adhésion, les observations au MEB

et la modélisation mécanique. La perméabilité à la vapeur d'eau (WVP) des deux matrices a augmenté en présence des charges SF et F0, tandis que la perméabilité à l'oxygène n'est pas significativement affectée par les charges. A titre d'exemple, la WVP a augmenté de $0,9 \pm 0,1 \times 10^{-12} \text{ mol m}^{-1} \text{ s}^{-1} \text{ Pa}^{-1}$ pour le PHBV pur jusqu'à $15,1 \pm 2,6 \times 10^{-12} \text{ mol m}^{-1} \text{ s}^{-1} \text{ Pa}^{-1}$ pour PHBV-F0 (30%). Cela favorise une utilisation prometteuse des fractions SF / F0 dans les emballages biocomposites durables pour les produits alimentaires respirants par contre, les formulations à base de PF sont plus appropriées pour les produits non-respirants et sensibles à l'eau. Nos résultats ont démontré que le fractionnement par voie sèche de la biomasse lignocellulosique est intéressant pour le contrôle des propriétés des charges biosourcées et des fonctionnalités des biocomposites résultants. Par ailleurs, les films composites à base de PP développés dans cette étude permettent de réduire les coûts et la dépendance aux ressources fossiles, tandis que les biocomposites à base de PHBV ont également l'avantage d'être entièrement biosourcés et biodégradables.

Mots-clés : grignon d'olives, fractionnement à sec, biocomposites, propriétés mécaniques, propriétés barrières, emballage alimentaire

Abstract

Three lignocellulosic fractions with contrasted properties were produced by dry fractionation of olive pomace (OP): a stone-rich fraction (SF) rich in cellulose and having high polarity, a pulp-rich fraction (PF) richer in lignin and less polar, and a crude pomace fraction (F0) with intermediate properties. These fractions were used as fillers in two thermoplastic matrices, *i.e.* polypropylene (PP) and polyhydroxybutyrate-co-valerate (PHBV). Tensile tests showed a decrease of both the stress and the elongation at break for all biocomposites, while the Young's modulus was not significantly affected. At low filler contents, no effect of filler composition was observed whereas at high filler content (30 wt%), the decrease in the stress at break was less pronounced for PHBV-PF, with respective reduction values of 36%, 65% and up to 78% for PHBV-PF (30%), PHBV-F0 (30%) and PHBV-SF (30%) composites, as compared to the neat PHBV. The elongation at break also greatly decreased according to the filler content. The highest reduction was recorded in the case of SF fillers, with a reduction of 74% for PHBV-SF composites. Mechanical properties were better preserved in the case of the PF filler due to better interfacial adhesion towards the matrices, as revealed by work of adhesion calculations, SEM observations and mechanical modelling. Water vapour permeability (WVP) of both matrices was increased in presence of both SF and F0 fillers, while oxygen permeability was not

significantly affected by the fillers. As an example, WVP increased from $0.9 \pm 0.1 \times 10^{-12}$ mol $m^{-1} s^{-1} Pa^{-1}$ for the neat PHBV up to $15.1 \pm 2.6 \times 10^{-12}$ mol $m^{-1} s^{-1} Pa^{-1}$ for PHBV-F0 (30%). This supports a promising use of SF/F0 fractions in sustainable biocomposites packaging for respiring food products, the PF-based formulations being more appropriate for non-respiring and water sensitive products. Our results demonstrated that the conditioning of lignocellulosic biomass by dry fractionation is important for the control of bio-based fillers properties and the resulting functionalities of biocomposites. Besides, the PP-based composites developed in this study allow reducing costs and dependence to fossil resources, while PHBV-based biocomposites also have the advantage of being fully bio-based and biodegradable.

Keywords: olive pomace; dry fractionation; biocomposites; mechanical properties; barrier properties; food packaging

III.2.1. Introduction

Food packaging is the sector consuming most plastics, with about 40% of the global demand worldwide. Polypropylene (PP) is at the head with more than 19% of usages (Plastics Europe, 2016). In view of reducing food waste while limiting the harmful effects of petrochemical-derived plastic residues on the environment, the conception of fully bio-based and biodegradable packaging materials having tailored mass transfer properties constitutes one alternative to overcome these issues (Angellier-Coussy *et al.*, 2013). Among them, polyhydroxyalkanoates (PHA) are bacterially-derived thermoplastic polymers that can be produced from renewable resources, including solid or liquid agro-residues and municipal wastes. They have gained major importance worldwide due to their macromolecular structure diversity and close properties to conventional plastics that make them highly competitive with respect to PP. The copolyester polyhydroxy-(3-butyrate-*co*-3-valerate) (PHBV) is one of the best characterized PHA (Reddy *et al.*, 2003). Besides its higher price as compared to conventional plastics, the main limitation restricting its commercial application at a large scale is its barrier properties which are too high to fit respiring products needs such as fruits and vegetable (Berthet *et al.*, 2016).

One environmentally virtuous strategy to modulate PHBV barrier properties while reducing the final cost of materials is to mix it with low cost lignocellulosic fillers obtained from food industry solid by-products (Berthet *et al.*, 2015; 2016). Olive pomace (OP), which is the solid lignocellulosic residue of olive oil extraction, is a very good candidate for this purpose due to its very high availability and low cost. Its production is mainly concentrated in Mediterranean

area, but the emergence of new producer countries leads to an intense accumulation of OP that is estimated to reach 2,881,500 tons/year worldwide (Ravindran and Jaiswal, 2016). Olive pomace is a mixture of residual skin, pulp and fragments of the crushed stone. Until now, only the part corresponding to the olive stone has been valorized in the field of biocomposites by combining it either with synthetic polymers such as unsaturated polyesters (Gharbi *et al.*, 2014), polyvinyl chloride (PVC) (Djidjelli *et al.*, 2007), PP (Naghmouchi *et al.*, 2015; Siracusa *et al.*, 2001), or biodegradable polymers such as wheat gluten (Hammoui *et al.*, 2015), polylactic acid (PLA) (Koutsomitopoulou *et al.*, 2014) and PHBV (Hassaini *et al.*, 2017). Neither the whole crude OP nor the olive pulp has been yet exploited in this way. In addition, all these studies mainly focused on mechanical and thermal properties of the resulting biocomposites. Only Hassaini *et al.* (2017) were interested about oxygen and water vapour permeability of these biocomposites after chemical treatment of the stone-based filler to improve its affinity toward the PHBV matrix. It is also worth noting that OP is often exclusively treated using wet processes consuming a large amount of water and chemicals (hexane and/or acetone) in order to separate the pulp from the stone, thus generating pollutant and toxic effluents. In the perspective to reduce the harmful environmental impact of OP by its sustainable valorization, dry fractionation combining grinding and sorting processes (electrostatic separation, friction or sieving) has been recently demonstrated to be a sustainable technology to produce fillers from crude olive pomace. It was shown that friction in a ball mill was the most adapted mechanical treatment to produce pulp-rich and stone-rich powders with high yield and purity, and contrasted biochemical composition and polarity (Lammi *et al.*, 2018a).

In this context, the present work aims at exploring the potential use of the two main parts of olive pomace, *i.e.* the stone and the pulp, as fillers in biocomposites and to compare it to that of the crude OP. For this purpose, pulp-rich and stone-rich fractions with contrasted biochemical composition and physico-chemical surface properties were produced by dry fractionation and used as fillers in a petroleum based polymer matrix, polypropylene (PP) and a bio-based polymer matrix, polyhydroxy-butyrates-co-valerates (PHBV). Biocomposites with increasing filler contents were prepared by melt compounding and thermo-compression and their optical (color), microstructural, thermal, mechanical (tensile tests) and barrier (water vapour and oxygen permeability) properties were characterized. Changes in material functional properties are discussed in relation to the intrinsic characteristics of olive pomace-based fillers, including their color, density, size, morphology, biochemical composition, thermal stability and surface free energy. Special attention is given to understand the impact of the composition of OP-based fillers and especially their physico-chemical affinity with the thermoplastic matrices on

biocomposites functional properties. Finally, their possible application in the food packaging sector was discussed based on all the results.

III.2.2. Materials and methods

III.2.2.1. Raw materials

Algerian crude olive pomace (OP) of the *Chemlal* variety was kindly provided in December 2016 by local olive producers in the region of Azeffoun (Tizi-Ouzou) located in north-central of Algeria. OP was stored in a cold room at $4^{\circ}\text{C} \pm 1$ until its use. This residue was composed of partially crushed stones, pulp and skin and displayed an initial moisture content of 53 wt%. Prior to dry fractionation, the fresh olive pomace was dried in an oven at 60°C for 24 hours until reaching a moisture content of 9 wt%.

A commercial grade of polyhydroxy-(butyrate-co-valerate) (PHBV) containing 5% of valerate was purchased from NaturePlast company (France) in the form of pellets (PHI002 grade). Data given by the supplier were the following: PHBV density of 1.25 ± 0.05 , melt flow index ranging between 15 and 30 g.10 min⁻¹ ($190^{\circ}\text{C}/2.16$ kg) and melt temperature ranging from 145 to 155°C . Pellets were dried overnight at 60°C before processing. Polypropylene (PP) in the form of pellets (PPH 9020 grade) was purchased from Total Petrochemicals (Belgium). Data given by the supplier were the following: PP density of 0.905, melt flow index of 25 g.10 min⁻¹ ($230^{\circ}\text{C}/2.16$ kg) and melt temperature of 165°C .

Sulfuric acid, arabinose, xylose and glucose (Sigma-Aldrich), formamide, diiodomethane (Acros Organics, Geel, Belgium), ethylene glycol (Aldrich chemical Co. Inc., Milwaukee, USA) and glycerol (Merk, Darmstadt, Germany) were used for characterization of olive pomace fractions.

III.2.2.2. Preparation of olive pomace-based fillers

A dry fractionation process was applied to separate the pulp and the stone from the crude olive pomace (OP). Dry OP was first submitted to frictional forces in a ball mill (Marne n°55, FAURE, France) operating at ambient temperature, 86 rpm and during 30 min. A jar of 2 L was used, with 1/3 in volume of ceramic balls (diameter of 15, 20 and 25 mm) and 1/3 in volume of crude OP. The resulting powder was then passed into an electric sieve (RITEC, model 400, France) through a 1.25 mm mesh. Two fractions were obtained: the fine fraction was recovered at the bottom of the sieve and corresponds to the pulp-rich fraction (PF), while a coarse fraction was retained on the sieve (Lammi *et al.*, 2018a). This coarse fraction was further ground using

a knife milling (SM 300, Retch, Germany) with a grid size of 1 mm and speed of 1500 rpm. The ground product was then sieved through a 0.4 mm mesh in order to separate the stone-rich fraction (SF) from the intermediate fraction (Figure 14). Finally, in order to obtain powders with similar particle sizes, the SF and PF fractions as well as the crude OP, corresponding to the starting biomass (named F0), were first reduced by knife milling using a 0.25 mm grid at 1500 rpm and then further reduced using a 0.3 mm impact milling (Hosokawa-alpine, type 100UPZ, Augsburg, Germany) operating at 18000 rpm (Figure 14).

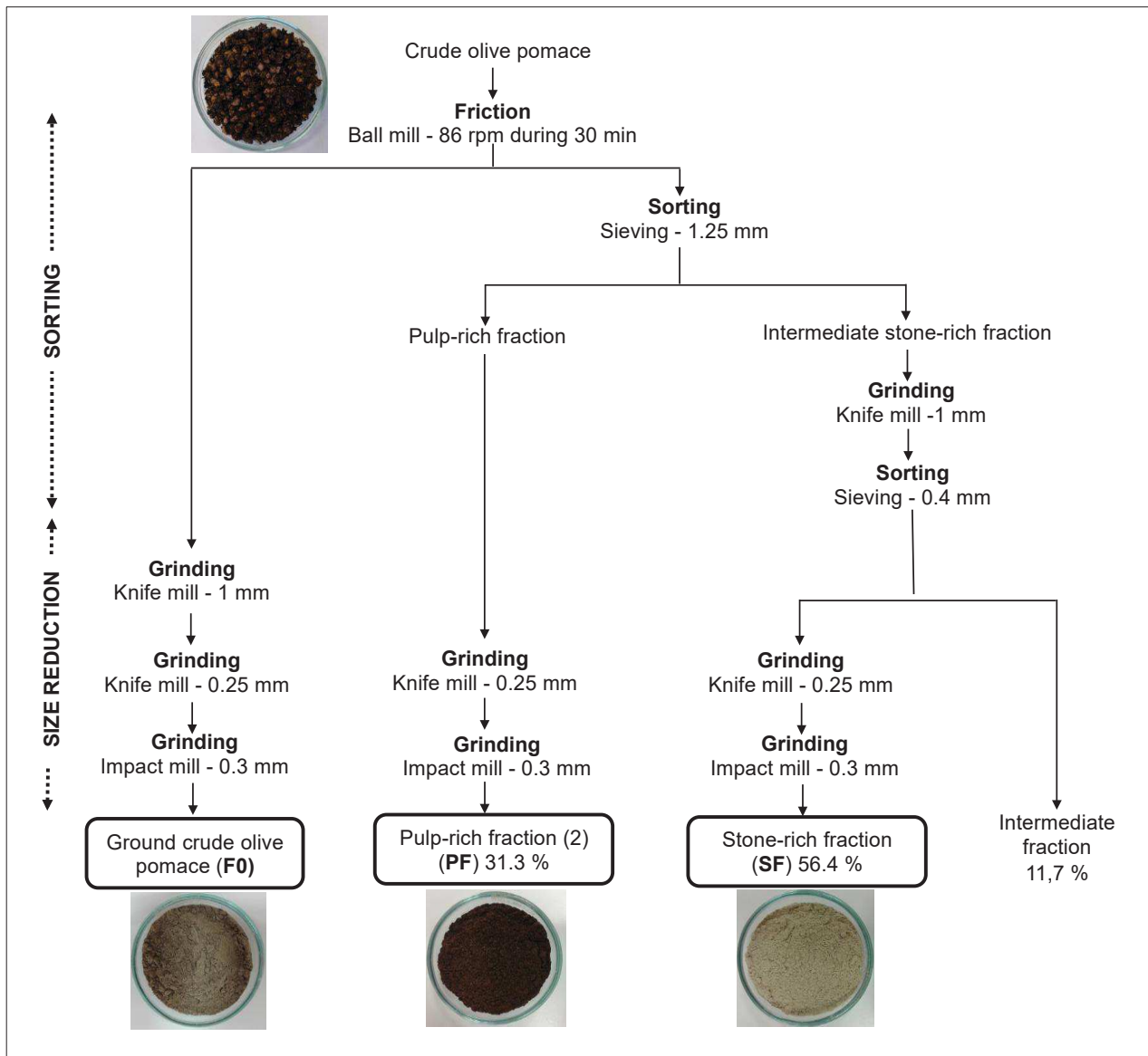


Figure 14: Dry fractionation process of crude olive pomace.

III.2.2.3. Preparation of olive pomace-based composite films

III.2.2.3.1. Compounding

To minimize hydrolytic degradation, all constituents (PHBV pellets, F0, SF and PF powders) were dried in a vacuum oven at 60°C over night prior to compounding. Composites were blended at various polymer/filler ratios (100/0, 95/5, 85/15, 70/30 w/w) using a HAAKE Rheomix internal mixer. The polymer pellets and the OP-based fillers were first mixed manually. The resulting mixture was then introduced all at once into the mixer operating at a rotor speed of 60 rpm. The mixture was blended during 5 min at temperatures of 170°C and 180°C for PHBV and PP matrices, respectively. The obtained compounds were cooled to room temperature and then, ground in a knife mill (SM 300, Retch, Germany) at a speed of 2200 rpm through a 4 mm grid to obtain composite pellets, which were then stored in sealed plastic bags containing silica gel. The codification of sample was done as follows: matrix-OP based fraction (weight filler content). For example, PHBV-F0 (5%) corresponds to a PHBV-based composite filled with 5 wt% of the F0 fraction.

III.2.2.3.2. Film shaping

Compounds were dried at 60°C for at least 8 hours before the preparation of films. Biocomposite films (10.5 cm wide squares, average thickness about 250 µm) were prepared by hot pressing the pellets between two Teflon coated plates, at 170°C and 180°C for PHBV and PP-based biocomposites respectively, using a hydraulic thermopress (PLM 10 T, Techmo, Nazelles, France). Samples were allowed to melt for 3 min then, a pressure of 150 bars was applied for 2 min as described by Martino *et al.* (2015). Finally, films were cooled at room temperature before being removed from the mold (no control of the cooling rate). Exactly the same process was applied to the neat PP and PHBV matrices.

III.2.2.3.3. Film thickness and conditioning

Film thickness was measured using a precision thickness gauge (Hanatek-model FT3, UK) on at least ten different positions for each film sample. Thickness mean values were considered in the calculation of mechanical properties, oxygen and water vapour permeability. All analyses were carried out on films samples stored in desiccators in presence of silica gel (relative humidity of 3 %).

III.2.2.4. Characterization of olive pomace-based fillers and biocomposites

III.2.2.4.1. Particle size and morphology

Particle size distributions were determined using a laser diffraction particle size analyzer (Mastersizer 2000, Malvern Instruments Ltd., United Kingdom). Powders were suspended in ethanol 95% (v/v) directly in the experimental cell. Quantitative morphological analysis of particles was performed by image analysis using the Image J software. For each sample, mosaic images were assembled by reconstructing 10 x 4 images using the imaging software NIS-Elements (Nikon, Japon) operating with the Multizoom AZ100 system, as described by Montano *et al.* (2013). Number- and surface-weighted distributions of maximum Feret diameters, *i.e.* the maximum length inside the particle projection, were determined based on the analysis of roughly 300 particles. Image analysis was performed on an increasing number of particles, until the mean of the considered indicator stabilized, *i.e.* with a variation lower than 5%, which was obtained with 80 particles in the present study. Aspect ratio of particles was calculated as the maximum Feret diameter (maximum dimension inside the particle projection) divided by the minimum Feret diameter (equivalent rectangle short side).

III.2.2.4.2. Particle density

The true density of OP-based powders was measured with a helium pycnometer (ULTRAPYCNOMETER 1000, Quantachrome instruments) using approximately 2 g of sample.

III.2.2.4.3. Biochemical composition

The moisture content of OP-based powders was determined by drying two grams of sample in an oven at 110°C until reaching weight equilibrium. The ashes content was obtained by igniting about one gram of sample in a muffle furnace at 600°C for five hours using porcelain crucibles. Cellulose and hemicellulose contents were measured after concentrated acid hydrolysis. 10 mg of dried samples were treated with 72% H₂SO₄ for 1 h at 30 °C followed by hydrolysis with 4% sulfuric acid for 1 h at 120 °C. The released monosaccharides were analyzed by a combined HPLC water system, using a BioRad HPX-87H column at 40°C and 0.3mL.min⁻¹ according the protocol described by Barakat *et al.* (2014). The lignin content was determined by the Klason method (Nicholson *et al.*, 2014). The protein content (N x 6.25) was determined after estimation

of the nitrogen content (N) by elementary analysis according to Jones (1941). All experiments were carried out in triplicate for each OP fraction.

III.2.2.4.4. Surface free energy and work of adhesion

Contact angles were measured using a goniometre (Digidrop, GBX, France) instrument, on samples fractions compressed beforehand with a hydraulic press (Perkin-Elmer) to form tablets that were stored over night with silicagel. In order to estimate the surface free energy of compressed OP-based fillers (polar γ^p , and dispersive γ^d components), five reference liquids were used, *i.e.* distilled water, formamide, diiodomethane, ethylene glycol and glycerol. Surface free energy values were calculated by using the Owens-Wendt approach (Owens and Wendt, 1969). To calculate the work of adhesion (W_A) between the matrix m (PP or PHBV) and the OP-based filler f , the following equation derived from the Owens-Wendt approach was used:

$$W_A = 2 \left[\sqrt{\gamma_m^d \gamma_f^d} + \sqrt{\gamma_m^p \gamma_f^p} \right] \quad (\text{Equation 1})$$

III.2.2.4.5. Color

The color attributes of every OP-based fractions and biocomposites were measured with a colorimeter (Minolta), using the L^* , a^* , b^* color system. The total color difference (ΔE) was calculated according to CIE (2004) as following (Equation 2):

$$\Delta E = [(L^* - L_0^*)^2 + (a^* - a_0^*)^2 + (b^* - b_0^*)^2]^{0.5} \quad (\text{Equation 2})$$

With L^* , a^* and b^* the color components of each sample. The references were respectively F0 for SF and PF fractions, and the neat polymer matrices for biocomposites. All measurements were carried out in triplicate.

III.2.2.4.6. Thermogravimetric analysis (TGA)

The thermal stability of OP-based fractions and biocomposites was evaluated by TGA carried out by heating about 10 mg of samples from room temperature up to 900°C, at a heating rate of 10°C min⁻¹ under either air or nitrogen (flow rate of 50mL.min⁻¹). Three thermal degradation temperatures were recorded: T_{peak} which was measured from the maximum value of weight loss derivative, $T_{5\%}$ and $T_{20\%}$, which corresponds to the temperatures at which respectively 5wt% and 20wt% of initial weight were lost.

III.2.2.4.7. Differential scanning calorimetry (DSC)

Differential scanning calorimetry was used to measure the crystallization (T_c) and melting (T_m) temperatures of materials, as well as their crystallinity (X_c). Measurements were done with a thermo-modulated calorimeter (Q200 modulated DSC, TA Instruments, New Castle, USA). Around 10 mg of film were placed in hermetic aluminum pans (Zero Aluminium Hermetic pan, TA Instruments New Castle, USA). Each sample was first heated up to 200°C then cooled down to -40°C at 10°C min⁻¹, and finally heated again up to 200°C at a heating rate of 10°C min⁻¹, the first scan was used to erase the thermo-mechanical history of the samples. Crystallization temperature (T_c) was measured from the exothermic peak of the cooling ramp. Melting temperatures were deduced from the endothermic peaks of the first (T_{m1}) and second (T_{m2}) heating ramp. Melting enthalpies were determined by the DSC software, from the area under the peak observed on both the first (ΔH_{m1}) and the second heating (ΔH_{m2}) ramp. Crystallinity of each sample was calculated with the Equation 3:

$$X_c = \left(\frac{\Delta H_m}{W \times \Delta H_m^*} \right) \times 100 \quad (\text{Equation 3})$$

where ΔH_m is the apparent melting enthalpy of the sample, W is polymer weight fraction in the sample and ΔH_m^* the theoretical melting enthalpy of a 100% crystalline polymer. Values of 146 J.g⁻¹ and 148 J.g⁻¹ were respectively used for ΔH_m^* of PHBV and PP, as reported by Barham *et al.* (1984) and Monasse and Haudin (1985).

III.2.2.4.8. Tensile tests

The mechanical properties of the different films were evaluated at room temperature through tensile tests performed with a texture analyzer (Zwick BZ2.5/TN1S, France) on dog-bone shape specimens pre-cut with a piece cutter (width of 4 mm and gauge length of 45 mm) and using a cross-head speed of 10 mm.min⁻¹. Nominal stress at break (σ_b), nominal elongation at break (ϵ_b) and Young's modulus (E) were determined from stress-strain curves. Ten replicates were realized for each formulation.

III.2.2.4.9. Scanning electron microscopy (SEM)

SEM observations were performed using a scanning electron microscope (SEM S-4500, Hitachi, Japan) with an acceleration voltage of 2 kV and a detector for secondary electrons. For the observation of cryo-fractured surfaces, films were previously frozen under liquid nitrogen, then fractured, mounted and coated with gold/palladium on an ion sputter coater.

III.2.2.4.10. Water vapour permeability (WVP)

Water vapour permeability of films ($\text{mol}\cdot\text{m}^{-1}\cdot\text{s}^{-1}\cdot\text{Pa}^{-1}$) was determined at 20°C using a gravimetric method according to the protocol described by Angellier-Coussy *et al.* (2011) between 0% (permeation cells placed in a dessicator containing silicagel) and 100 % of relative humidity (cells containing water). Cells were weighed using a four-digit balance (BALCO - Type LX 220A, Switzerland) every 24 hour during one week. Five samples of each film were tested and water vapour permeability was calculated from the following equation:

$$WVP = \frac{w \cdot x}{A \cdot \Delta p} \quad (\text{Equation 4})$$

where w is the slope of the weight loss versus time ($\text{mol}\cdot\text{s}^{-1}$), x is the film thickness at equilibrium measured at the end (m), A is the area of exposed film (m^2), and Δp is the water vapour pressure differential across the film (at 20°C, $\Delta p = 2338 \text{ Pa}$).

III.2.2.4.11. Oxygen permeability

Oxygen transmission rate (OTR) ($\text{m}^3\cdot\text{m}^{-2}\cdot\text{d}^{-1}$) of films was measured at 20°C and 0% RH on 16 cm^2 circular films using an oxygen permeation cell (OTR-Pst6, PresSens-GmbH, Germany) and a modified ASTM F1927-07 (2007) procedure. The oxygen transmission rate through the material can be detected with the oxygen sensor in the upper chamber. It was determined for all specimens in duplicate and calculated according to the following formula:

$$\text{OTR} = \frac{VO_2}{A \cdot t} \quad (\text{Equation 5})$$

With VO_2 is oxygen volume in the upper chamber (cm^3), A is surface of the specimen area (m^2), t is the time (day).

The permeability (PO_2) ($\text{cm}^3\cdot\text{m}^{-2}\cdot\text{d}^{-1}\cdot\text{Pa}^{-1}$) of the films was calculated according to equation 6:

$$PO_2 = \frac{\text{OTR}}{P} \quad (\text{Equation 6})$$

Where P is the partial pressure of oxygen in the upper chamber.

The oxygen permeability coefficient $P'O_2$ ($\text{mol}\cdot\text{m}^{-1}\cdot\text{s}^{-1}\cdot\text{Pa}^{-1}$) was determined as follows:

$$P'O_2 = PO_2 \times l \quad (\text{Equation 7})$$

Where l (m) is the average thickness of the specimen, which was determined at five points distributed over the entire test area.

III.2.3. Results and discussion

III.2.3.1. Effect of dry fractionation on the characteristics of olive pomace-based fillers

III.2.3.1.1. Effect of dry fractionation on biochemical composition, color and particle density

On the whole, the lignocellulosic complex represented more than two thirds of the biochemical composition of OP fractions (Figure 15). The concentration in cellulose and hemicellulose was the highest in the stone-rich fraction, with values of 36, 24.8 and 18.8 wt% d.b. for the SF, F0 and PF fractions, respectively. On the opposite, lignin was more concentrated in the pulp-rich fraction, with values of 48.9, 44.3 and 37.8 wt% dry basis (d.b.) for the PF, F0 and SF samples respectively. The pulp-rich fraction was also characterized by higher protein and ashes contents (protein contents of 8.7, 4.9 and 0.6 wt% d.b. and ashes content of 4.6, 2.6 and 0.8wt%d.b. for PF, F0 and SF, respectively). To summarize, the stone-rich fraction was richer in holocellulose whereas the pulp-rich fraction was richer in lignin, proteins and ashes, as compared to the crude olive pomace. These results were consistent with those already obtained from a previous study (Lammi *et al.*, 2018a) and are close to those reported by Hassaini *et al.* (2017) and Rodríguez-Gutiérrez *et al.* (2014). This confirmed that the three produced fractions displayed contrasted compositions, with an intermediate composition for the fraction F0. Such differences in biochemical compositions may be responsible for variations in intrinsic properties of powders, including their physico-chemical and mechanical properties as well as their thermal stability.

The pulp-rich fraction (PF) was visually darker than the stone-rich fraction (SF), with a dark brown and almost black color. The stone-rich fraction was characterized by a light beige color. These differences in color are related to the oxidation of fatty acids mainly in the pulp due the presence of residual oil, and also to the heterogeneous distribution of chlorophyll pigments through the different tissues of the olive. These pigments, which are responsible for the color of the fruit, are more concentrated in the pulp and the skin. The darker color of the PF fraction could also be due to a higher content in lignin and polyphenols, as compared to SF and the crude F0 fractions. As expected, the F0 fraction, which is a mixture of pulp and stone, displayed a light brown color intermediate between the two preceding samples. These observations were quantitatively confirmed by the measurements of the colorimetric parameters L^* , a^* and b^* , with L^* characterizing the lightness, a^* the range of color from red to green, and b^* the range

of color from yellow to blue (Table 16). Big differences in lightness were noticed, with L^* values of respectively 57.8, 25.2 and 36.8 for the SF, PF and F0 fractions, knowing that the lower the L^* value, the darker the sample. Some significant differences were also recorded for b^* , with values of respectively 15.3, 7.7 and 13.5 for the SF, PF and F0 fractions, that can be associated with the difference in lignin content.

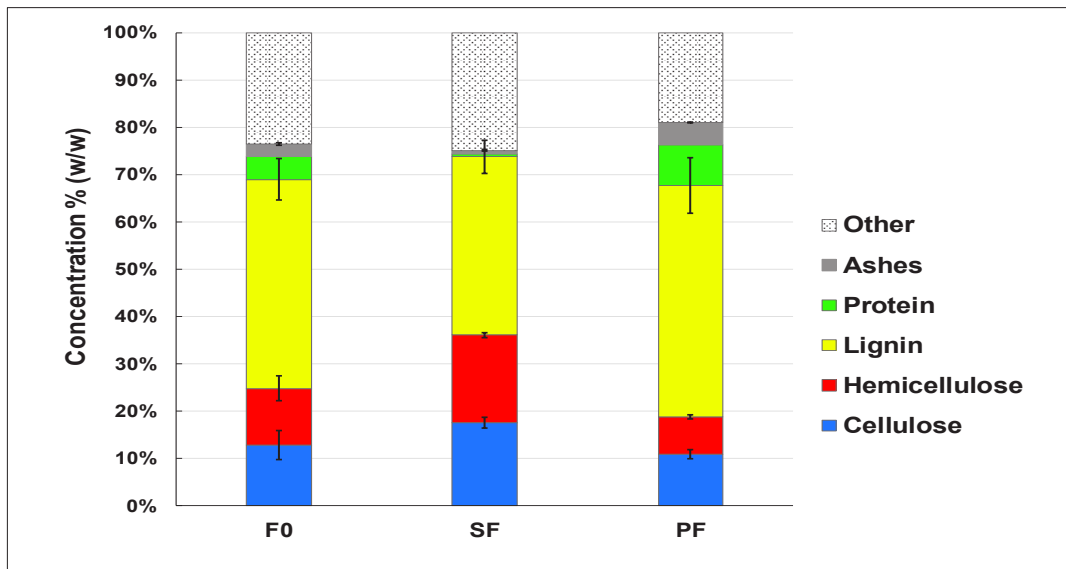


Figure 15: Biochemical composition (dry basis) of olive pomace-based fractions, *i.e.* F0 (ground crude olive pomace), SF (stone-rich fraction) and PF (pulp-rich fraction).

Finally, as regards the true density, a significant difference was noticed between the PF fraction having a density of 1.35 g.cm^{-3} and the SF and F0 having higher densities of respectively 1.42 and 1.43 g.cm^{-3} (Table 16). Since composite materials have been formulated by considering polymer/filler weight ratios, this means that for a given filler weight content, PF-based biocomposites will have slightly higher filler volume contents (V_f) than F0- and SF-based biocomposites (e.g. for PP-PF(15%), V_f is 10.6% while for PP-F0(15%) and PP-SF(15%), V_f is roughly 10.1%).

III. Résultats et discussion

Table 16: True density, color parameters (L^* , a^* , b^* and ΔE), morphological parameters and thermal degradation temperatures recorded under air flow ($T_{5\%}$, $T_{20\%}$ and T_{peak}) of olive pomace-based fillers.

	True density ($\text{g}\cdot\text{cm}^{-3}$)	L^*	a^*	b^*	ΔE	Median d_{50} in volume (μm) ^a	Median d_{50} in number (μm)	Median aspect ratio in surface ^b	$T_{5\%}$ ($^{\circ}\text{C}$)	$T_{20\%}$ ($^{\circ}\text{C}$)	T_{peak} ($^{\circ}\text{C}$)
F0	1.43 ± 0.01	36.8 ± 0.2	8.2 ± 0.0	13.5 ± 0.0	-	59 ± 2 (4.4)	0.55 ± 0.02	1.47 (0.71)	227 ± 4	272 ± 1	320 ± 0
SF	1.42 ± 0.00	57.8 ± 0.2	6.6 ± 0.1	15.3 ± 0.0	21.2 ± 0.2	56 ± 2 (3.6)	0.59 ± 0.01	1.42 (0.52)	250 ± 0	278 ± 1	282 ± 3
PF	1.35 ± 0.00	25.2 ± 0.3	7.4 ± 0.1	7.7 ± 0.3	13.0 ± 0.4	84 ± 7 (4.2)	0.53 ± 0.02	1.47 (0.43)	212 ± 2	264 ± 0	321 ± 1

^aValue in parenthesis corresponded to the span value ($span = (d_{90} - d_{10})/d_{50}$)

^bCalculated from image analysis results

III.2.3.1.2. Effect of dry fractionation on particle size and morphology

Grinding steps have been applied in such a way to obtain similar size distributions and median apparent diameters. All the fractions displayed bimodal volume-based size distributions, with a first population around 0.5 μm and a second one around 40-60 μm depending on the sample (Figure 16). Median apparent diameters deduced from volume-weighted distributions (d_{50}) were 84, 59 and 56 μm for the PF, F0 and SF fractions, respectively (Table 16). The PF fraction had a slightly higher d_{50} (about 30 μm more) than the other two fractions, probably due to its composition richer in lignin, which is known to promote plant tissues cohesion and to make the biomass more recalcitrant towards the grinding processes (Barakat *et al.*, 2013). However, this is in contradiction with other results. Indeed, Berthet *et al.* (2015), who compared the grindability of several lignocellulosic biomass, reported that in the case of wheat straw, the high content in cellulose and hemicellulose may hinder the obtaining of fine powders. These authors supposed that olive mills were more prone to produce fine powders due to the higher lignin content. When considering the number-weighted distributions, median diameters were respectively 0.5, 0.6 and 0.6 μm for the PF, F0 and SF fractions (Table 16), highlighting the presence of numerous submicronic size particles in the three samples.

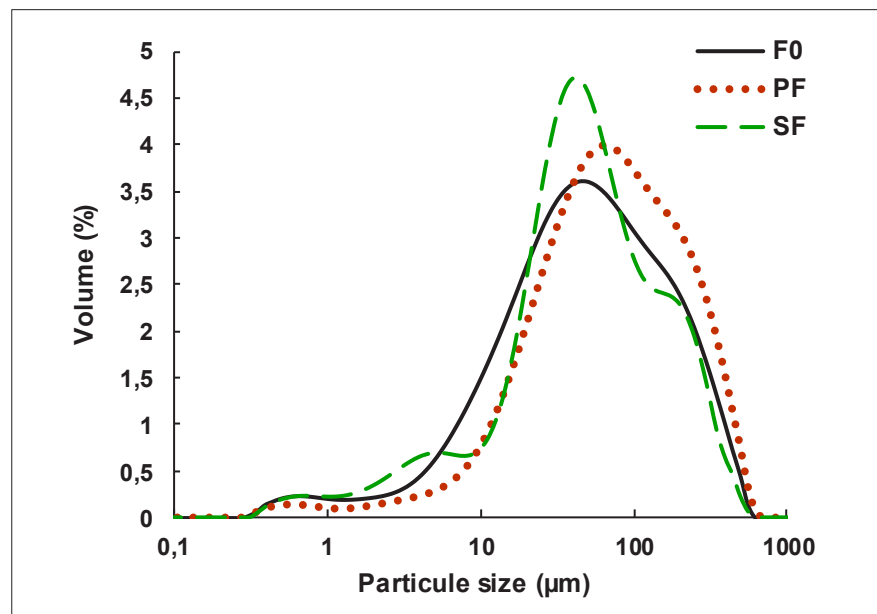


Figure 16: Particle size distribution of olive pomace fractions

SEM observations revealed that, globally, the three fractions primarily displayed a quite similar sphere-like shape with low aspect ratio (Figure 16). This was confirmed by quantitative image analysis based on surface-weighted distributions (Berthet *et al.*, 2017), with aspect ratio around

1.5 for the three samples. Some elongated particles were observed on SEM pictures in the case of the stone-rich fraction, but this population of particles had no significant impact on the median aspect ratio of this sample (Table 16).

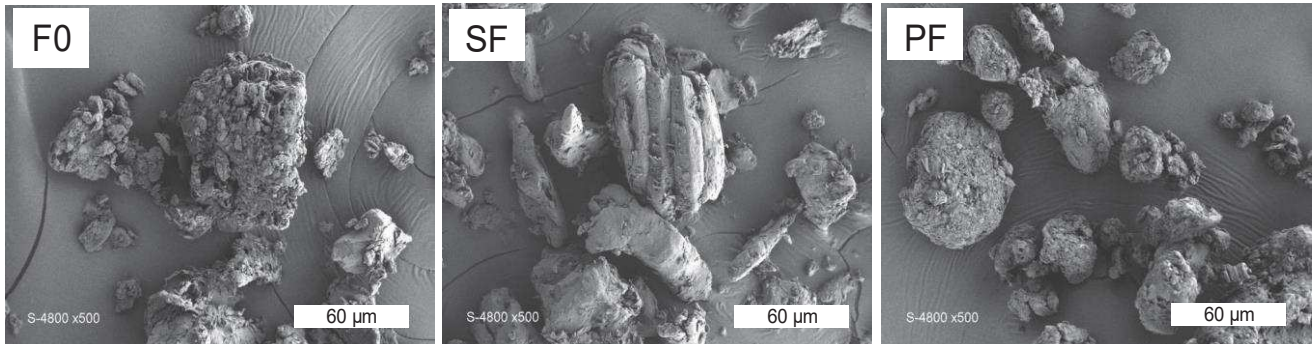


Figure 17: SEM images of F0, SF and PF fillers (scale bar = 60 μm).

III.2.3.1.3. Effect of dry fractionation on the thermal stability of olive pomace-based fillers

All the fractions exhibited a similar behavior: a first weight loss occurring up to 130°C corresponding to water loss (3.3, 4.5 and 7.2 wt% w.b. for SF, F0 and PF respectively), and one main weight loss between 150 and 350°C under air (or until 650°C under nitrogen), which corresponds to the thermal degradation of main organic compounds found in olive pomace, *i.e.* cellulose, hemicellulose, lignin and other non-cellulosic components (Figure 18 a1 and a2). Either under air or nitrogen conditions, the SF fraction was slightly more thermally stable than the F0 and PF fractions, with a higher $T_{5\%}$ and $T_{20\%}$ values (250°C and 278°C, respectively), whereas its degradation temperature at the maximal rate (T_{peak}) was 282°C against 320°C for F0 and PF (Table 16), this is certainly explained by lignin contents in each fractions. Furthermore, considering DTG curves, the degradation peak was clearly sharper for the SF fraction richer in cellulose and hemicellulose than for F0 and PF displaying broader peaks (Figure 18 b1 and b2). In the case of F0 and PF, the main degradation could be deconvoluted in at least two peaks. This was ascribed to the higher content of lignin in F0 and PF samples, which is known to thermally decompose over a wide temperature range from 150 to 500°C due to the presence of various oxygen functional groups (Ozveren and Ozdogan, 2013). Under nitrogen, thermal degradation leaves 24.9, 25.7 and 26.5 wt% w.b. of residue for SF, F0 and PF, respectively. Under air conditions, a third weight loss was observed from 360 to 510°C, corresponding to the oxidation reactions of aromatic rings of lignin and of the residue formed during the first degradation step (Shafizadeh *et al.*, 1972; Tejado *et al.*, 2007; Yang *et al.* 2007).

The residual matter corresponds to ashes and was 3.3, 3.5 and 6.5 wt% w.b for SF, F0 and PF, respectively.

Based on these results, it should be pointed out that thermal degradation of all OP-based fractions occurs at temperatures much higher than the melting point (T_m) of many conventional thermoplastic polymers, including PP and PHBV. As an example, a weight loss of 5 wt% w.b. was recorded at 212, 227 and 250°C for the PF, F0 and SF fractions, respectively. This makes OP-based fractions sufficiently thermally stable to be used as fillers in thermoplastic biocomposites.

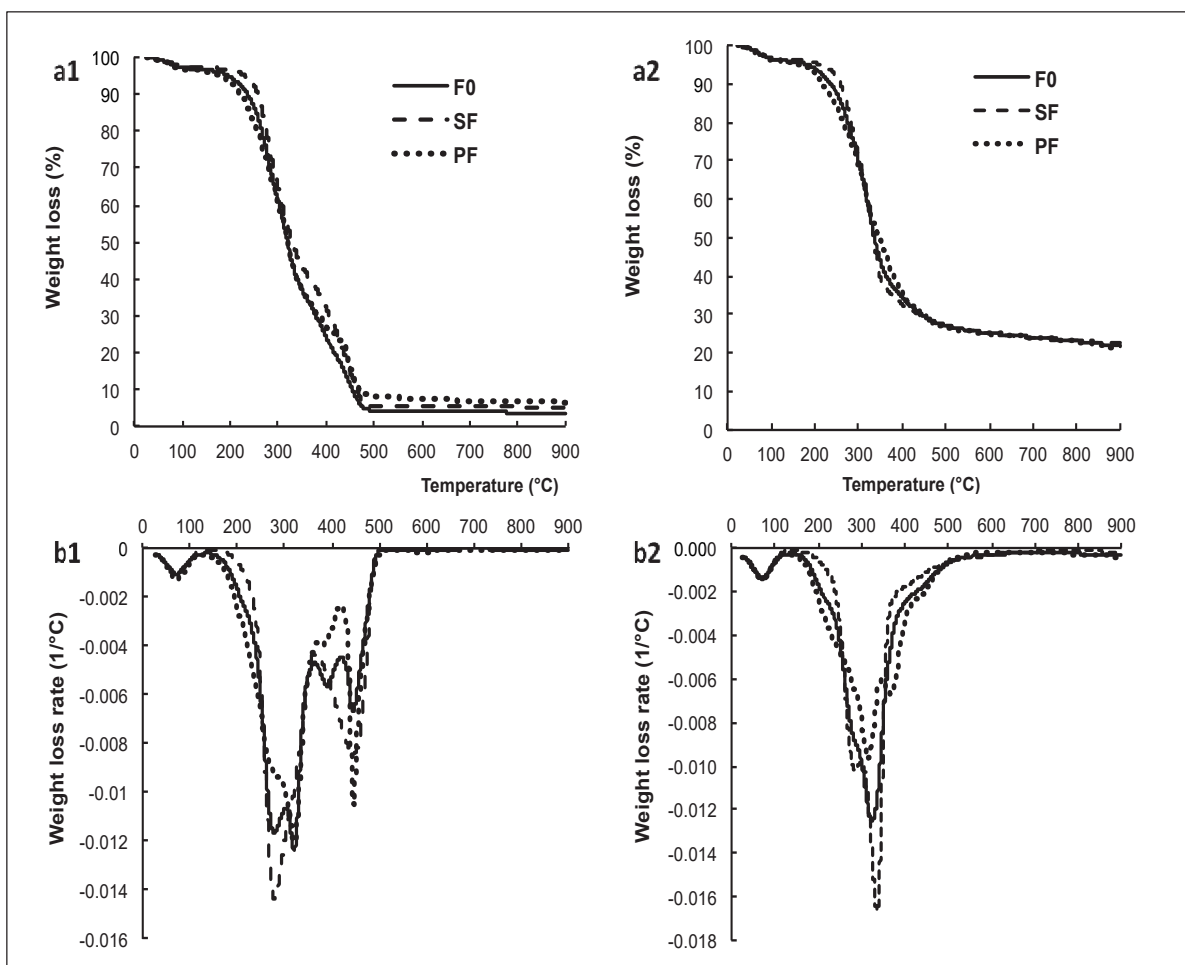


Figure 18: TGA (a) and DTG (b) curves of F0, SF and PF fractions under air (a1 and b1) and nitrogen (a2 and b2).

III.2.3.1.4. Effect of dry fractionation on the surface energy of olive-pomace based fillers

On the basis of contact angle θ ($^{\circ}$) measurements and calculated surface free energy γ (mJ.m^{-2}), it appears that the three produced fractions displayed different wettability properties (Table 2). SF appeared as the most polar fraction, with the lowest contact angle with water ($\theta = 59^{\circ}$), the highest polar component ($\gamma^p = 9.7 \text{ mJ.m}^{-2}$) and the lowest dispersive component ($\gamma^d = 28.9 \text{ mJ.m}^{-2}$) of the surface free energy. These results were explained by the higher content of hydrophilic compounds, i.e. cellulose and hemicelluloses, in the stone-rich fraction. On the other hand, the PF fraction was the most apolar. This latter displayed the highest contact angle value with water ($\theta = 75^{\circ}$), the lowest polar component ($\gamma^p = 2.7 \text{ mJ.m}^{-2}$) and the highest dispersive component ($\gamma^d = 37.6 \text{ mJ.m}^{-2}$) of the surface free energy. This was explained by the richer composition in lignin of PF fraction as compared to the two other fractions, which is known to bring water impermeability to plants and reduce the polar character of the filler surface (Le Digabel *et al.*, 2004). The higher hydrophobicity of the pulp-rich fraction could also be attributed to the presence of residual oil in this tissue. As reported by Rigane *et al.* (2012), the fat content of olive pomace is less than 2% and Maymone *et al.* (1961), confirmed that the pulp is rich in oil, i.e. more than 50%). Regarding the starting fraction F0, it displayed intermediate wettability properties between those of the pulp and stone-rich fractions. These results highlighted the efficiency of the applied dry fractionation process to separate the pulp from the stone and produce olive pomace-based fractions with contrasted surface properties.

The predicted work of adhesion between the matrix and the filler was calculated for each formulation based on surface free energy of each constituent, i.e. fillers and matrices (Table 17). Work of adhesion values are similar to those reported in literature for other ligno-cellulosic substrates with thermoplastic matrices (Fuentes *et al.* 2015; Tran *et al.* 2013). Little differences could be noticed between the three fractions towards PP and PHBV. The pulp-rich fraction is expected to exhibit the highest affinity towards both matrices due to its lower polar character and highest surface free energy (work of adhesion of 72 mJ.m^{-2} for the two matrices) while the stone-rich fraction is expected to be slightly less compatible with the matrices due to its higher polar character and lower surface free energy (work of adhesion of 69 and 66 mJ.m^{-2} with PP and PHBV, respectively).

III. Résultats et discussion

Table 17: Contact angle (θ), polar (γ^p) and dispersive (γ^d) components of the solid surface free energy (γ) and predicted work of adhesion (W_{mf}) between polymer matrices and OP-based fillers.

	Contact angle θ (°)					Surface free energy (mJ.m ⁻²)			Predicted work of adhesion (W _A) (mJ.m ⁻²)	
	Water	Ethylene glycol	Diiodomethane	Formamide	Glycerol	γ	γ^p	γ^d	W _{PP-filler}	W _{PHBV-filler}
F0	66 ± 1	56 ± 2	30 ± 5	53 ± 7	83 ± 3	38.5	6.3	31.8	69	68
SF	59 ± 1	58 ± 4	35 ± 4	46 ± 3	82 ± 3	38.5	9.7	28.9	69	66
PF	75 ± 2	56 ± 2	26 ± 3	45 ± 3	87 ± 3	40.2	2.7	37.6	72	72
PP	80 ± 6	71 ± 6	40 ± 7	67 ± 3	85 ± 5	32.1	2.8	29.3	-	-
PHBV	90 ± 6	75 ± 4	45 ± 4	69 ± 5	83 ± 8	32.2	1	31.2	-	-

III.2.3.2. Structure of olive pomace-based biocomposites

III.2.3.2.1. Visual appearance of films

PF-based composites appeared homogeneous for all tested filler contents, whereas SF- and F0-based composites exhibited a macroscopic heterogeneity for filler contents higher than 15 wt%. This heterogeneity was characterized by irregularities at the surfaces of films, resulting in a rough surface and was accentuated at a filler ratio of 30 wt%. This was particularly pronounced in the case of SF-based materials, which became more friable with the presence of micro-cracks and holes due to visible filler particles agglomerations. Such differences in the appearance of films could be explained by the respective affinity of fillers towards matrices, in particular by their respective polarity and surface free energy (Figure 14 and Table 17). It is assumed that the lignin-rich PF fraction being more hydrophobic should show a better affinity towards PP and PHBV, thus leading to a better dispersion of the fillers within both matrices.

Colorimetric parameters are very important in the field of food packaging as regards consumer acceptability. Transparency or even translucence is often requested by consumers in order to be able to see the product. However, it is worth noting that in the case of rigid and opaque composite materials dedicated to trays applications, the use of a transparent lid film would allow to fulfill this requirement. Finally, the opacity could be required for some food products such as fatty foods in order to hinder oxidative degradation reactions by acting as a barrier to light (Romani *et al.* 2017). Concerning the produced biocomposite films, PF-based formulations were visually dark brown and opaque while SF-based composites were also opaque and had a light beige color. F0-based materials displayed an intermediate light brown color. These observations were confirmed by colorimetric analyzes carried out on PP and PHBV biocomposites filled with 15wt% of olive pomace-based fractions (Table 18). The difference of color (ΔE) between biocomposites and the respective virgin polymer matrix was 63.1 and 56.7 for the PP-PF and PHBV-PF formulations, against 31.8 and 25.7 for the PP-SF and PHBV-SF formulations. The lightness values (L^*) recorded for the PP-PF and PHBV-PF were 35.8 and 34.7, respectively, indicating that the difference in lightness between the two matrices was erased in presence of the PF fraction. Furthermore, whatever the formulation, increasing filler content led to an increase in the darkness of the films. The resulting color of biocomposites was clearly dependent on the color of the fillers, which is an intrinsic property related to their biochemical composition.

Table 18: Colorimetric attributes (L^* , a^* , b^* and ΔE) of biocomposites filled with 15 wt% of OP-based fillers.

	L^*	a^*	b^*	ΔE
PHBV (control)	88.5 ± 0.3	-0.5 ± 0.0	20.6 ± 0.4	-
PHBV-F0(15%)	41.5 ± 0.1	8.7 ± 0.1	10.3 ± 0.1	49.0 ± 0.1
PHBV-SF(15%)	65.1 ± 0.2	4.6 ± 0.0	26.4 ± 0.0	25.7 ± 0.2
PHBV-PF(15%)	34.7 ± 0.5	8.6 ± 0.2	3.2 ± 0.0	56.7 ± 0.5
PP (control)	97.8 ± 0.0	-0.8 ± 0.0	4.4 ± 0.0	-
PP-F0(15%)	48.4 ± 0.1	11.7 ± 0.1	22.8 ± 0.1	54.1 ± 0.0
PP-SF(15%)	74.6 ± 0.1	4.7 ± 0.4	25.6 ± 0.4	31.8 ± 0.2
PP-PF(15%)	35.8 ± 0.2	10.7 ± 0.0	8.4 ± 0.1	63.1 ± 0.1

III.2.3.2.2. Observation of the microstructure

SEM observations on cryo-fractured films were done to qualitatively investigate the microstructure of biocomposites. Figure 19 presents images obtained for PP-based biocomposites. The cross-section of neat PP films was quite smooth and uniform. The incorporation of either F0 or SF fillers led to a very heterogeneous and rough section with the presence of many holes, due to debonding of particles. This evidences the very poor interfacial adhesion between the PP polymer matrix and F0 or SF particles. This certainly justifies the different chemical treatments of olive stone powders applied by several authors in order to improve their compatibility with polymer matrices (Djidjelli *et al.*, 2007; Gharbi *et al.*, 2014; Hammoui *et al.*, 2015; Hassaini *et al.*, 2017). In contrast, the cryo-fractured section of PF-based biocomposites appeared very homogeneous with particles well embedded by the polymer, highlighting a good interfacial adhesion between the two constituents. It is worth noting that similar observations were found for PHBV-based biocomposites. Furthermore, these results are in agreement with the predicted values of work of adhesion. Based on these observations, variations in functional properties between the different PP- and PHBV-based biocomposites are expected.

III.2.3.2.3. Melting and crystallization behavior

DSC analysis was carried out on biocomposites filled with 15 w% of OP-based particles (Table 19). The effect of processing was analysed based on the comparison of the first and second heating thermograms. PP-based materials were thermally very stable, with identical values of

melting temperatures for either the first or the second heating ramp. In the case of PHBV-based materials, T_{m1} were significantly higher than T_{m2} values (from 4 to 7°C) for all the formulations,

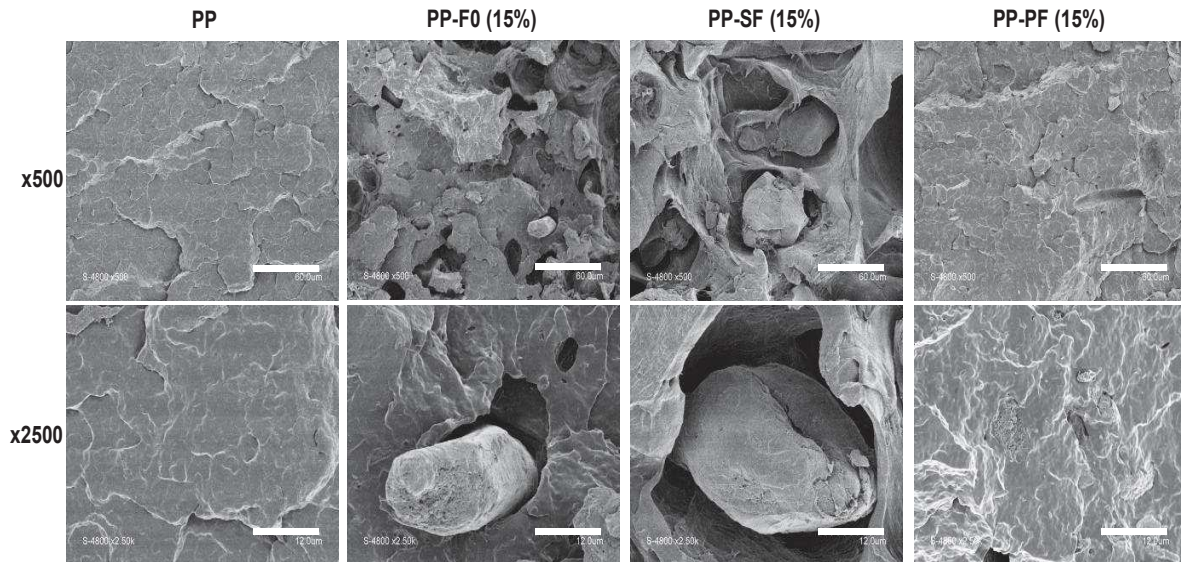


Figure 19: SEM images of cryo-fractured surfaces of PP-based composites filled with 15 wt% of either F0, SF and PF fillers (x 500: scale bar = 60 µm; x 2500: scale bar = 12 µm).

meaning that PHBV crystals with higher thermal stability (corresponding to higher melting temperature) were formed during processing. This could be related to the slow cooling rate applied during the manufacturing of the biocomposite films by thermocompression that could induce changes in the crystallization process of PHBV, possibly the formation of more perfect crystals.

Besides, the melting temperature T_m of PHBV was significantly decreased after the incorporation of OP-based fillers. As an example, T_{m2} decreased from 171°C to 167, 164 and 162 for films filled with 15 wt% of SF, PF and F0, respectively. As already demonstrated by Berthet *et al.* (2015), this decrease in melting temperature in the presence of lignocellulosic fillers is most probably related to a decrease in PHBV molecular weight owing to both thermal and hydrolytic degradation reactions of chains during the thermo-mechanical processing of materials. As regards the crystallization temperature T_c , it decreased from 121°C for the neat PHBV matrix to 118°C and 114°C for PHBV-SF and PHBV-F0 composites respectively, while it was not impacted by the presence of PF fillers. This suggests that the presence of F0 and SF fillers could hinder the crystallization process by delaying the nucleation. Additional analyses by polarized light microscopy and isothermal DSC should be performed to investigate the effect

of OP-based fillers on the crystallization kinetics of PHBV matrix. Finally, the degree of crystallinity X_c of PHBV-based materials was significantly decreased in the presence of SF and F0 fillers until 68 % and 65 % respectively, while it was increased in the case of PF fillers from 75 % up to 78% (Table 19). This phenomenon is not process-dependent since it is observed for both first and second heating. It suggests that PF particles favoured the crystallization of PHBV, in relation with the higher ashes content in PF and/or to enhanced interactions with the matrix, as already reported by Calabia *et al.* (2013). In the case of PP-based biocomposites, thermal properties and degree of crystallinity of the polymer matrix were not significantly impacted by the introduction of olive pomace-based fillers (Table 19).

III.2.3.3. Functional properties of olive-pomace based biocomposites films

III.2.3.3.1. Thermal stability

Thermal stability of biocomposites is an important property for packaging likely to be heated during their service use. It was investigated by thermogravimetric analysis under oxidative atmosphere (Figure 20). Both polymer matrices displayed one main degradation peak, with a clearly sharper drop in the case of neat PHBV. Biocomposites showed a thermal behavior similar to their main constituents, *i.e.* the polymer matrix and lignocellulosic fillers. Globally, the introduction of olive pomace-based fillers resulted in a reduction of the thermal stability of materials, with a thermal degradation beginning at low temperatures and occurring in a wider temperature range as compared to the neat matrix (Table 19). This was due to the previously reported lower thermal stability of lignocellulosic fillers as compared to the polymer matrices (Table 16). As expected, the more thermally stable the filler, the more thermally stable the biocomposites, as illustrated by the higher thermal stability of SF-based biocomposites. In the case of PP-based composites, the decrease in thermal stability follows a rule of mixture according to the respective contents of PP and fillers (see Figure 20a for PP-F0(15%)). This evidences the high thermal stability of PP and the fact that the thermal stability of the composites was not influenced by negative filler / polymer interactions. In the case of PHBV-based materials, the reduction of the thermal stability was more pronounced and did not follow a simple rule of mixture (see Figure 20b for PHBV-F0(15%)). PHBV is known to be very sensitive towards temperature, especially above its melting point, due to the concomitance of two thermal degradation mechanisms of PHBV, *i.e.* a random chain scission by cis-elimination and trans-esterification reactions in a lesser extent (Leroy *et al.*, 2012). As already well described by Berthet *et al.* (2015) and later by Hassaini *et al.* (2017), the introduction of

III. Résultats et discussion

Table 19: Thermal properties (crystallization temperature (T_c), melting temperature (T_m), melting enthalpy (ΔH_m), degree of cristallinity (X_c) and degradation temperature (T_{onset} , T_{peak} , T_{offset})) of biocomposites filled with 15 wt% of OP-based fillers.

	T_c (°C)	T_{m1} (°C)	ΔH_{m1} (J.g ⁻¹)	X_{c1} (%)	T_{m2} (°C)	ΔH_{m2} (J.g ⁻¹)	X_{c2} (%)	T_{onset} (°C)	T_{peak} (°C)	T_{offset} (°C)
PHBV (control)	121 ± 0	175 ± 2	85 ± 2	59 ± 2	171 ± 1	93 ± 2	75 ± 1	249±3	293±0	312±1
PHBV-F0(15%)	114 ± 1	169 ± 1	77 ± 1	46 ± 4	162 ± 1	80 ± 3	65 ± 2	199±2	260±1	531±1
PHBV-SF(15%)	118 ± 0	171 ± 1	79 ± 2	43 ± 0	167 ± 0	85 ± 2	68 ± 1	208±0	272±0	517±1
PHBV-PF(15%)	122 ± 3	168 ± 1	81 ± 1	53 ± 3	164 ± 1	96 ± 6	78 ± 1	196±1	254±1	514±4
PP (control)	132 ± 0	165 ± 1	94 ± 1	63 ± 1	164 ± 0	110 ± 1	74 ± 1	220±0	402±2	425±2
PP-F0(15%)	127 ± 1	165 ± 0	86 ± 5	68 ± 5	164 ± 1	92 ± 4	73 ± 3	201±1	390±1	494±1
PP-SF(15%)	127 ± 0	166 ± 1	82 ± 1	65 ± 1	165 ± 0	94 ± 2	75 ± 2	213±2	389±1	504±5
PP-PF(15%)	122 ± 6	166 ± 1	80 ± 2	63 ± 1	164 ± 0	91 ± 1	72 ± 0	194±4	400±4	490±3

lignocellulosic fillers induces additional hydrolytic degradation reactions through chain scission reactions at ester linkages due to the inherent presence of residual water molecules (even if dried before processing) and degradation products (alcohols and carboxylates) on lignocellulosic particles. It was demonstrated that the introduction of lignocellulosic fillers negatively impacts the thermal stability of PHBV (Berthet *et al.*, 2015). Hopefully, the degradation temperatures remained relatively high for all the formulations, i.e. above 200°C, if considering the heating up temperatures typically used for food products protected by packages.

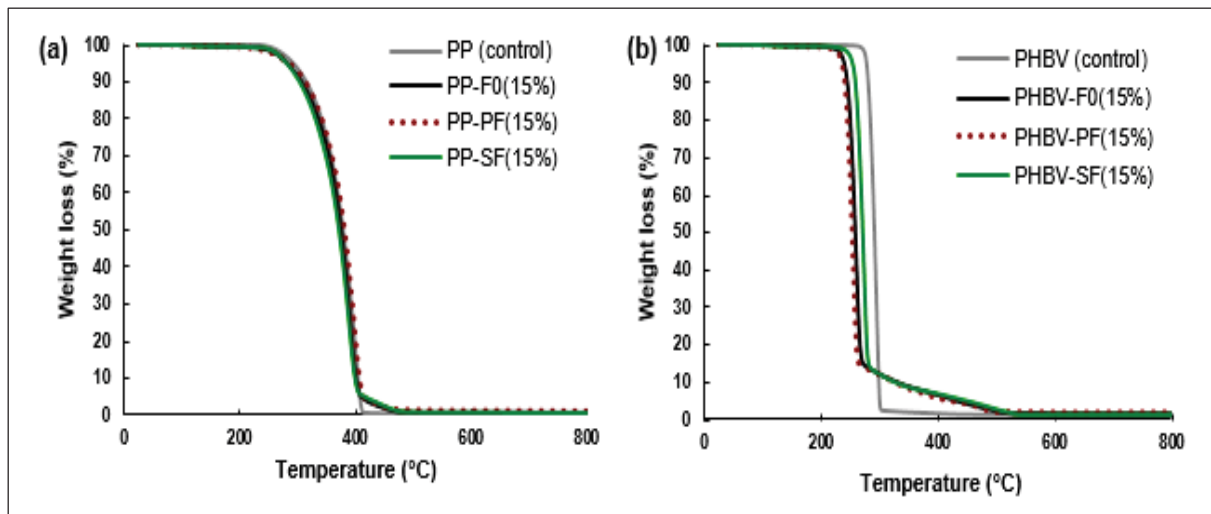


Figure 20: TGA and DTG curves of (a) PP and (b) PHBV-based biocomposites under air.

III.2.3.3.2. Mechanical properties

Mechanical properties of materials were investigated through tensile tests. Due to their low aspect ratio, the introduction of olive pomace-based fillers did not significantly impact the Young's modulus of either PP or PHBV within the range of tested filler contents (Table 20). However, a strong effect was noticed regarding ultimate properties. Whatever the filler or the matrix, a reduction of the material stress and strain at break was noticed. This decrease was all the more important with increasing filler amounts and depending on OP-based filler type. At low filler contents (below 15 wt%), no effect of filler type was observed while for higher filler contents (30wt%), the decrease in stress at break was more pronounced for SF and F0 fractions. As an example, a stress at break reduction of 36% was recorded for the PHBV-PF (30%), while it was more than the double (78%) for the PHBV-SF (30%) material. A similar effect was noticed for the elongation at break. In general, the highest reduction rates were recorded with SF-based composites, which were for example 39%, 61% and 74% for PHBV-SF materials filled with respectively 5, 15 and 30 wt% of SF. On the other hand, the elongation at break of

Table 20: Mechanical properties (Young's modulus, stress at break and elongation at break), water vapor permeability (WVP) and oxygen permeability of olive pomace-based biocomposites (n.d.: not determined).

Samples	Elongation at break (%)	Stress at break (MPa)	Young's modulus (GPa)	WVP x 10 ¹² (mol m ⁻¹ s ⁻¹ Pa ⁻¹)	PO ₂ x 10 ¹⁷ (mol m ⁻¹ s ⁻¹ Pa ⁻¹)
PHBV control	2.3 ± 0.3	34.2 ± 4.0	2.7 ± 0.4	0.9 ± 0.1	78.9 ± 5.6
PHBV-F0(5%)	1.7 ± 0.2	27.8 ± 3.5	2.9 ± 0.2	1.1 ± 0.2	n.d.
PHBV-F0(15%)	1.2 ± 0.2	18.1 ± 3.0	2.4 ± 0.2	1.5 ± 0.0	80.1 ± 3.9
PHBV-F0(30%)	1.0 ± 0.2	11.9 ± 2.0	2.2 ± 0.2	15.1 ± 2.6	n.d.
PHBV-SF(5%)	1.4 ± 0.2	26.5 ± 3.6	2.7 ± 0.2	0.3 ± 0.0	n.d.
PHBV-SF(15%)	1.2 ± 0.2	18.5 ± 4.8	2.5 ± 0.4	1.8 ± 0.2	85.9 ± 10.6
PHBV-SF(30%)	0.6 ± 0.1	7.7 ± 3.0	2.2 ± 0.5	3.9 ± 0.2	n.d.
PHBV-PF(5%)	2.1 ± 0.1	26.7 ± 2.1	2.4 ± 0.2	0.5 ± 0.1	n.d.
PHBV-PF(15%)	1.5 ± 0.3	17.9 ± 2.6	2.2 ± 0.2	0.7 ± 0.2	87.2 ± 2.6
PHBV-PF(30%)	1.5 ± 0.1	21.7 ± 1.3	2.4 ± 0.1	1.0 ± 0.2	n.d.
PP control	8.5 ± 1.1	28.8 ± 3.6	1.3 ± 0.1	0.6 ± 0.1	63.9 ± 2.7
PP-F0(15%)	3.7 ± 0.5	18.9 ± 1.1	1.3 ± 0.1	1.1 ± 0.1	63.6 ± 3.9
PP-SF(15%)	3.3 ± 0.3	17.5 ± 2.4	1.4 ± 0.2	1.2 ± 0.3	64.8 ± 2.4
PP-PF(15%)	5.2 ± 0.6	19.1 ± 1.2	1.2 ± 0.1	0.7 ± 0.1	67.0 ± 2.4

PF-based formulations was better preserved, with reductions of 9% and 35% for filler contents of respectively 5 and 30 wt%. It is worth noting that ultimate properties were better preserved in the case of PP-based materials. As an example, a reduction of the stress of break of respectively 34-39% and 47% for PP and PHBV filled with 15 wt% of fillers (whatever the composition). Similar results were also reported for olive pomace/polypropylene-based biocomposites (Ayrilmis and Buyuksari, 2010; Siracusa *et al.*, 2001).

In general, the functional properties of composite materials are governed by (i) intrinsic properties of each constituent, including their chemical composition and structure, (ii) the filler aspect ratio, dispersion state and content, and (iii) the quality and quantity of interactions at the filler/matrix interface (Berthet *et al.*, 2015; 2017). For all the formulations considered in the present study, the loss in the ultimate tensile performances could be directly related to the quality of the filler/matrix interfacial adhesion. It should also be pointed out that the low aspect ratios (Table 16) of OP-based fillers do not favour the development of large interfacial areas. In the case of poor filler/matrix interactions, as revealed for SF- and F0-based composites by SEM observations, mechanical failure will occur at the interface and be favoured by the presence of gaps between the matrix and the fillers. Furthermore, increasing filler content would favour the agglomeration of lignocellulosic particles, leading to the creation of microscopic and macroscopic defects, including voids, within the material, hence constituting a fragile zone conducive to the initiation and propagation of macro-cracks. This agglomeration phenomenon

should be more pronounced for the fractions having a poor affinity towards the polymer matrix. Finally, in the case of PHBV-based materials, changes in tensile properties could also be related to matrix structural changes induced by the presence of fillers, including the degradation of the polymer molecular weight and decrease in degree of crystallinity, that favour a loss of both stress and strain at break. In the case of PHBV/PF composites, the higher degree of crystallinity (calculated from the first heating ramp, Table 19) as well as better interfacial adhesion (slightly higher work of adhesion) could explain the better preservation of ultimate properties compared to SF- and F0-based composites. The fact that mechanical properties of PP-based materials were better preserved than those based on PHBV could be explained by a slightly higher affinity of fillers towards PP, as suggested by the predicted work of adhesion, and also to the fact that macromolecular and crystalline structure of PP was not significantly affected by the presence of olive pomace-based fillers, in particular no degradation occurred upon processing by extrusion and thermocompression.

It is possible to describe the composition dependence of the tensile strength of polymer composites using interfacial adhesion models as proposed by Pukánszky (1990):

$$(\sigma_c = \sigma_m \lambda^n \left(\frac{1-x_f}{1+2.5x_f} \right) e^{(Bx_f)} \quad \text{(Equation 8)})$$

Where σ_c , and σ_m are the tensile strength of the composite and the matrix, respectively, λ is the relative elongation of the specimen, n is a parameter characterizing the strain hardening tendency of the matrix and which was calculated by the curve fitting procedure, x_f is the filler volume fraction, and B an empirical fitting parameter characterizing the quality of the interfacial adhesion, related to filler/matrix interactions and the size of the interface (Pukánszky, 1990). The lower the B value, the worst is the interfacial adhesion. This model was applied to the PHBV-based composites.

As seen in Figure 21, the model satisfactorily fits the evolution of the tensile strength over the all range of filler contents for SF- and F0-based composites, with B parameters of -2.31 and -1.08, respectively, and n values of roughly 1, i.e. limited strain hardening. Considering the negative values of B for these formulations, this suggests that the reduction of the tensile strength was not only related to filler/matrix interfacial adhesion effects but also to large microscopic and macroscopic defects that drastically favour macro-cracks initiation and propagation. Besides, the intrinsic properties of the PHBV matrix were affected by the presence of fillers and their amount, which cannot be considered in the model. Indeed, the intrinsic properties of the degraded polymer matrix within a composite material are difficult to approach. It is worth mentioning that a low but positive value of B was obtained for the PHBV-PF

formulation ($B=0.23$), meaning that for the PF filler, the negative effect of polymer degradation, and defects could be counterbalanced by the positive effect of a better interfacial adhesion and higher degree of crystallinity. Concluding, the creation of favorable filler/matrix physico-chemical interactions (i.e. higher work of adhesion) appear as a key for the control of the ultimate mechanical properties of such biocomposite systems in which the aspect ratio of the fillers and the resulting size of filler/matrix interfaces are low.

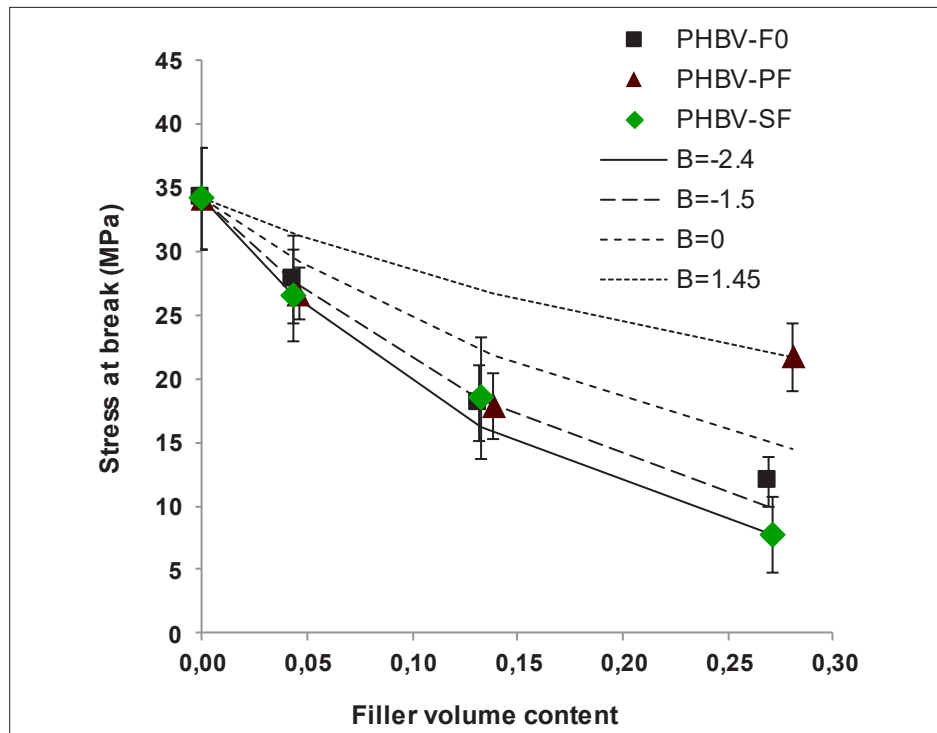


Figure 21: Experimental values of the stress at break of PHBV and PBHV-based composites filled with 5, 15 and 30 wt% of SF (●), F0 (□) or PF (▲) fillers and resulting fitted curves with Pukanszky's model.

III.2.3.3.3. Water vapour and oxygen permeability

Results revealed that water vapour permeability WVP ($\times 10^{12} \text{ mol.m}^{-1}.\text{s}^{-1}.\text{Pa}^{-1}$) strongly depended on the concentration and the nature of the filler (Table 20). Globally, the introduction of F0 or SF fillers (except for the PHBV-SF(5%) formulation) led to a significant increase in WVP of either PP or PHBV. As measured for PHBV-based materials, this increase in WVP was more pronounced for increasing filler contents. WVP increased from $0.9 \times 10^{-12} \text{ mol.m}^{-1}.\text{s}^{-1}.\text{Pa}^{-1}$ for the neat PHBV up 1.1, 1.5 and $15.1 \times 10^{-12} \text{ mol.m}^{-1}.\text{s}^{-1}.\text{Pa}^{-1}$ for PHBV-CF(5%), PHBV-CF(15%) and PHBV-CF(30%) respectively, which corresponded to increases of respectively 22%, 67% and more than 1500%. The WVP increase was in the same range for PP, with an

increase of 83% for PP-CF (15%). In contrast, the introduction of pulp-rich particles in PHBV led to a reduction in WVP of about 44% for PHBV-PF(5%) and 22% for PHBV-PF(15%), while WVP value remained constant for a high filler content of 30 wt%. In the case of PP, WVP was not significantly impacted by the introduction of PF fillers.

As already reported for PHBV/wheat straw fibres biocomposites, this was mainly ascribed to the hydrophilic character of fillers (Berthet *et al.*, 2015; Hassaini *et al.* 2017) and the existence of water vapour clustering (Wolf *et al.*, 2016). It is sure that the presence of interfacial gaps would have an effect on WVP, but this effect is not yet well understood. Indeed, the assumption of Berthet *et al.* (2015), that a bad filler/matrix interfacial adhesion would favour the creation of a preferential pathway for the diffusion of water vapour is in contradiction with the decrease in diffusivity showed by Wolf *et al.* (2016). In this study, the very high WVP (increase of a factor of about 25) recorded for PHBV-F0(30%) was ascribed to the presence of cracks on the surface of films. As already observed by Berthet *et al.* (2015), the incorporation of lignocellulosic fillers (at a filler content of 20 wt%) on WVP of PHBV had not the same impact according to the nature of the filler. Wheat straw fillers led to a significant increase in WVP of PHBV, whereas the introduction of olive mills led to a decrease in WVP. The barrier effect brought by the introduction of PF fillers could be attributed to the apolar nature of this lignin-rich filler, and overall to the better interfacial interactions between PF fillers and PHBV, inducing a tortuosity effect and hence an increase in the water vapour diffusion pathway. The tortuosity effect could also be ascribed to the previously mentioned higher degree of crystallinity (Table 4), PHBV crystallites being less permeable to water vapor.

In the case of food packaging, the large variety of food products to be packaged requires a wide range of mass transfer properties (Petersen *et al.*, 1999). As an example, respiring food products, would require permeable packaging materials to avoid condensation of water vapour inside the packaging, while dry products such as bakery or delicatessen would need barrier packaging materials (Siracusa *et al.*, 2008). Consequently, olive stone (SF)-based composites appeared as promising materials to reach the requirements of respiring food products such as cheese, fruits and vegetable because of their transpiration, whereas olive pulp (PF)-based composites would be more adapted for water sensitive products like sandwiches (Petersen *et al.*, 1999).

Based on tensile properties and WVP results, materials filled with 15 wt% of olive pomace-based particles were selected for measuring oxygen permeability (Table 20). Hassaini *et al.* (2017) reported a significant decrease in the oxygen barrier properties after the incorporation

of stone-based filler to PHBV. According to these authors, the non-compatibility of the system filler/matrix leads to the formation of micro-voids due to the poor interfacial adhesion between the two components, which make oxygen permeation easier. In this study, oxygen permeability of either PP or PHBV was not significantly impacted by the incorporation of olive pomace-based fillers. These results could be explained by two concomitant and competitive phenomena. Structural changes of PHBV matrix that would be in favour of an increase of oxygen permeability (effect on diffusion, as shown for water vapour) are compensated by the fact that oxygen is an apolar molecule displaying a poor affinity towards lignocellulosic particles (effect on sorption). Only a very slight increase in oxygen permeability (raise of 11%) was noticed in the case of PHBV-PF(15%), probably due to the higher apolar character of pulp-rich fractions, and thus higher affinity towards oxygen.

III.2.4. Conclusion

In response to the ecological concerns aimed at stimulating the development of new materials from renewable sources without competition with food usage, olive pomace, the solid lignocellulosic residue of olive oil extraction, was processed by dry fractionation so as to obtain contrasted fillers for the formulation of petroleum-based (PP) and fully bio-based and biodegradable (PHBV) biocomposites materials.

Our results evidences that OP-based fillers displayed different affinities towards PP and PHBV matrices depending on their dry fractionation route. Such observations were confirmed by contact angle measurements and SEM analysis. Filler/matrix adhesion has a preponderant impact as regards the functional properties of biocomposite. An appropriate choice of the filler-matrix combination could thus allow modulating the biocomposites properties according to the requirements of the targeted application.

In general, the incorporation of olive pomace fillers resulted in a reduction of both the stress and the elongation at break for either PP and PHBV-based biocomposites. This effect was more pronounced at high filler content. A better preservation of mechanical characteristics was achieved in the case of pulp-rich filler (PF), due to better filler/matrix interactions and hence higher interfacial adhesion. It is worth noting that mechanical properties were less preserved in the case of PHBV-based composites, probably due to the thermal degradation of PHBV occurring during melt extrusion and thermocompression and favored by the presence of lignocellulosic fillers. Considering the barrier characteristics of the biocomposites, water vapour permeability was increased in presence of SF and CF fillers for both PP and PHBV

formulations. Our results suggest that according to their biochemical composition and physicochemical characteristics, OP-based fillers can be used in packaging materials for various range of foods, from fresh respiring products such as cheeses, fruits or vegetables until the water sensitive products like dry or fatty foods and prepared meals. For Zeman and Kubik (2007), the absolute barrier does not exist. It is necessary to adapt barrier properties to the real life.

Finally, the combination of OP-based fillers with thermoplastic polymers to develop low cost and functional biocomposite materials is a relevant and sustainable approach to value one of the main by-products of olive oil industry. Given that PP is the most widely used polymer in the packaging sector, PP/OP-based composites have the advantage of being less expensive than virgin PP materials, with an overall reduced fossil resource content. Concerning PHBV-based biocomposites, the additional huge advantage is that they are fully bio-based and biodegradable even in non-composting conditions.

Acknowledgments

This research was supported by MALICE project co-financed by the European Regional Development Fund, and the PNE Program (2016-2017) of the Algerian Ministry of Higher Education and Scientific Research. Authors would like to thank Benjamin GALLARD from C2MA (IMT Mines Alès) for his technical support in the preparation of the compounds and Amélie BREYSSE from IATE (Montpellier-France) for her help with image analysis.

III.3. Biodegradability of olive pomace-based biocomposites: Impact of filler composition

(Article n°3)

III.3. Biodegradability of olive pomace–based biocomposites: Impact of filler composition

Article en préparation pour soumission

Sarah Lammi^{1,2}, Emmanuelle Gastaldi¹, Fabrice Gaubiac¹, Djamel Djenane², Nathalie Gontard¹, Hélène Angellier-Coussy¹

¹JRU IATE 1208 – CIRAD/INRA/Montpellier SupAgro/University of Montpellier, 2 place Pierre Viala, F-34060 Montpellier, France.

²Laboratory of Food Quality and Food Safety, Department of Agronomic Sciences, University of Mouloud MAMMERI, BP 17, 15000 Tizi-Ouzou, Algeria.

Résumé

Le polyhydroxybutyrate-co-valérate (PHBV) est un polyester bactérien biosourcé et biodégradable très prometteur, dont le développement commercial est encore limité par son coût élevé. D'autre part, l'extraction de l'huile d'olive génère une grande quantité de résidus solides lignocellulosiques, appelés grignons d'olive (OP). Son élimination soulève des préoccupations environnementales, notamment l'inhibition des populations microbiennes du sol et la réduction de la germination des graines. Pour résoudre ces problèmes, des biocomposites à base de PHBV / OP ont été produits (teneur en charge de 15%) en utilisant trois charges différentes obtenues par fractionnement sec de l'OP, une fraction riche en noyau (SF), une fraction riche en pulpe (PF) et le grignon brut (F0). L'objectif du présent travail était d'étudier l'influence de la composition des charges à base d'OP sur la biodégradabilité des biocomposites résultants. La biodégradation du PHBV, des charges à base d'OP et des biocomposites à base d'OP / PHBV a été étudiée dans le sol par des tests respirométriques sur 4 mois. Les résultats ont montré que l'incorporation de charges à base d'OP dans le PHBV favorisait la biodégradabilité globale des matériaux. En effet, 100% de la biodégradation a été enregistrée après 75, 79 et 87 jours respectivement, pour les formulations PHBV-F0, PHBV-SF et PHBV-PF, alors qu'un taux de biodégradation de seulement 91% était obtenu après 123 jours dans le cas du PHBV pur. Cela a été attribué à l'effet stimulant des charges. Ces résultats ont été confirmés par des mesures d'angle de contact, le degré de cristallinité (DSC) et la structure des surfaces des biocomposites (observations MEB).

Mots clés : Biodégradation, biocomposites, PHBV, grignons d'olive, sol, emballage.

Abstract

Polyhydroxybutyrate-co-valerate (PHBV) is a very promising biosourced and biodegradable bacterial polyester, the commercial development of which is still limited by its high cost. On the other hand, olive oil extraction generates a large amount of lignocellulosic solid residue, called olive pomace (OP). Its disposal raises environmental concerns, including the inhibition of soil microbial populations and the reduction in seed germination. To address these issues, PHBV/OP based composites were produced (filler content of 15 wt %) by using three different fillers obtained by dry fractionation of OP, *i.e.* a stone-rich fraction (SF), a pulp-rich fraction (PF) and a crude pomace (F0). The objective of the present work was to investigate the influence of the composition of OP-based fillers on the biodegradability of resulting biocomposites. The biodegradation of PHBV, OP-based fillers and OP/PHBV-based biocomposites was carried out in the soil by respirometric tests over 4 months. Results showed that the incorporation of OP-based fillers in PHBV favored the overall biodegradability of the materials. Indeed, 100% of biodegradation was achieved after 75, 79 and 87 days for PHBV-F0, PHBV-SF and PHBV-PF formulations respectively, while a biodegradation rate of only 91% was obtained after 123 days in the case of neat PHBV. This was attributed to the priming effect of fillers. These results were confirmed by contact angle measurements, the degree of crystallinity (DSC) and the surfaces structure of biocomposites (SEM observations).

Keys words: Biodegradation, biocomposites, PHBV, olive pomace, soil, packaging.

III.3.1. Introduction

Most of today's synthetic polymers are produced from petrochemicals and are not biodegradable. Persistent polymers generate significant sources of long-term negative impacts on environment and human health, due to their accumulation in the environment and to the diffusion of degraded plastic micro- and nano-particles towards the soil, the water and finally the food. That is why biosourced polymers that are biodegradable in natural conditions have raised great interest, particularly for short-term applications such as packaging and agriculture (Avérous and Pollet, 2012). It is worth noting that food and agriculture sectors represent the largest plastic consumption sectors, with respectively 40% and 5% of the total consumption, and more than 75% of uncollectable and dispersed plastics.

Biodegradation is a process in which the molecular structure of materials is broken down through metabolic or enzymatic mechanisms. The decomposition process occurs via enzymes secreted by naturally present or naturally occurring microorganisms such as bacteria, some

fungi or actinomycetes. Biodegradation can occur in aerobic (requiring oxygen) or anaerobic (without oxygen) conditions. Biomass (humus) and biogas (carbon dioxide and methane) are the products of a biodegradation process. Under aerobic conditions carbon dioxide is the primary gas emitted while in the case of anaerobic conditions methane is the primary gas (Andrady, 2011; Kumar *et al.*, 2013; Stoleru, 2017). The key factors that affect the biodegradation of plastics are both chemical and physical like the surface properties (surface area, hydrophilic, and hydrophobic properties), the first order structures (chemical structure, molecular weight and molecular weight distribution) and the high order structures (glass transition temperature, melting temperature, modulus of elasticity, crystallinity and crystal structure) Tokiwa *et al.* (2009). The molecular weight is also important for the biodegradability because it determines many physical properties of the polymer. Increasing the molecular weight of the polymer decreased its degradability. The degree of crystallinity is a crucial factor affecting biodegradability, since enzymes mainly attack the amorphous domains of a polymer. The molecules in the amorphous region are loosely packed, and thus make it more susceptible to degradation. The crystalline part of the polymers is more resistant than the amorphous region. The aliphatic polyesters [ester bond (-CO-O-)] and polycarbonates [carbonate bond (-O-CO-O-)] are two typical plastic polymers that show high potential for use as biodegradable plastics, owing to their susceptibilities to lipolytic enzymes and microbial degradation. Among the bio-sourced polymers able to biodegrade in natural conditions, polyhydroxyalkanoates (PHAs) are a class of polyesters that present the advantage to be naturally produced by a wide variety of bacteria able to accumulate from 30 to 80 % of their dry weight in the form of intracellular granules as carbon and energy reserves (Madison and Huisman, 1999; Singh Saharan *et al.*, 2014). The copolymer poly(3-hydroxybutyrate-co-3-hydroxyvalerate) (PHBV) is one of the most well-known PHA already commercially available for the production of disposable items and food packaging materials (Kourmentza *et al.*, 2017). The high crystallinity degree is a parameter that negatively affects the degradation performance of PHBV in environments (Tsuji and Suzuyoshi, 2002; Wei *et al.*, 2015). Furthermore, as compared to conventional plastics, PHBV is still more expensive (around 5 €/kg), which limits its large applications. To decrease the overall cost of materials while modulating their properties and maintaining their biodegradability, the incorporation of lignocellulosic fillers stemming from agricultural residues has become an attractive strategy (Barkoula *et al.*, 2010; Berthet *et al.*, 2016; Berthet *et al.*, 2017; Mousavioun *et al.*, 2013).

Olive pomace (OP) is an agro-waste that has already been combined with PHBV to produce full biocomposites (Berthet *et al.*, 2015; Dufresne *et al.*, 2003; Hassaini *et al.*, 2017; Lammi *et al.*, 2018b). This solid lignocellulosic residue represents 30 to 40% of the olive oil extraction by-products. It is mainly composed of skin, pulp and fragments of crushed stone (Gharbi *et al.*, 2014; Gómez-Muñoz *et al.*, 2012). The production of OP reaches 2,881,500 tons/year worldwide (Ravindran and Jaiswal, 2016). If OP is let on soil, it will cause a harmful effect for the environment due to its phytotoxic and antimicrobial properties, low pH, relatively high salinity, phenolic and lipidic constituents, or either because it is contaminated with fungi. Fungal toxins or polyphenolic compounds are resistant to bacterial degradation, so consequently making OP a source of environment pollution (Cardelli and Benitez, 1998; Gómez-Muñoz *et al.*, 2012; Niaounakis and Halvadakis, 2004). To date, most of available studies on the incorporation of OP in composite materials have focused specifically on the use of olive stone, which is very rich in cellulose. In a previous study, it has been demonstrated that the use of either the whole OP or a pulp-rich fraction could be interesting in terms of final performance of materials (Lammi *et al.*, 2018b). However, it has never been checked if the presence of lignin could have a negative impact on the biodegradability of resulting composites.

In this context, the objective of the present work is to investigate for the first time the impact of the composition of OP fillers on the biodegradability of PHBV/OP-based biocomposites. For that purpose, three types of fillers displayed contrasted biochemical composition have been produced following a dry fractionation process already published (Lammi *et al.*, 2018a), *i.e.* a stone-rich filler, a pulp-rich filler and a filler produced from the whole OP residue. PHBV/OP-based biocomposites were prepared by melt extrusion, with a filler content of 15 wt%. The biodegradability of materials was measured by respirometric tests in soil, at 28°C and in aerobic conditions during 4 months. Biodegradability was discussed in relation to the structure of materials, as well as to the antibacterial activity of the OP samples evaluated by direct contact technique on solid medium.

III.3.2. Materials and methods

III.3.2.1. Materials

Olive pomace (OP) was kindly supplied in December 2016 by a local olive producer in the region of Azeffoun (Tizi-Ouzou, north-centre of Algeria). It was obtained from the olive oil extraction of the *Chemlal* variety. Raw olive pomace was dried in an oven at 60°C for 24 hours

before further usage. A commercial grade of polyhydroxy-(butyrate-co-valerate) (PHBV) containing 3% of valerate was purchased from NaturePlast (France) in the form of pellets (PHI002 grade).

The soil used in this study was taken from the park of the University of Montpellier (France) in April 2017, after removal of the superficial vegetation layer. The big pebbles and foreign objects were removed manually to obtain a homogeneous sample. The soil was dried in open air for one week and then sieved through a 2 mm mesh. The total dry solids content was determined by drying the soil at 105 °C until a constant weight and was around 97%.

Sulfuric acid, arabinose, xylose and glucose (Sigma-Aldrich), formamide, diiodomethane (Acros Organics, Geel, Belgium), ethylene glycol (Aldrich chemical Co. Inc., Milwaukee, USA) and glycerol (Merck, Darmstadt, Germany) were used for characterization of OP fillers. Barium chloride-Dihydrat (VWR Chemicals, Germany), sodium hydroxide (Grosseron, France), thymolphtalein (Alfa Aesar, Germany), hydrochloric acid and microcrystalline cellulose (Merck, Germany) were used for biodegradation tests.

III.3.2.2. Preparation and characterization of olive pomace-based fillers

OP-based fillers were produced by dry fractionation of crude OP using friction solicitations in a ball mill with a succession of grinding and sieving steps as described by Lammi *et al.* (2018a). The obtained powders, *i.e.* the pulp-rich fraction (PF), the stone-rich fraction (SF) and the crude OP fraction (F0), displayed a median apparent diameter of respectively 55, 59 and 85 µm (Lammi *et al.*, 2018b).

The cellulose, hemicellulose and lignin contents of OP-based fillers were characterized in a two-stage acid hydrolysis. The first hydrolysis was carried out using a 72 wt% H₂SO₄ solution at 30°C for 1 hour, while the second one was performed using a 4 wt% H₂SO₄ solution at 121°C for 1 hour following the protocol described by Barakat *et al.* (2014). The lignin content was determined by the Klason method (Nicholson *et al.*, 2014). The protein content was estimated according to the formula (N x 6.25) (Jones, 1941) after the determination of nitrogen content (N) by elementary analysis. The moisture content was determined by drying about two grams of sample in an oven at 110°C until reaching weight equilibrium. The ashes content was obtained by igniting about one gram of sample in a muffle furnace at 600°C for 5 hours. pH measurements were carried out with a pH electrode (VWR 1100L, Germany) on an aqueous suspension (five grams of sample mixed with 50 mL of distilled water.) put under magnetic stirring during 30 min (Haddadin *et al.*, 2009). All the analyses were performed in triplicate.

III.3.2.3. Preparation and characterization of OP/PHBV-based biocomposites

PHBV pellets and OP-based fillers (15 wt%) were blended in a HAAKE Rheomix internal mixer operating at a rotor speed of 60 rpm and 170°C during 5 min. Obtained compounds were cooled to room temperature and then, ground in a knife mill (SM 300, Retch, Germany) at a speed of 2200 rpm through a 4 mm grid to obtain composite pellets. Compounds were dried at 60°C for at least 8 hours before the preparation of materials. Biocomposite films (10.5 cm wide squares, average thickness about 250 µm) were prepared by hot pressing the pellets between two Teflon coated plates at 170°C, using a hydraulic thermopress (PLM 10 T, Techmo, Nazelles, France). Samples were first allowed to melt for 3 min. Then, a pressure of 150 bars was applied for 2 min. The films were cooled at room temperature before being removed from the mould.

The percentage of carbon of OP fillers, neat PHBV, biocomposites and microcrystalline cellulose was determined using an elemental analyzer Vario Micro Cube (Elementar, Germany).

The surface morphology of the OP-fillers and the cross-section of the PHBV-based films (obtained after cryo-fracturing under liquid nitrogen) was analysed by scanning electron microscopy (SEM) using a scanning electron microscope (SEM S-4500, Hitachi, Japan) with an acceleration voltage of 2 kV and a detector for secondary electrons. The samples were previously coated with gold/palladium by ion beam sputtering.

Antibacterial tests were carried out to evaluate the antibacterial effect of both fillers and composites films following the direct contact technique on Mueller-Hinton agar against two selected bacterial strains (*Staphylococcus aureus* CIP 53156 and *Escherichia coli* 55B5 CIP 52170). The tests were performed on young pre-cultures of both bacteria in a Mueller-Hinton broth. Bacterial suspensions turbidity was standardized to 0.5 McFarland. The OP-based fillers (in the form of powders) were deposited in wells of 10 mm in diameter obtained with a piece-cutter on the agar medium. In the case of materials, discs of 10 mm diameter pre-cut from the biocomposite films were putted on the surface of the agar previously inoculated with the target bacteria. The incubation of Petri dishes was carried out at 30°C for 24 hours. The occurrence of an antibacterial effect of both materials was evidenced by the appearance a clear inhibition zone around the wells/discs.

III.3.2.4. Biodegradation tests

Respirometric tests were conducted in aerobic conditions to evaluate the biodegradability of OP-based fillers, PHBV matrix and OP/PHBV composites in soil medium. The method was adapted from the US standard ASTM D5988-96, which is a Standard Test Method for Determining Aerobic Biodegradation in Soil of Plastic Materials. The released CO₂ being proportional to the percentage of biodegraded substrate, the CO₂ evolution measures ultimate degradation (i.e. mineralization) in which a substance is broken down to its final products. Beforehand, film samples were frozen under liquid nitrogen and then ground with a domestic grinder (Moulinex type DPA1, France) to obtain particles around 1–2 mm.

Biodegradation tests were carried out in cylindrical hermetic glass vessels (1000 mL capacity) containing three small open polypropylene flasks (60 mL capacity) as described by Chevillard *et al.* (2012). The first flask contained 25 g of dry soil (previously sieved at 2 mm) mixed with samples whose weight corresponded to 50 mg of carbon. The water content of soil samples was adjusted to reach 80% of the soil water retention capacity (SWRC). Soil characteristics were as follows: pH 6.8 (H₂O), 2.3 wt% of organic matter, 16.85 wt% of clay, 26.85 wt% of lime and 56.3 wt% of sand. The second flask contained 10 mL NaOH solution (0.1 M) to trap the CO₂ produced by microorganisms. The third flask contained distilled water, in order to maintain the relative humidity at 100% inside the vessel. The glass vessels were hermetically closed and incubated in the dark at 28±1°C. Every week, glass vessels were open to ensure the back titration of the excess of NaOH, which has not reacted with CO₂. Before titrating the residual NaOH with HCl solution (0.1 M) in the presence of thymophthaleine 0.10% (prepared in ethanol 95.5), 5 mL of barium chloride solution (20% in water) were added in each flask to precipitate carbonate ions. The flasks containing soil were weighted and appropriate amount of water was added in order to keep constant the water content initially fixed at 80% of SWRC. During this procedure, the glass vessels were left open during 2 min in order to be aerated. At each dosage, a new flask containing 10 mL NaOH 0.1 M was placed in each glass vessel before being closed and put in the dark at 28°C until the next measurement. Biodegradation experiments included control and blank samples. The control samples were microcrystalline cellulose, a positive reference material well-known for its biodegradation properties. The blank samples corresponded to the soil alone, without addition of an external carbon source to measure both the CO₂ produced by the soil carbon substrate and the CO₂ present in the air of the glass vessel. All experiments were run in triplicate.

Results were calculated by subtracting the CO₂ production of the blank. The theoretical maximum CO₂ potential (CO₂ max (mg)) produced by total oxidation of the material is calculated using the following equation:

$$\text{CO}_2 \text{ max} = C \times \frac{44.01}{12.01} \text{ (equation 1)}$$

where C is the amount of carbon of the sample introduced in the soil for the test (mg).

The percentage of biodegradation (B) is calculated by equation (2):

$$B = \frac{\text{CO}_2 \text{ material} - \text{CO}_2 \text{ blank}}{\text{CO}_2 \text{ max}} \text{ (equation 2)}$$

As required by the ASTM D5988-96 standard, cellulose is used as a reference substance in order to check the activity of the soil and its biodegradation percentage should be higher than 70 % after six months. Otherwise, the test must be regarded as invalid and should be repeated using another fresh soil.

III.3.3. Results and discussion

III.3.3.1. Biodegradability of OP-based fillers

Respirometric tests were used to evaluate the degree and rate of aerobic biodegradation of OP-based fillers and related PHBV composites in contact with soil. CO₂ evolution provides an indicator of the ultimate biodegradability ascribed to the mineralization of the test samples. The experimental degradation data were modeled with the Hill equation:

$$\text{Deg} = \text{Degmax} \cdot \frac{t^n}{(k^n + t^n)}$$

where Deg [%] is the percentage of degradation at time t [days], Degmax [%] the percentage of degradation at infinite time, k [days], the time for which Deg = ½ Deg_{max} and n the curve radius of the sigmoid function.

The characteristic Hill sigmoidal shape of the biodegradation curves is known to reflect the two phases commonly ascribed to the polymer degradation process involving microorganisms. Firstly, the polymer chains are cleaved in small fragments due the action of extracellular enzymes, and then, these latter are transported into the cell where they are ultimately mineralized mainly in CO₂, water vapour, minerals, and biomass [Bastioli, 2005].

The biodegradation kinetic of the three OP-based fillers is presented in Figure 22. As compared to cellulose known to rapidly biodegrade in soil, all the OP-based fillers biodegraded rather well, ranking as follows $F0 < SF < PF$, with a biodegradation threshold of at least 70% (relative to cellulose) reached in 65, 43 and 37 days respectively. They all reached their rate of maximum degradation ($Time_{rate\ max}$) in less than 20 days, and it took less than 6 months for F0 and SF samples to reach 50% of Deg_{max} as indicated by k values. Regarding the pulp-rich fraction (PF) which exhibited the highest maximum rate of biodegradation (with a $Deg_{rate\ max}$ value twice higher than these observed for the two others fillers), it is worth noting that this sample displayed a peculiar biodegradation curve shape reflected by a low radius of the sigmoid function.

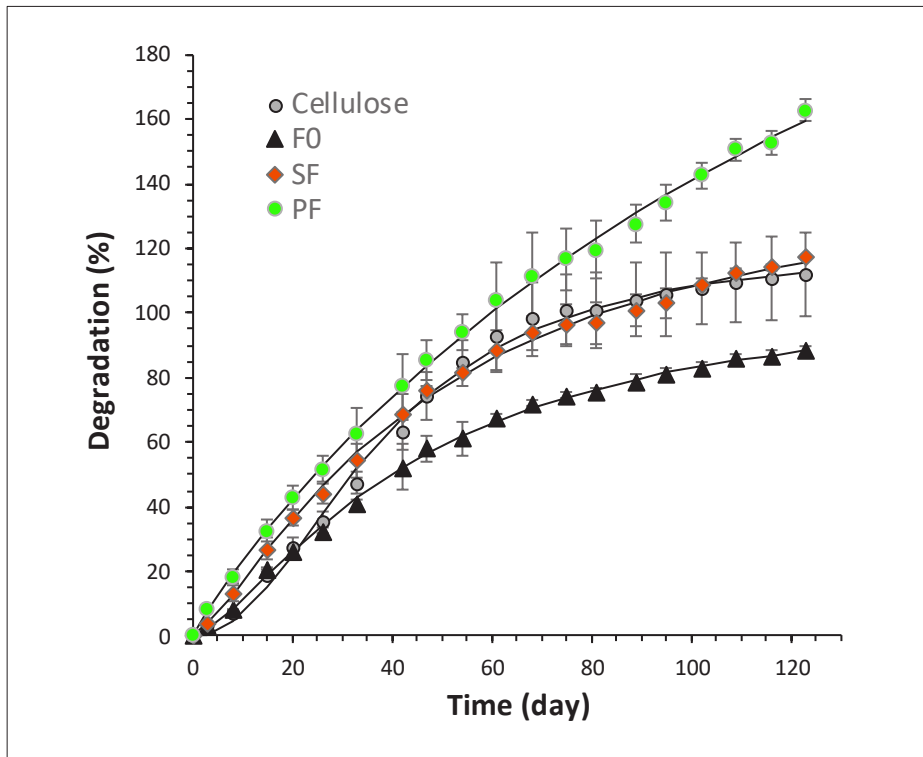


Figure 22: Kinetic of biodegradation of OP-based fillers in soil

The biodegradation curve of the stone-rich fraction (SF) was almost superimposed on that of the reference, which is ascribed to its richer cellulose content as compared to the other fillers (around 10, 12 and 17% for PF, F0 and SF respectively) (Table 21). Contrary to our expectations, the highest rate of biodegradation was recorded for the pulp-rich sample (PF), despite its highest lignin content (48.9 wt%) as compared to F0 (44.2 wt%) and SF (37.7 wt%) samples (Table 21). Indeed, lignin is a complex polyphenolic polymer that is known for its resistance to microbial degradation. Furthermore, the biodegradability of organic substances

was demonstrated follows this order: carbohydrates > hemicellulose > cellulose > lignin (Cooperband (2002)).

In addition, as already evidenced by contact angle measurements (Lammi *et al.*, 2018b), lignin was shown to confer a greater hydrophobicity to the PF fraction compared to the other OP-based ones. The hydrophobic character of PF should theoretically reduce its contact with soil water and therefore with microorganisms.

As a consequence, other reason should thus be evoked to explain the highest biodegradation rate displayed by the pulp-rich fraction (PF). Indeed, the protein content of PF (8.7%) was higher than these of F0 (4.9%) and SF (0.6%) (Table 21). Recent researches have highlighted that factors such as organic carbon (C), nitrogen (N) content, carbon to nitrogen ratio (C/N), would be key elements to improve the biodegradation process, since they regulated conditions for the microbial growth and development involved in the decomposition of organic matter (De Bertoldi *et al.*, 1983; Muktadirul Bari Chowdhury *et al.*, 2013). The optimal C/N ratio for composting ranged from 25 to 35, since it is assumed that microorganisms require 30 parts of C per unit of N. Medium exhibiting high C/N ratios are known to delay the composting process due to a surplus of degradable substrate for the microorganisms (Bishop and Godfrey, 1983). In the present work, the C/N ratio was about 37, 65 and 555 for PF, F0 and SF samples respectively (Table 21), which may explain the fact that PF biodegraded at a higher rate than F0 and SF.

Table 21: Biochemical composition (% dry basis) of olive pomace fractions

	Yield	pH	Humidity	Ashes	Cellulose	Hemicellulose	Lignin	Proteins	C	N
F0	100	4.9± 0.0	4.5± 0.0	2.6± 0.2	12.8±3.1	11.9±2.6	44.2±4.3	4.9	51.07	0.78
SF	56.4	4.9± 0.0	3.3± 0.0	0.8 ±0.0	17.4±1.1	18.5±0.4	37.7±3.4	0.6	49.97	0.09
PF	31.3	5.0± 0.0	7.2 ±0.0	4.6± 0.1	10.8±0.9	7.9±0.4	48.9±5.9	8.7	52.05	1.38

Given that the crude OP sample (F0) consisted of a mixture of the pulp and stone tissues, composed of about 31% of PF and 56% of SF (Table 21), it was expected to display an intermediate biodegradation kinetic, compared to the two other fractions that compose it. However, results showed that F0 exhibited a slower biodegradation rate than both the stone-rich (SF) and the pulp-rich (PF) fractions. It is worth noting that all the samples underwent the same grinding route in such a way to obtain similar average particle sizes (Lammi *et al.*, 2018b) (Figure 23). The slow biodegradation kinetic of F0 was probably due to a more complex organization of the lignocellulosic structure in the particles of the raw sample. The slow

biodegradation kinetic of F0 was probably due to a more complex organization of the lignocellulosic structure in the particles of the raw sample that would make them less accessible to the soil microorganisms as compared to the two other pure and contrasted fractions (PF and SF). Indeed, the accessibility of surface for enzymatic attack could be correlated to cellulose crystallinity, lignin, and hemicellulose content as already suggested by Taherzadeh and Karimi (2008). In the same context, Mais *et al.* (2002), indicated that milling can be employed to alter the inherent ultra-structure of lignocelluloses and degree of crystallinity, reducing the size of the material and consequently making it more amenable to enzymatic degradation. However, this hypothesis would deserve to be further explored by crystallinity measurement since, in the present study, the physical treatments applied to mill the pomace fractions were probably too superficial and mild to induce such structural changes.

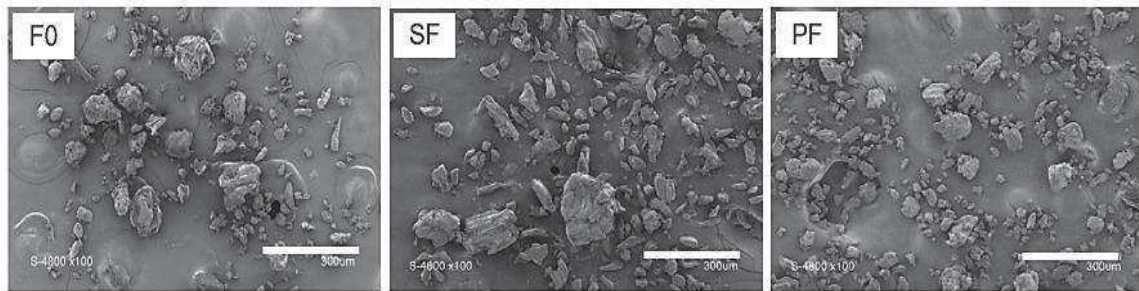


Figure 23: SEM pictures of olive pomace-based fillers (scale bar = 300 µm)

After 123 days, the recorded biodegradation rates of OP samples exceeded 100% and reaching 88.6, 111.8, 117.2 and 162.8% for F0, cellulose, SF and PF samples respectively (Figure 22). Such an effect is known as priming, and generally occurs when the soil inoculum in the test reactor containing the samples produces more CO₂ than the soil inoculum in the blank reactors. This peculiar behaviour results from a stimulation of the organic matter mineralization due to easily-decomposable organic matter that would be released in the medium during the biodegradation of specific materials. This phenomenon would arise from particular interactions occurring between the transformation of the added substances and the natural soil cycle of carbon (Kuzyakov *et al.*, 2000).

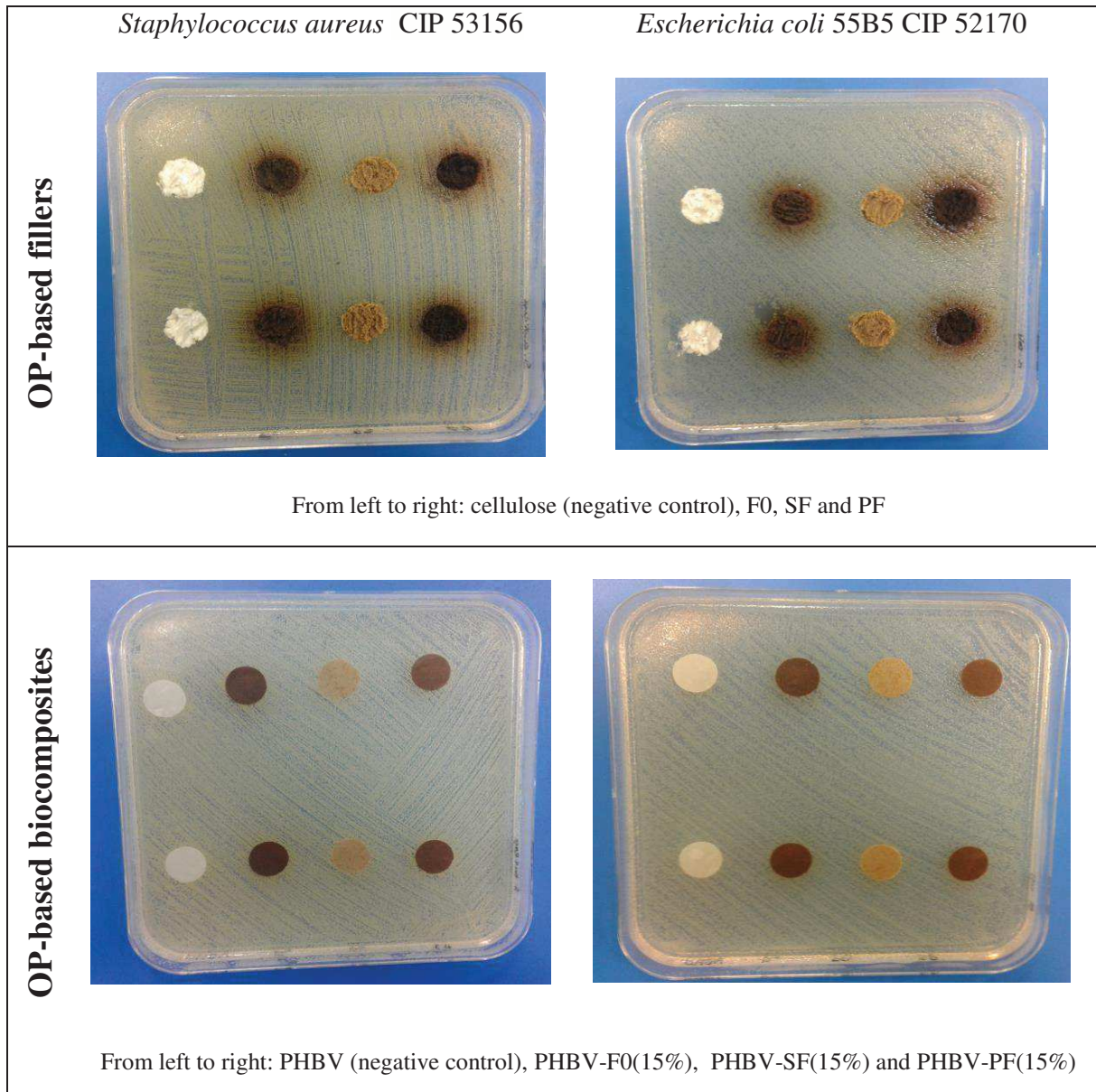


Figure 24: Antibacterial results of OP-based fillers and OP-based composites after 24h incubation at 37°C

Based on our results, the biodegradation patterns of the OP-fillers did not support the different literature data emphasizing on the antibacterial effect of crude olive pomace, which would prevent their biodegradation in soil, being consequently at the origin of environmental pollution. Indeed, according to Cardoso *et al.* (2005), the most of the phenolic compounds, including hydroxytyrosol and glucoside well known to exert significant biological activities, would be not degraded during olive oil extraction. As a consequence, like olive pulp, the olive pomace would be expected to be a good source of those compounds. Nevertheless, no antibacterial activity was evidenced from the antibiogram tests conducted with the OP-based samples and two targeted bacterial strains (*S. aureus* and *E. coli*) (Figure 24).

To explain this unexpected result, it could be assumed that the preliminary stage consisting in the drying of the raw biomass for 24 hours at 60°C would be at the origin of a thermal denaturation of the active compounds resulting in a loss of its inhibiting effect. In addition, during the successive grinding operations, the various OP-based samples were exposed to thermal heating when in contact with appliances. Such a temperature increase would also contribute to denature the bioactive substances involved in the targeted antibacterial effect. To finish with, it cannot be excluded that the OP-based fillers were also probably already microbiologically contaminated. These microorganisms might enhance the biodegradation of the OP-based fillers acting in cooperation with the soil microorganisms, both contributing to a faster biodegradation rate.

These observations clearly showed the interest of crude OP fractionation and led us to propose another exploitation field for the SF and PF fractions as natural and biodegradable fertilizers for the agricultural grounds.

III.3.3.2. Biodegradability of OP-based biocomposites

After 4 months of incubation at 28°C in the soil and under aerobic conditions, PHBV biodegradation reached 91%. According to Boopathy (2000), biodegradation is dependent on a number of factors such as microbial activity of the environment, exposed surface area, moisture content, temperature, pH and molecular weight.

Regarding all composite films, the obtained results showed that the incorporation of the OP-fillers accelerated their biodegradation as compared to the neat PHBV control (Figure 25). It is also interesting to note that, unexpectedly, the composites biodegradation rate evolved inversely to the OP-filler biodegradation order. Indeed, the PHBV-F0 formulation was the fastest biodegraded, while PHBV-SF recorded an intermediate behavior, and PHBV-PF exhibited a slightly lower biodegradation profile (Figure 25). Monitoring the evolution of respirometric tests over time revealed that the biodegradation kinetics of the biocomposite materials followed the order: PHBV control < PHBV-PF (15%) < PHBV-SF (15%) < PHBV-F0 (15%). After 123 days of incubation in the soil, PHBV-PF and PHBV-SF formulations overpassed 134% of biodegradation, and the PHBV-F0 film exceeded 143%. This peculiar behavior resulted from the priming effect already mentioned above for the OP-fractions which all reached biodegradation rates greater than 100. This synergistic effect was certainly related to the presence of the fillers, which further boost the biodegradation process of the composites

compared to the matrix alone. Biodegradation rates of biocomposites exceeding 100% have already been reported by other authors (Balaguer *et al.*, 2015) for bioplastics made of gliadins cross-linked by cinnamaldehyde, starch-polystyrene foams (Pushpadass *et al.*, 2010), or of L-poly lactide-polycaprolactone co-polymer films (Plackett, 2006).

This phenomenon may be the result of three concomitant effects. Firstly, the increased biodegradability of composite materials could be attributed to the increased hydrophilicity of biocomposites as compared to virgin PHBV, due to the incorporation of fillers that are much more hydrophilic than virgin PHBV, even the pulp-rich fraction PF (Lammi *et al.*, 2018b). A higher hydrophilicity would favor the adsorption and then the transport of water within the composite material, which would promote microbial degradation of material (Karlsson and Albertsson, 1998; Chevillard *et al.*, 2012).

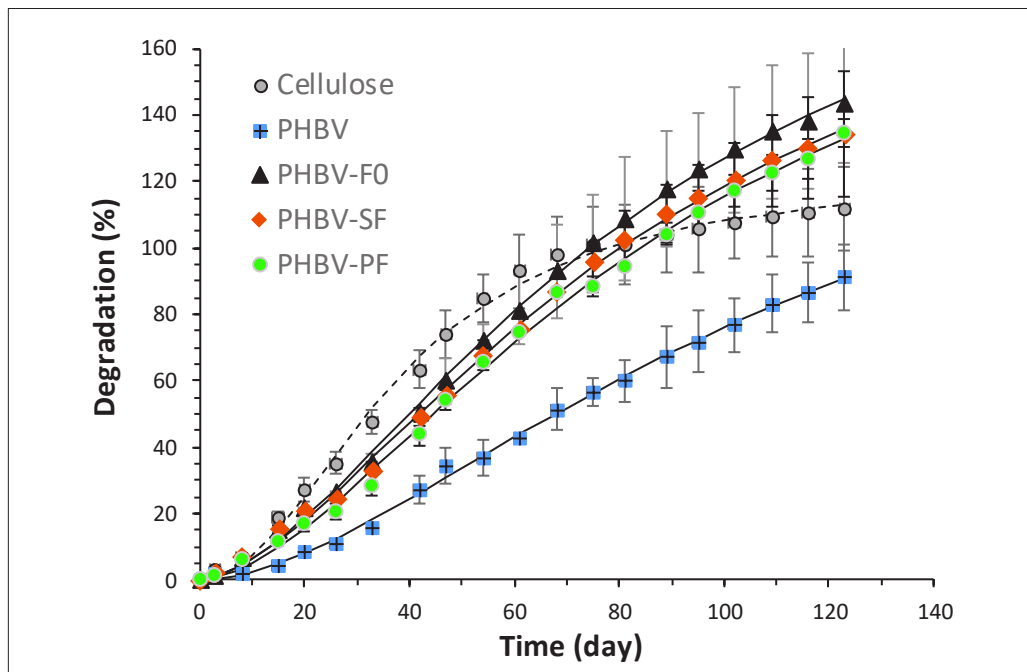


Figure 25: Kinetic of biodegradation and biodegradation rate of OP/PHBV-based composites in sol

Secondly, differences in biodegradation patterns between composite materials could be attributed to differences in the microstructure of materials. A poor affinity between the filler and the polymer matrix would result in a poor dispersion of the fillers and the formation of aggregates as well as in a poor filler/matrix adhesion that would induce the creation of voids between the filler and the matrix. These two phenomena would lead to the creation of a bulk porosity and therefore to (i) the creation of a preferential pathway for the transport of water

within the composite material, (ii) a favored disintegration of materials due to a higher fragility of materials, and (iii) in a higher surface contact to microorganisms. This hypothesis was supported by the microstructural investigation of the composite materials qualitatively characterized by SEM (Figure 26). As evidenced on SEM images, PHBV cross-section displayed a homogeneous and smooth surface. Contrariwise, the cross sections of PHBV-F0 and PHBV-SF films were rough, with the evidence of cracks and voids at the filler/matrix interface (may be) due to filler debonding. As described above, this would allow microorganisms to attach and form biofilms colonizing the material. In the case of PHBV/PF composites, the particles were entirely wetted by the polymer matrix, indicating a good filler/matrix interfacial adhesion. This was attributed to the increased similarity of the surface free energy of the PF surface and PHBV, as previously demonstrated (Lammi *et al.*, 2018b). This more homogenous and compact microstructure would hinder the diffusion of water and thus the accessibility to microorganisms, as compared to PHBV/F0 and PHBV/SF composites.

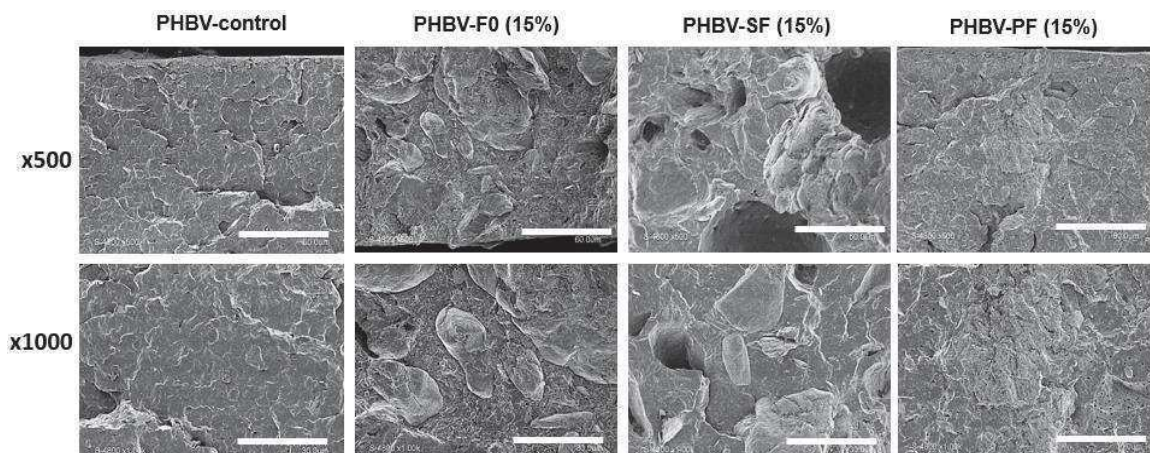


Figure 26: SEM pictures of OP/PHBV-based biocomposites surfaces (x 500: scale bar = 60 μm , x 1000: scale bar = 30 μm)

Finally, difference in cristallinity between the materials might be at the origin of changes in their biodegradation patterns. Indeed, the kinetic of enzymatic degradation is known to depend on the overall cristallinity of the material (El-Hadi *et al.*, 2002). An increase in polymer cristallinity is detrimental for the polymer biodegradability since crystalline zones are less accessible for the microorganisms (Wei *et al.*, 2015), Indeed, as previously demonstrated by the authors (Lammi *et al.*, forthcoming), the presence of F0 and SF as fillers in the PHBV led to a decrease in the cristallinity degree X_c of the neat matrix whereas the cristallinity of the PHBV/PF was increased. The recorded degrees of cristallinity X_c (%) were 65, 68, 75 and 78%

for PHBV-F0, PHBV-SF, PHBV and PHBV-PF films, respectively (Lammi *et al.*, 2018b). Such an anti-nucleating effect might contribute to facilitate the biodegradability of PHBV/F0 and PHBV/SF composites as compared to PHBV/PF. This phenomenon was previously observed for biocomposites based on polyhydroxybutyrate and potato peel waste fermentation residue (Wei *et al.*, 2015). In the case of the PHBV/PF composite formulation and as compared to the neat PHBV matrix, it is worth noting that the effect of the increased crystallinity was compensated by the opposite effect resulting from the increased hydrophilicity and the more heterogenous microstructure.

The absence of any antibacterial effect of all materials formulations towards the target bacteria selected in this study appeared in full agreement with their fast biodegradation in soil medium. Such results enabled to explore other routes for valorizing the different fractions stemming from olive pomace wastes and justified the approach consisting in introducing them as fillers for developing biodegradable composites based on PHBV.

III.3.4. Conclusion

The present work is recorded in an environmental context. With a view to a complete valorisation of the olive pomace, powders coming from the constitutive tissues of the olive fruit, namely the pulp and the stone and produced by dry fractionation of the raw biomass as well as the crude pomace, were used to develop PHBV-based biocomposites. The impact of the filler on the biodegradability of the obtained materials was been investigated. Results revealed that the incorporation of the fillers accelerated the biodegradation kinetics of the films compared to the neat PHBV, which exceeded 100% after 4 months. These results were verified by measurements of crystallinity as well as SEM observations. On the other hand, the absence of any antibacterial effect of both the olive pomace-based fillers and biocomposites towards the target bacteria, confirms the obtained results and justifies the interest of this study. To conclude, this research presents a promising track for the valorisation of olive pomace in the elaboration of biocomposites, notably materials intended for short-term use such as packaging.

Acknowledgments

The authors are grateful to the MALICE project co-financed by the European Regional Development Fund, and the PNE Program (2016-2017) of the Algerian Ministry of Higher Education and Scientific Research.

IV. Discussion générale

L'objectif appliqué de cette thèse consistait à la mise en œuvre et à la caractérisation de nouveaux matériaux biocomposites, fonctionnels et biodégradables, qui seront appliqués en emballage alimentaire ; dont les constituants étaient issus de sous-produits des industries agroalimentaires. L'enjeu scientifique de ce travail était de comprendre l'impact des caractéristiques de la charge (composition et propriétés de surface) sur les propriétés fonctionnelles (thermique, mécanique et barrière) et la biodégradabilité des matériaux développés.

Afin de répondre à l'objectif de notre étude, nous avons opté pour la valorisation du grignon d'olives, sous-produit solide lignocellulosique de l'industrie oléicole. Ce choix a été fait pour plusieurs raisons : outre la vocation oléicole de la région d'étude, la disponibilité et l'abondance de cette biomasse font d'elle une matière première « bon marché » pour une éventuelle application à grande échelle.

IV.1. Valorisation de grignon d'olives pour la production de charges de renfort

Etant donné que la présente étude s'enregistre dans un contexte de diminution des impacts environnementaux, nous avons dans un premier temps exploré la potentialité d'utiliser le fractionnement par voie sèche pour séparer la pulpe du noyau à partir du grignon d'olives brut. Le but était de produire des fractions contrastées en terme de composition, avec la plus grande pureté, un rendement élevé et une faible consommation d'énergie, tout en préservant leur intégrité (Article 1).

Différents itinéraires technologiques combinant des opérations de broyage (solicitations mécaniques de type compression, cisaillement et impact, friction) et de tri (tamisage ou fractionnement électrostatique) ont été testés. Les propriétés intrinsèques des fractions résultantes ont été caractérisées et discutées en lien avec les procédés de fractionnement appliqués. Un procédé de séparation par voie humide a été également utilisé pour comparaison. Les deux fractions (fraction riche en pulpe et fraction riche en noyau) obtenues par la voie humide ont été considérées comme références, afin d'évaluer l'efficacité des différentes voies alternatives de fractionnement sec proposées dans la présente étude.

Le premier paramètre indiquant l'efficacité de la séparation était la couleur : la pulpe étant très foncée (presque noire) et le noyau jaune/brune, en raison d'une distribution hétérogène des pigments chlorophylliens à travers les différents tissus de l'olive. Les autres critères étaient la composition biochimique et les propriétés de surfaces des particules de poudres : la **pulpe** est

caractérisée par une **teneur plus élevée en lignine**, protéines et cendres et par une **surface apolaire**, tandis que le **noyau** est caractérisé par une **teneur plus élevée en cellulose-hémicellulose** et une **surface plus polaire**. Les résultats ont révélé que la séparation de la pulpe du noyau par **friction** dans un broyeur à boulets fonctionnant dans des conditions douces (pendent seulement 2 min à une fréquence de 15 Hz), sur un échantillon préalablement broyé à l'aide d'un broyeur à couteaux, était la voie de fractionnement la plus efficace. Les poudres obtenues ont présenté une composition biochimique, une énergie libre de surface, une couleur et une stabilité thermique similaires aux fractions produites par voie humide. Il a également été démontré que le fractionnement par voie sèche permettait d'atteindre un **rendement total plus élevé** que le fractionnement humide (99,4% contre seulement 82,1% dans le cas du fractionnement humide) et **sans production d'effluents**. De plus, **le fractionnement par voie sèche n'exigeait pas l'utilisation d'eau** ; alors qu'un rapport eau/biomasse de 5/1 était nécessaire dans le cas du fractionnement conventionnel par voie humide.

Il est également intéressant de noter que toutes les fractions de grignon étaient **thermiquement stables** jusqu'à au moins 210°C, température largement supérieure à la température de fusion de nombreux polymères thermoplastiques, les rendant aptes à la production de matériaux biocomposites.

IV.2. Développement de biocomposites pour l'emballage alimentaire

La deuxième partie de la thèse était consacrée à l'étude de l'effet de renfort des deux principaux compartiments du grignon d'olives, à savoir la « pulpe » et le « noyau », en comparaison avec celui du « grignon d'olives brut » (OP) (Article 2).

A cet effet, les fractions riches en pulpe (PF) et en noyau (SF) préalablement produites par fractionnement par voie sèche ont été introduites dans deux matrices thermoplastiques, i.e. un polymère conventionnel dérivé du pétrole le « polypropylène » (PP), et un polymère biosourcé le « polyhydroxy-butyrates-co-valérate » (PHBV), avec un taux de charges allant jusque 30 % massique. Les matériaux composites ont été préparés par voie fondue via un procédé thermomécanique disponible à échelle industrielle. Les propriétés fonctionnelles des matériaux développés ont été discutées en relation avec les caractéristiques intrinsèques des charges de grignon, y compris leur couleur, densité, taille, morphologie, composition

biochimique, stabilité thermique, l'énergie libre de surface, et la microstructure des matériaux composites.

Les **paramètres colorimétriques** sont très importants dans le domaine de l'emballage alimentaire du point de vue de l'acceptabilité du consommateur. La transparence ou même la translucidité est souvent demandée par les consommateurs afin de pouvoir voir le produit. Cependant, il est à noter que dans le cas de matériaux composites rigides et opaques dédiés à la fabrication de barquette, l'utilisation d'un couvercle en film transparent permettrait de répondre à cette exigence. D'une autre part, l'opacité pourrait être nécessaire pour certains produits alimentaires tels que les aliments gras, afin d'empêcher les réactions de dégradation oxydative en agissant comme une barrière à la lumière (Romani *et al.*, 2017). Les films biocomposites développés dans cette étude sont tous opaques, avec une couleur brun foncé pour les formulations à base de pulpe, une couleur beige clair pour les biocomposites à base de noyau, et une couleur brun clair intermédiaire pour les matériaux à base de grignon brut. Ces observations ont été confirmées par des analyses colorimétriques réalisées sur des biocomposites PP et PHBV à 15% de charges. De plus, quelle que soit la formulation, l'augmentation de la teneur en charge conduit à une couleur sombre des films. La couleur des biocomposites dépend donc clairement de celle des charges, celle-ci étant intrinsèquement liée à leur composition biochimique.

D'autre part, la **stabilité thermique des matériaux** est une propriété importante pour les emballages qui doivent être chauffés avant leur utilisation. Elle a été étudiée par analyse thermogravimétrique sous atmosphère oxydante. Nous avons constaté que les biocomposites avaient un comportement thermique similaire à leurs constituants principaux, c'est-à-dire la matrice polymère et les charges lignocellulosiques. Globalement, l'introduction de charges de grignons entraîne une réduction de la stabilité thermique des matériaux, en raison de leurs dégradations à des températures inférieures par rapport aux matrices polymères. La réduction de la stabilité thermique est plus prononcée dans le cas des matériaux à base de PHBV. Ce dernier est connu pour être très sensible à la température, surtout au-dessus de son point de fusion, en raison de la concomitance de deux mécanismes de dégradation thermique du PHBV, à savoir une scission aléatoire par cis-élimination et trans-estérification (Leroy *et al.*, 2012). De plus, l'introduction de charges lignocellulosiques induit des réactions de dégradation hydrolytique supplémentaires, dues à la présence de molécules d'eau résiduelles et de produits de dégradation (alcools et carboxylates) sur les particules lignocellulosiques (Berthet *et al.*, 2015 ; Hassaini *et al.*, 2017). Cependant, les températures de dégradation

enregistrées restent relativement élevées pour toutes les formulations, c'est-à-dire au-dessus de 200°C, température de chauffage typiquement utilisée pour les produits alimentaires emballés.

Les tests de traction ont révélé une diminution des **propriétés mécaniques**, notamment la contrainte et l'allongement à la rupture pour tous les biocomposites, tandis que le module de Young n'était pas significativement affecté. À forte teneur en charge (30% massique), la diminution de la contrainte à la rupture était de 36%, 65% et 78% pour les formulations PHBV-PF, PHBV-F0 et PHBV-SF respectivement, par rapport au PHBV vierge. L'allongement à la rupture a également fortement diminué en fonction de la teneur en charge. La réduction la plus élevée a été enregistrée dans le cas de la charge SF, elle est estimée de 74% pour les composites PHBV-SF. Les propriétés mécaniques sont mieux conservées dans le cas de la charge PF grâce à une meilleure adhésion inter-faciale envers les matrices polymères. Ces résultats ont été confirmés par les calculs du travail d'adhésion, les observations au MEB et la modélisation mécanique.

D'une manière générale, les propriétés fonctionnelles des matériaux composites sont régies par (i) les propriétés intrinsèques de chaque constituant, y compris la composition chimique et la structure, (ii) le taux de charge, (iii) l'état de dispersion des charges au sein de la matrice et (iv) la nature des interactions à l'interface charge/matrice (Berthet *et al.*, 2015 ; 2017). A titre d'exemple, une faible adhésion interfaciale charge/matrice, comme cela a été révélé qualitativement pour les composites à base de noyau et du grignon d'olive brut par des observations de surfaces de fracture au MEB, conduit à une dégradation des propriétés mécaniques aux grandes déformations. Par ailleurs, l'augmentation du taux de charge favorise les phénomènes d'agglomération entre les particules lignocellulosiques (agglomération d'autant plus favorisée que l'affinité entre la charge et la matrice est faible), entraînant la création de défauts microscopiques et macroscopiques, y compris des vides à l'intérieur du matériau, constituant ainsi une zone fragile favorisant l'initiation et la propagation des macro-fissures. Les changements de propriétés mécaniques peuvent également être liés aux changements structuraux de la matrice, induits par la présence de charges notamment la dégradation du poids moléculaire du polymère et la diminution du taux de cristallinité.

Par ailleurs, l'étude des **propriétés de transfert** des films développés à base de particules de grignon révèle que la **perméabilité à la vapeur d'eau** (WVP) dépend fortement de la concentration et de la nature de la charge. Dans l'ensemble, l'introduction des charges de

noyau ou de grignon brut conduit à une augmentation significative de la WVP, aussi bien pour les films biocomposites à base de PP et de PHBV. Cette augmentation est plus prononcée pour les taux de charges élevés. La WVP augmentait de $0,9 \times 10^{-12} \text{ mol.m}^{-1}.\text{s}^{-1}.\text{Pa}^{-1}$ pour le PHBV contrôle jusqu'à 1,1 ; 1,5 et 15,1 $\times 10^{-12} \text{ mol.m}^{-1}.\text{s}^{-1}.\text{Pa}^{-1}$ pour PHBV-F0 (5%), PHBV-F0 (15%) et PHBV-F0 (30%) respectivement. L'augmentation de WVP était de 83% pour PP-F0 (15%). Au contraire, l'introduction de la fraction riche en pulpe dans le PHBV, conduit à une réduction de la WVP d'environ 44% pour le PHBV-PF (5%) et de 22% pour le PHBV-PF (15%), tandis que la valeur WVP reste constante pour la formulation à 30%. Dans le cas de PP, l'introduction de charges de PF n'a pas eu d'impact significatif sur la WVP.

L'augmentation de la perméabilité à la vapeur d'eau est expliquée principalement par le caractère hydrophile des particules de charges comparativement à la matrice polymère (loi de mélange), ainsi qu'à une mauvaise adhérence inter-faciale matrice/charge, qui contribuerait à la création d'une voie favorable pour la diffusion de la vapeur d'eau comme il a déjà été rapporté par Berthet *et al.* (2015) et Hassaini *et al.* (2017). L'effet barrière apporté par l'introduction de la charge PF est attribué à sa nature apolaire en raison de sa teneur élevée en lignine et aux meilleures interactions interfaciales avec les matrices polymères, induisant un effet de tortuosité et donc à la création d'un chemin plus long pour la diffusion de la vapeur d'eau. Cet effet de tortuosité pourrait également être attribué à l'effet nucléant des charges (augmentation de la cristallinité de la matrice en présence des charges).

Notre étude montre que la **perméabilité à l'oxygène** des films de PP et de PHBV n'est pas significativement affectée par l'incorporation de charges de grignons. Ce résultat a été expliqué par les changements structurels de la matrice PHBV qui seraient en faveur d'une augmentation de la perméabilité à l'oxygène (effet sur la diffusion, comme pour la vapeur d'eau) et compensé par le fait que l'oxygène est une molécule apolaire à faible affinité avec les particules lignocellulosiques. Seule une légère augmentation de la perméabilité à l'oxygène (augmentation de 11%) a été observée dans le cas du PHBV-PF (15%), probablement en raison du caractère apolaire plus élevé des fractions riches en pulpe et donc une plus grande affinité pour l'oxygène.

Dans le cas des emballages alimentaires, la grande variété de produits à emballer nécessite un large éventail de propriétés de transfert de matière (Petersen *et al.*, 1999). À titre d'exemple, les produits alimentaires respirants nécessiteraient des matériaux d'emballage perméables pour éviter la condensation de la vapeur d'eau à l'intérieur de celui-ci (l'emballage), tandis que

les produits secs, nécessiteraient des matériaux d'emballage barrière (Siracusa *et al.*, 2008). Par conséquent, les **formulations à base de noyau** pourraient répondre aux besoins de **produits alimentaires respirants** comme certains fromages, les fruits et les légumes, en raison de leur transpiration ; par contre, les **biocomposites à base de pulpe** d'olive conviendraient mieux aux exigences de **produits sensibles à l'eau** comme les sandwiches, les corps gras et les plats cuisinés (Petersen *et al.*, 1999).

IV.3. Etude de la biodégradabilité des biocomposites de grignon d'olives

En raison de l'importance croissante que suscite les matériaux biodégradables en tant que substituts aux plastiques conventionnels pétrochimiques, nous nous sommes intéressés dans le dernier volet de cette thèse à l'étude de l'influence de la composition des fractions de grignon d'olives sur la biodégradabilité des films de PHBV à 15% de charge, dans le sol (Articles 3). Afin de mieux comprendre l'évolution de la cinétique de biodégradation des matériaux composites, des tests respirométriques ont été réalisés sur les charges de grignon, la matrice non chargée et les bicomposites, dans les mêmes conditions opératoires.

Les résultats ont démontré que toutes **les charges** étaient biodégradables. Leur cinétique de dégradation évolue dans l'ordre $F0 < SF < PF$, avec un taux de biodégradation de 70% après 65, 43 et 37 jours, respectivement. Contrairement à nos attentes, la fraction riche en pulpe présente la plus grande vitesse de dégradation malgré sa teneur élevée en lignine (environ 49%) par rapport aux autres fractions, F0 (44,2%) et SF (37,7%). En effet, la lignine est un polymère polyphénolique complexe connu pour sa résistance à la dégradation microbienne (Dashtban *et al.*, 2010 ; Singh *et al.*, 2016). De plus, la lignine confère à la fraction PF un caractère hydrophobe plus important par rapport aux autres fractions de grignon déjà démontré dans notre étude ; ce qui réduirait théoriquement son contact avec l'eau du sol et par conséquent avec les microorganismes.

Cependant, la pulpe se distingue par une concentration élevée en protéines (8,7%) comparativement au grignon brut (4,9%) et au noyau (0,6%). Des recherches récentes ont montré que des facteurs tels que le carbone organique (C), l'azote (N) et le rapport carbone/azote (C/N) sont des éléments clés pour améliorer le processus de biodégradation, car ils régulent les conditions de croissance microbienne et la décomposition de la matière organique (De Bertoldi *et al.*, 1983, Mukhtadirul Bari Chowdhury *et al.*, 2013). Selon Bishop et Godfrey (1983), le rapport C/N idéal pour le compostage varie de 25 à 35 et que les rapports C/N élevés ralentissent le processus de compostage, car il y a un surplus de substrat

dégradable pour les microorganismes. Les rapports C/N enregistrés avec nos fractions étaient de 37, 65 et 555 pour les échantillons PF, F0 et SF respectivement, ce qui peut expliquer la biodégradation rapide de la pulpe.

Il est important de souligner que les résultats obtenus sur la biodégradation des poudres de grignon s'opposent aux données de littérature qui s'accordent sur la présence d'un puissant effet antibactérien du grignon d'olive brut, qui empêcherait sa dégradation par voie naturelle et serait par conséquent, à l'origine de sa pollution de l'environnement. En effet, Cardoso et al. (2005), ont affirmé que la plupart des composés phénoliques, y compris l'hydroxytyrosol et le glucoside, qui peuvent avoir des activités biologiques, ne sont pas dégradés lors de l'extraction de l'huile d'olive, suggérant que le grignon ainsi que la pulpe d'olive pourraient être une bonne source de ces composés.

Afin de confirmer ces résultats, nous avons également évalué l'**activité antibactérienne** des différentes fractions de grignon envers deux souches bactériennes de référence (*Staphylococcus aureus* CIP 53156 et *Escherichia coli* 55B5 CIP 52170), par la technique de contact direct sur le milieu de culture Mueller-Hinton. Après incubation, l'antibiogramme a révélé l'absence de l'effet antibactérien pour les trois fractions de grignon. En effet, aucune zone d'inhibition de la croissance bactérienne n'a été observée autour des échantillons de grignon, ce qui justifie leur cinétique de dégradation. Pour expliquer ce résultat inattendu, nous avons supposé que le séchage préalable de la biomasse brute pendant 24 heures à 60°C, était à l'origine de la dénaturation des substances bioactives et la perte de l'effet inhibiteur.

Selon la norme EN 13432, pour qu'un matériau soit considéré biodégradable, celui-ci doit être en mesure d'atteindre 90% de biodégradation en moins de 6 mois. Concernant **les films** de grignon, les résultats ont révélé que l'incorporation des charges accélère leur **biodégradabilité** dans le sol par rapport au PHBV contrôle. En effet, un taux de biodégradation de 100% a été enregistré après 75, 79 et 87 jours pour les formulations PHBV-F0, PHBV-SF et PHBV-PF respectivement, alors que seulement 91% de biodégradation était obtenu après 123 jours dans le cas du PHBV vierge. Ces valeurs ont été expliquées par l'effet stimulant des charges qui favoriserait la biodégradation des biocomposites de grignon par les microorganismes du sol comparés à la matrice polymère seule. Les différences dans les profils de biodégradation entre les matériaux composites ont été attribuées aux différences dans leurs microstructures. Une faible affinité entre la charge et la matrice polymère, conduirait à la formation d'agrégats de particules de charge ainsi qu'à une mauvaise adhérence charge/matrice, qui induirait à la

création de vides entre ces deux éléments. Ces phénomènes entraîneraient l'augmentation de la porosité et la création d'une voie préférentielle pour le transport de l'eau dans le matériau composite, qui favoriserait par conséquent sa désintégration due à une importante surface de contact avec les micro-organismes.

La **microstructure des matériaux** a été qualitativement caractérisée par des observations au MEB. Le PHBV a montré une surface homogène et lisse. Par contre, les surfaces des films composites étaient rugueuses et présentaient des fissures et des vides à l'interface charge/matrice. Ceci permettrait aux micro-organismes de se fixer et de former des biofilms pour coloniser le matériau.

D'autre part, il est à noter que la cinétique de dégradation enzymatique dépend de la cristallinité globale du matériau (El-Hadi *et al.*, 2002). Une **cristallinité** élevée du polymère freinerait sa biodégradabilité, puisque les zones cristallines sont moins accessibles aux microorganismes (Wei *et al.*, 2015). Les taux de cristallinité enregistrés X_c (%) étaient respectivement de 65, 68, 75 et 78% pour les films PHBV-F0, PHBV-SF, PHBV-contrôle et PHBV-PF. Cette réduction du degré de cristallinité des matériaux peut contribuer à l'accélération de leur biodégradabilité.

Enfin, l'absence d'effet antibactérien de toutes les formulations de matériaux vis-à-vis des bactéries cibles sélectionnées dans cette étude, s'accordent parfaitement aux résultats de biodégradation enregistrés ; justifiant une fois de plus, l'intérêt de valoriser les différentes fractions du grignon d'olives et d'évaluer leurs effets sur la biodégradation des biocomposites de PHBV.

Tenant compte de ces données sus-énumérées, nous pouvons rappeler que les sous-produits de l'olive, fortement polluant, représentent un plus grand tonnage que l'huile d'olive et leur composition les prête à une multitude d'usages. Ils peuvent jouer un rôle essentiel dans le développement durable du secteur oléicole. Il est donc important de les considérer comme des matières premières au même titre que l'huile et d'évaluer les conditions économiques pour développer des solutions reproductibles à grande échelle. Il est également nécessaire que les voies de valorisation émergentes évitent la création de problèmes supplémentaires au lieu de la résolution des problèmes existants. Ainsi, nous pourrions résoudre les contraintes environnementales et augmenter la compétitivité du secteur de l'huile d'olive.

V. Conclusion

Dans le but de voir si les grignons d'olives pouvaient être introduits dans une formule de valorisation en tant que matériaux d'emballage alimentaire fonctionnels et biodégradables, nous avons mené des investigations expérimentales dans le cadre de cette présente thèse qui ont permis d'aboutir aux principaux résultats suivants :

- ✓ la séparation de la pulpe du noyau par friction à partir du grignon d'olives brut, était la voie de fractionnement la plus efficace permettant de produire des fractions contrastées avec un rendement élevé. La pulpe étant caractérisée par une teneur plus élevée en lignine, protéines et cendres et par une surface apolaire, tandis que le noyau présente une teneur plus élevée en cellulose-hémicellulose et une surface plus polaire ;
- ✓ toutes les fractions de grignon étaient thermiquement stables jusqu'à au moins 210°C, ce qui les rend aptes à la production de matériaux biocomposites ;
- ✓ l'introduction de charges de grignons entraîne une réduction de la stabilité thermique des matériaux biocomposites développés essentiellement ceux à base de PHBV ;
- ✓ les tests de traction ont révélé une diminution des propriétés mécaniques, notamment la contrainte et l'allongement à la rupture pour tous les biocomposites, tandis que le module de Young n'était pas significativement affecté ;
- ✓ la perméabilité à la vapeur d'eau des films développés dépend fortement de la concentration et de la nature de la charge. Dans l'ensemble, l'introduction des charges de noyau ou de grignon brut conduit à une augmentation significative de la WVP, aussi bien pour les films biocomposites à base de PP et de PHBV. Par contre, l'introduction de la fraction riche en pulpe, conduit à une réduction de la WVP ;
- ✓ la perméabilité à l'oxygène des films développés n'est pas significativement affectée par l'incorporation de charges de grignons ;
- ✓ toutes les charges étaient biodégradables. Leur cinétique de dégradation évolue dans l'ordre F0 <SF <PF, avec un taux de biodégradation de 70% après 65, 43 et 37 jours, respectivement.
- ✓ l'incorporation des charges accélère la biodégradabilité des matériaux composites dans le sol par rapport au PHBV contrôle. En effet, un taux de biodégradation de 100% a été enregistré après 75, 79 et 87 jours pour les formulations PHBV-F0, PHBV-SF et PHBV-PF respectivement, alors que seulement 91% de biodégradation était obtenu après 123 jours dans le cas du PHBV vierge ;
- ✓ aucune activité antibactérienne n'a été enregistré aussi bien pour les charges que les matériaux biocomposites de grignon d'olives.

Au terme de ce travail, les conclusions suivantes se dégagent :

- une nouvelle voie prometteuse est explorée pour transformer le grignon d'olives en produits à plus haute valeur ajoutée (production de charges de renfort ou autres applications), à travers une technologie propre permettant une meilleure valorisation écologique. L'approche durable développée a consisté en la combinaison de charges des grignons avec des polymères thermoplastiques en vue d'obtenir des matériaux biocomposites, à faible coût, fonctionnels et biodégradables ;
- une valorisation totale du grignon d'olives a été rendue possible, par la mise en œuvre de douze formulations de biocomposites, présentant des propriétés de perméabilité à l'oxygène et à la vapeur d'eau différentes, ce qui permet d'envisager leur application dans l'emballage d'une large gamme de produits alimentaires ;
- un choix approprié du couple charge/matrice permettrait de moduler les propriétés fonctionnelles du biocomposite produit selon les exigences de l'application ciblée et par conséquent, le développement de matériaux d'emballage adaptés.

D'autres perspectives pourraient être envisagées suite à ces travaux pour approfondir la compréhension de l'impact des charges sur les propriétés des matériaux développés :

- vérifier l'effet anti-oxydant des biocomposites de grignon mis en œuvre ;
- réaliser et suivre l'effet des tests de migration afin d'évaluer l'aptitude de ces biocomposites au contact des aliments, avant leur application dans l'emballage alimentaire pour garantir une sécurité optimale du consommateur ;
- appliquer les différents matériaux biocomposites à base de grignon d'olives développés dans cette thèse sur une gamme variée de matrices alimentaire et évaluer leurs effets sur la durée de conservation des aliments emballés.

Références bibliographiques

- **Abdessemed S., Muzzalupo I., Benbouza H. 2015.** Assessment of genetic diversity among Algerian olive (*Olea europaea* L.) cultivars using SSR marker. *Scientia Horticulturae* 192, 10-20.
- **Abou-Zeid R.E., Hassan E.A., Bettaieb F., R.Khiari, Hassan M. L. 2015.** Use of Cellulose and Oxidized Cellulose Nanocrystals from Olive Stones in Chitosan Bionanocomposites. *Journal of Nanomaterials*. Article ID 687490.
- **Abu Tayeh H., Najami N., Dosoretz C., Tafesh A., Azaizeh H. 2014.** Potential of bioethanol production from olive mill solid wastes. *Bioresource Technology* 152, 24–30.
- **Ahankari S.S., Mohanty A.K., Misra M. 2011.** Mechanical behavior of agro-residue reinforced poly(3 hydroxybutyrate-co-3-hydroxyvalerate), (PHBV) green composites: a comparison with traditional polypropylene composites. *Composites Science and Technology* 71, 653–657.
- **Ahvenainen R. 2003.** Novel Food Packaging Techniques. Woodhead Publishing Limited, Cambridge: England. (eBook ISBN: 9781855737020).
- **Akaraonye E., Keshavarz T., Roy I. 2010.** Production of polyhydroxyalkanoates: the future green materials of choice. *Journal of Chemical Technology and Biotechnology* 85(6),732-743.
- **Akay F., Kazan A., Celiktas M. S., Yesil-Celiktas O. 2015.** A holistic engineering approach for utilization of olive pomace. *Journal of Supercritical Fluids* 99, 1–7.
- **Al bkoor Alrawashdeh K., Slopicka K., Alshorman A.A., Bartocci P., Fantozzi F. 2017.** Pyrolytic Degradation of Olive Waste Residue (OWR) by TGA: Thermal Decomposition Behavior and Kinetic Study. *International Journal of Energy and Power Engineering* 11, 497-510.
- **Alfano G., Belli C., Lustrato G., Ranalli, G. 2008.** Pile composting of two-phase centrifuged olive husk residues: Technical solutions and quality of cured compost. *Bioresource Technology* 99, 4694-4701.
- **Aliakbarian B., Casale M., Painsi M., Casazza A.A., Lanteri S., Perego P. 2015.** Production of a novel fermented milk fortified with natural antioxidants and its analysis by NIR spectroscopy. *LWT — Food Science and Technology* 62 (1, Part 2), 376–383.
- **Amar B., Salem K., Hocine D., Chadia I., Juan M.J. 2011.** Study and characterization of composites materials based on polypropylene loaded with olive husk flour. *Journal of Applied Polymer Science* 122, 1382–1394.

- **Amro M.A. 2016.** Olives pomace as renewable energy source. *Journal of Multidisciplinary Engineering Science Studies* 2(1), 245-250.
- **Anastopoulos I., Massas I., Ehaliotis C. 2015.** Use of residues and by-products of the olive-oil production chain for the removal of pollutants from environmental media: A review of batch biosorption approaches. *Journal of Environmental Science and Health. Part A Toxic/Hazardous Substances & Environmental Engineering* 50(7), 677-718.
- **Andersen H.J., Rasmussen M.A. 1992.** Interactive packaging as protection against photodegradation of the colour of pasteurized sliced ham. *International Journal of Food Science and Technology* 27, 1-8.
- **Andrady A.L. 2011.** Microplastics in the marine environment. *Marine Pollution Bulletin* 62,1596–1605.
- **Angellier H. 2005.** Nanocristaux d'amidon de maïs cireux pour applications matériaux composites. Thèse de **Doctorat de** l'Université Joseph-Fourier - Grenoble I, France.
- **Angellier-Coussy H., Gastaldi E., Gontard N., Guillard V. 2011.** Influence of processing temperature on the water vapour transport properties of wheat gluten based agromaterials. *Industrial Crops and Products* 33, 457–461.
- **Angellier-Coussy H., Guillard V., Guillaume C., Gontard N. 2013.** Role of packaging in a smorgasbord of action for sustainable food consumption. *Agro-Food Industry High-Tech Journal* 24 (3), 15-19.
- **Aniszewska M., Gendek A. 2014.** Comparison of heat of combustion and calorific value of the cones and wood of selected forest trees species. *Forest Research Papers* 75 (3), 231–236.
- **Antónia Nunes M., Pimentel F.B., Costa A.S.G., Alves R.C., Oliveira M. B. P.P. 2016.** Olive by products for functional and food applications: Challenging opportunities to face environmental constraints. *Innovative Food Science and Emerging Technologies* 35,139–148.
- **Araújo M., Pimentel F.B., Alves R.C., Oliveira M.B.P.P. 2015.** Phenolic compounds from olive mill wastes: Health effects, analytical approach and application as food antioxidants (Review). *Trends in Food Science and Technology* 45, 200-211.
- **Argenson C. 1999.** **L'Olivier**. Les éditions **Ctifl**, 204 p.
- **ASTM Standard F 1927-07, 2007.** Standard test method for determination of oxygen gas transmission rate, permeability and permeance at controlled relative humidity through barrier materials using a colorimetric detector. West Conshohocken, PA: ASTM International.
- **Avella, M., La Rota, G., Martuscelli, E., Raimo, M., Sadocco, P., Elegir, G., Riva, R. 2000.** Poly(3-hydroxybutyrate-co-3-hydroxyvalerate) and wheat straw fibre composites: thermal, mechanical properties and biodegradation behaviour. *Journal of Material Science* 35, 829–836.

- **Avérous L. and Pollet E. 2012.** Chapter 2: Biodegradable Polymers. Environmental Silicate Nano-Biocomposites, Green Energy and Technology ©Springer-Verlag London.
- **Aydinoglu T., Sargin S. 2013.** Production of laccase from *Trametes versicolor* by solid-state fermentation using olive leaves as a phenolic substrate. *Bioprocess and Biosystems Engineering* 36, 215–222.
- **Ayrilmis N., Buyuksari U. 2010.** Utilization of olive mill sludge in manufacture of lignocellulosic/polypropylene composite. *Journal of Material Science* 45, 1336–1342.
- **Babul Reddy A., Manjula B., Sudhakar K., Jayaramudu T. and Sadiku E. R. 2016.** Polyethylene/Other Biomaterials-Based Biocomposites and Bionanocomposites. Scrivener Publishing LLC, 279–314.
- **Balaguer M. P., Villanova J., Cesar G., Gavara R., Hernandez-Munoz P. 2015.** Compostable properties of antimicrobial bioplastics based on cinnamaldehyde cross-linked gliadins. *Chemical Engineering Journal* 262, 447–455.
- **Baley C., Busnel F., Grohens Y., Sire O. 2006.** Influence of chemical treatments on surface properties and adhesion of flax fibre–polyester resin. *Composites : Part A* 37, 1626–1637.
- **Ballesteros I., Ballesteros M., Cara C., Sáez F., Castro E., Manzanares P., Negro M.J., Oliva J.M. 2011.** Effect of water extraction on sugars recovery from steam exploded olive tree pruning. *Bioresource Technology* 102, 6611–6616.
- **Banat R., Fares M.M. 2015.** Olive oil waste filled high density polyethylene biocomposite: Mechanical, morphological and water absorption properties. *International Journal of Composite Material* 5(5), 133-141.
- **Barakat A., De Vries H., Rouau X. 2013.** Dry fractionation process as an important step in current and future lignocellulose biorefineries: A review. *Bioresource Technology* 134, 362–373.
- **Barakat A., Chuetor S., Monlau F., Solhy A., Rouau X. 2014.** Eco-friendly dry chemo-mechanical pretreatments of lignocellulosic biomass: Impact on energy and yield of the enzymatic hydrolysis. *Applied Energy* 113, 97–105.
- **Barakat A., Jérôme F., Rouau X. 2015.** A dry platform for separation of Proteins from biomass-containing polysaccharides, lignin, and polyphenols. *ChemSusChem* 8, 1161-1166.

- **Barbaro B., Toietta G., Maggio R., Arciello M., Tarocchi M., Galli A. Balsano C. 2014.** Review: Effects of the Olive-Derived Polyphenol Oleuropein on Human Health. *International Journal of Molecular Sciences* 15, 18508-18524.
- **Barbera A.C., Maucieri C., Cavallarp V., Ioppolo A., Spagna G. 2013.** Effects of spreading olive mill wastewater on soil properties and crops, a review. *Agric. Water Management* 119, 43-53.
- **Barham P.J., Keller A., Otun E.L., Holmes P.A. 1984.** Crystallization and morphology of a bacterial thermoplastic: poly-3-hydroxybutyrate. *Journal of Material Science* 19, 2781–2794.
- **Barkoula N.M., Garkhail S.K., Peijs T. 2010.** Biodegradable composites based on flax/polyhydroxybutyrate and its copolymer with hydroxyvalerate. *Industrial Crops and Products* 31, 34–42.
- **Basset C., Kedidi S., and Barakat A. 2016.** Chemical- and Solvent-Free Mechanophysical Fractionation of Biomass Induced by Tribo-Electrostatic Charging. *ACS Sustainable Chemistry and Engineering* 4, 4166–4173.
- **Belkharchouche D., Chaker A. 2017.** Thermo-mechanical characterization of construction material lightened by olive pomace. *Materials for Renewable and Sustainable Energy* 6, 15.
- **Benavente V., Fullana A. 2015.** Torrefaction of olive mill waste. *Biomass and bioenergy* 73, 186 -194.
- **Bengana M., Bakhouch A., Lozano-Sánchez J., Amir Y., Youyou A., Segura-Carretero A., Fernández-Gutiérrez A. 2013.** Influence of olive ripeness on chemical properties and phenolic composition of Chemlal extra-virgin olive oil. *Food Research International* 54, 1868–1875.
- **Benhayoun G., Lazzeri Y. 2007.** L'olivier en Méditerranée, du symbole à l'économie, Editions L'Harmattan, Paris.
- **Bentayeb K., Rubio C., Batlle R., Nerín C. 2007.** Direct determination of carnosic acid in a new active packaging based on natural extract of rosemary. *Analytical and Bioanalytical Chemistry* 389,1989–1996.
- **Benzekri M.B., Benderdouche N., Bestani B., Douara N., Duclaux L. 2018.** Valorization of olive stones into a granula activated carbon for the removal of methylene blue in batch and fixed bed modes. *Journal of Materials and Environmental Science* 19(1), 272-284.

- **Benzie I. F. F. 1996.** Lipid peroxidation: A review of causes, consequences, measurement and dietary influences. *International Journal of Food Science and Nutrition* 47, 233–261.
- **Berthet M.A., Angellier-Coussy H., Machado D., Hilliou L., Staebler A., Vicente A., Gontard N. 2015a.** Exploring the potentialities of using lignocellulosic fibers derived from three food by-products as constituents of biocomposites for food packaging. *Industrial Crops and Products* 69, 110–122.
- **Berthet M.A., Angellier-Coussy H., Chea V., Guillard V., Gastaldi E., Gontard N. 2015b.** Sustainable food packaging: Valorising wheat straw fibres for tuning PHBV-based composites properties. *Composites: Part A* 72, 139–147.
- **Berthet M.A., Angellier-Coussy H., Guillard V., Gontard N. 2016.**Vegetal fibre-based biocomposites: Which stakes for food packaging applications. *Journal of Applied Polymer Science* 133(2), SI (42528).
- **Berthet M.A., Mayer-Laigle C., Rouau X., Gontard N., Angellier-Coussy H. 2017.** Sorting natural fibres: A way to better understand the role of fibre size polydispersity on the mechanical properties of biocomposites. *Composites: Part A* 95, 12–21.
- **Bhatnagar A., Kaczala F., Hogland W., Marques M., Paraskeva C.A., Papadakis V.G., Sillanpää M. 2014.**Valorization of solid waste products from olive oil industry as potential adsorbents for water pollution control - a review. *Environmental Science and Pollution Research* 21(1), 268-98. DOI: 10.1007/s11356-013-2135-6.
- **Bianchi G. 2003.** Lipids and phenols in table olives. *European Journal of Lipid Science and Technology* 105, 229–242.
- **Bishop P.L., Godfrey C. 1983.** Nitrogen transformations during sludge composting. *BioCycle* 24, 34-39.
- **Blázquez G., Hernáinz F., Calero M., Martín-Lara M.A., Tenorio G. 2009.** The effect of pH on the biosorption of Cr(III) and Cr(VI) with olive stone. *Chemical Engineering Journal* 148, 473–479.
- **Bledzki A.K. and Gassan J. 1999.** Composites reinforced with cellulose based fibers. *Progress in Polymer Science* 24, 221–274.
- **Bledzki A.K., Mamun A., and Volk J. 2010.** Barley husk and coconut shell reinforced polypropylene composites: The effect of fibre physical, chemical and surface properties. *Composites Science and Technology* 70, 840–846.

- **Bledzki, A.K., Jaszkiwicz, A. 2010.** Mechanical performance of biocomposites based on PLA and PHBV reinforced with natural fibres – a comparative study to PP. *Composites Science and Technology* 70, 1687–1696.
- **Boopathy R. 2000.** Factor limiting bioremediation technologies. *Bioresource Technology* 74, 63–67.
- **Borja R., Alba J., Banks C.J. 1996.** Anaerobic digestion of wash water derived from the purification of virgin olive oil using a hybrid reactor combining a filter and sludge blanket. *Process Biochemistry* 31, 219–224.
- **Borja R., Alba J., Banks C.J. 1997.** Impact of the main phenolic compounds of olive mill wastewater (OMW) on the kinetics of aceto clastic methanogenesis. *Process Biochemistry* 32, 121-133.
- **Borja R., Martín A., Rincón B., Raposo F. 2003.** Kinetics for substrate utilization and methane production during the mesophilic anaerobic digestion of two phases olive pomace (TPOP). *Journal of Agricultural and Food Chemistry* 51, 3390-3395.
- **Borja R., Rincon B., Raposo F., Sanchez E., Martin A. 2004.** Assessment of kinetic parameters for the mesophilic anaerobic biodegradation of two-phase olive pomace. *International Biodeterioration and Biodegradation* 53,71-78.
- **Borja R., Raposo F., Rincón B. 2006.** Treatment technologies of liquid and solid wastes from two-phase olive oil mills. *Grasas Aceites* 57, 32-46.
- **Boskou D. 1996.** History and characteristics of the olive tree. In *Olive Oil Chemistry and Technology*; Boskou, D., Ed.; Am. Oil Chem. Soc. Press: Champaign, IL, USA.
- **Bouaziz M., Feki I., Ayadi M., Jemai H., Sayadi S. 2010.** Stability of refined olive oil and olive-pomace oil added by phenolic compounds from olive leaves. *European Journal of Lipid Science and Technology* 112, 894-905.
- **Boussehel H., Meghzi A., Nebbache N. 2016b.** The effect of alkali treatment on the mechanical and water absorption characteristics of olive stone flour reinforced polystyrene composites. *Research Journal of Pharmaceutical, Biological and Chemical Sciences* 7(1), 26-33.
- **Brozzoli V., Crognale S., Sampedro I., Federici, F., D’Annibale A., Petruccioli M. 2009.** Assessment of olive-mill wastewater as a growth medium for lipase production by *Candida cylindracea* in bench-top reactor. *Bioresource Technology* 100, 3395–3402.

- **Budinova T., Petrov N., Razvigorova M., Parra J., Galiatsatou P. 2006.** Removal of arsenic (III) from aqueous solution by activated carbons prepared from solvent extracted olive pulp and olive stones. *Industrial & Engineering Chemistry Research* 45, 1896–1901.
- **Buratti C., Mousavi S., Barbanera M., Lascaro E., Cotana F., Bufacchi M. 2016.** Thermal behaviour and kinetic study of the olive oil production chain residues and their mixtures during co-combustion. *Bioresource Technology* 214, 266-275. DOI: 10.1016/j.biortech.2016.04.097
- **Cagri A., Ustunol Z., Ryser E. 2001.** Antimicrobial edible films and coatings. *Journal of Food Science* 66, 865–870.
- **Calabia B.P., Ninomiya F., Yagi H., Oishi A., Taguchi K., Kunioka M., Funabashi M. 2013.** Biodegradable poly(butylene succinate) composites reinforced by cotton fiber with silane coupling agent. *Polymer* 5, 128-141.
- **Calatayud M., López-de-Dicastillo C., López-Carballo G., Vélez D., Muñoz P. H., Gavara R. 2013.** Active films based on cocoa extract with antioxidant, antimicrobial and biological applications. *Food Chemistry*, 139, 51–58.
- **Camo J., Lorés A., Djenane D., Beltrán J. A., Roncalés P. 2011.** Display life of beef packaged with an antioxidant active film as a function of the concentration of oregano extract. *Meat Science* 88, 174–178.
- **Campanari S., Augelletti F., Rossetti S., Sciubba F., Villano M., Majone M. 2017.** Enhancing a multi-stage process for olive oil mill wastewater valorization towards polyhydroxyalkanoates and biogas production. *Chemical Engineering Journal* 317, 280-289.
- **Cardelli R., Benitez E. 1998.** Changes of chemical properties in two soils amended with moist olive residues. *Agricol. Medit.* 128, 171–177.
- **Cardoso S. M., Guyot S., Marnet N., da-Silva J. A. L., Renard C.M.G.C., Coimbra M. A. 2005.** Characterisation of phenolic extracts from olive pulp and olive pomace by electrospray mass spectrometry. *Journal of The Science of Food and Agriculture* 85, 21–32. DOI: 10.1002/jsfa.1925
- **Carofiglio V.E., Romano R., Servili M., Goffredo A., Alifano P., Veneziani G., Demitri C., Centrone D., Stufano P. 2015.** Complete valorization of olive mill wastewater through an integrated process for poly-3-hydroxybutyrate production. *Journal of Life Sciences* 9, 481-493.

- **Carraro L., Trocino A., Xiccato G. 2005.** Dietary supplementation with olive stone meal in growing rabbits. *Ital. J. Anim. Sci.*4, 88–90.
- **Cavalheiro C. V., Picoloto R. S., Cichoski A. J., Wagner R., de Menezes, C. R., Zepka, L. Q., Barin J. S. 2015.** Olive leaves offer more than phenolic compounds— Fatty acids and mineral composition of varieties from Southern Brazil. *Industrial Crops and Products*, 71, 122–127.
- **Caynak S., Guru M., Bicer A., Keskin A., Icingur Y. 2009.** Biodiesel production from pomace oil and improvement of its properties with synthetic manganese additive. *Fuel* 88, 534–538.
- **Centre d'Activités Régionales pour la Production Propre (CAR/PP). 2000.** Prévention de la pollution dans la production d'huile d'olive. Plan d'Action pour la Méditerranée. 142 p.
- **Cerrone F., Sánchez-Peinado M.M., Juárez-Jimenez B., González-López J., Pozo C. 2010.** Biological treatment of two-phase olive mill wastewater (TPOMW, alpeorujó): polyhydroxyalkanoates (PHAs) production by azotobacter strains. *Journal of Microbiology and Biotechnology* 20, 594–601.
- **Chanprateep S. 2010.** Current trends in biodegradable polyhydroxyalkanoates. *Journal of Bioscience and Bioengineering* 110(6), 621-632.
- **Che F., Sarantopoulos I., Tsoutsos T., Gekas V. 2011.** Exploring a promising feedstock for biodiesel production in Mediterranean countries: a study on free fatty acid esterification of olive pomace oil. *Biomass Bioenergy* 36, 427-431.
- **Chemani H. 2013.** Valorisation des déchets solides d'huilerie et leur adjonction dans les masses pour la fabrication des tuiles de terre cuite, en vue d'améliorer leurs propriétés physico mécaniques. 21ème Congrès Français de Mécanique. (Bordeaux, 26 au 30 août 2013).
- **Chemrak M.A., Benderdouche N., Bestani B., Benallou M.B., Cagnon B. 2018.** Removal of mercury from natural gas by a new activated adsorbent from olive stones. *The Canadian Journal of Chemical Engineering* 96(1), 241-249.
- **Chen G.Q. 2009.** A microbial polyhydroxyalkanoates (PHA) based bio- and materials industry. *Chemical Society Reviews* 38(8), 2434-2446.
- **Chevillard A., Angellier-Coussy H., Guillard V., Gontard N., Gastaldi E. 2012.** Investigating the biodegradation pattern of an ecofriendly pesticide delivery system based

on wheat gluten and organically modified montmorillonites. *Polymer Degradation and Stability* 97, 2060-2068.

- **Chollet E., Sebti I., Martial-Gros A., Degraeve P. 2008.** Nisin preliminary study as a potential preservative for ripened cheese: NaCl, fat and enzymes influence on nisin concentration and its antimicrobial activity. *Food Control* 19, 982–989.
- **Chouchene A. 2010.** Etude expérimentale et théorique de procédés de valorisation de sous-produits oléicoles par voies thermique et physico-chimique. Food and Nutrition. Thèse de Doctorat. Université de Haute Alsace - Mulhouse, French. 221p.
- **Chouchene A., Jeguirim M., Khiari B., Zagrouba F., Trouvé G. 2010.** Thermal degradation of olive solid waste: influence of particle size and oxygen concentration. *Resources, Conservation and Recycling* 54, 271-277.
- **Christoforou E., Kylili A., Fokaidis P.A. 2016.** Technical and economical evaluation of olive mills solid waste pellets. *Renewable Energy* 96, 33-41.
- **Chuetor S., Luque R., Barron C., Solhy A., Rouau X. and Barakat A. 2015.** Innovative combined dry fractionation technologies for rice straw valorization to biofuels. *Green Chemistry* 17, 926–936.
- **Cioffi G., Pesca M. S., De Caprariis P., Braca A., Severino L., De Tommasi N. 2010.** Phenolic compounds in olive oil and olive pomace from Cilento (Campania, Italy) and their antioxidant activity. *Food Chemistry* 121, 105-111.
- **Ciolacu D., Ciolacu F., Popa V.I. 2008.** Supramolecular Structure - A Key Parameter for Cellulose Biodegradation. *Macromolecular Symposia* 272, 136–142.
- **Cirillo G., Spizzirri U. G., Iemma F. 2015.** Functional polymers in food science from technology to biology. Volume 1: Food Packaging. Edition WILEY. ISBN 978-1-118-59489-6.
- **Commission Internationale de l’Eclairage (CIE). 2004.** Technical report-Colorimetry. 3rd Edition. ISBN 3 901 906 33 9.
- **Cooperband L. 2002.** The Art and Science of Composting: A Resource for Farmers and Compost Producers. University of Wisconsin-Madison.
- **Cosmoliva, 2014.** Available from <<http://www.cosmoliva.co.uk>>.
- **Crocker J. 2008.** Natural materials innovative natural composites. *Materials Technology* 3, 174-178.

- **Cuevas M., Sánchez S., Bravo V., García J.F., Baeza J., Parra C., Freer J. 2010.** Determination of optimal pretreatment conditions for ethanol production from olive-pruning debris by simultaneous saccharification and fermentation. *Fuel* 89, 2891–2896.
- **Cuq B., Redl A. 2000.** Activités antimicrobiennes des films d’emballages. In : Gontard N. 2000. Les emballages actifs. Edition Tec et Doc. Paris. ISBN : 2-7430-0387-1.
- **Davies L.C., Vilhena A. M., Novais J.M. and Martins-Dias S. 2004.** Olive mill wastewater characteristics: modelling and statistical analysis. *Grasas Aceites* 55(3), 233-241.
- **Day B. P. F. 2003.** Active packaging. In Food Packaging Technology, eds. R. Coles, D. McDowell, M. J. Kirwan, pp. 283–302. Oxford (UK): Blackwell Publishing Ltd.
- **Day B.P.F. 2008.** Active packaging of food. In Smart Packaging Technologies for Fast Moving Consumer Goods, eds. J. Kerry, P. Butler, pp. 1–18. West Sussex: John Wiley & Sons Ltd.
- **De Bertoldi M., Vallini G., Pera A. 1983.** The biology of composting: a review. *Waste Management and Research* 1, 157-176.
- **De la Casa J., Castro E. 2014.** Recycling of washed olive pomace ash fired clay brick manufacturing. *Construction Building Materials* 61, 320-326.
- **De la Lama D., Borja R., Rincón B. 2017.** Performance evaluation and substrate remove alkinetics in the semi-continuous anaerobic digestion of thermally pretreated two-phase olive pomace or “Alperujo”. *Process Safety and Environmental Protection* 105, 288–296
- **De Moraes Crizel T., De Oliveira Rios A., Alves V.D., Bandarra N., Moldão-Martins M., Hickmann Flôres S. 2018.** Active food packaging prepared with chitosan and olive pomace. *Food hydrocolloids* 74, 139-150.
- **Demirbas A. 2004.** Effects of temperature and particle size on bio-char yield from pyrolysis of agricultural residues. *Journal of Analytical and Applied Pyrolysis* 72, 243-251.
- **Dermeche S., Nadour M., Larroche C., Moulti-Mati F., Michaud P. 2013.** Olive mill wastes: Biochemical characterizations and valorization strategies. A review. *Process Biochemistry* 48, 1532–1552.
- **Díaz-García A., Martínez-García C., Cotes-Palomino T. 2017.** Properties of Residue from Olive Oil Extraction as a Raw Material for Sustainable Construction Materials. Part I: *Physical Properties Materials* 10(2), 1-15.

- **Djadouf S. 2011.** Etude de l'influence des ajouts (grignon d'olive et foin) sur les caractéristiques physicomécaniques de la brique de terre cuite. *Science & technologie* 9, 3-7.
- **Djefel D., Makhoul S., Khedache S., Lefebvre G., Royon L. 2015.** Preparation and characterization of stearic acid/ olive pomace powder composite as form-stable phase change material. *International journal of hydrogen energy* 40, 13764-13770
- **Djidjelli H., Benachour D., Boukerrou1 A., Zefouni O., Martinez-Véga J., Farenc J., Kaci M. 2007.** Thermal: dielectric and mechanical study of poly (vinyl chloride)/olive pomace composites. *Express Polymer Letters* 1, 846–852.
- **Doymaz I., Gorel O., Akgun N.A. 2004.** Drying characteristics of the solid by-product of olive oil extraction. *Biosystemstry Engineering* 88(2), 213-219.
- **Dufresne A., Kellerhals M.B. and Witholt B. 1999.** Transcrystallization in mcl-HAs/cellulose whiskers composites. *Macromolecules* 32(22): 7396–7401.
- **Dufresne A., Dupeyre D., Paillet M. 2003.** Lignocellulosic flour-reinforced poly(hydroxybutyrate-co-valerate) composites. *Journal of Applied Polymer Science* 87, 1302–1315.
- **Dupont F.J.L., Guignard. 2007.** Botanique systématique moléculaire. Edition Elsevier Masson. 14^eédition révisée. 285p.
- **El Mouhtadi I., Agouzzal M., Guy F. 2014.** L'olivier au Maroc. *Oil seeds & fats Crops and Lipids* 21, 1-3.
- **El S.N., Karakaya S. 2009.** Olive tree (*Olea europaea*) leaves: potential beneficial effects on human health. *Nutrition Research* 67, 632–638.
- **El-Abbassi A., Kiai H., Hafidi A. 2012.** Phenolic profile and antioxidant activities of olive mill wastewater. *Food Chemistry* 132, 406-412.
- **El-Hadi A., Schnabel R., Straube E., Müller G., Henning S. 2002.** Correlation between degree of crystallinity, morphology, glass temperature, mechanical properties and biodegradation of poly(3-hydroxyalkanoate) PHAs and their blends. *Polymer Test* 21(6), 665–674.
- **Eliche-Quesada D., Leite-Costa J. 2016.** Use of bottom ash from olive pomace combustion in the production of eco-friendly fired clay bricks. *Waste Management* 48, 323-333.
- **Ellen MacArthur Foundation. 2016.** The new plastics economy. Rethinking the future of plastics.

- **Eriksson C. E. 1987.** Oxidation of Lipids in Food Systems: Autoxidation of Unsaturated Lipids. Academic Press Inc.: London.
- **European Bioplastics. 2017.** FACT SHEET: What are bioplastics? <http://en.european-bioplastics.org/news/publications>.
- **FAOSTAT. 2016.** Website of Food and Agriculture Organization of the United Nations. <http://faostat.fao.org> (consulted the 03th of October 2017).
- **Fathy S.A., Mahmoud A.E., Rashad M.M., Ezz M.K., Mohammed A.T. 2018.** Improving the nutritive value of olive pomace by solid state fermentation of *Kluyveromyces marxianus* with simultaneous production of gallic acid. *International Journal of Recycling of Organic Waste in Agriculture*. doi.org/10.1007/s40093-018-0199-5.
- **Fellows P. 2000.** Food Processing Technology: Principles and Practice, 2nd ed. Cambridge: Woodhead Publishing Ltd. ISBN 1 85573 533 4.
- **Fernández-Bolaños J., Rodríguez G., Rodríguez R., Guillén R. and Jiménez A. 2006.** Potential use of olive by-products. Extraction of interesting organic compounds from olive oil waste. *Grasas y aceites* 57, 95-106.
- **Fernandez-Orozco R., Roca M., Gandul-Rojas B., Gallardo-Guerrero L. 2011.** DPPH-scavenging capacity of chloroplastic pigments and phenolic compounds of olive fruits (cv. Arbequina) during ripening. *Journal of Food Composition and Analysis* 24, 858–864.
- **Fki I., Bouaziz M., Sahnoun Z., Sayadi S. 2005.** Hypocholesterolemic effects of phenolic-rich extracts of Chemlali olive cultivar in rats fed a cholesterol-rich diet. *Bioorganic and Medicinal Chemistry* 13, 5362–70.
- **Fuentes C.A., Brughmans G., Tran L.Q.N., Dupont-Gillain C., Verpoest I., Van Vure A.W. 2015.** Mechanical behaviour and practical adhesion at a bamboo composite interface: Physical adhesion and mechanical interlocking. *Composites Sciences and Technology* 109, 40-47.
- **Gajdoš J., Galić K., Kurtanjek Ž., Ciković N. 2000.** Gas permeability and DSC characteristics of polymers used in food packaging. *Polymer Testing* 20, 49–57.
- **Galotto M. J., Valenzuela X., Rodriguez F., Bruna J., Guarda A. 2012.** Evaluation of the effectiveness of a new antimicrobial active packaging for fresh Atlantic Salmon (*Salmon Salar* L.) shelf life. *Packaging Technology and Science* 25, 363–372.
- **Galotto M. J., Guarda A., de Dicastillo C. L. 2015.** Antimicrobial active polymers in food packaging. In: Functional polymers in food science from technology to biology. Cirillo G., Spizzirri U. G., Iemma F (Eds.), ISBN: 978-1-118-59489-6.

- **Gandul-Rojas B., Cepero M.R., Mínguez-Mosquera M.I. 2000.** Use of chlorophyll and carotenoid pigment composition to determine authenticity of virgin olive oil. *Journal of the American Oil Chemists' Society* 77, 853- 858.
- **García G.B., Calero de Hoces M., Martínez García C., Cotes Palomino M.T., Gálvez A.R., Martín-Lara M.Á. 2014.** Characterization and modeling of pyrolysis of the two-phase olive mill solid waste. *Fuel Processing Technology* 126, 104-111.
- **Garcia-Ibanez P., Sanchez M., Cabanillas A. 2006.** Thermogravimetric analysis of olive-oil residue in air atmosphere. *Fuel Processing Technology* 87.103 – 107.
- **García-Maraver M., Salvachúa D., Martínez M.J., Díaz L.F., Zamorano M. 2013.** Analysis of the relation between the cellulose, hemicellulose and lignin content and the thermal behavior of residual biomass from olive trees. *Waste Manage* 33, 2245–2249.
- **Garcia-Maraver A., Perez-Jimenez J.A., Serrano-Bernardo F, Zamorano M.2015.** Determination and comparison of combustion kinetics parameters of agricultural biomass from olive trees. *Renew Energy* 83, 897-904.
- **Gardner K. and Blackwell J. 1974.** The structure of native cellulose. *Biopolymers* 13, 1975-2001.
- **Garlotta D. 2001.** A literature review of poly (lactic acid). *Journal of Polymers and the Environment* 9(2), 63–84.
- **Geyer R., Jambeck J.R., Law K.L. 2017.** Production, use, and fate of all plastics ever made. *Science Advance* 3, e1700782. doi:DOI: 10.1126/sciadv.1700782.
- **Ghanbari R., Anwar F., Alkharfy K.M., Gilani A. and Saari N. 2012. Valuable Nutrients and Functional Bioactives in different Parts of Olive (Olea europaea L.): Review.** *International Journal of Molecular Sciences* 13, 3291-3340.
- **Gharbi A., BelHassen R., Boufi S. 2014.** Composite materials from unsaturated polyester resin and olive nuts residue: The effect of silane treatment. *Industrial Crops and Products* 62, 491–498.
- **Ghazy S.E., Samra S.E., May A.E.M., El-Morsy S.M. 2006.** Removal of aluminium from some water samples by sorptive-flotation using powdered modified activated carbon as a sorbent and oleic acid as a surfactant. *Analytical Science* 22, 377–82.
- **Goldsmith C.D., Stathopoulos C.E., Golding J.B., Roach P.D. 2014.** Fate of the phenolic compounds during olive oil production with the traditional press method. *International Food Research Journal* 21(1), 101-109.

- **Gomes M.E. 2004.** Biodegradable polymers and composites in biomedical applications: From catgut to tissue engineering. Part 1: Available systems and their properties. *International Materials Reviews* 12(4), 65–81.
- **Gomez-de la Cruz F.J., Casanova-Pelaez P.J., Lopez-Garcia R., Cruz-Peragon F. 2015.** Review of the drying kinetics of olive oil mill wastes: Biomass recovery. *Bioresources* 10(3), 6055-6080.
- **Gómez-Muñoz B., Hatch D. J., Bol R., García-Ruiz R. 2012.** The Compost of Olive Mill Pomace: From a Waste to a Resource – Environmental Benefits of Its Application in Olive Oil Groves. Chapter from the book Sustainable Development - Authoritative and Leading Edge. Content for Environmental Management. <http://dx.doi.org/10.5772/48244>
- **Gontard N. 2000.** Les emballages actifs. Edition Tec et Doc. Paris. ISBN : 2-7430-0387-1.
- **Gontard N. 2015.** L'emballage Alimentaire. L'Alimentation à Découvert, C. Esnouf J. Fioramonti et B. Laurieux Eds., CNRS Editions, Paris, Fr. ISBN : 978-2-271-07896-4, p90.
- **Gontard N., Guillard V., Gaucel S., Guillaume C. 2017.** L'emballage alimentaire et l'innovation écologique dans toutes leurs dimensions. Innovations Agronomiques, INRA, , 58, pp.1-9. <hal-01668195> .
- **Guilbert S., Guillaume C., Gontard N. 2011.** New Packaging Materials Based on Renewable Resources: Properties, Applications, and Prospects. doi:10.1007/978-1-4419-7475-4_26.
- **Guillard V., Gontard N. 2017.** Des emballages qui ne polluent pas, ça existe ! The conversation. 14 février 2017.
- **Haddadi M., Yakoub-Bougdal S. 2010.** Olive rootstock production from Oleaeuropea var. Chemlal cultured in vitro. *Cahiers Agricultures*, 19, 288–291.
- **Haddadin M.S.Y., Haddadin J., Arabiyat O.I., Hattar B.2009.** Biological conversion of olive pomace into compost by using *Trichoderma harzianum* and *Phanerochaete chrysosporium*. *Bioresource Technology* 100, 4773–4782.
- **Hamelinck C.N., Hooijdonk G.V., Faaji A.P.C.2005.**Ethanol from lignocellulosic biomass: techno-economic performance in short-middle and long-term. *Biomass Bioenergy*, 28: 384-410.
- **Hammad M., Badarneh D., Tahboub K. 1999.** Evaluating variable organic waste to produce methane. *Energy Conversion and Management* 40, 1463-1475.

- **Hammoui Y., Molina-Boisseau S., Duval A., Djerrada N., Adjeroud N., Remini H., Dahmoune F., Madani K. 2015.** Preparation of plasticized wheat gluten/olive pomace powder biocomposite: Effect of powder content and chemical modifications. *Materials and Design* 87, 742–749.
- **Harikumar K.R., Joseph K., Thomas S. 1999.** Jute sack cloth reinforced polypropylene composites: mechanical and sorption studies. *Journal of Reinforced Plastics and Composites* 18, 346–372.
- **Harmsen P., Huijgen W., Bermudez L., Bakker R. 2010.** Literature review of physical and chemical pretreatment processes for lignocellulosic biomass. Report n°1184, pp 1–49.
- **Hassaini, L., Kaci, M., Benhamida A., Bruzard, S., Pillin, I., Grohens Y. 2016.** The effects of PHBV-g-MA compatibilizer on morphology and properties of poly(3-hydroxybutyrate-co-3-hydroxyvalerate)/olive husk flour composites. *Journal of Adhesion Science and Technology* 30(19), 2061-2080.
- **Hassaini L., Kaci M., Touati N., Pillin I., Kervoelen A., Bruzard S. 2017.** Valorization of olive husk flour as a filler for biocomposites based on poly(3-hydroxybutyrate-co-3-hydroxyvalerate): Effects of silane treatment. *Polymer Testing* 59, 430-440.
- **Hassan M.L., Abouzeid R., El-Sakhawy M., Khiari R. 2014.** Cellulose nanocrystals and carboxymethyl cellulose from olive stones and their use to improve paper sheets properties. *International Journal of Nanoparticles* 7(3/4), 261-277.
- **Hauser C., Wunderlich J. 2011.** Antimicrobial packaging films with a sorbic acid based coating. *Procedia – Food Science* 1, 197–202.
- **Hemery Y., Holopainen U., Lampi A.M., Lehtinen, P., Nurmi T., Piironen V., Edelmann M., Rouau X. 2011.** Potential of dry fractionation of wheat bran for the development of food ingredients, part II: Electrostatic separation of particles. *Journal of Cereal Science* 53 (1), 9–18.
- **Hepworth D.G., Hobson R.N., Bruce D.M. and Farrent J.W. 2000.** The use of unretted hemp fibre in composite manufacture. *Composites Part A: Applied Science and Manufacturing* 31(11), 1279–1283.
- **Hon D.N.S. 1996.** Chemical Modification of Lignocellulosic Materials. New York: Marcel Dekker.
- **Houmani M., Tisserand J.L. 1999.** Complémentation d'une paille de blé avec des blocs multi nutritionnels : effets sur la digestibilité de la paille et intérêt pour des brebis taries et des agneaux en croissance. *Annales de Zootechnie*, 199-209.

- **Inglezakis V.J., Moreno J.L., Doula M. 2012.** Olive oil waste management EU legislation: Current situation and policy recommendations. *International Journal of Chemical and Environmental Engineering Systems* 3(2), 65-77.
- **International Olive Council. 2014.** <http://www.internationaloliveoil.org/>
- **International Olive Council. 2016.** <http://www.internationaloliveoil.org/>
- **International Olive Council. 2017.** <http://www.internationaloliveoil.org/>
- **Isikgor F.H. and Becer C.R. 2015.** Lignocellulosic biomass: a sustainable platform for the production of bio-based chemicals and polymers. *Polymer Chemistry* 6(25), 4497–4559.
- **Jamshidian M., Tehrani E.A., Imran M., Jacquot M., Desobry S. 2010.** Poly-Lactic Acid: production, applications, nanocomposites, and release studies. *Comprehensive reviews in food science and food safety* 9 (5), 552-571.
- **Jauhainen J. Martín-Gullón I., Conesa Juan A., Font R. 2005.** Emissions from pyrolysis and combustion of olive oil solid waste. *Journal of Analytical and Applied Pyrolysis* 74, 512-517.
- **Jerman Klen T., Mozetic Vodopivec B. 2012.** The fate of olive fruit phenols during commercial olive oil processing: Traditional press versus continuous two- and three-phase centrifuge. *Food Science technology* 49(2), 267-274.
- **John M.J. and Thomas S. 2008.** Biofibers and biocomposites. *Carbohydrate Polymers* 71, 343–364.
- **Johnstone B. 1990.** A throw away answer. *Far Eastern Economic Review* 147 (6), 62–63.
- Jones D.B., 1941. Factors for converting percentages of nitrogen in foods and feeds into percentages of proteins. Circular N°183. United States Department of Agriculture. Washington, 22 p.
- **Joshi S.V., Drzal L.T., Mohant, A.K. and Arora S. 2004.** Are natural fiber composites environmentally superior to glass fiber reinforced composites? *Composites Part A: Applied Science and Manufacturing* 35, 371–376.
- **Justino C.I., Pereira R., Freitas A.C., Rocha-Santos T.A., Panteleitchouk T.S., Duarte A.C. 2012.** Olive oil mill wastewaters before and after treatment: a critical review from the ecotoxicological point of view. *Ecotoxicology* 21(2), 615-629.
- **Kalderis D., Diamadopoulos E. 2010.** Valorization of Solid Waste Residues from Olive Oil Mills: A Review. *Terrestrial and Aquatic Environmental Toxicology* 4 (1), 7-20.

- **Kalipci E. 2016.** Removal of methylene blue from aqueous solutions with natural olive pomace modified with ultrasounds and acid. *Environment Protection Engineering* 42 (3), 6-17. DOI: 10.5277/epe160301.
- **Karakaya, S.E.S. 2009.** Studies of olive tree leaf extract indicate several potential health benefits. *Nutrition Reviews* 67, 632–639.
- **Karus M. and Kaup M. 2002.** Natural fibres in the European automotive industry. *Journal of Industrial Hemp* 7(1), 119–131.
- **Kengkhetkit N. Amornsakchai T. 2014.** A new approach to “Greening” plastic composites using pineapple leaf waste for performance and cost effectiveness. *Materials and Design* 55. 292–299.
- **Kerry J. P., O’Grady M. N., Hogan S. A. 2006.** Past, current and potential utilisation of active and intelligent packaging systems for meat and muscle-based products: A review. *Meat Science* 11, 113–130.
- **Khalifa I., Barakat H., El-Mansy H. A., Soliman S. A. 2017.** Preserving apple (*Malus domestica* var. Anna) fruit bioactive substances using olive wastes extract-chitosan film coating. *Information processing in agriculture* 4, 90–99.
- **Khayal M.T., El-Ghazaly M.A., Abdallah D.M., Nassar N.N., Okpanyi S.N., Kreuter M.H. 2002.** Blood pressure lowering effect of an olive leaf extract (*Olea europaea*) in L-NAME induced hypertension in rats. *Arzneimittelforschung* 52, 797–802.
- **Khemakhem M., Lamnawar K., maazouz A., Jaziri M. 2016.** Biocomposites based on polylactic acid and olive solid waste fillers: Effect of two compatibilization approaches on the physicochemical, rheological and mechanical properties. *Polymer Composites*. DOI 10.1002/pc.24094
- **Khoufi S., Aloui F., Sayadi S. 2008.** Extraction of antioxidants from olive mill wastewater and electro-coagulation of exhausted fraction to reduce its toxicity on anaerobic digestion. *Journal of Hazardous Materials* 151, 531–539.
- **Kim J-K., Mai Y-W. 1998.** Engineered Interfaces in Fiber Reinforced Composites. 1st Edition. pages: 416. eBook ISBN: 9780080530970
- **Kourmentza C., Plácido J., Venetsaneas N., Burniol-Figols A., Varrone C., Gavala H.N., Reis M.A.M. 2017.** Recent Advances and Challenges towards Sustainable Polyhydroxyalkanoate (PHA) Production: a review. *Bioengineering* 4, 55. doi:10.3390/bioengineering4020055

- **Koutsomitopoulou A.F., Bénézet J.C., Bergeret A., Papanicolaou G.C. 2014.** Preparation and characterization of olive pit powder as a filler to PLA-matrix biocomposites. *Powder Technology* 255, 10–16.
- **Krokida M.K., Maroulis Z.B., Kremas C. 2002.** Process design of rotary dryers for olive cake. *Drying Technology* 20(4/5), 771:788.
- **Kuhad R.C., Singh A., Eriksson K.E.L. 1997.** Microorganisms and enzymes involved in the degradation of plant fiber cell walls. *Advance in Biochemical Engineering/ Biotechnology* 57, 45-125.
- **Kumar S., Das P.M., Rebecca L.J., Sharmila S. 2013.** Isolation and identification of LDPE degrading fungi from municipal solid waste. *Journal of Chemical and Pharmaceutical Research* 5(3), 78-81.
- **La Rubia-García M.D., Yebra-Rodríguez A., Eliche-Quesadac D., Corpas-Iglesias F.A., López-Galindo A. 2012.** Assessment of olive mill solid residue (pomace) as an additive in lightweight brick production. *Construction Building Materials* 36, 495-500.
- **Lafka T.I., Lazou A. E., Sinanoglou V. J., Lazos E. S. 2011.** Phenolic and antioxidant potential of olive oil mill wastes. *Food Chemistry* 125, 92-98.
- **Lammi S., Barakat A., Mayer-Laigle C., Djenane D., Gontard N., Angellier-Coussy H. 2018a.** Dry fractionation of olive pomace as a sustainable process to produce fillers for biocomposites. *Powder Technology* 326, 44-53. DOI.org/10.1016/j.powtec.2017.11.060
- **Lammi S., Le Moigne N., Djenane D., Gontard N., Angellier-Coussy H. 2018b.** Dry fractionation of olive pomace for the development of food packaging biocomposites. *Industrial Crop and Products* 120, 250-261. DOI.org/10.1016/j.indcrop.2018.04.052
- **Laufenberg G., Kunz B., Nystroem M. 2003.** Transformation of vegetable waste into value added products: (A) the upgrading concept; (B) practical implementation. *Bioresource Technology* 87, 167-198.
- **Le Digabel F., Boquillon N., Dole P., Monties B., Averous L. 2004.** Properties of thermoplastic composites based on wheat-straw lignocellulosic fillers. *Journal of Applied Polymer Science* 93, 428–436.
- **Lee K. T. 2010.** Quality and safety aspects of meat products as affected by various physical manipulations of packaging materials. *Meat Science* 86, 138–150.
- **Lee O.H., Lee B.Y. 2010.** Antioxidant and antimicrobial activities of individual and combined phenolics in *Olea europaea* leaf extract. *Bioresource Technology* 101, 3751–3754.

- **Lee S.Y. 1996.** Plastic bacteria? Progress and prospects for polyhydroxyalkanoates production in bacteria. *Trends in Biotechnology* 14, 431–438.
- **Leite P., Salgado J. M., Venâncio A., Domínguez J. M., Belo I. 2016.** Ultrasounds pretreatment of olive pomace to improve xylanase and cellulase production by solid-state fermentation. *Bioresource Technology* 214, 737–746.
- **Leroy E., Petit I., Audic J.L., Colomines G., Deterre R. 2012.** Rheological characterization of a thermally unstable bioplastic in injection molding conditions. *Polymer Degradation and Stability* 97(10), 1915-21.
- **Lesage-Meessen L., Navarro D., Maunier S., Sigoillot J.C., Lorquin J., Delattre M., Simon J.L., Asther M., Labat M. 2001.** Simple phenolic content in olive oil residues as a function of extraction systems. *Food Chemistry* 75, 501-507.
- **Li X., Panigrahi S., Tabil L. G. 2009.** A study on flax fiber-reinforced polyethylene biocomposites. *Applied Engineering in Agriculture* 25 (4), 25-531.
- **Li X.H., Hua-jun Yang H.J, Roy B., Wang D., Yue W.F., Jiang L.J., Park E.Y., Miao Y.G. 2009.** The most stirring technology in future: Cellulase enzyme and biomass utilization. *African Journal of Biotechnology* 8(11): 2418-2422.
- **Licari A., Monlau F., Solhy A., Buche P., Barakat A. 2016.** Comparison of various milling modes combined to the enzymatic hydrolysis of lignocellulosic biomass for bioenergy production: Glucose yield and energy efficiency. *Energy* 102, 335-342.
- **Licciardello F., Wittenauer J., Saengerlaub S., Reinelt M., Stramm C. 2015.** Rapid assessment of the effectiveness of antioxidant active packaging— Study with grape pomace and olive leaf extracts. *Food Packaging and Shelf Life* 6, 1–6.
- **Lin L., Ying D., Chaitep S., Vittayapadung S. 2009.** Biodiesel production from crude rice bran oil and properties as fuel. *Applied Energy* 86, 681-688.
- **Lin T.H., Huang C.F., Guo G.L., Hwang W.S. & Huang S.L. 2012.** Pilot-scale ethanol production from rice straw hydrolysates using xylose-fermenting *Pichia stipitis*. *Bioresource Technology* 116: 314-319.
- **Loizzo M.R., Di Lecce G., Boselli E., Menichini F., Frega N.G. 2011.** Inhibitory activity of phenolic compounds from extra virgin olive oils on the enzymes involved in diabetes, obesity and hypertension. *Journal of Food Biochemistry* 35, 381–99.
- **Long J and Bonnet P. 1951.** L'olivier à fruits de table. Ministère de l'agriculture, Direction de la production agricole, 1 vol. Paris, France, 59 p.

- **López J.P., Boufi S., Mansouri N.E., Mutjé P., Vilaseca F. 2012.** PP composites based on mechanical pulp, deinked newspaper and jute strands: a comparative study. *Composites Part B: Engineering* 43, 3453–3461.
- **Lopez O., Garcia M. A., Zaritzky N. 2015.** Films based on starches. In: Functional polymers in food science from technology to biology. Cirillo G., Spizzirri U. G., Iemma F (Eds.), ISBN: 978-1-118-59489-6.
- **Luo S. and Netravali A.N. 1999.** Mechanical and thermal properties of environmentally friendly green composites made from pineapple leaf fibres and poly(hydroxybutyrate-co-valerate) resin. *Polymer Composite* 20(3), 367–378.
- **Madison L.L., Huisman G.W. 1999.** Metabolic engineering of poly(3-hydroxyalkanoates): from DNA to plastic. *Microbiology and Molecular Biology Review* 63 (1), 21–53.
- **Mais U., Esteghlalian A.R., Saddler J.N., Mansfield S.D. 2002.** Enhancing the enzymatic hydrolysis of cellulosic materials using simultaneous ball milling. *Applied Biochemistry and Biotechnology* 98, 815-832.
- **Markarian J. 2005.** Automotive and packaging offer growth opportunities for nanocomposites. *Journal of Plastics Additives and Compounding* 7, 18–25.
- **Market of Olive Residues for Energy (M.O.R.E). 2010.**
<https://ec.europa.eu/energy/intelligent/projects>
- **Martínez-Nieto L., Driss Alamia S.B., Hodaifa G., Faur C., Rodríguez S., Giménez J.A., Ochando J. 2010.** Adsorption of iron on crude olive stones. *Industrial Crops and Products* 32, 467–471.
- **Martin-Lara M.A., Trujillo Miranda M.M., Galvez A.R., Munoz A.P., de Hoces M.C. 2016.** Valorization of olive stone as adsorbent of chromium(VI) : comparison between laboratory- and pilot-scale fixed-bed columns. *International Journal of Environmental Science Technology* 14(12), 2661-2674.
- **Martino L., Berthet M.A., Angellier-Coussy H., Gontard N. 2015.** Understanding external plasticization of melt extruded PHBV–wheat straw fibers biodegradable composites for food packaging. *Journal of Applied Polymer Science* DOI : 10.1002/APP.41611
- **Martone T.P., Estevez, M.J., Lu F., Ruel K., Denny W. M., Somerville C., Ralph J. 2009.** Discovery of Lignin in Seaweed Reveals Convergent Evolution of Cell-Wall Architecture. *Current Biology* 19, 169-175.

- **Mastromateo M., Danza A., Conte A., Muratore G., Del Nobile M. A. 2012.** Shelf life of ready to use peeled shrimps as affected by thymol essential oil and modified atmosphere packaging. *International Journal of Food Microbiology* 14, 4250–256.
- **Matos M., Barreiro M.F., Gandini A. 2010.** Olive stone as a renewable source of biopolyols. *Industrial Crops and Products* 32, 7–12.
- **Maymone B., Battaglini A., Tiberio M. 1961.** Ricerche sul valore nutritive del la sansa d'olive. *Alimentazione Animale* 4, 219–250.
- **Mehdi Emadian S., Onay T.T., Demirel B. 2017.** Biodegradation of bioplastics in natural environments. *Waste Management* 59, 526–536.
- **Mehmeti E., Dogan Ö., Tiris M., Kiran N.C., Matuschek G. 2008.** Thermolysis product distribution of solid waste obtained from olive oil production. *Clean* 36, 315-319.
- **Mekki H., Anderson M., Ben Zina M., Ammar E. 2008.** Valorization of olive mill wastewater by its incorporation in building bricks. *Journal of Hazardous Materials* 158, 308–315.
- **Meksi N., Haddar W., Hammami S., Mhenni M.F. 2012.** Olive mill wastewater: A potential source of natural dyes for textile dyeing. *Industrial Crops and Products* 40, 103–109.
- **Michailides M., Christou G., Akrotos C.S., Tekerlekopoulou A.G., Vayenas D.V. 2011.** Composting of olive leaves and pomace from a three-phase olive mill plant. *Int. Biodeterior. Biodegradation* 65, 560-564.
- **Misra M., Nagarajan V., Reddy J., Mohanty A. K. 2011.** Bioplastics and green composites from renewable resources: where we are and future directions. 18th International conference on composite materials, Korea.
- **Monasse B., Haudin J. M. 1985.** Growth transition and morphology change in polypropylene. *Colloid & Polymer Science* 263, 822–831.
- **Montano-Leyva B., Ghizzi Da Silva G., Gastaldi E., Torres-Chávez P., Gontard N., Angellier-Coussy H. 2013.** Biocomposites from wheat proteins and fibers: Structure/mechanical properties relationships. *Industrial Crops Products* 43, 545–555.
- **Monteiro S.N., Calado V., Rodriguez R.J., Margem F.M. 2012.** Thermogravimetric stability of polymer composites reinforced with less common lignocellulosic fibers—an overview. *Journal of Materials Research and Technology* 1, 117–126.

- **Moore M. E., Han I. Y., Acton J. C., Ogale A. A., Barmore C. R., Dawson P. L. 2000.** Effects of antioxidants in polyethylene film on fresh beef color. *Journal of Food Science* 68, 99–104.
- **More (Market of olive residues for energy) project. 2008.** deliverable 3.1. (contributors : Regional Energy Agency of Central Macedonia, Anatoliki S.A., ARE Liguria, UC Liguria, AGENER, IPTPO, UP ZRS).
- **Mosca M., Cuomo F., Lopez F., Palumbo G., Bufalo G., Ambrosone L. 2015.** Adsorbent properties of olive mill wastes for chromate Removal. *Desalination and Water Treatment*: 1-9. DOI: 10.1080/19443994.2014.951694.
- **Mousavioun P., Halley P.J., Doherty, W.O.S., 2013.** Thermophysical properties and rheology of PHB/lignin blends. *Industrial Crops and Products* 50, 270–275.
- **Muktadirul Bari Chowdhury A. K.M., Akkratos C.S., Vayenas D.V., Pavlou S. 2013.** Olive mill waste composting: A review. *International Biodeterioration & Biodegradation* 85, 108-119.
- **Multon J.L. 1998.** Les emballages et conditionnement alimentaires, auxiliaires technologiques de la conservation des denrées. In : Multon J.L. et Bureau G. (1998). *L'emballage des denrées alimentaires de grande consommation*. Tec et Doc Lavoisier, Paris, 3-25.
- **Muñoz P.V., Morales M.P. O., Letelier V. G., Mendivil M.A. G. 2016.** Fired clay bricks made by adding wastes: Assessment of the impact on physical, mechanical and thermal properties. *Construction and Building Materials* 125, 241-252.
- **Muzzalupo I., Vendramin G.G., Chiappetta A. 2014.** Genetic biodiversity of Italianolives (*Olea europaea*) germplasm analyzed by SSR markers. *Scientific World Journal* (ID296590).
- **Nabinejad O., Sujan D., Rahman M., Davies I.J. 2015.** Effect of oil palm shell powder on the mechanical performance and thermal stability of polyester composites. *Material Design* 65, 823–830.
- **Naghmouchi I., Mutjé P., Boufi S. 2014.** Polyvinyl chloride composites filled with olive stone flour: Mechanical, thermal, and water absorption properties. *Journal of Applied Polymer Science* 131(22).
- **Naghmouchi I., Mutjé P., Boufi S. 2015.** Olive stones flour as reinforcement in polypropylene composites: A step forward in the valorization of the solid waste from the olive oil industry. *Industrial Crops and Products* 72,183–191.

- **Najar-Souissi S., Ouederani A., Ratel A. 2005.** Adsorption of dyes onto activated carbon prepared from olive stones. *Journal of Environmental Science in China* 17, 998–1003.
- **Nascimento D.C.O., Lopes F.P.D., Monteiro S.N. 2010.** Tensile behavior of lignocellulosic fiber reinforced polymer composites: Part I piassava/epoxy. *Revista Matéria* 2, 189-194.
- **Nasopoulou C., Zabetakis I. 2013.** Agricultural and aquacultural potential of olive pomace : A review. *Journal of Agricultural Science* 5(7), 116-127.
- **Nefzaoui A. 1983.** Etude de l'utilisation des sous-produits de l'olivier en alimentation animale en Tunisie. Division de la production et de la santé animale. FAO, Rome.
- **Nefzaoui A. 1987.** Contribution à la rentabilité de l'oléiculture par la valorisation optimale des sous-produits. OLIVAE IV, Tunisie.
- **Nerín C., Tovar L., Djenane D., Camo J., Salafranca J., Beltrán J. 2006.** Stabilization of beef meat by a new active packaging containing natural antioxidants. *Journal Agriculture and Food Chemistry* 54, 7840–7846.
- **Netravali A.N. and Chabba S. 2003.** Composites get greener. *Materials Today* 6(4): 22–29.
- **Niaounakis M., Halvadakis C.P. 2004.** Olive-Mill Waste Management, first ed. Typothito-George Dardanos, Athens.
- **Niaounakis M., Halvadakis C.P. 2006.** Olive Processing Waste Management: Literature Review and Patent Survey. Elsevier, Amsterdam. Olive tree pruning acid-hydrolysates by Pachysolentannophilus. *Biochemical Engineering Journal* 36, 108–115.
- **Nicholson D.J., Leavitt A.T., Francis R.C. 2014.** A three-stage klason method for more accurate determinations of hardwood lignin content. *Cellulose Chemistry and Technology* 48 (1-2), 53-59.
- **Obied H.K., Bedgood D.R.Jr., Prenzler P.D., Robards K. 2007.** Bioscreening of Australian olive mill waste extracts: Biophenol content, antioxidant, antimicrobial and molluscicidal activities. *Food and Chemical Toxicology* 45, 1238–1248.
- **Observatoire National des Filières Agricoles et Agroalimentaires (ONFAA). 2016.** Bilan de la campagne oléicole 2015/2016 « Segment huile d'olive ». Ministère de l'Agriculture, du Développement Rural et de la Pêche, Algérie. onfaa.inraa.dz
- **Oksman K. and Sain M. 2008.** Wood-Polymers Composites. Boca Raton, FL: CRC Press.

- **Omar A., Saed M.M., Abdalkarim M.M., Iedeelah H.A., Beaj W. 2016.** Olive pomace as an abundant, low-cost adsorbent for nitrate removal from aqueous solution. *MAYFEB Journal of Environmental Science* 1, 10-19.
- **Ouajai S. and Shanks R.A. 2009a.** Biocomposites of cellulose acetate butyrate with modified hemp cellulose fibres. *Macromolecular Materials and Engineering* 294, 213–221.
- **Ouajai S. and Shanks R.A. 2009b.** Preparation, structure and mechanical properties of allhemp cellulose biocomposites. *Composites Sciences and Technology* 69, 2119–2126.
- **Ouazzane H., Laajine F., El Yamani M., El Hilaly J, Rharrabti Y., Amarouch M-Y., Mazouzi D. 2017.** Olive Mill Solid Waste Characterization and Recycling opportunities: A review. *Journal of Materials and Environmental Science* 8(8), 2632-2650.
- **Ounas A., Aboulkas A., El harfi K., Bacaoui A., Yaacoubi A. 2011.** Pyrolysis of olive residue and sugar cane bagasse: Non-isothermal thermogravimetric kinetic analysis *Bioresource Technology* 102, 11234–11238.
- **Owen R.W., Giacosa A., Hull W.E., Haubner R., Spiegelhalder B., Bartsch H. 2000.**The antioxidant/anticancer potential of phenolic compounds isolated from olive oil. *European Journal of Cancer* 36, 1235–47.
- **Owens D.K., Wendt R.C. 1969.** Estimation of the Surface Free Energy of Polymers. *Journal of Applied Polymer Science* 13,1741-1747.
- **Ozdemir M., Floros J. D. 2004.** Active food packaging technologies. *Critical Reviews in Food Science and Nutrition* 44, 185–193.
- **Ozveren U., Ozdogan Z. S. 2013.**Investigation of the slow pyrolysis kinetics of olive oil pomace using thermo-gravimetric analysis coupled with mass spectrometry. *Biomass and bioenergy* 58, 168-179.
- **Pantaleo A., Carone M. T., Pellerano A. 2009.** Olive residues to energy chains in the apulia region part I: biomass potentials and costs. *Journal of Agriculture* 1, 1-11.
- **Papadaki E., Mantzouridou F.T. 2016.** Current status and future challenges of table olive processing wastewater valorization. *Biochemical Engineering Journal* 112, 106-113.
- **Papanicolaou G. C., Koutsomitopoulou A. F., Sfakianakis A. 2011.** Effect of Thermal Fatigue on the Mechanical Properties of Epoxy Matrix Composites Reinforced with Olive Pits Powder. *Journal of Applied Polymer Science* 124, 67–76.
- **Paraskeva P., Diamadopoulos E. 2006.** Technologies for olive mill wastewater (OMW) treatment: a review. *Journal of Chemical Technology and Biotechnology* 81, 1475–1485.

- **Parisi S. 2002.**The prediction of minimum durability in dairy products through analysis of bacterial and chemical physical contents. *Italian Food Technology* 29, 5–14.
- **Peelman N., Ragaert P., De Meulenaer B., Adons D., Peeters R., Cardon L., Van Impe F., Devlieghere F. 2013.** Application of bioplastics for food packaging. Review. *Trends in Food Science and Technology* 32, 128-141.
- **Perez-Jimenez F., Alvarez de Cienfuegos G., Badimon L., Barja. 2005.** International conference on the healthy effect of virgin olive oil. Consensus report, Jaen (Spain) 2004. *European Journal of Clinical Investigation* 35, 421-424.
- **Perinovic S., Andricic B., Erceg M. 2010.** Thermal properties of poly(L-lactide)/olive stone flour composites. *Thermochimica Acta* 510, 97-102.
- **Persson T., Matusiak M., Zacchi G., Jonsson A.S. 2006.** Extraction of hemicelluloses from process water from the production of masonite. *Desalination* 199, 411-412.
- **Petersen K., Nielsen P.V., Bertelsen G., Lawther M., Olsen M.B., Nilsson N.H., Mortensen G. 1999.** Potential of biobased materials for food packaging. *Trends in Food Science and Technology* 10, 52–68.
- **Philip S., Keshavarz T., Roy I. 2007.** Polyhydroxyalkanoates: biodegradable polymers with a range of applications, *Journal of Chemical Technology and Biotechnology* 82(3), 233-247.
- **Pillai S. K., Ray S.S. 2015.** Inorganic-organic hybrid polymers for food packaging. In: Functional polymers in food science from technology to biology Cirillo G., Spizzirri U. G., Iemma F. (Eds.), ISBN 978-1-118-59489-6.
- **Plackett D.V., Holm V.K., Johansen P., Ndoni S., Nielsen P.V., Sipilainen-Malm T., Sodergard A., Verstichel S. 2006.** Characterization of L-poly(lactide) and L-poly(lactide–polycaprolactone co-polymer films for use in cheese-packaging applications. *Packaging Technology and Science* 19,1–24.
- **Plastics Europe Plastics—The Facts 2016.** An analysis of European plastics production, demand and waste data. www.plasticseurope.org
- **Plaza C., Nogales R., Senesi N., Benitez E., Polo A. 2008.** Organic matter humification by vermin composting of cattle manure alone and mixed with two-phase olive-mill pomace. *Bioresource Technology* 99, 5085–5089.
- **Plaza M.G., Pevida C., Arias B., Feroso J., Casal M.D., Martín C.F., Rubiera F., Pis J.J. 2009.** Development of low-cost biomass-based adsorbents for postcombustion CO₂ capture. *Fuel* 88, 2442–2447.

priming effects. *Soil Biology and Biochemistry* 32, 1485–1498.

- **Pukánszky B.1990.** Influence of interface interaction on the ultimate tensile properties of polymer composites. *Composites* 21(3), 255-62.
- **Pushpadass H.A., Weber R.W., Dumais J.J., Hanna M.A. 2010.** Biodegradation characteristics of starch–polystyrene loose-fill foams in a composting medium. *Bioresource Technology* 101, 7258–7264.
- **Puthussery H., Prasad R., Gorazda K., Roy I. 2015.** Production, chemistry and properties of biopolymers in food science. In: Functional polymers in food science from technology to biology. Cirillo G., Spizzirri U. G., Iemma F. (Eds.), ISBN 978-1-118-59489-6.
- **Quattara B., Simard R., Piette G., Begin A., Holley R. 2000.** Diffusion of acetic and propionic acids from chitosan-based antimicrobial packaging films. *Journal Food Science* 65, 768–773.
- **Rabouhi A., Boukerrou A., Kaci M., Djidjelli H., Martinez-Vega J. J. 2010.** Chemical Modification of Olive Pomace by Various Esters and Silane. *Journal of Applied Polymer Science* 116, 535–540.
- **Ragni M., Melodia L., Bozzo F. Colonna M.A., Megna V., Toteda F., Vicenti A. 2003.** Use of a de-stoned olive pomace in feed for heavy lamb production. *Italian Journal Animal Science* 2(1S), 485-487.
- **Rahmanian N., Jafari S. M., Galanakis C.M. 2014.** Recovery and Removal of Phenolic Compounds from Olive Mill Wastewater. *Journal of American Oil Chemist's Society* 91, 1-18.
- **Rajaeifar M.A., Akram A., Ghobadian B., Rafiee S., Heijungs R., Tabatabaei M. 2016.** Environmental impact assessment of olive pomace oil biodiesel production and consumption: A comparative life cycle assessment. *Energy* 106, 87-102.
- **Ravindran R. and Jaiswal A. K. 2016.** Exploitation of food industry waste for high-value products. *Trends in Biotechnology* 34, 58–69.
- **Rebouillat S., Letellier B., Steffenino B.1999.**Wettability of single fibres-beyond the contact angle approach. *International Journal of Adhesion & Adhesives* 19, 303-314.
- **Reddy C.S.K., Ghai R., Rashmi, Kalia V.C.2003.** Polyhydroxyalkanoates: an overview. *Bioresource Technology* 87: 137–146.
- **Regional Energy Agency of Central Macedonia (REACM). 2008.** Market of Olive Residues for Energy.

- **Reinsch, V.E., Kelley, S.S. 1997.** Crystallization of poly(hydroxybutyrate-co-hydroxyvalerate) in wood fibre-reinforced composites. *Journal of Applied Polymer Science* 64, 1785–1796.
- **Reis M., Albuquerque M., Villano M., Majone M. 2011.** Mixed Culture Processes for Polyhydroxyalkanoate Production from Agro-Industrial Surplus/Wastes as Feedstocks. *Comprehensive Biotechnology* 6, 669-683.
- **Restuccia D., Puoci F., Parisi O. I., Picci N. 2015.** Food Applications of Active and Intelligent Packaging: Legal Issues and Safety Concerns. Cirillo G., Spizzirri U. G., Iemma F (Eds.), ISBN 978-1-118-59489-6.
- **Restuccia D., Spizzirri U. G., Parisi O. I., Cirillo G., Curcio M., Iemma F., Puoci F., Vinci G., Picci N. 2010.** New EU regulation aspects and global market of active and intelligent packaging for food industry applications. *Food Control* 21, 425–1435.
- **Rigane G., Bouaziz M., Sayadi S., Ben Salem R. 2012.** Identification and characterization of a new iridoid compound from two-phase Chemlali olive pomace. *European Food Research Technology* 234,1049–1054.
- **Rizzi V., D’Agostino F., Gubitosa J., Fini P., Petrella A., Agostiano A., Semeraro P., Cosma P. 2017.** An alternative use of olive pomace as a wide-ranging bioremediation strategy to adsorb and recover disperse orange and disperse red industrial dyes from wastewater. *Separations* 4, 29, 1-12. DOI:10.3390/separations4040029.
- **Roca M. and Minguéz-Mosquera M.I. 2001.** Changes in chloroplast pigments of olive varieties during fruit ripening. *Journal of Agriculture and Food Chemistry* 49, 832-839.
- **Rodis P. S., Karathanos V. T., Mantzavinou A. 2002.** Partitioning of olive oil antioxidants between oil and water phases. *Journal of Agriculture and Food Chemistry* 50, 596-601.
- **Rodrigues F., Pimentela F.B., Oliveira M.B.P.P. 2015.** Olive by-products: Challenge application in cosmetic industry. *Industrial Crops and Products* 70, 116–124.
- **Rodríguez G., Lama A., Rodríguez R., Jiménez A., Guillén R., Fernández-Bolanos J. 2008.** Olive stone as an attractive source of bioactive and valuable compounds. *Bioresource Technology* 99, 5261–5269.
- **Rodríguez-Gutierrez G., Rubio-Senent F., Lama-Munoz A., García A., Fernandez-Bolanos J. 2014.** Properties of lignin, cellulose, and hemicelluloses isolated from olive cake and olive stones: Binding of water, oil, bile acids, and glucose. *Journal of Agriculture and Food Chemistry* 62(36), 8973-81.

- **Romani V.P., Prentice-Hernández C., Martins V.G. 2017.** Active and sustainable materials from rice starch, fish protein and oregano essential oil for food packaging. *Industrial Crops and Products* 97, 268–274.
- **Romero I., Sánchez S., Moya M., Castro E., Ruiz E., Bravo V. 2007.** Fermentation of olive tree pruning acid-hydrolysates by *Pachysolen tannophilus*. *Biochemical Engineering Journal* 36, 108–115.
- **Romero-García J.M., Niño L., Martínez-Patiño C., Álvarez C., Castro E., Negro M.J. 2014.** Biorefinery based on olive biomass. State of the art and future trends: Review. *Bioresource Technology* 159, 421–432.
- **Roussos S., Perraud-Gaime I., Lakhtar H., Aouidi F., Labrousse Y., Belkacem N., Macarie H., Artaud J. 2009.** Valorisation biotechnologique des sous-produits de l'olivier par Fermentation en Milieu Solide. *Olivebioteq*, 293-300.
- **Rowell R.M. 2012.** Handbook of Wood Chemistry and Wood Composites. Boca Raton, FL: Taylor and Francis.
- **Rubio-Senent F., Rodriguez-Gutierrez G., Lama-Munoz, A., Fernandez Bolanos J.G. 2012.** New phenolic compounds hydrothermally extracted from the olive oil byproduct alperujo and their antioxidative activities. *Journal of Agricultural and Food Chemistry* 60, 1175-1186.
- **Rubio-Senent F., Martos S., Lama-Muñoz A., Fernández-Bolaños J.G., Rodríguez-Gutiérrez G., Fernández-Bolaños J. 2015.** Isolation and identification of minor secoiridoids and phenolic components from thermally treated olive oil by-products. *Food Chemistry* 187, 166–173.
- **Rudawska A., Jacniacka E. 2009.** Analysis for determining surface free energy uncertainty by the Owen–Wendt method. *International Journal of Adhesion & Adhesives* 29, 451–457.
- **Sabbah I., Marsook T., Basheer S. 2004.** The effect of pretreatment on anaerobic activity of olive mill wastewater using batch and continuous systems. *Process Biochemistry* 39, 1947–1951.
- **Sánchez de Medina V., Priego-Capote F., Luque de Castro M.D. 2011.** Quality and stability of edible oils enriched with hydrophilic antioxidants from the olive tree: the role of enrichment extracts and lipid composition. *Journal of Agriculture and Food Chemistry* 59, 11432–11441.

- **Sánchez de Medina V., Priego-Capote F., Luque de Castro M. D. 2012.** Characterization of refined edible oils enriched with phenolic extracts from olive leaves and pomace. *Journal of Agriculture and Food Chemistry* 60, 5866–5873.
- **Sanchez E., Rincon B., Borja R., Travieso L., Raposo F., Colmenarejo M.F. 2007.** Aerobic degradation kinetic of the effluent derived from the anaerobic digestion of two-phase olive mill solid residue. *International Journal of Biodeterioration and Biodegradation* 60, 60–67.
- **Sansoucy R. 1991.** Problèmes généraux de l'utilisation des sous-produits agroindustriels en alimentation animale dans la région méditerranéenne. CIHEAM-Options méditerranéennes. Série séminaire N°16, 75-79.
- **Santos F., Iulianelli G., Tavares M. 2016.** The Use of Cellulose Nanofillers in Obtaining Polymer Nanocomposites: Properties, Processing, and Applications. *Materials Sciences and Applications* 7, 257-294. DOI:10.4236/msa.2016.75026.
- **Schievano A., D'Imporzano G., Adani F. 2009.** Substituting energy crops with organic wastes and agro-industrial residues for biogas production. *Journal of Environmental Management* 90, 2537-2541.
- **Sebban A., Bahloul A., Saadoune M., Ait Kassi A., Berrada M., Pineau J.L., Kitane S. 2004.** Schéma de valorisation des grignons d'olives produits par les maasras Marocaines. Déchets - Revue francophone d'écologie industrielle- N° 34, 39-43.
- **Senneca O. 2007.** Kinetics of pyrolysis, combustion and gasification of three biomass fuels. *Fuel Processing Technology* 88, 87-97.
- **Shafizadeh F., McGinnis G.D., Philpot C.W., 1972.** Thermal degradation of xylan and related model compounds. *Carbohydrate Research* 25, 23–33.
- **Sharma Y.C., Singh B., Madhu D., Liu Y., Yaakob Z. 2014.** Fast synthesis of high quality biodiesel from 'waste fish oil' by single step transesterification. *Biofuel Research Journal* 1, 78-80.
- **Shibata M., Yamazoe K., Kuribayashi M., Okuyama Y. 2013.** All-wood biocomposites by partial dissolution of wood flour in 1-butyl-3-methylimidazolium chloride. *Journal of Applied Polymer Science* 127, 4802–4808.
- **Singh R., Kumar M., Mittal A., Mehta P.K. 2016.** Lignocellulolytic enzymes: Biomass to biofuel. *International Journal of Advanced Research* 4(10), 2175-2182. DOI: 10.21474/IJAR01/2039

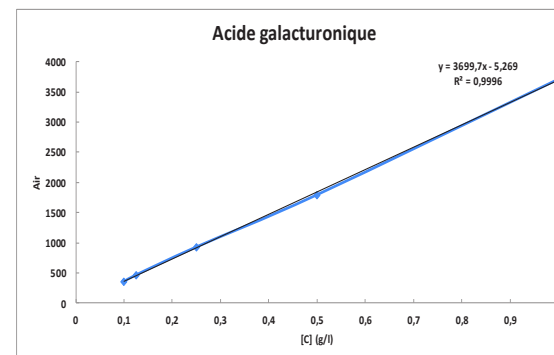
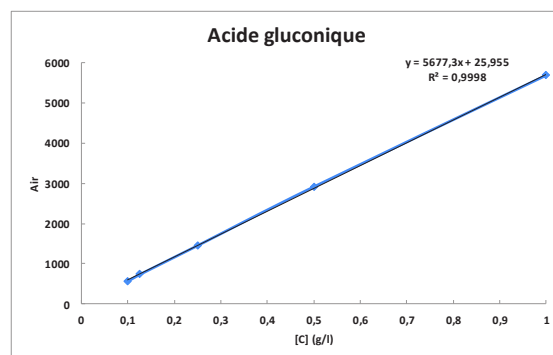
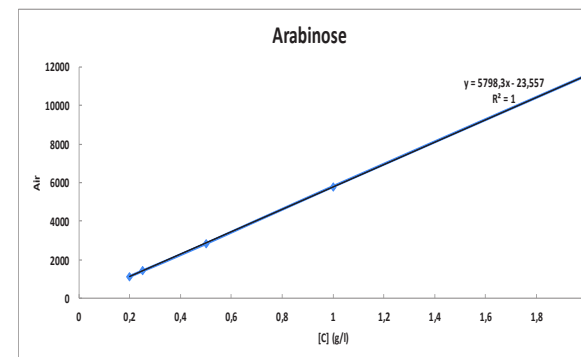
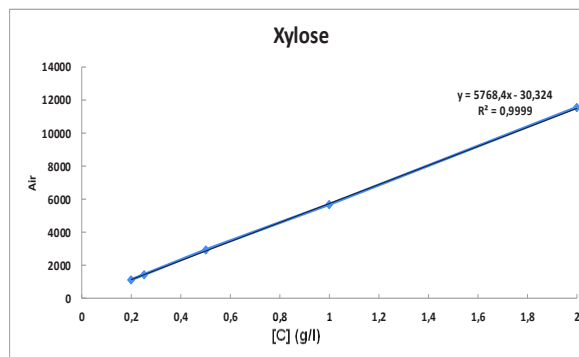
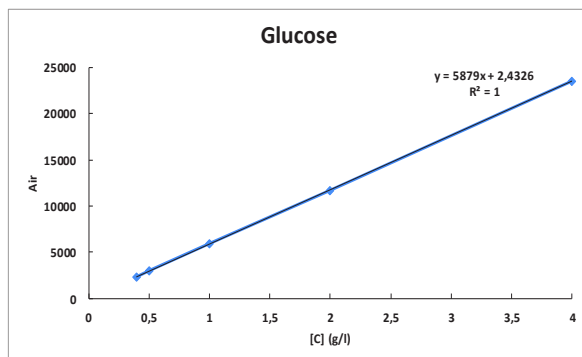
- **Singh Saharan B., Grewal A., Kumar P. 2014.** Biotechnological Production of Polyhydroxyalkanoates: A Review on Trends and Latest Developments. *Chinese Journal of Biology* 2014, 1–18.
- **Singha, A.S. and Thakur V.K. 2012.** Green Polymer Materials. Houston, TX: Studium Press LLC.
- **Siracusa G., La Rosa A.D., Siracusa V., Trovato M. 2001.** Eco Compatible use of olive husk as filler in thermoplastic composites. *Journal of Polymers Environment* 9, 157–161.
- **Siracusa V., Rocculi P., Romani S., Rosa M.D. 2008.** Biodegradable polymers for food packaging: a review. *Trends in Food Science & Technology* 19, 634–643.
- **Siracusa V. 2012.** Food packaging permeability behaviour: A report. International Journal of Polymer Science. Article ID 302029, 11 pages <http://dx.doi.org/10.1155/2012/302029>.
- **Siripatrawan U., Noipha S. 2012.** Active film from chitosan incorporating green tea extract for shelf life extension of pork sausages. *Food Hydrocolloids* 27, 102–108.
- **Smith J. S., Hui Y. H. 2004.** Food Processing Principles and Applications. Iowa :Blackwell. ISBN 0-8138-1942-3.
- **Somova L.I., Shode F.O., Ramnanan P., Nadar A. 2003.** Antihypertensive, antiatherosclerotic and antioxidant activity of triterpenoids isolated from *Olea europaea*, subspecies *africana* leaves. *Journal Ethnopharmacology* 84, 299–305.
- **Sorieul M., Dickson A., Hill S.J., Pearson H. 2016.** Plant Fibre: Molecular Structure and Biomechanical Properties, of a Complex Living Material, Influencing Its Deconstruction towards a Biobased Composite. *Materials* 9(8), 618. DOI:10.3390/ma9080618.
- **Spinelli R., Picchi G. 2010.** Industrial harvesting of olive tree pruning residue for energy biomass. *Bioresource Technology* 101, 730 –735.
- **Stamatelatou K., Kopsahelis A., Blika P.S., Paraskeva C.A., Lyberatos G. 2009.** Anaerobic digestion of olive mill wastewater in a periodic anaerobic baffled reactor (PABR) followed by further effluent purification via membrane separation technologies. *Journal of Chemical Technology and Biotechnology* 84, 909–917.
- **Steele R. 2004.** Understanding and measuring the shelf-life of food, 1st ed Steele R (ed) Woodhead Publishing Limited: Cambridge, UK.
- **Suarez M., Romero M.P., Motilva M.J. 2010.** Development of a phenol enriched olive oil with phenolic compounds from olive cake. *Journal of Agricultural and Food Chemistry* 58, 10396-10403.

- **Sukumaran R.K., Singhania R.R., Pandey A. 2005.** Microbilcellulases-production, applications and challenges. *Journal of Scientific & Industrial Research* 64, 832-844.
- **Suvorova A. I., Tyukova I. S., Trufanova E. I. 2000.** Biodegradable starch-based polymeric materials. *Russian Chemical Reviews* 69, 451–459.
- **Taherzadeh M.J. and Karimi K. 2008.** Pretreatment of Lignocellulosic Wastes to Improve Ethanol and Biogas Production: A Review. *International Journal of Molecular Science* 9, 1621-1651.
- **Tejado A., Kortaberria G., Pen, C., Labidi J., Echeverría J.M., Mondragon I. 2007.** Lignins for phenol replacement in novolac-type phenolic formulations, Part I: Lignophenolic resins synthesis and characterization. *Journal of Applied Polymer Science* 106, 2313–2319.
- **Thakur V.K., Singha A.S. and Thakur M.K. 2011.** Green Composites from Natural Cellulosic Fibers. Germany: GmbH & Co. KG.
- **Thakur V.K. 2014.** Green Composites from Natural Resources. ISBN-13: 978-1-4665-7070-2 (eBook - PDF).
- **Theriez M., Boule G. 1970.** Valeur alimentaire du tourteau d'olive. *Annales de zootechnie, INRA/EDP Sciences* 19 (2), 143-157.
- **Tian J., Sinskey A.J., Stubbe J. 2005.** Kinetic Studies of Polyhydroxybutyrate Granule Formation in *Wautersia eutropha* H16 by Transmission Electron Microscopy. *Journal of Bacteriology* 187 (11), 3814-3824. doi: 10.1128/JB.187.11.3814-3824.2005
- **Toledano A., Serrano L., Labidi J. 2012.** Process for olive tree pruning lignin revalorization. *Chemical Engineering Journal* 193-194, 396-403.
- **Tran L.Q.N., Fuentes C.A., Dupont-Gillain C., Van Vuure A.W. I. 2013.** Understanding the interfacial compatibility and adhesion of natural coir fibre thermoplastic composites. *Composites Sciences and Technology* 80, 23-30.
- **Tserki V., Matzinos P., Kokkou S., Panayiotou C. 2005.** Novel biodegradable composites based on treated lignocellulosic waste flour as filler. Part I. Surface chemical modification and characterization of waste flour. *Composites Part A* 36(7), 965–974.
- **Tserki V., Matzinos P., Panayiotou C. 2006.** Novel biodegradable composites based on treated lignocellulosic waste flour as filler. Part II. Development of biodegradable composites using treated and compatibilized waste flour. *Composites Part A* 37, 1231-1238.

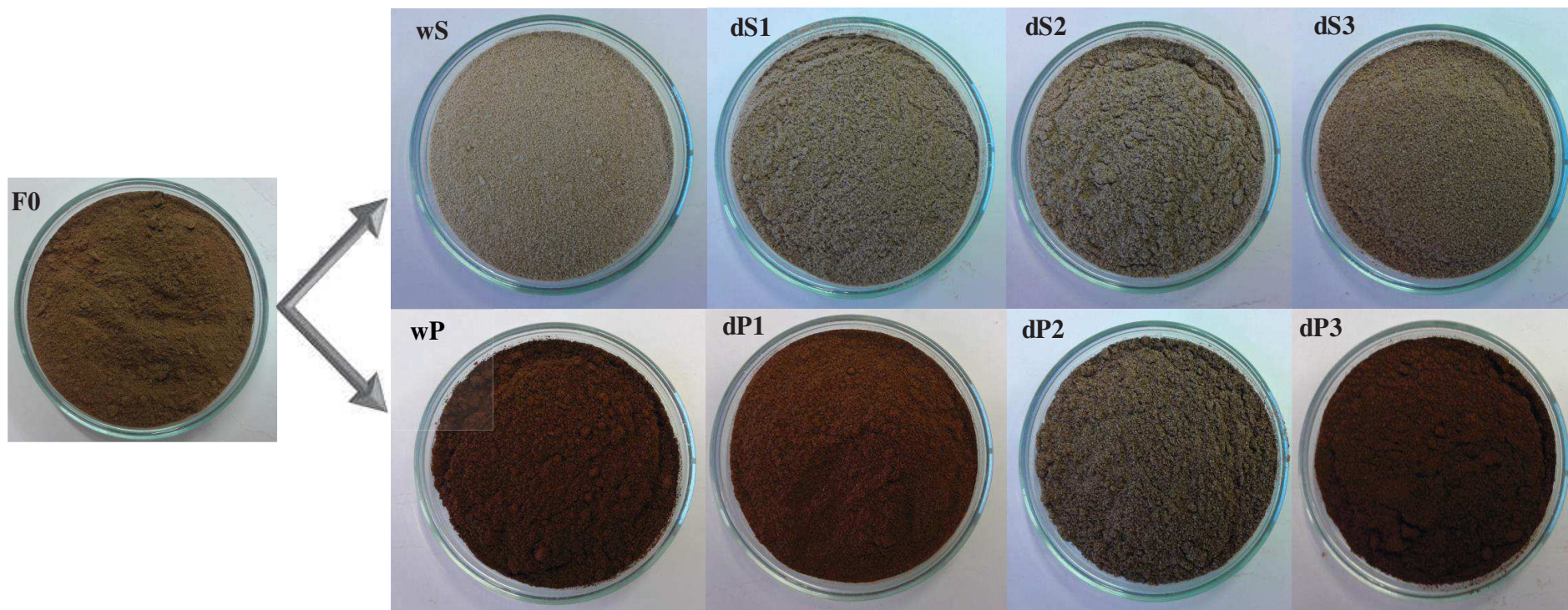
- **Tsuji H., Suzuyoshi K. 2002.** Environmental degradation of biodegradable polyesters 1. Poly(ϵ -caprolactone), poly[(R)-3-hydroxybutyrate], and poly(L-lactide) films in controlled static seawater. *Polymer Degradation and Stability* 75, 347–355.
- **Tuck K.L., Hayball P.J. 2002.** Major phenolic compounds in olive oil: metabolism and health effects. *Journal of Nutritional Biochemistry* 13, 636-644.
- **Ture H., Gallstedt M., Hedenqvist M. 2012.** Antimicrobial compression-moulded wheat gluten films containing potassium sorbate. *Food Research International* 45, 109–115.
- **Uma Devi L., Bhagawan S.S. and Thomas S. 2010.** Dynamic mechanical analysis of pineapple leaf/glass hybrid fiber reinforced polyester composites. *Polymer Composites* 31(6), 956–965.
- **Vermeiren L., Devlieghere F., Van Beest M., de Kruijf N., Debevere J. 1999.** Development in the active packaging of foods. *Trends in Food Sciences and Technology* 10, 77–86.
- **Villa P. 2003.** La culture de l'olivier. Edition De Vicchi, 143 pages.
- **Vlyssides A.G., Loizidou M., Gimouhopoulos K., Zorpas A. 1998.** Olive oil processing wastes production and their characteristics in relation to olive oil extraction methods. *Fresenius Environmental Bulletin* 7 (5/6), 308–313.
- **Voichita B. 2006.** Acoustics of Wood. Dordrecht: Springer-Verlag Berlin and Heidelberg GmbH & Co. KG.
- **Voichita B. 2011.** Delamination in Wood, Wood Products and Wood-Based Composites. Berlin, Heidelberg, Germany: Springer.
- **Volpe M. G., Di Stasio M., Paolucci M., Moccia S. 2015.** Polymers for food shelf-life extension. In: Functional polymers in food science from technology to biology. Cirillo G., Spizzirri U. G., Iemma F (Eds.), ISBN: 978-1-118-59489-6.
- **Wagner J. 1989.** The advent of smart packaging. *International Journal of Food Engineering*, December 11.
- **Wei L., Liang S., McDonald A.G. 2015.** Thermophysical properties and biodegradation behavior of green composites made from polyhydroxybutyrate and potato peel waste fermentation residue. *Industrial Crops and Products* 69, 91–103.
- **Wolf C., Guillard V., Angellier-Coussy H., Ghizzi Da Silva G., Gontard N., 2016.** Water vapour sorption and diffusion in wheat straw particles and impact on mass transfer properties of biocomposites. *Journal of Applied Polymer Science* 133 (16), article number 43329.

- **Wong, S., Shanks, R., Hodzic, A., 2004.** Interfacial improvements in poly(3-hydroxybutyrate)-flax fibre composites with hydrogen bonding additives. *Composites Science and Technology* 64, 1321–1330.
- **Wu C.S., Liao H.T. 2014.** The mechanical properties, biocompatibility and biodegradability of chestnut shell fibre and polyhydroxyalkanoate composites. *Polymer Degradation and Stability* 99, 274-282.
- **Yam K. L., Takhistov P. T., Miltz J. 2005.** Intelligent packaging: Concepts and applications. *Journal of Food Science* 70, R1–R10.
- **Yang B., Wyman C.E. 2008.** Pretreatment: the key to unlocking low-cost cellulosic ethanol. *Biofuels, Bioproducts and Biorefining* 2, 26–40.
- **Yang H., Yan R., Chen H., Lee D.H., Zheng C. 2007.** Characteristics of hemicellulose, cellulose and lignin pyrolysis. *Fuel* 86, 1781–1788.
- **Zabaniotou A., Kalogiannis G., Kappas E., Karabelas A.J. 2000.** Olive residues (cuttings and kernels) rapid pyrolysis product yields and kinetics. *Biomass Bioenergy* 18, 411- 420.
- **Zbakh H., El Abbassi A. 2012.** Potential use of olive mill wastewater in the preparation of functional beverages: A review. *Journal of Functional Foods* 4(1), 53-65.
- **Zeman S., Kubik L., 2007.** Permeability of polymeric packaging materials. *Technical Science* 10, 27-34.
- **Zhang H., Mittal G. 2010.** Biodegradable protein-based films from plant resources: A review. *Environmental Progress & Sustainable Energy* 29, 203 - 220.

Annexes



Courbes étalons des différents sucres



Fractions de grignon d'olives produites

Abstract

The aim of this thesis project is to design a packaging material - functional and biodegradable under natural conditions - from renewable resources, as an ecological alternative to conventional fossil-based materials and better adapted for the preservation of various food products. Olive pomace is the solid by-product of the extraction of olive oil, consisting mainly of pulp and stone. This agro-food residue causes serious environmental problems and their valorization must be encouraged.

A first study carried out on the dry fractionation of the olive pomace by combination of grinding and sorting processes, made it possible to select the most suitable method for this lignocellulosic biomass to separate the pulp from the stone and produce fractions with the highest purity, and the best yield. The physico-chemical characteristics (composition, thermal stability, color, surface free energy) of the obtained powders were evaluated. It has been demonstrated that the use of a ball mill under very mild conditions, allows, by friction forces, to successfully transform the pomace into useful fractions, while avoiding the consumption of water and the generation of water effluents or co-products.

The second part of this work was devoted to the implementation of biocomposite materials based on olive pomace. Three lignocellulosic fractions with contrasting properties previously produced by dry fractionation of the olive cake were selected: a core rich fraction (SF) with a high cellulose content and having a high polarity, a rich pulp fraction (PF) which is richer lignin and less polar; a fraction of crude pomace (F0) having intermediate properties. These powders are incorporated as fillers in two thermoplastic matrices, polypropylene and polyhydroxybutyrate-co-valerate (PHBV) at concentrations of 5, 15 and 30% by weight using a thermomechanical process. The structure / property relationships of the resulting biocomposites were studied. The tensile tests revealed that the mechanical properties were better preserved in the case of the FP load thanks to better interfacial adhesion to the polymer matrices. The water vapor permeability of the two matrices increased in the presence of the SF and F0 charges, while the oxygen permeability was not significantly affected by the incorporation of the charges. These results suggest a promising use of stone and crude pomace fractions in the development of sustainable biocomposites for the packaging of breathable food products. As for the pulp formulations, they have proved more suitable for the packaging of non-breathable and water-sensitive products.

In the third part, we studied the influence of the composition of the pomace fractions on the biodegradability of biocomposites based on PHBV (loading rate of 15% by mass). Biodegradation of the matrix, fillers and biocomposite materials was evaluated in the soil by respirometric tests over 4 months. The results showed that the incorporation of the pomace loads leads to the acceleration of the biodegradability of the biocomposites compared to the PHBV alone. In fact, the biodegradation reached a level of 100% after 75, 79 and 87 days for the formulations PHBV-F0, PHBV-SF and PHBV-PF respectively. After 123 days, the biodegradation of PHBV reached only 91%, whereas it exceeded 100% for all OP / PHBV films, which was attributed to the stimulating effect of the charges. These results were confirmed by contact angle measurements, degree of crystallinity (DSC) and surface structure of biocomposites (SEM observations).

Keywords: olive pomace, dry fractionation, characterization, PHBV, PP, food packaging, biocomposites, mechanical properties, barrier properties, thermal properties, biodegradation, soil.

Résumé

L'objectif de ce projet de thèse consiste à concevoir un matériau d'emballage - fonctionnel et biodégradable en conditions naturelles - à partir de ressources renouvelables, comme alternative écologique aux matériaux conventionnels d'origine fossile et mieux adapté pour la conservation de divers produits alimentaires. Le grignon d'olives est le sous-produit solide issu de l'extraction de l'huile d'olive, composé essentiellement de pulpe et de noyau. Ce résidu agroalimentaire cause de sérieux problèmes environnementaux et sa valorisation doit être encouragée.

Une première étude réalisée sur le fractionnement par voie sèche du grignon par combinaison de procédés de broyage et de tri, a permis de sélectionner le procédé le plus adapté à cette biomasse lignocellulosique pour séparer la pulpe du noyau et produire des fractions avec la plus grande pureté et le meilleur rendement. Les caractéristiques physico-chimiques (composition, stabilité thermique, couleur, énergie libre de surface) des poudres obtenues ont été évaluées. Il a été démontré que l'utilisation d'un broyeur à boulets dans des conditions très douces, permettait, par des forces de friction, de transformer avec succès le grignon en fractions utiles, tout en évitant la consommation d'eau et la génération d'effluents ou de coproduits.

La deuxième partie de ce travail était consacrée à la mise en œuvre de matériaux biocomposites à base de grignon. Trois fractions lignocellulosiques avec des propriétés contrastées préalablement produites par fractionnement sec du grignon ont été sélectionnées : une fraction riche en noyau (SF) avec une teneur en cellulose importante et ayant une polarité élevée, une fraction riche en pulpe (PF) qui est plus riche en lignine et moins polaire ; une fraction de grignons brute (F0) présentant des propriétés intermédiaires. Ces poudres sont incorporées comme charges dans deux matrices thermoplastiques, le polypropylène et polyhydroxybutyrate-co-valérate (PHBV) à des concentrations de 5, 15 et 30% massique en utilisant un procédé thermo-mécanique. Les relations structure/propriétés des biocomposites résultants ont été étudiées. Les essais de traction ont révélé que les propriétés mécaniques étaient mieux préservées dans le cas de la charge PF grâce à une meilleure adhérence interfaciale envers les matrices polymères. La perméabilité à la vapeur d'eau des deux matrices a augmenté en présence des charges SF et F0, tandis que la perméabilité à l'oxygène n'a pas été significativement affectée par l'incorporation des charges. Ces résultats suggèrent une utilisation prometteuse des fractions de noyau et du grignon brut dans le développement de biocomposites durables pour l'emballage des produits alimentaires respirants. Quant aux formulations à base de pulpe, elles se sont avérées plus appropriées pour l'emballage des produits non-respirants et sensibles à l'eau.

Dans la troisième partie, on s'est intéressé à l'étude de l'influence de la composition des fractions de grignon sur la biodégradabilité des biocomposites à base de PHBV (taux de charge de 15% massique). La biodégradation de la matrice, des charges et des matériaux biocomposites a été évaluée dans le sol par des tests respirométriques sur 4 mois. Les résultats ont montré que l'incorporation des charges de grignon entraîne l'accélération de la biodégradabilité des biocomposites par rapport au PHBV seul. En effet, la biodégradation a atteint un taux de 100% après 75, 79 et 87 jours pour les formulations PHBV-F0, PHBV-SF et PHBV-PF respectivement. Après 123 jours, la biodégradation du PHBV n'a atteint que 91%, alors qu'elle a dépassé 100% pour tous les films OP/PHBV, ce qui a été attribué à l'effet stimulant des charges. Ces résultats ont été confirmés par des mesures d'angle de contact, le degré de cristallinité (DSC) et la structure des surfaces des biocomposites (observations MEB).

Mots clés : grignon d'olives, fractionnement par voie sèche, caractérisation, PHBV, PP, emballage alimentaire, biocomposites, propriétés mécaniques, propriétés barrières, propriétés thermiques, biodégradation, sol.